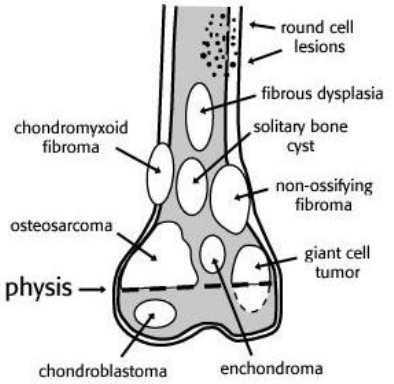

The tumor and the tumor-like condition Which aggressiveness features to search in multimodality imaging?

Frédéric Paycha, MD

Department of Nuclear Medicine

Lariboisière Hospital

Assistance Publique-Hôpitaux de Paris

Paris, France

frederic.paycha@wanadoo.fr

Epidemiology: Pick up best bet!

1000 pseudo-tumors
100 metastases
10 blood malignancies
1 primitive tumor

Pseudo-tumors group
4 categories

- Inflammations & Infections
  - Osteomyelitis/LCH/SAPHO
- T
  - Trauma/Brown tumors
- OSES
  - Sarcoidosis/Mastocytosis/Angiomatosis
- Bone scan+
  - FDB/Paget/Bone infarct

WHO classification of primary bone tumors

Histological Types	Benign	Malignant
Hematopoietic (40%)		Myeloma Malignant lymphoma
Chondrogenic (22%)	Osteochondroma Chondroma Chondroblastoma Chondromyxoid fibroma	Chondrosarcoma Dedifferentiated chondrosarcoma
Osteogenic (19%)	Osteoid osteoma Osteoblastoma, osteoma	Osteosarcoma
Unknown origin (10%)	Giant cell tumour	Ewing tumour Giant cell tumour Adamantinoma
Histiocytic origin Fibrogenic Notochordal Vascular, Cystic, lipogenic neurogenic	Fibrous histiocytoma Fibroma	MFH Fibrosarcoma Chordoma

Tumor Aggressiveness ⇆ Quiescence
A survival 10 criteria checklist for the imaging specialist

1. Localization
2. Age
3. Pain
4. Phenotype lytic/sclerotic
5. Margins
6. Activity/timeline
7. Cortical/Periosteum
8. Crossing or not the joint?
9. Soft tissue expansion
10. Number (⇒ distribution)

1. Localization criteria

Sclerotic and/or lytic phenotype

Localization

- Tubular bones
- Short bones
- Flat/irregular bones

Tumors & metastases in tubular bone

X-Rays/CT features

- Physeal localisation
- Sectional localisation
- Geometric features
  - Matrix type
  - Borders
- Transition zone/edema
- Cortical behaviour
- Periosteal reaction
- Soft tissue loco-regional extension
- Skip lesions
- Neighbouring joints reaction

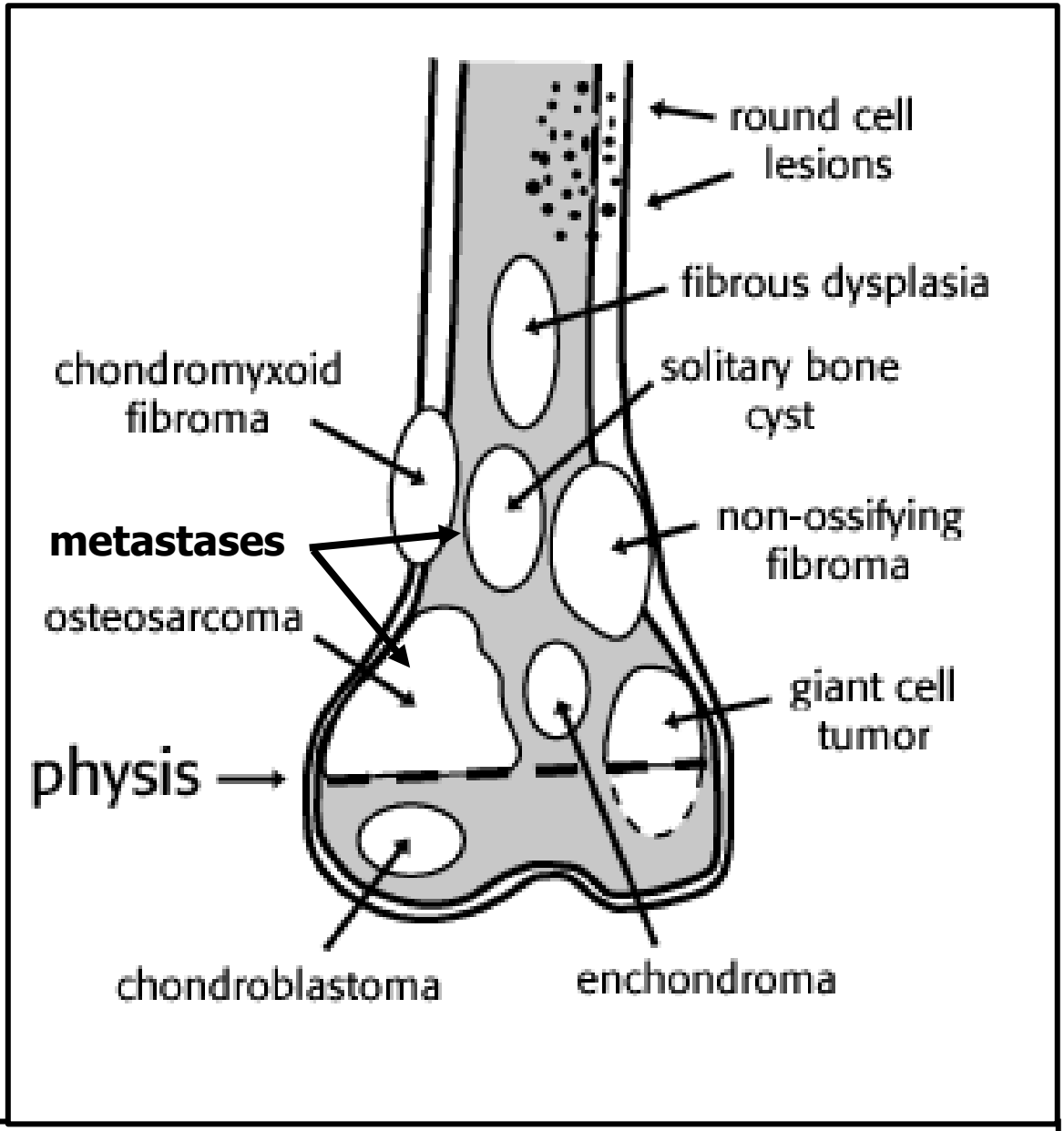

Adapted from:
Madewell JE, et al. Radiol Clin North Am 1981

Tumors & metastases in tubular bone

X-Rays/CT features

SPECT features

- Physeal localisation
- Sectional localisation
- Geometric features
  - Matrix type
  - Borders
- Transition zone/edema
- Cortical behaviour
- Periosteal reaction
- Soft tissue loco-regional extension
- Skip lesions
- Neighbouring joints reaction

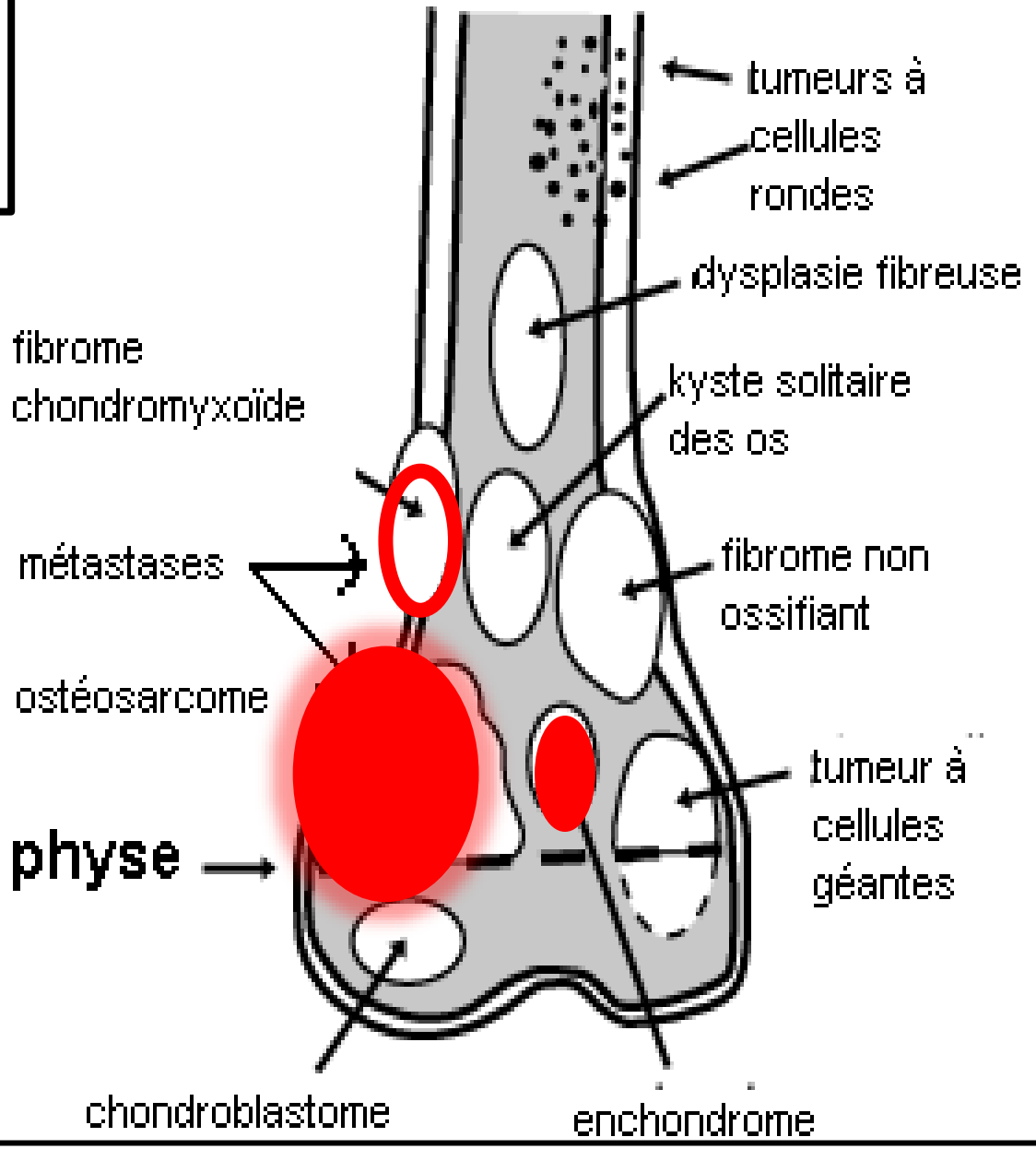

Adapté de:
Madewell JE, et al. Radiol Clin North Am 1981

Rule of the origin
Epiphyso-metaphyseal lesions

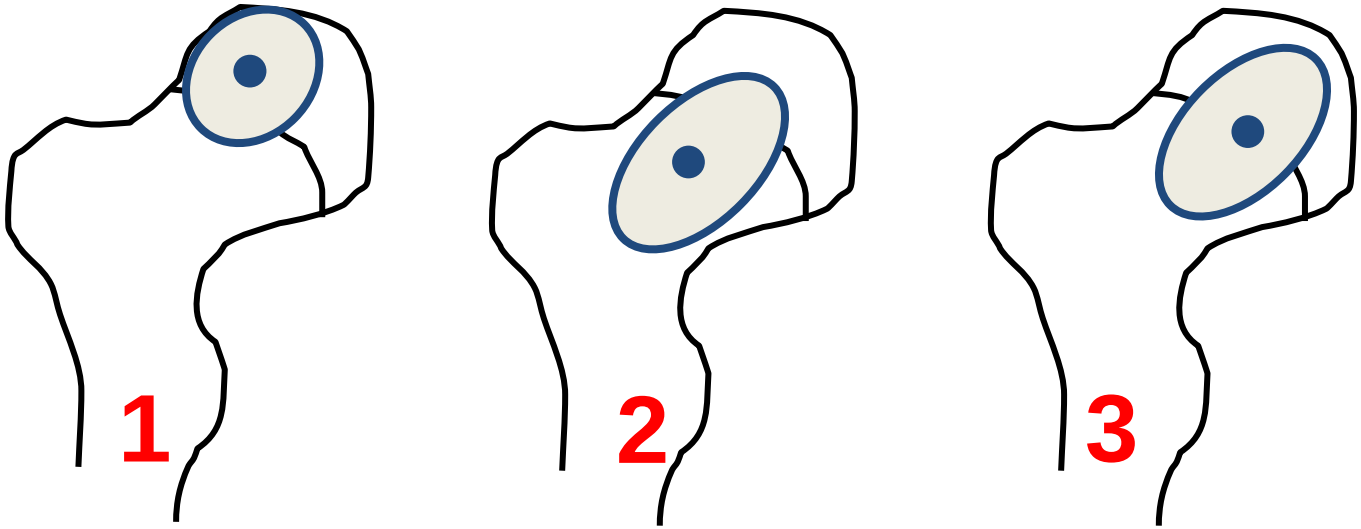

1. Juxta-articular cyst, chondroblastoma, CCC
2. Fibrous dysplasia
3. GCT

Rule of the origin: Axial views

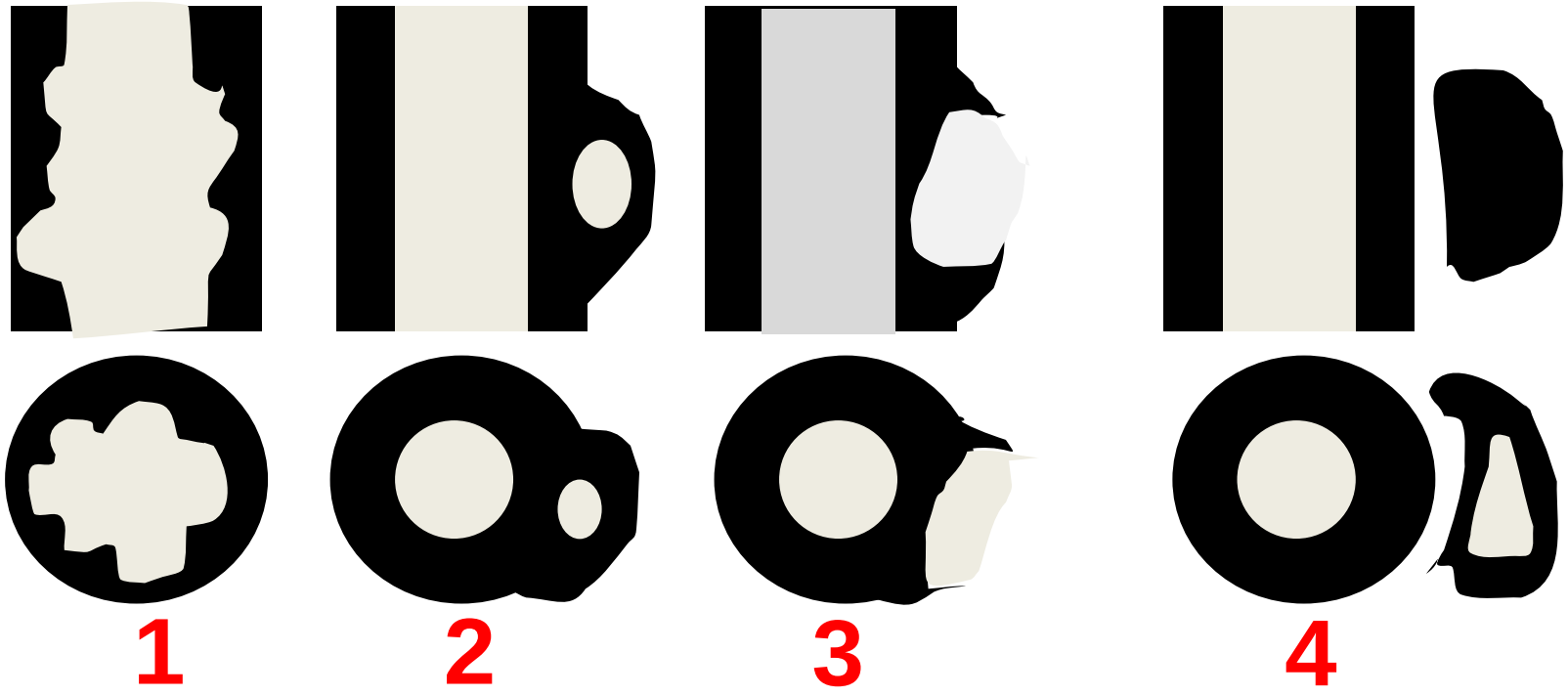

- 1. Endosteal defects: bone marrow
- 2. Intracortical : osteitis, OO,…
- 3. Subperiosteal : enchondroma, ABC,…
- 4. Paraosteal : MOC

Imaging abnormality in vertebra: Intra-somatic or posterior arch? Bone tumors & pseudo-tumors gamut

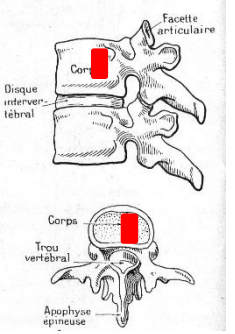

Rule: malignant lesions

-Metastasis

-Lymphoma

-Plasmocytoma/myeloma

-Chordoma

Exceptions: benign lesions

-Hemangioma

-Bone island

-Langerhans cell histiocytosis (LCH)

-Giant Cell Tumor (GCT)

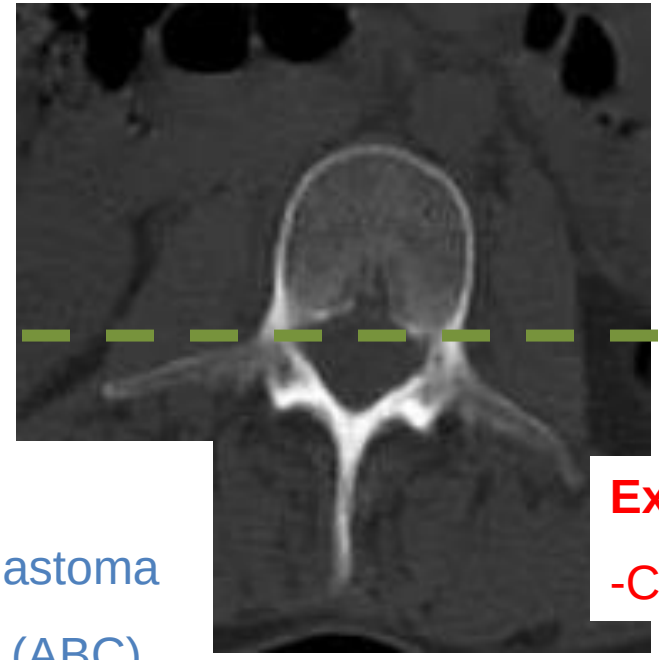

Rule: benign lesions

-Osteoid osteoma/Osteoblastoma

- Aneurysmal cyst of bone (ABC)

Exceptions: malignant lesions

-Chondrosarcoma

Metaphyseal equivalent for flat bones and irregular bones

Hematogenous Osteomyelitis of Metaphyseal-equivalent Locations

GEORGE W. NIXON[1]

AJR 1978; 130: 123-129

- Flat bones and irregular bones feature anatomical subdivisions ("physeal") analog to those of tubular bones
- Areas neighbouring cartilage are metaphyseal equivalent localizations
- Proof of concept: Human models of metastasis and osteomyelitis
- Radio-clinical interest: Solitary bone lesions

Flat bones

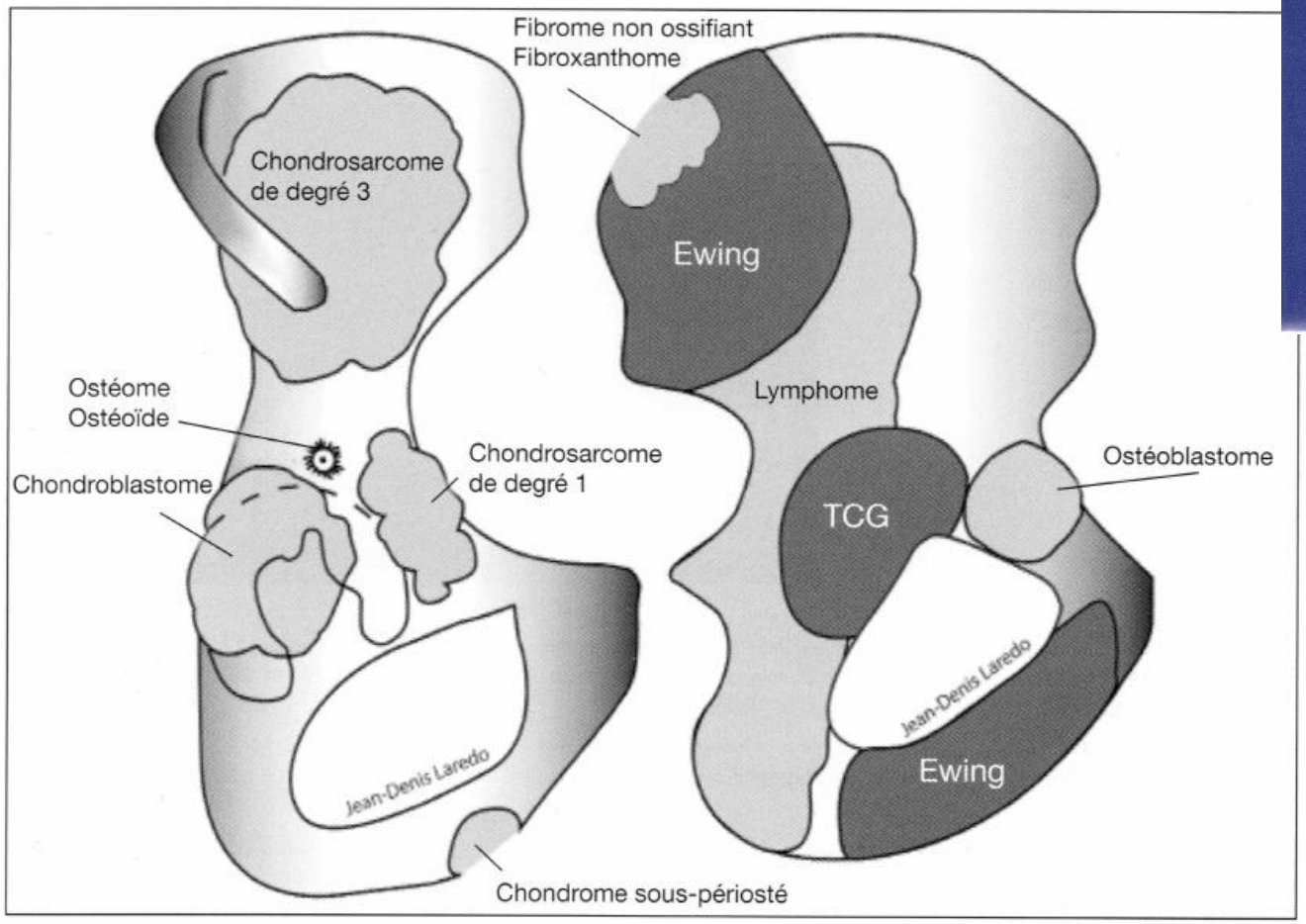
Fibrome non ossifiant
Fibroxanthome
Chondrosarcome
de degré 3
Ewing
Ostéome
Ostéoïde
Lymphome
Chondrosarcome
de degré 1
Ostéoblastome
Chondroblastome
TCG
Jean-Denis Laredo
Jean-Denis Laredo
Ewing
Chondrome sous-périosté

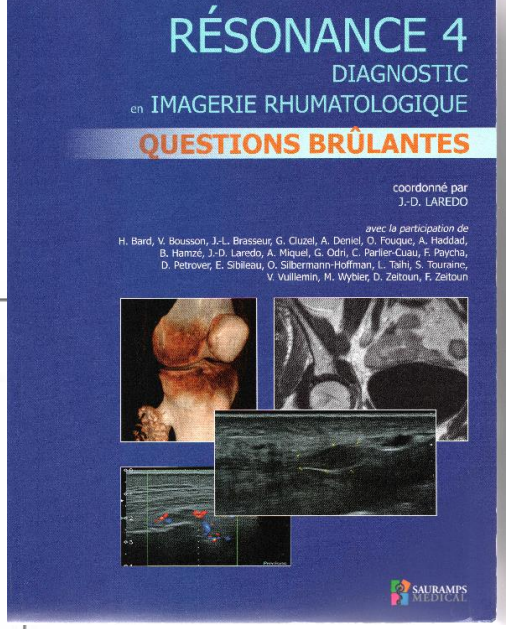
RÉSONANCE 4
DIAGNOSTIC
en IMAGERIE RHUMATOLOGIQUE
QUESTIONS BRÛLANTES
coordonné par
J.-D. LAREDO
avec la participation de
H. Bard, V. Bousson, J.-L. Brasseur, G. Cluzel, A. Deniel, O. Fouque, A. Haddad,
B. Hamzé, J.-D. Laredo, A. Miquel, G. Odri, C. Parlier-Cuau, F. Paycha,
D. Petrover, E. Sibileau, O. Silbermann-Hoffman, L. Taïh, S. Touraine,
V. Vuillemin, M. Wybier, D. Zeitoun, F. Zeitoun
SAURAMPS MEDICAL

Localization

Bone localization	Tumor & pseudo-tumor
Spheno-orbital region	Intraosseous meningioma
Vertebral posterior arch	ABC, osteoblastoma, osteoid osteoma
Sacrum	GCT, chordoma, chondrosarcoma
Lower limb	Hemangioendothelioma
Femur intertrochanteric	LSMF
Femur posterior cortex	Paraosteal osteosarcoma
Tibia anterior cortex	Adamantinoma, stress fracture
Phalanx	Enchondroma, Epidermoid cyst
Calcaneus	Lipoma, bone simple cyst

Intraosseous meningioma

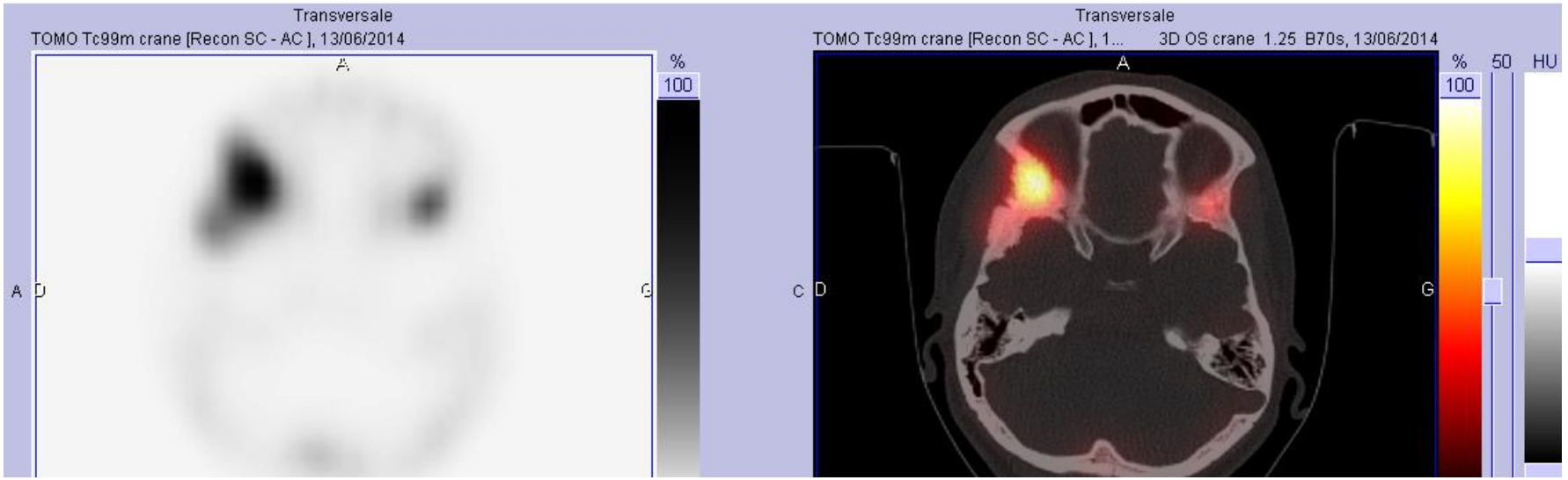

Hyperostosis, resulting in dedifferenciation between diploe and inner and outer tables
Periosteal reaction featuring crude spiculations, spheno-orbital localization (90%)

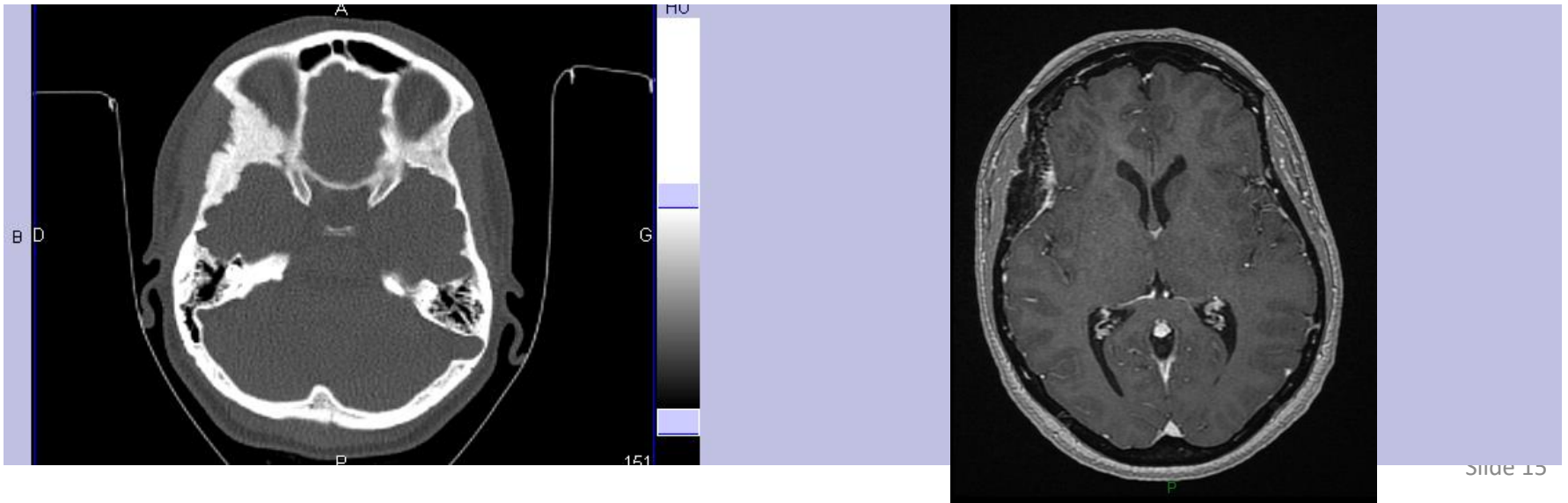

Clinical presentation

M, 50 YO
Chronic pain R ankle,
Mechanical rhythm
Medical history: ∅

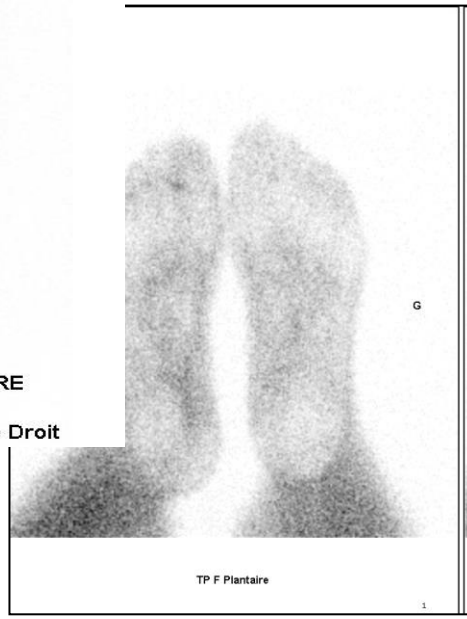

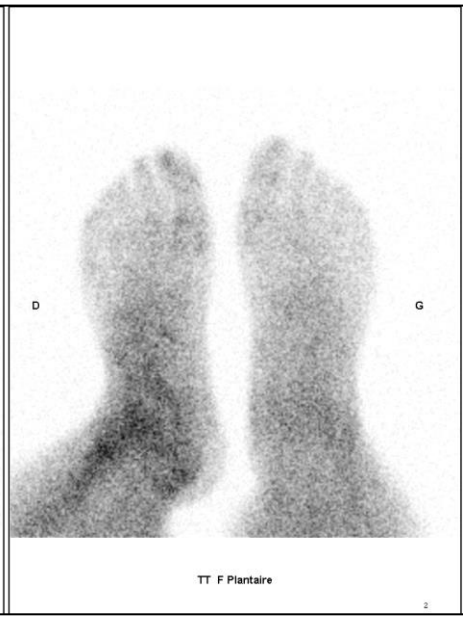

HYBRID_CT Coronals

HYBRID_CT Sagittals

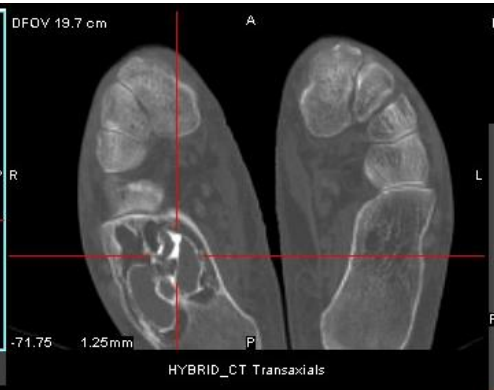

HYBRID_CT Transaxials

HYBRID_CT Scout

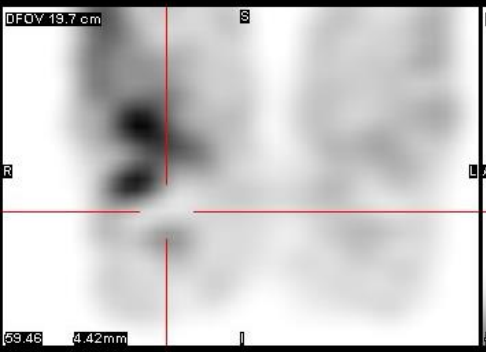

IRACSCRR Coronals

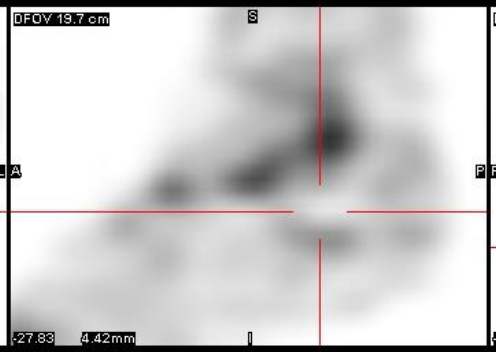

IRACSCRR Sagittals

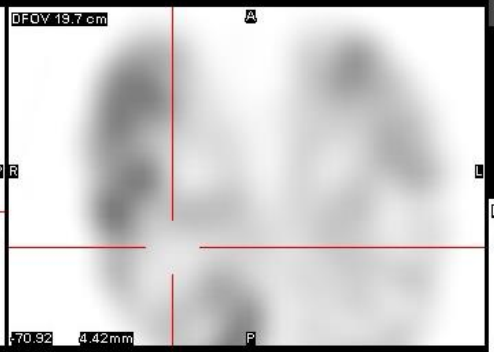

IRACSCRR Transaxials

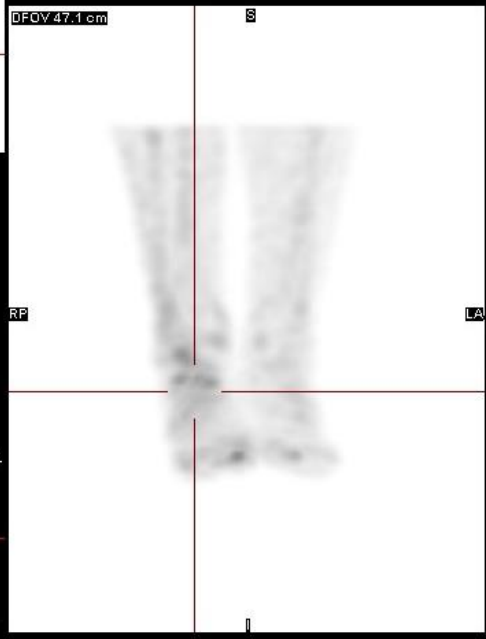

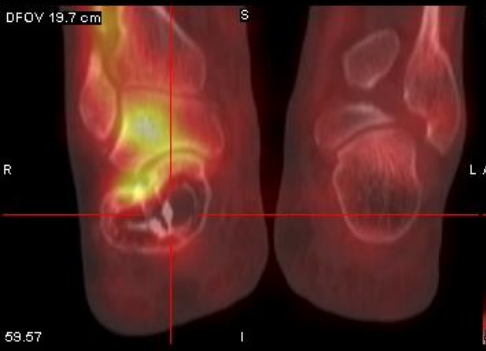

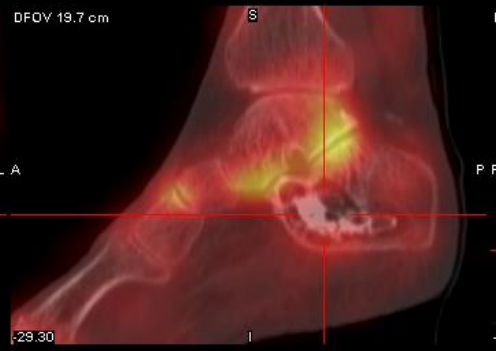

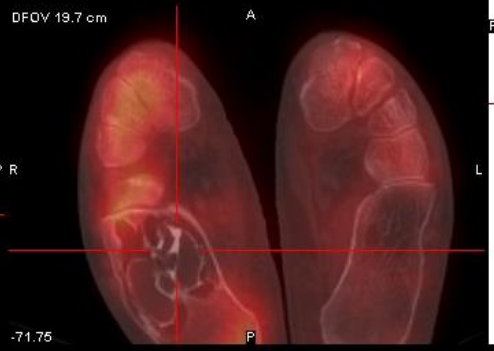

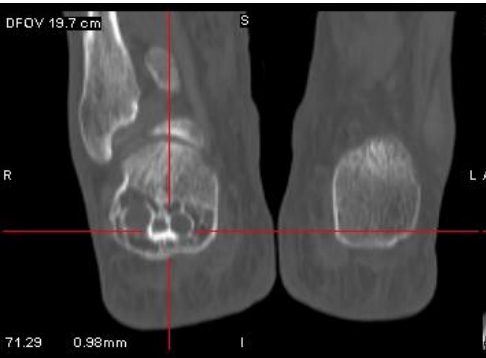

HYBRID_CT Coronals

HYBRID_CT Sagittals

HYBRID_CT Transaxials

HYBRID_CT Scout

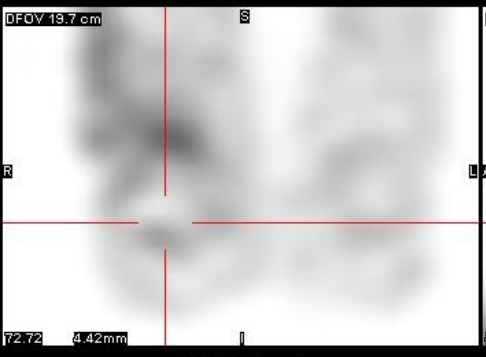

IRACSCRR Coronals

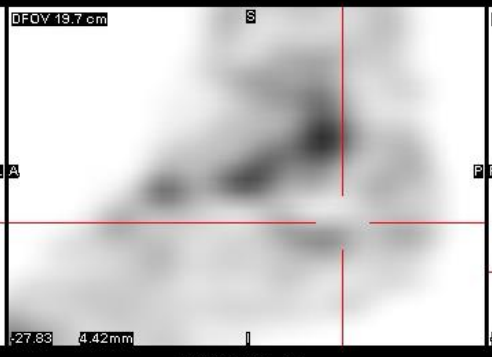

IRACSCRR Sagittals

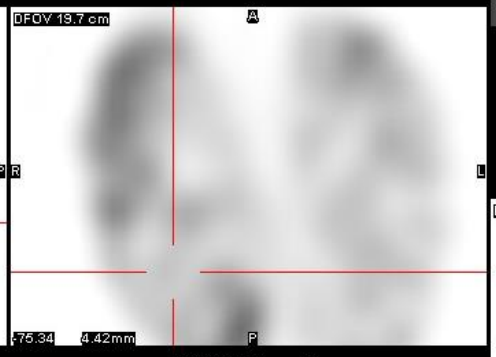

IRACSCRR Transaxials

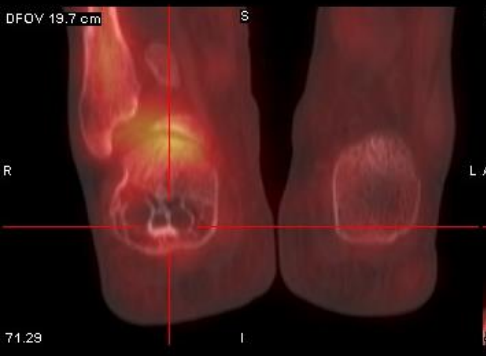

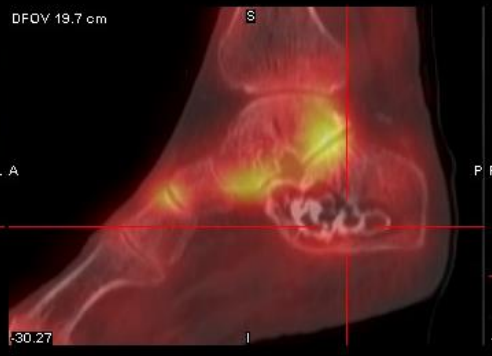

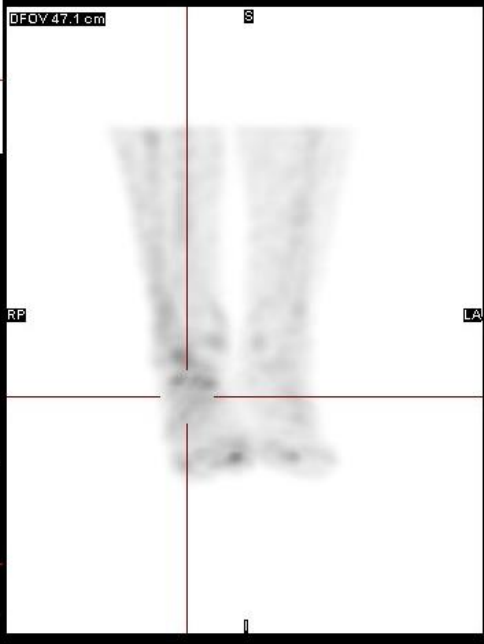

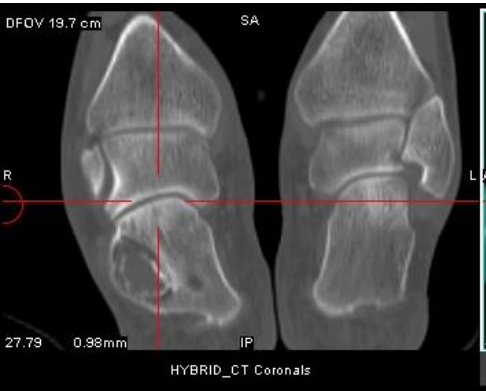

HYBRID_CT Coronals

HYBRID_CT Sagittals

HYBRID_CT Transaxials

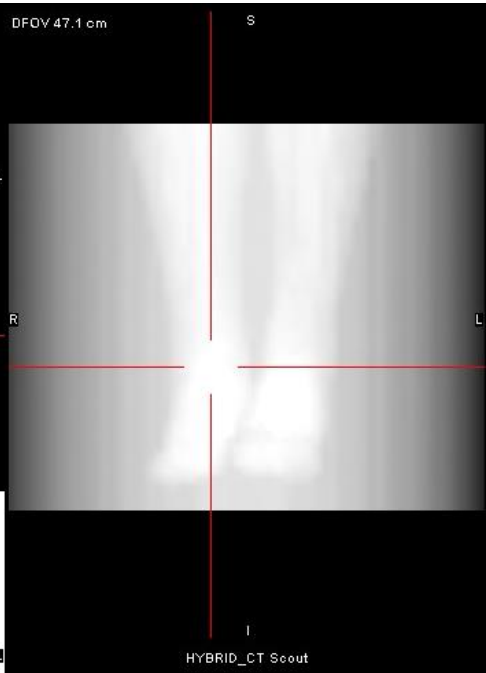

HYBRID_CT Scout

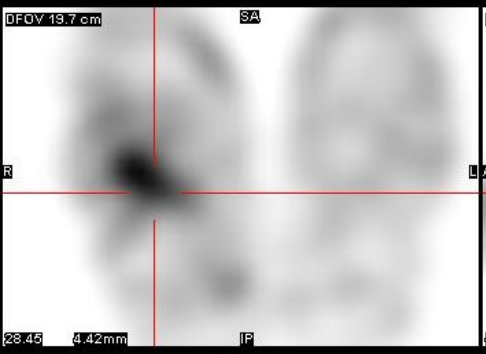

IRACSCRR Coronals

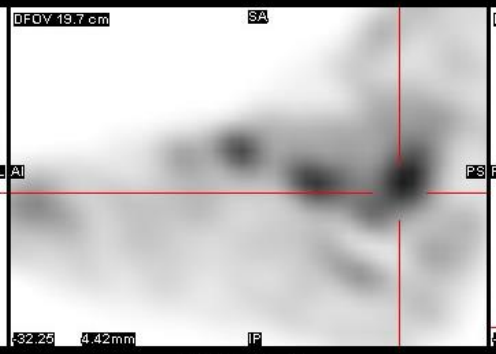

IRACSCRR Sagittals

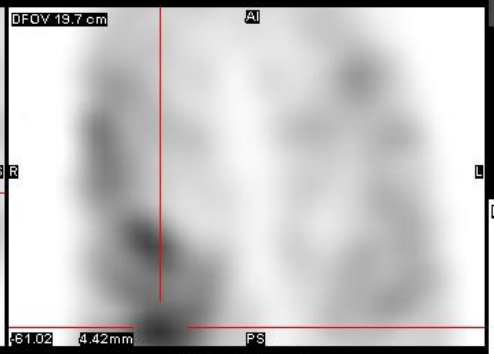

IRACSCRR Transaxials

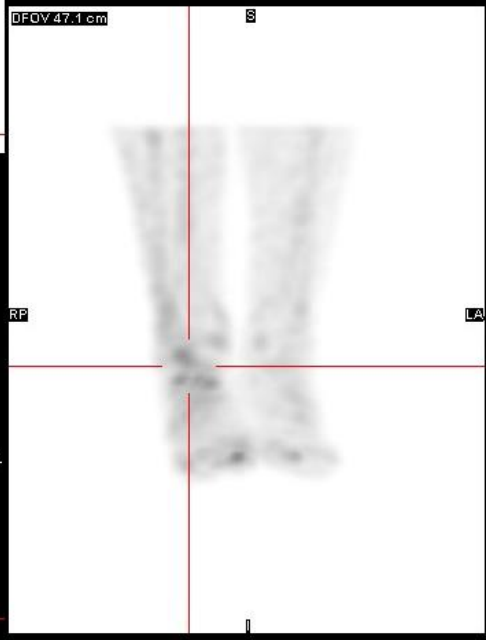

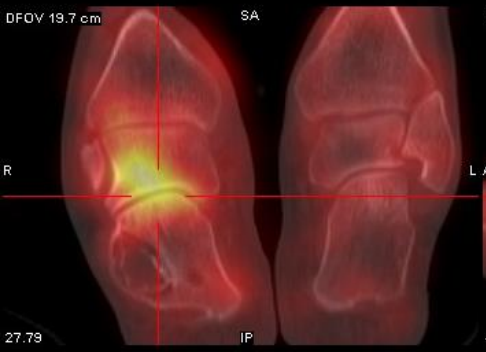

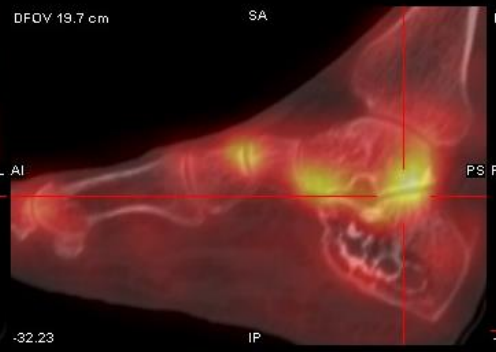

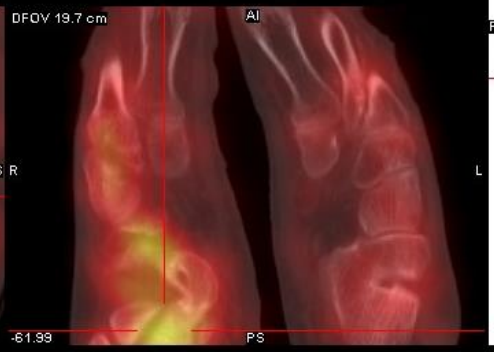

CT pattern deconstruction

No aggressiveness features!

Conclusion
Origin of pain?

- Intra-osseous lipoma calcaneus
  - Photopaenic
- Arthropathies sub-talar joint, tarsus, 1st ray
  - Increased uptake areas

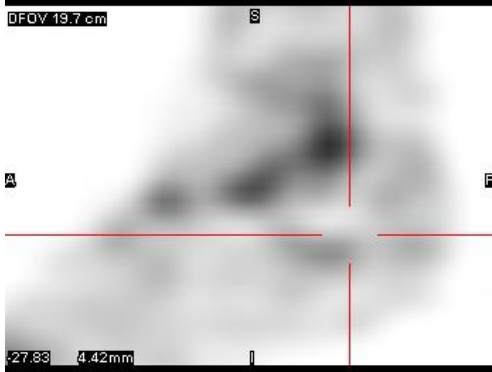

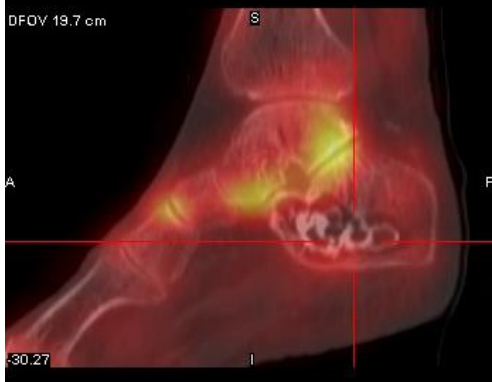

Intra-osseous lipoma "A black hole"

- Rare : 0.1% bone tumors
- Any age
- Clinical presentation :
  - Most frequently non-symptomatic
  - Rarely pathological fracture
- Localization :
  - Calcaneus
  - Metaphysis of tubular bones
  - Bone marrow

Intra-osseous lipoma

Milgram anatomo-pathological classification

3 grades

- Viable adipocytes
- Central necrosis and calcifications
- Myxoïd degenerescence with cystic changes

Milgram JW. Intraosseous lipomas: radiologic and pathologic manifestations. Radiology 1988

Clinico-scintigraphic presentation

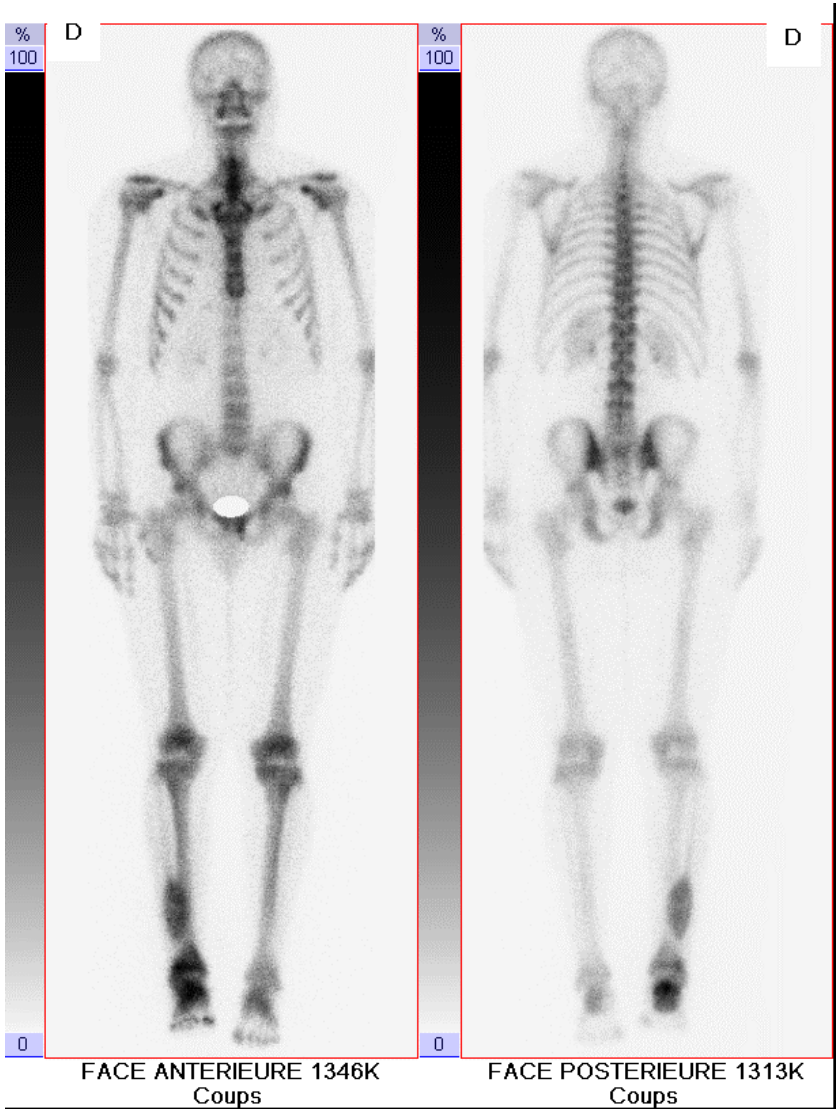

M, 40 YO

Worsening pain R talar for 2 years

Plain X-Rays R LL

Bone SPECT/CT
R fibula 1/3 distal diaphysis

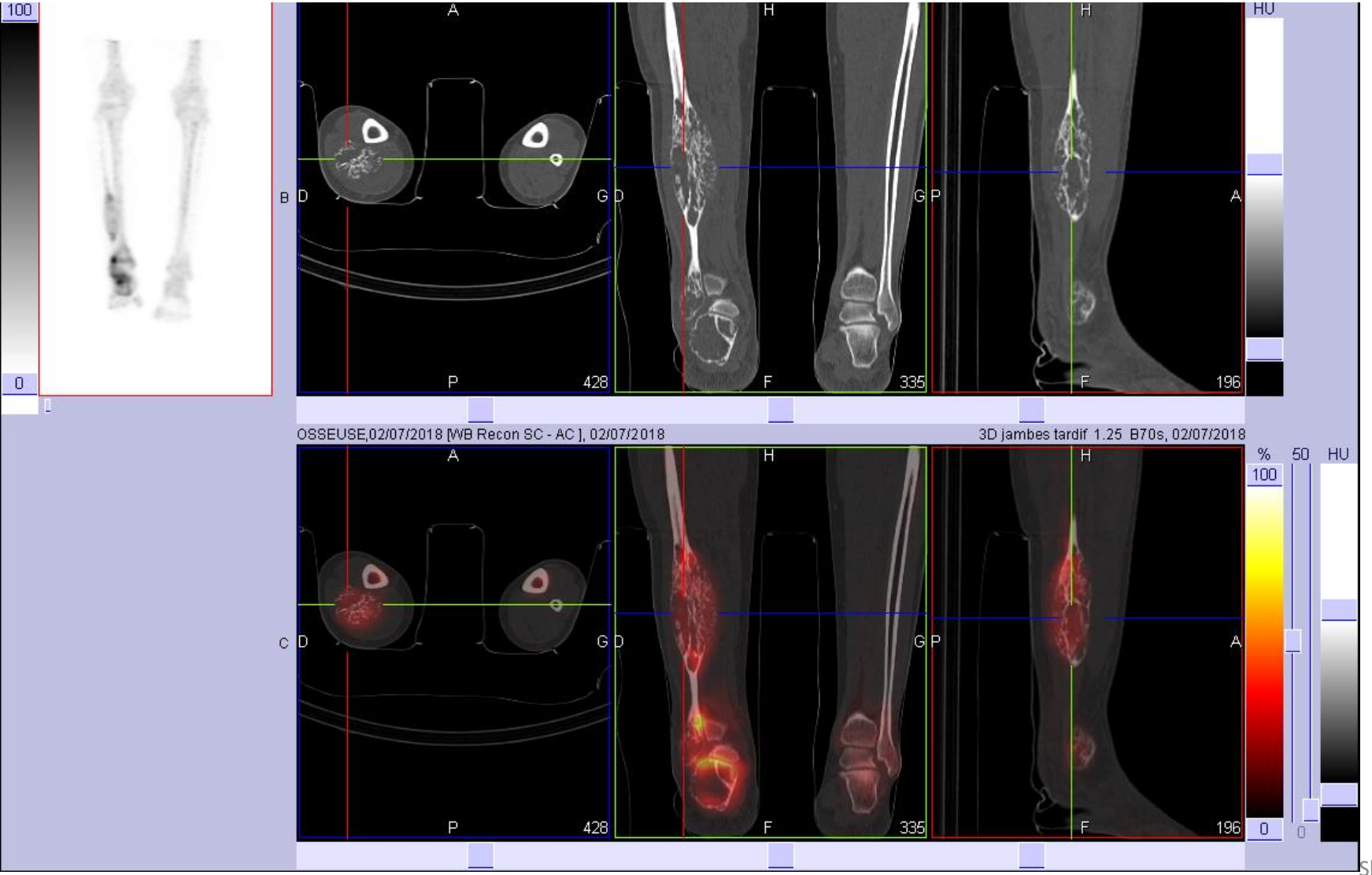

Bone SPECT/CT
R fibula distal metaphysis

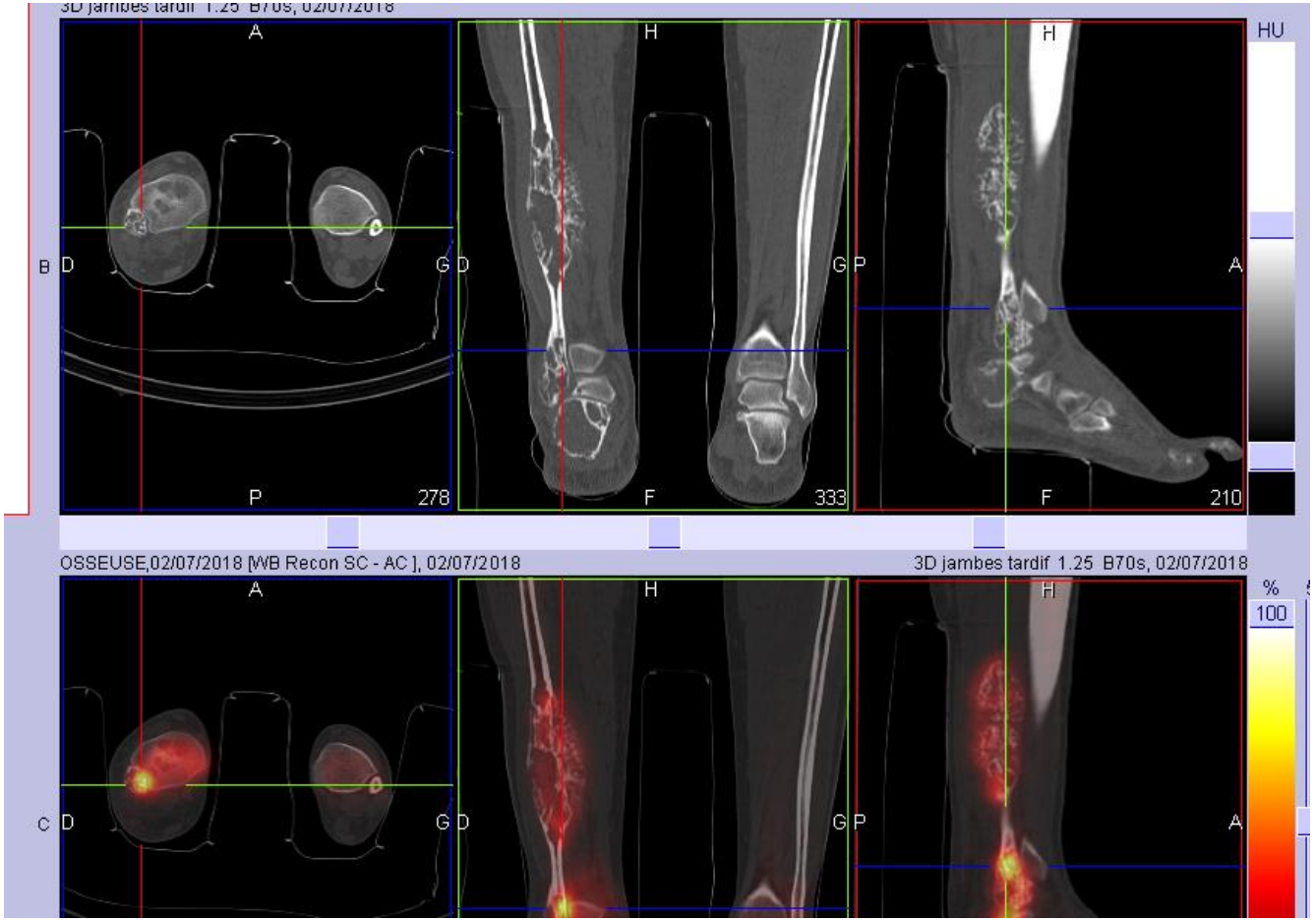

Bone SPECT/CT
R talus

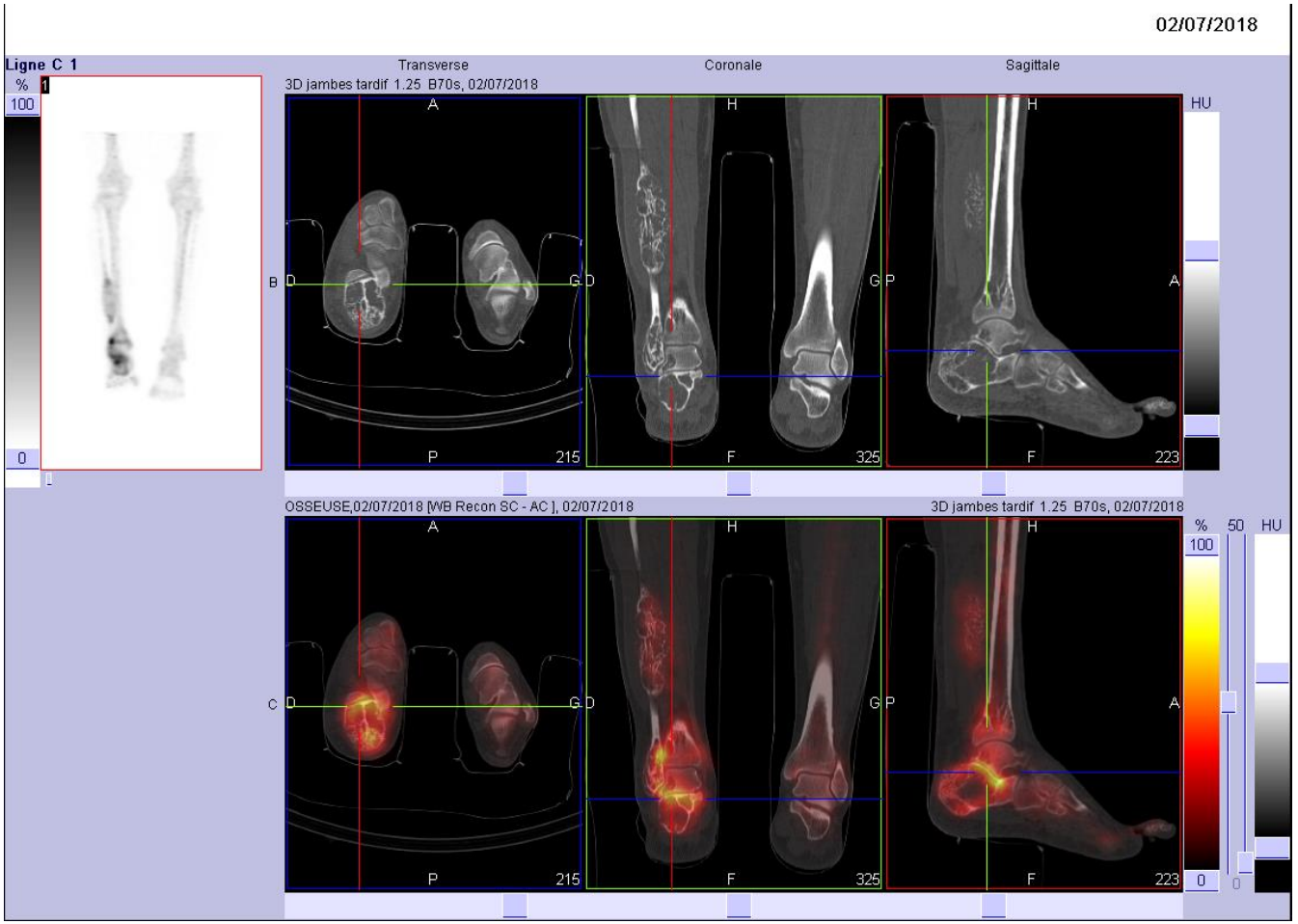

Fused VRT lower limbs

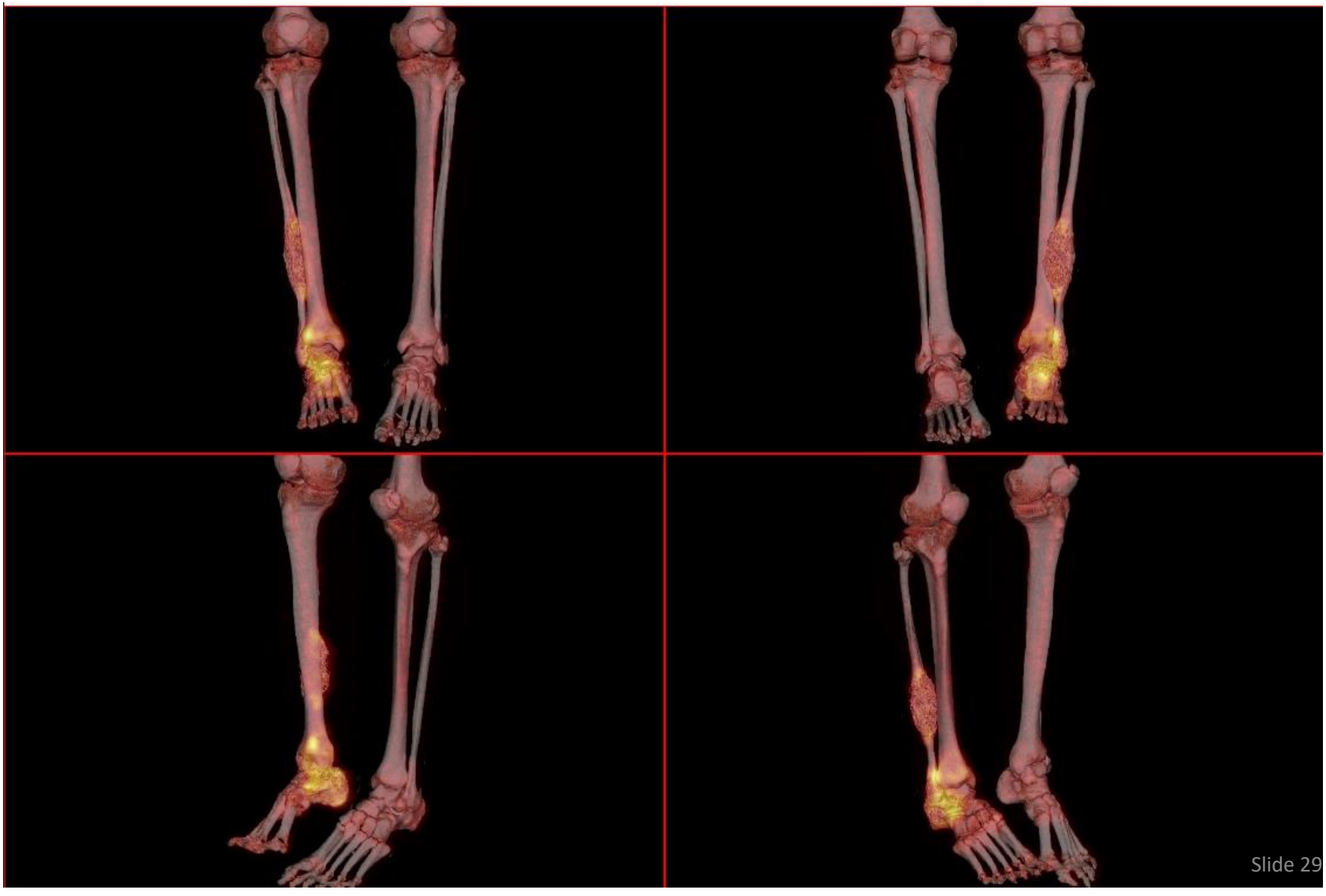

R rearfooot
MRI Axial T1 – DP FATSAT

FDG PET/CT
R fibula distal diaphysis

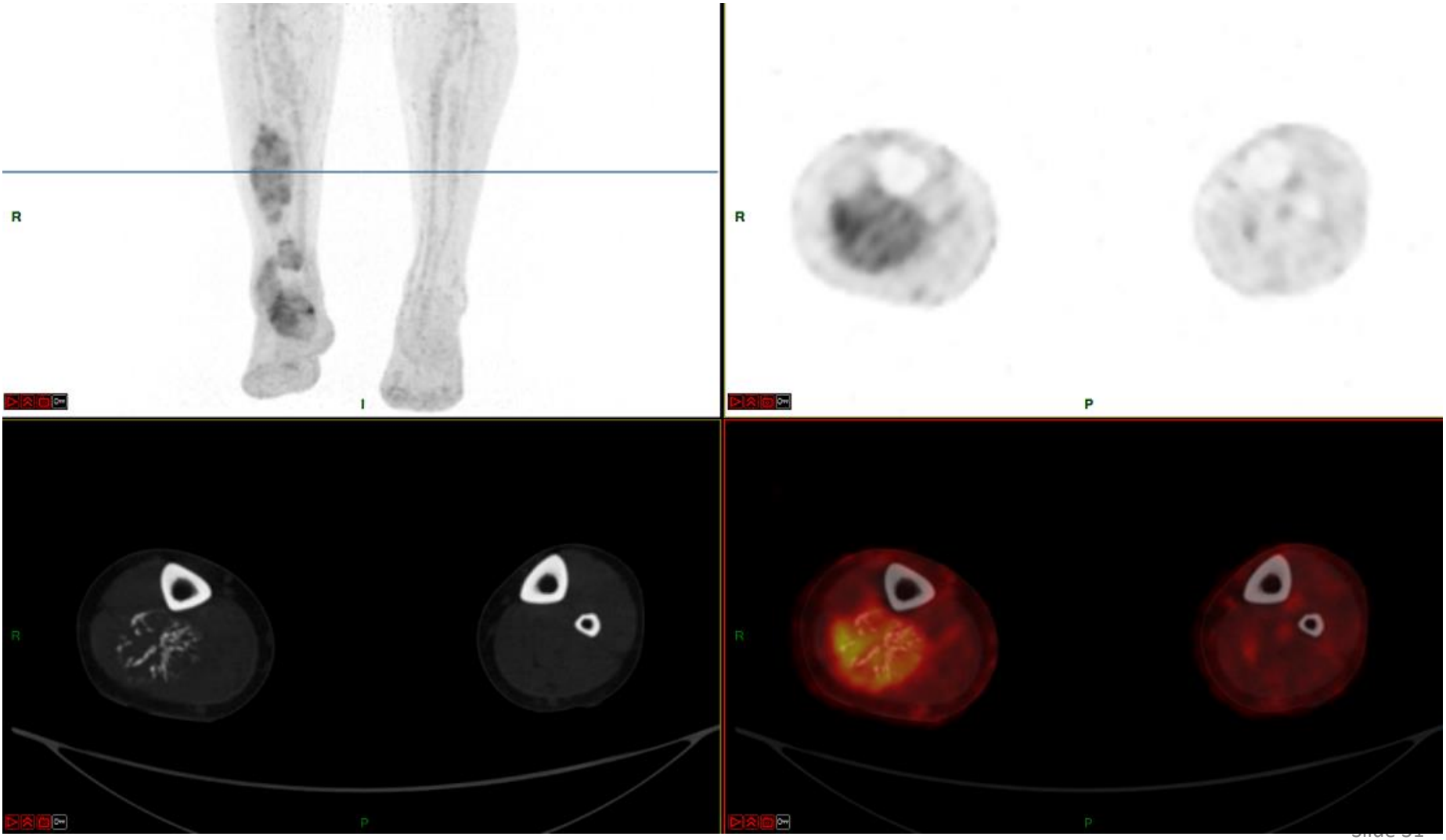

R leg arteriography

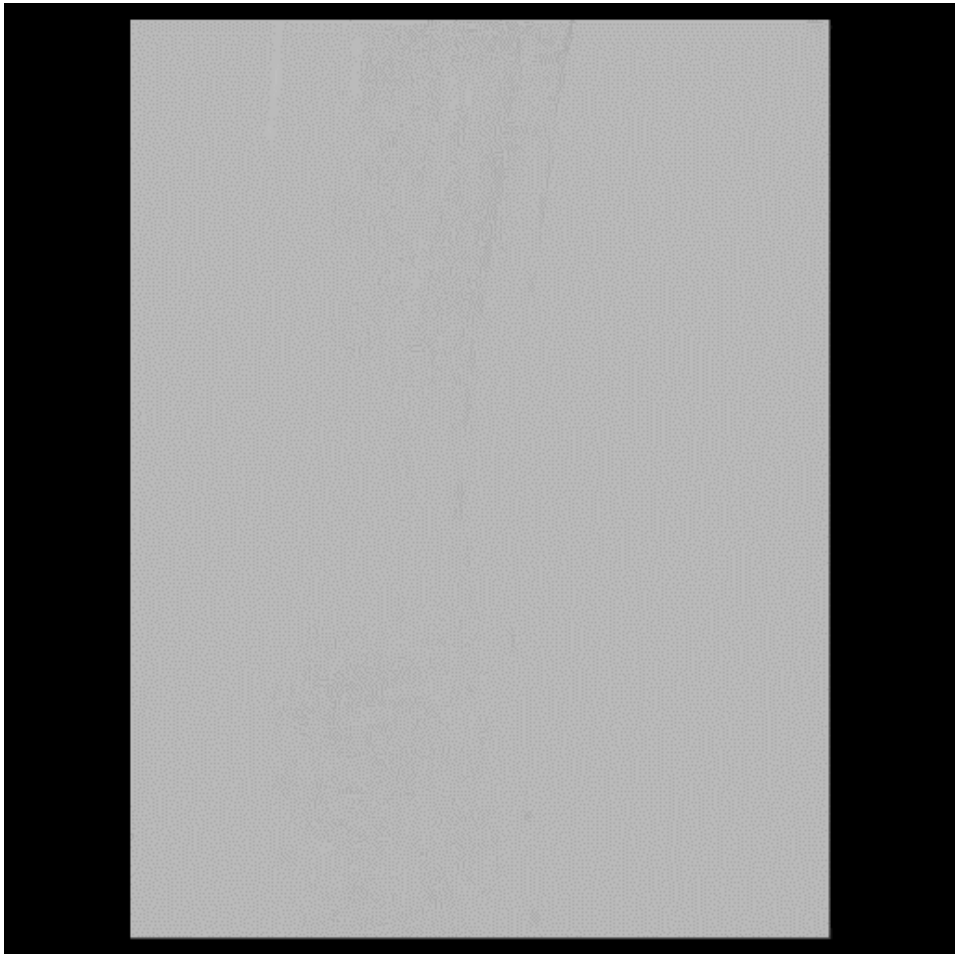

Diagnosis?

Epithelioid hemangioendothelioma

Summary of prognosis and treatment of vascular bone tumors

Classification	Entity	Prognosis	Treatment
Benign	Hemangioma	100% survival, 0% metastasis	Treat symptoms
Intermediate	Epithelioid hemangioma	100% survival, 2% metastases, 9% local recurrence	Curettage or marginal excision
	Pseudomyogenic hemangioendothelioma	Limited follow-up, stable or progressive osseous disease	
Malignant	Epithelioid hemangioendothelioma	85% survival, 25% metastases	Wide resection
	Angiosarcoma	30% survival	Wide resection, consider systemic therapy

DGP van Ijzendoorn, et al. Surgical Pathology 2017

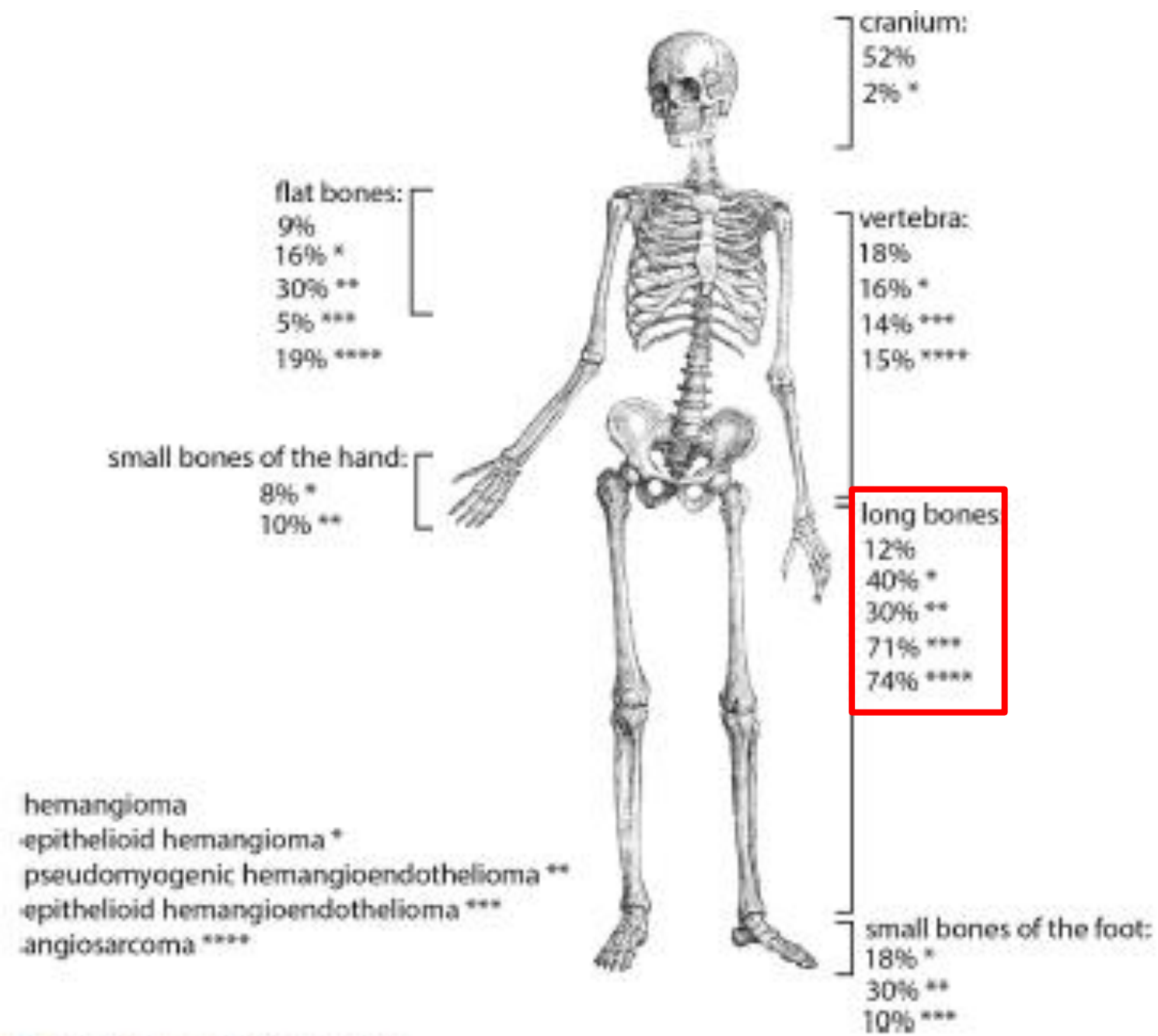

Fig. 1. Distribution of vascular tumors.

2. Age

Age

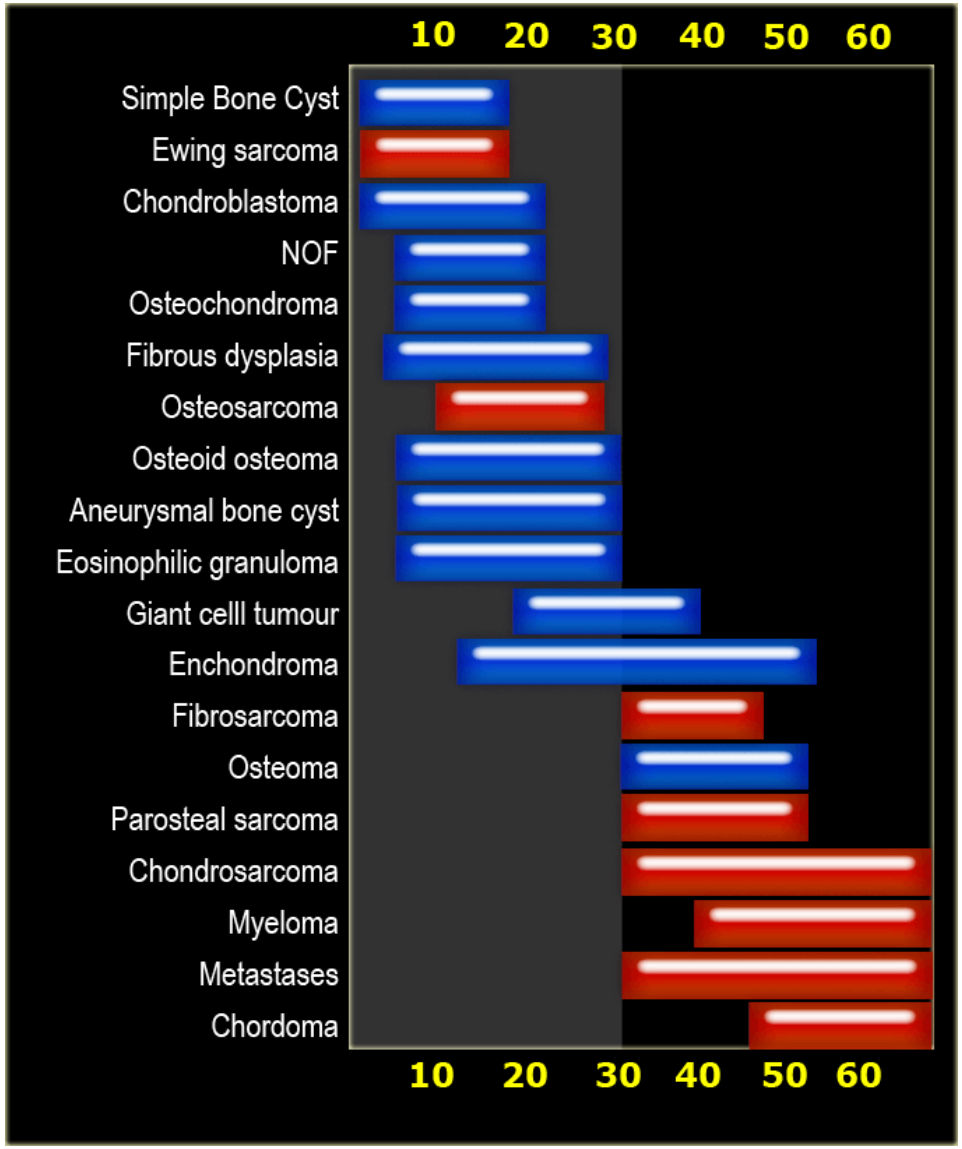
10
20
30
40
50
60
Simple Bone Cyst
Ewing sarcoma
Chondroblastoma
NOF
Osteochondroma
Fibrous dysplasia
Osteosarcoma
Osteoid osteoma
Aneurysmal bone cyst
Eosinophilic granuloma
Giant celll tumour
Enchondroma
Fibrosarcoma
Osteoma
Parosteal sarcoma
Chondrosarcoma
Myeloma
Metastases
Chordoma
10
20
30
40
50
60

3. Pain

Pain

First step: To rule out confusing origins of pain

1. May be related to pathological fracture
    1. Proximal metaphysis humerus: Bone simple cyst
    2. Proximal metaphysis femur: ABC, fibrous dysplasia, non ossifiying fibroma
    3. Phalanx: chondroma
2. Beware of referred pain

    Aching neighbouring osteoarthritic joint
3. NSAIDs diagnostic test
    1. Osteoid osteoma-related pain is, in rule, relieved by NSAIDs
    2. Osteoarthritis partially responds to NSAIDs
    3. Osteolytic metastasis partially responds to NSAIDs!

Second step: To assess tumor-related pain features

⇒ **Crucial role of the (Onco-)Rheumatologist**

5. Lytic/Sclerotic phenotype
+
Margins

Sclerotic/osteoblastic lesions

Sclerotic lesions

Analysis of sclerotic lesion

Tumoral sclerosis
(= Bone production by tumor)

Reactional sclerosis
(=Bone response to injury)

Cartilagineous type

Chondroïd matrix

- Chondroma ++ (enchondroma, periosteal chondroma)
- Chondrosarcoma centrale de faible degré de malignité
- Chondroblastoma

Osteochondroma

osteoid or osseous type

- OO
- OB
- OS
- Bone island
- Melorheostosis

Fibrous type

- Tumoral process (metastasis, Hodgkin's lymphoma, Ewing…)
- Infec$ous (osteomyeli$s)
- inflammatory process (SAPHO, psoriasic arthri$s)
- Degenera$ve (osteoarthri$s)
- Trauma$c (callus)
- Osteonecrosis

EF McCarthy, Semin Nucl Med 1997

Sclerotic lesions
List of lesions sorted by XR/CT hallmarks

- **Solitary sclerotic lesion**

  Metastasis - rarely solitary
  Lymphoma
  OO - cortical location with lucent nidus
  OB - similar to OO, but larger
  OS - aggressive periosteal reaction and new bone formation
  Osteoma - innocent
  Bone island - innocent
  FD - ground glass opacity
  Bone infarct - serpiginous
  Callus, healing fracture - compare with old films
  Sclerosing OM of Garré
  Paget's - bone expansion, thick coarse trabeculae
  Bone graft - well defined dense bone
  Melorheostosis - molten wax flowing down the burning candle, sclerotome, may have periosteal new bone formation

- **Solitary sclerotic lesion with lucent centre**
- OO
  OB
- Brodie's abscess
  TB

- **Sclerotic lesion with periosteal reaction**
- Healing fracture with callus
- Metastasis
  Lymphoma
  OO
- OB
  OS
- CS

- Melorheostosis

Uptake of sclerotic lesions on bone scintigraphy

- **Solitary sclerotic lesion**

Metastasis - rarely solitary
Lymphoma-Hodgkin
OO - cortical location with lucent nidus
OB - similar to OO, but larger
OS - aggressive periosteal reaction and new bone formation
Osteoma - innocent
Bone island - innocent
FD - ground glass opacity
Bone infarct - serpiginous
Callus **healing fracture** - compare with old films
Sclerosing OM of Garré
Paget's - bone expansion, thick coarse trabeculae
Bone graft - well defined dense bone
Melorheostosis - molten wax flowing down the burning candle, sclerotome, may have periosteal new bone formation

No uptake

Uptake of sclerotic lesions on bone scintigraphy

- **Solitary sclerotic lesion**

Metastasis rarely solitary
Lymphoma-Hodgkin
OO - cortical location with lucent nidus
OB - similar to OO, but larger
OS aggressive periosteal and new bone formation
Osteoma - innocent
Bone island innocent
FD - ground glass opacity
Bone infarct - serpiginous
Callus **healing fracture** - compare with old films
Sclerosing OM of Garré
Paget's - bone expansion, thick coarse trabeculae
Bone graft - well defined dense bone
Melorheostosis - molten wax flowing down the burning candle, sclerotome, may have periosteal new bone formation

Malignant

No uptake

Non-malignant harmful

Sclerotic metastases
Vargas classification

Sclerotic subtypes: Images

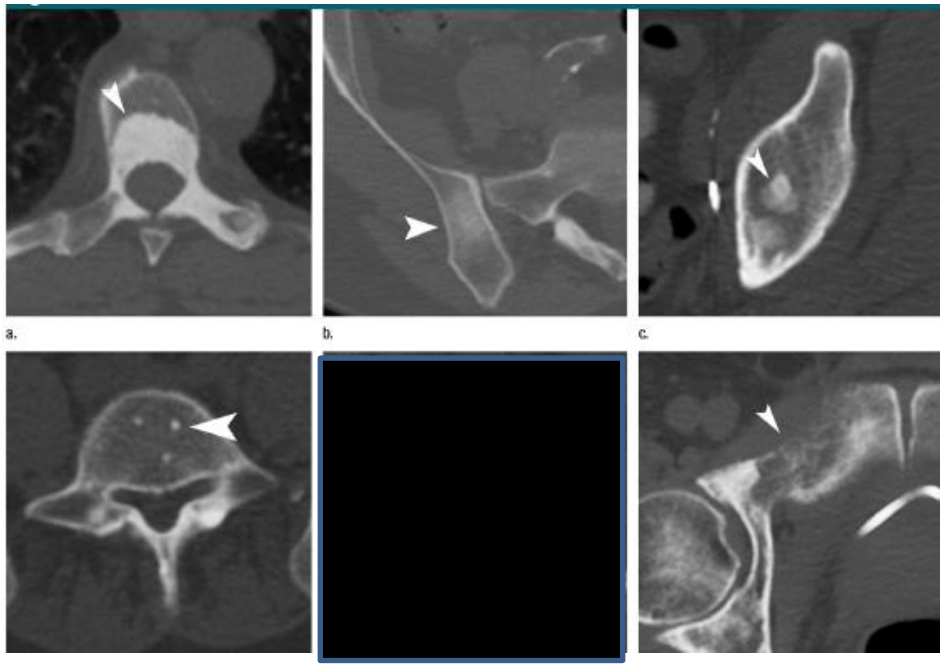

Sclerotic subtypes: Typology

- *(a)* osteoblastic dense areas
- (*b)* osteoblastic ground glass
- *(c)* osteoblastic mixed
- *(d)* osteoblastic miliary
- *(e)* mixed osteolytic and osteoblastic

Bone Metastases in Castration-Resistant Prostate Cancer: Associations between Morphologic CT Patterns, Glycolytic Activity, and Androgen Receptor Expression on PET and Overall Survival[1]

Radiology, 2014

Présentation clinique

- Homme 53 ans
- Bilan d'extension initial d'un adénocarcinome prostatique
- Score de Gleason : 7 (3+4)
- PSA total : 7,3 ng/mL
- Dorso-lombalgies
- TEMP-TDM au BP-(99mTc)

Scintigraphie HMDP 99mTc planaire et TEMP/TDM

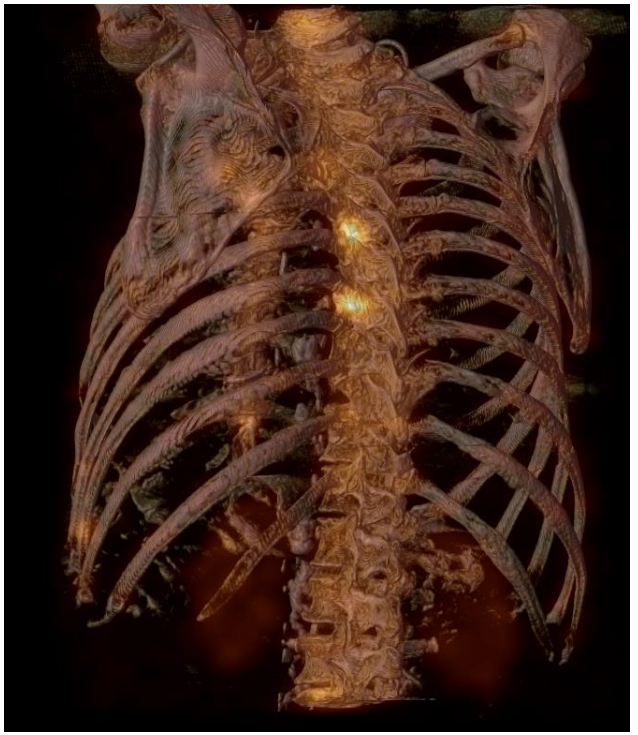

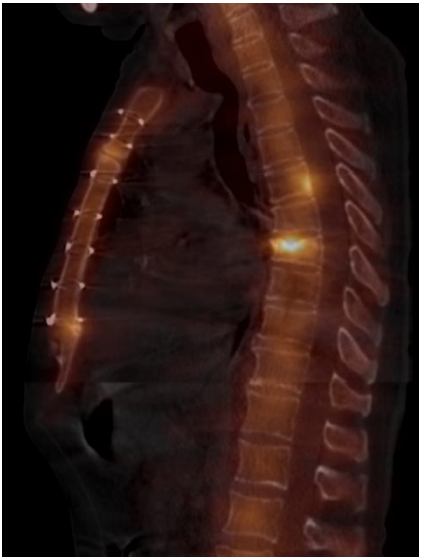

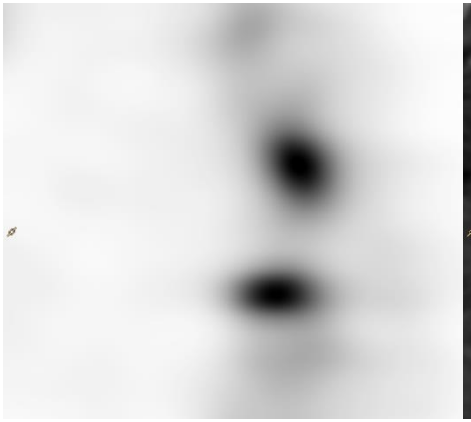

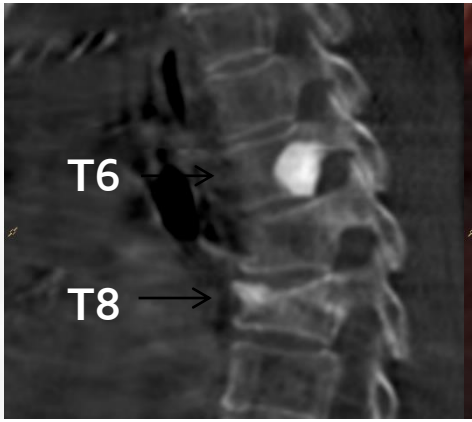
T6
T8

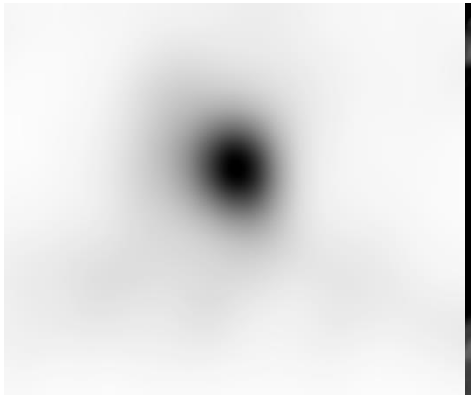

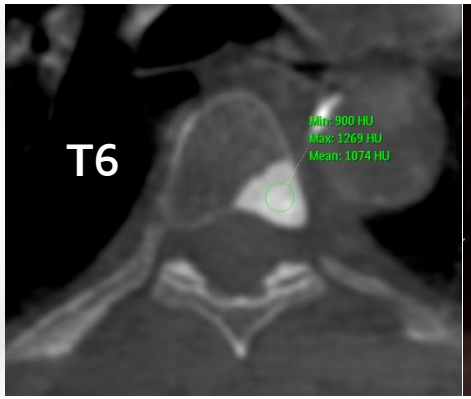
T6
Min: 900 HU
Max: 1269 HU
Mean: 1074 HU

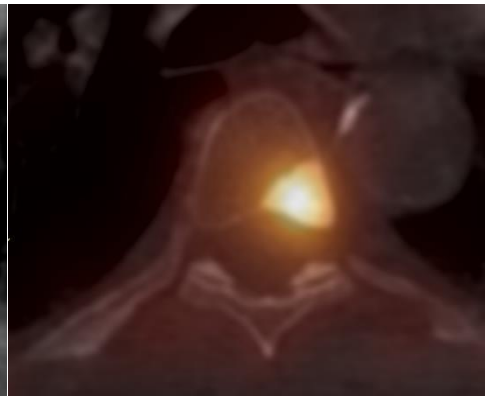

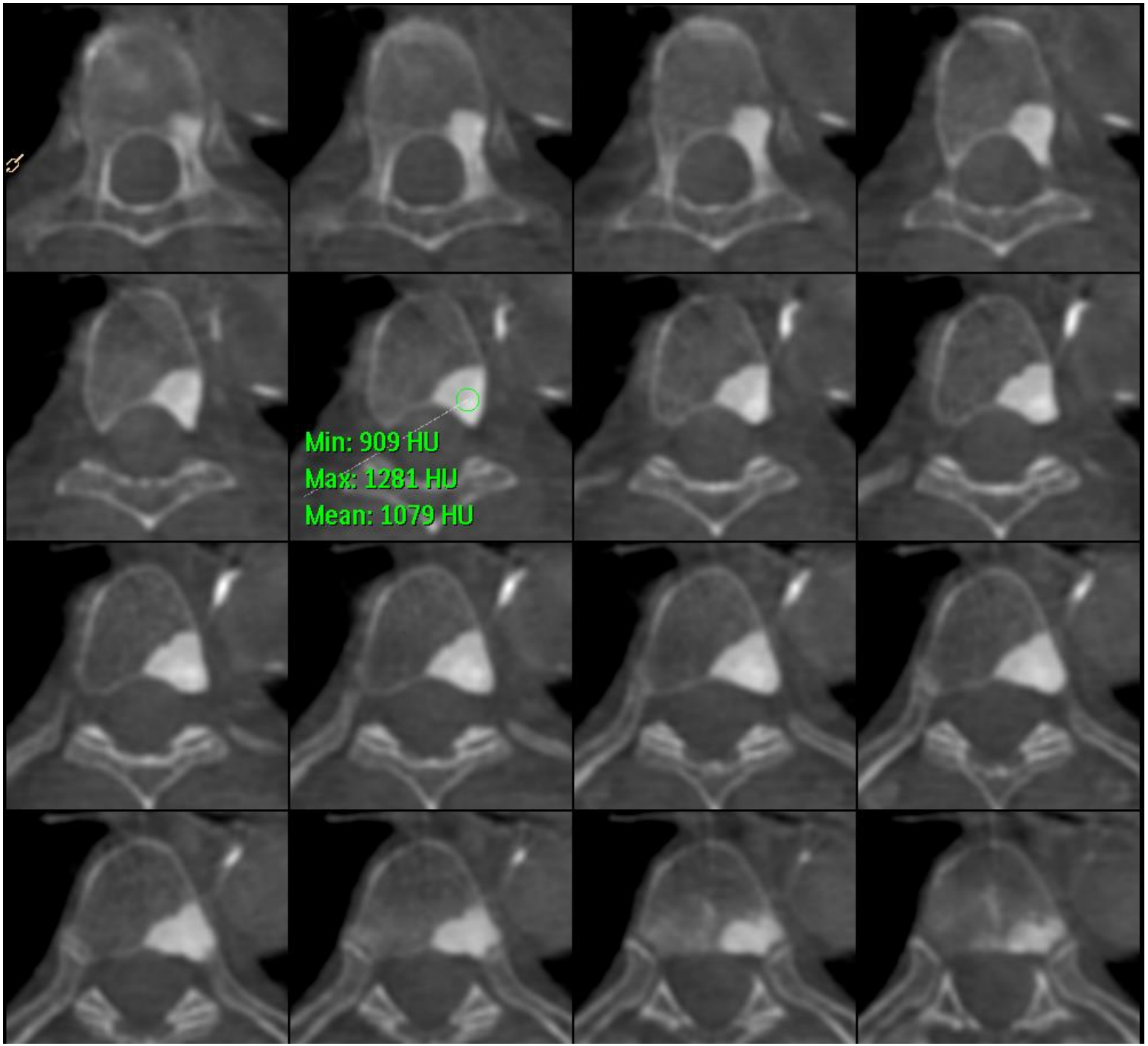
Min: 909 HU
Max: 1281 HU
Mean: 1079 HU

Suivi scintigraphique à 2 ans
Réascension du PSA total à 6 ng/mL

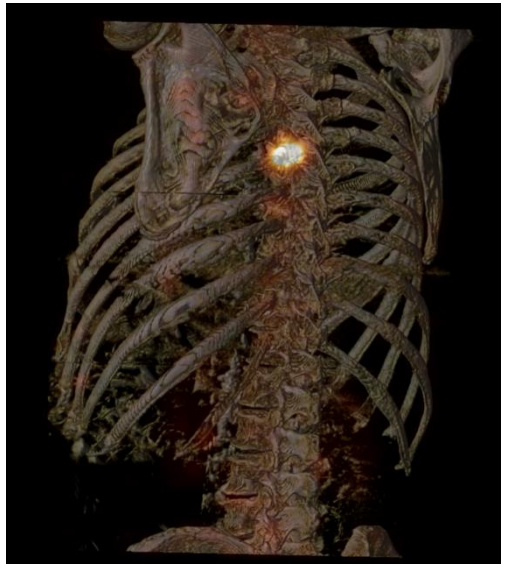

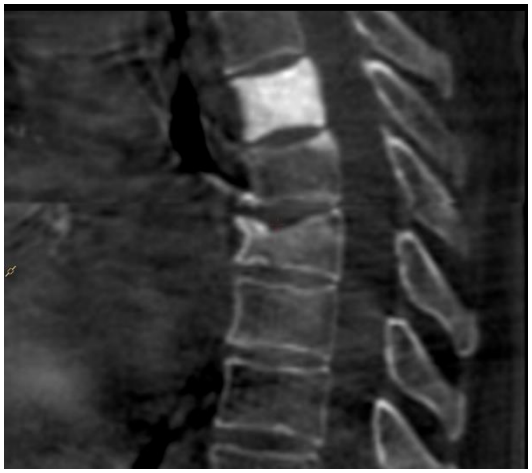

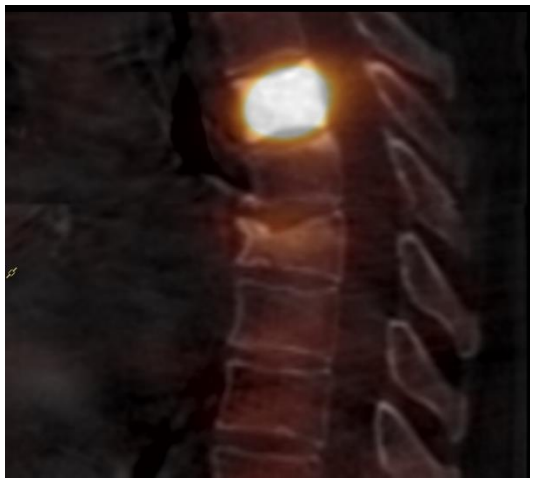

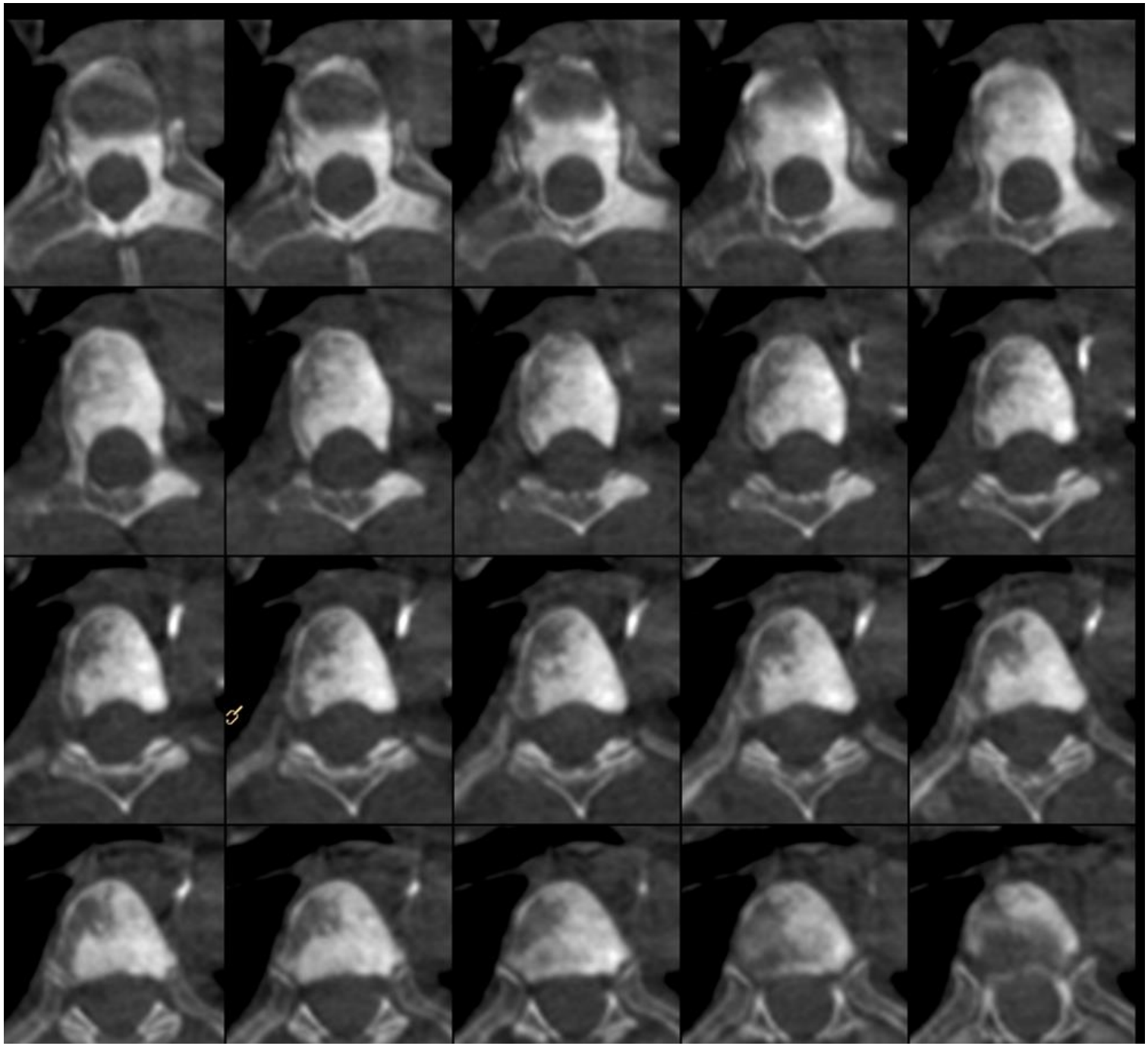

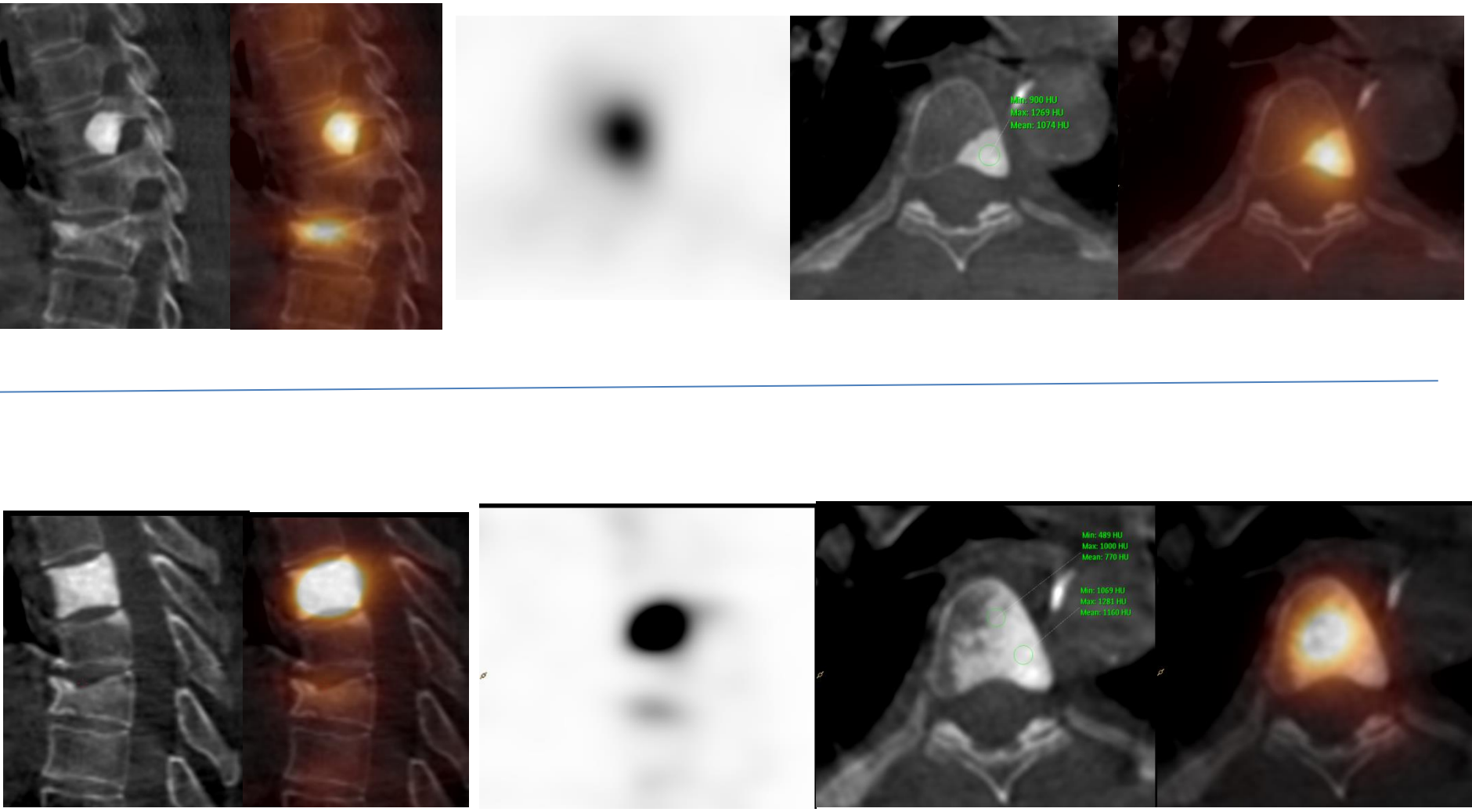

Métastase condensante à présentation pseudo-ilôt condensant bénin
Evolution vers la configuration de vertèbre ivoire

Lytic/osteoclastic lesions

Lodwick classification

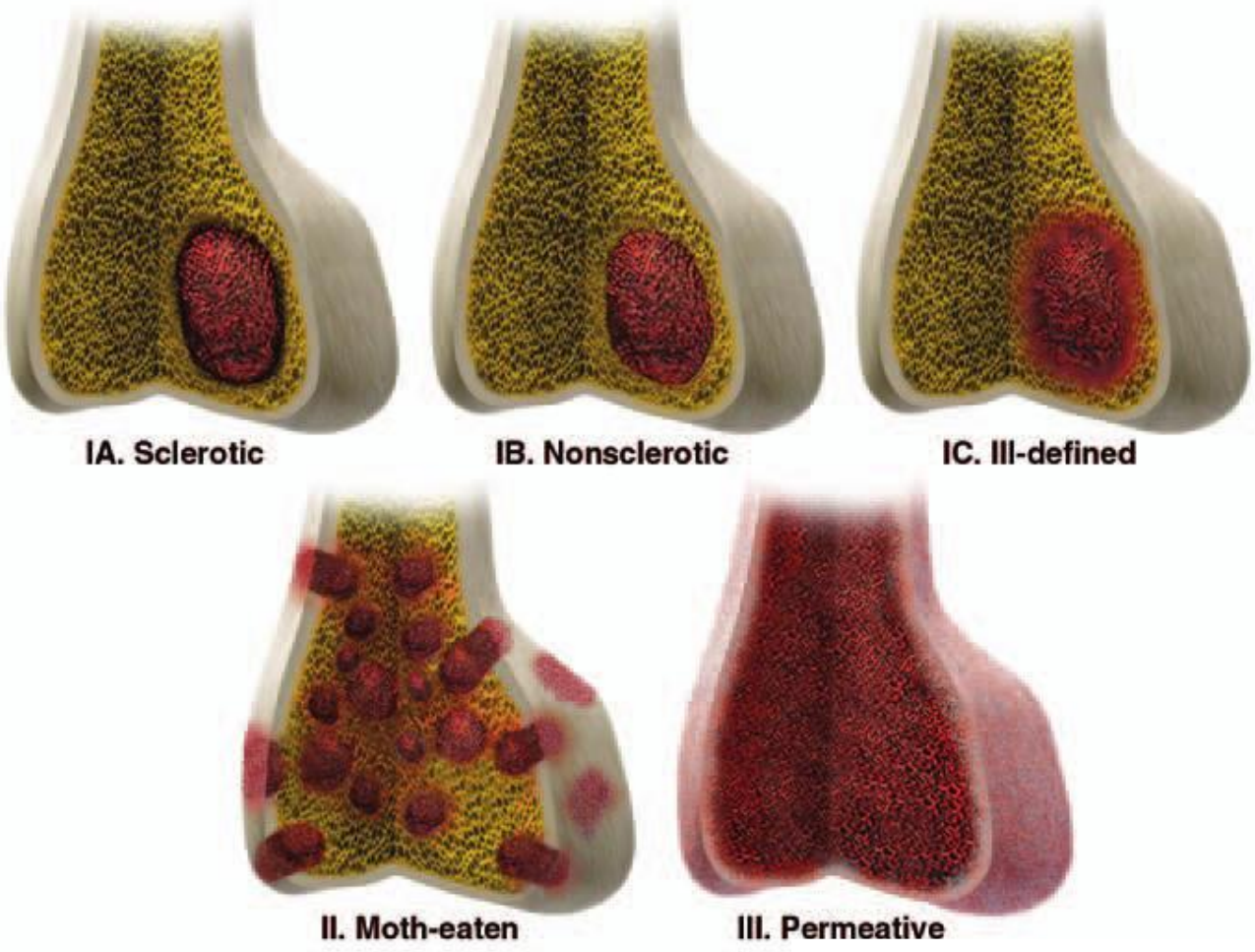

Geographic osteolysis

Lodwick type I

Type 1 A: osteolysis with clearcut borders + sclerosis rim (essential cyst)

Type 1 B: osteolysis with clearcut borders w/o sclerosis rim (cortical defect)

Type 1 C: osteolysis with fuzzy borders (osteomyelitis)

Radiography in the Initial Diagnosis of Primary Bone Tumors

Colleen M. Costelloe[1]
John E. Madewell

AJR, Janvier 2013

Radiography is the optimal initial imaging modality for evaluating undiagnosed primary bone tumors. The advantage of radiographic technique is to collapse the density of all points in the imaging plane into a 2D image. The resulting unique anatomic information allows the efficient evaluation of characteristics that reflect the biologic activity or growth rate of primary bone tumors, such as lesion margins, periosteal reaction, cortical expansion, thinning, and destruction.

Lodwick classification (C't'd)

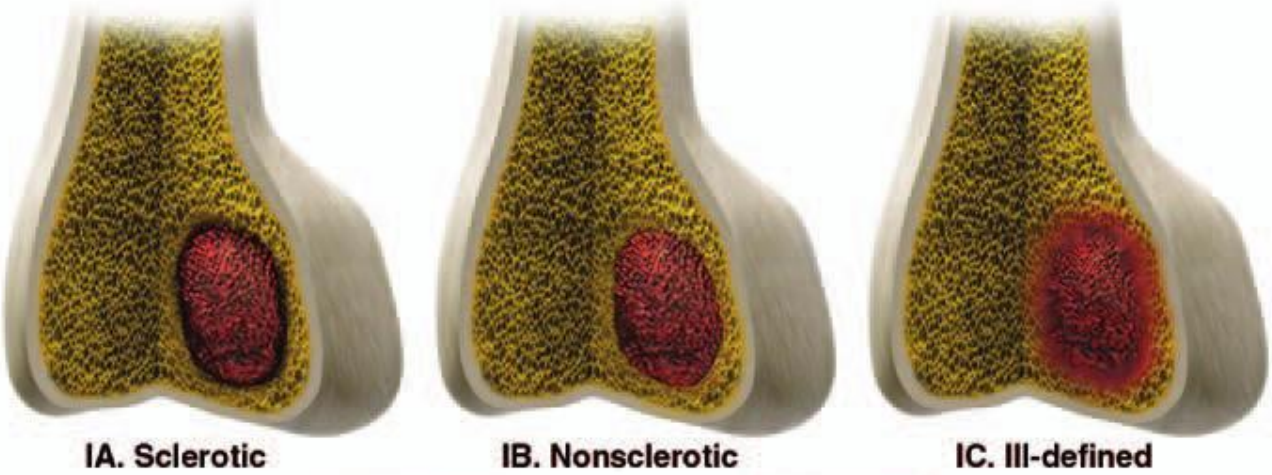

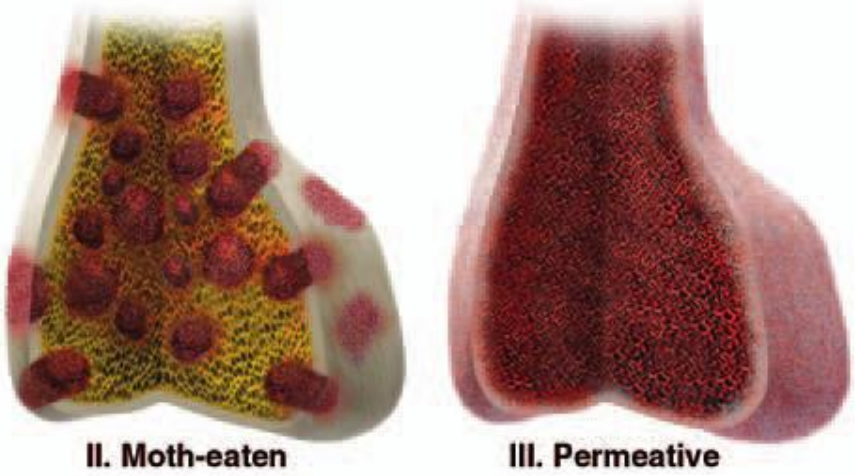

Type 2
Moth-eaten lesion

Type 3
Permeated lytic lesion

Radiography in the Initial Diagnosis of Primary Bone Tumors

Colleen M. Costelloe[1]
John E. Madewell

AJR, Janvier 2013

Radiography is the optimal initial imaging modality for evaluating undiagnosed primary bone tumors. The advantage of radiographic technique is to collapse the density of all points in the imaging plane into a 2D image. The resulting unique anatomic information allows the efficient evaluation of characteristics that reflect the biologic activity or growth rate of primary bone tumors, such as lesion margins, periosteal reaction, cortical expansion, thinning, and destruction.

Lodwick classification
Diagnostic orientation

	IA	IB	IC	II	III
Infection	X	X	X	X	X
Metastasis		X	X	X	X
Chondrosarcoma Fibrosarcoma	X	X	X	X	X
Ewing sarcoma Osteosarcoma			X	X	X
Osseous cyst Fibrous dysplasia Non ossifying fibroma	X	X			
Giant cell tumor Aneuvrismal bone cyst		X	X	X	
Langerhans cell histiocytosis	X	X	X	X	

Madewel, Radiol Clin North Am 1981
Radiologic and pathologic analysis of solitary bone lesions. Part I. Internal margins

A Modified Lodwick-Madewell Grading System for the Evaluation of Lytic Bone Lesions

Jamie T. Caracciolo[1]
H. Thomas Temple[2]
G. Douglas Letson[3]
Mark J. Kransdorf[4]

OBJECTIVE. Lodwick's well-established grading system of lytic bone lesions has been widely used in predicting growth rate for lytic bone lesions. We applied a Modified Lodwick-Madewell Grading System as an alternative means to categorize lytic bone tumors into those with low, moderate, and high risks of malignancy.

MATERIALS AND METHODS. A retrospective review of the radiographs of 183 bone lesions was performed. Cases were selected to include a broad range of benign and malignant tumors. Readers applied our Modified Lodwick-Madewell Grading System, and consensus was reached in all cases. This modified system consists of grade I, which is composed of grades IA and IB as listed in the Lodwick system; grade II, which is grade IC in the Lodwick system; and grade III, which is composed of IIIA (changing margination), IIB (moth-eaten and permeative patterns), and IIIC (radiographically occult). Grading was correlated with the final diagnosis.

RESULTS. Of the 183 tumors, 81 were classified as grade I, 54 as grade II, and 48 as grade III. When correlating grade with pathology, we found that 76 of 81 (94%) grade I lesions were benign and 39 of 48 grade III lesions (81%) were malignant. A nearly equal number of grade II lesions proved to be benign (29/54; 54%) and malignant (28/54; 53%).

CONCLUSION. By expanding Lodwick's grading system to include two additional patterns of disease described by Madewell and colleagues (changing margination and radiographically occult) and by reclassifying them into three distinct grades, we propose a modified system—the Modified Lodwick-Madewell Grading System. Application of this system shows correlation of tumor grade with tumor biologic activity and with risk of malignancy: Grade I lesions are usually benign, grade II lesions carry moderate risk of malignancy, and grade III lesions possess a high likelihood of malignancy.

AJR 2016; 20: W1-W7

Modified Lodwick-Madewell classification Rationale

TABLE 1: Modified Lodwick-Madewell Grading System

Grade	Description	Comment
IA	Well-defined geographic lytic lesion with a sclerotic rim	Slow-growing or indolent lesion; typically benign
IB	Well-defined geographic lytic lesion with a sharp margin without a sclerotic rim	Most lesions are benign, although differential diagnosis may include metastatic disease and myeloma
II[a]	Geographic lytic lesion with partial or circumferential ill-defined margins	Some benign causes, but differential diagnosis should include malignancy
IIIA[b]	Focal change in margin, changing margination, or progressive endosteal scalloping on serial radiographs	Focal changes or changes over time indicate increased biologic activity and should raise suspicion for malignancy
IIIB[c]	Moth-eaten and permeative patterns of osteolysis (nongeographic osteolysis)	Scattered and confluent holes in bone giving the impression of arising from multiple foci or innumerable tiny areas of bone destruction that fade imperceptibly from completely normal bone to markedly abnormal bone
IIIC[d]	Radiographically occult	Normal or near-normal radiographic findings; lesion is seen on advanced imaging such as MRI or PET

- Bone scan +
- PET +
- MRI +
- Bone biopsy +

SPECT classification of osteolytic/osteoclastic lesions

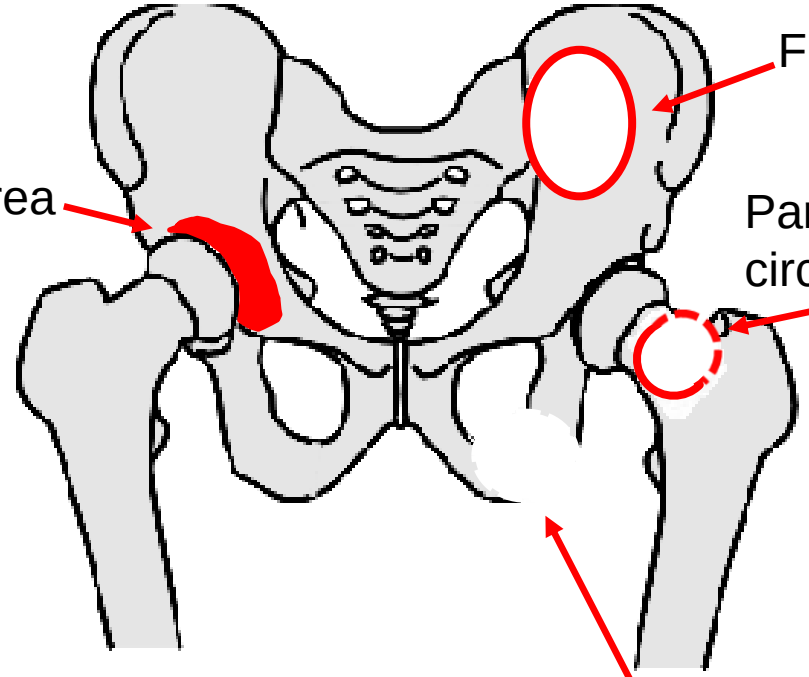

Full rim of increased uptake circumscribing cold spot

Hot spot filling lytic area ("FDG-like pattern")

Partial rim of increased uptake circumscribing cold spot

No or faint rim of increased uptake punched-out cold spot

Paycha F & Girma A, Méd Nucl 2011; 35: 332–335

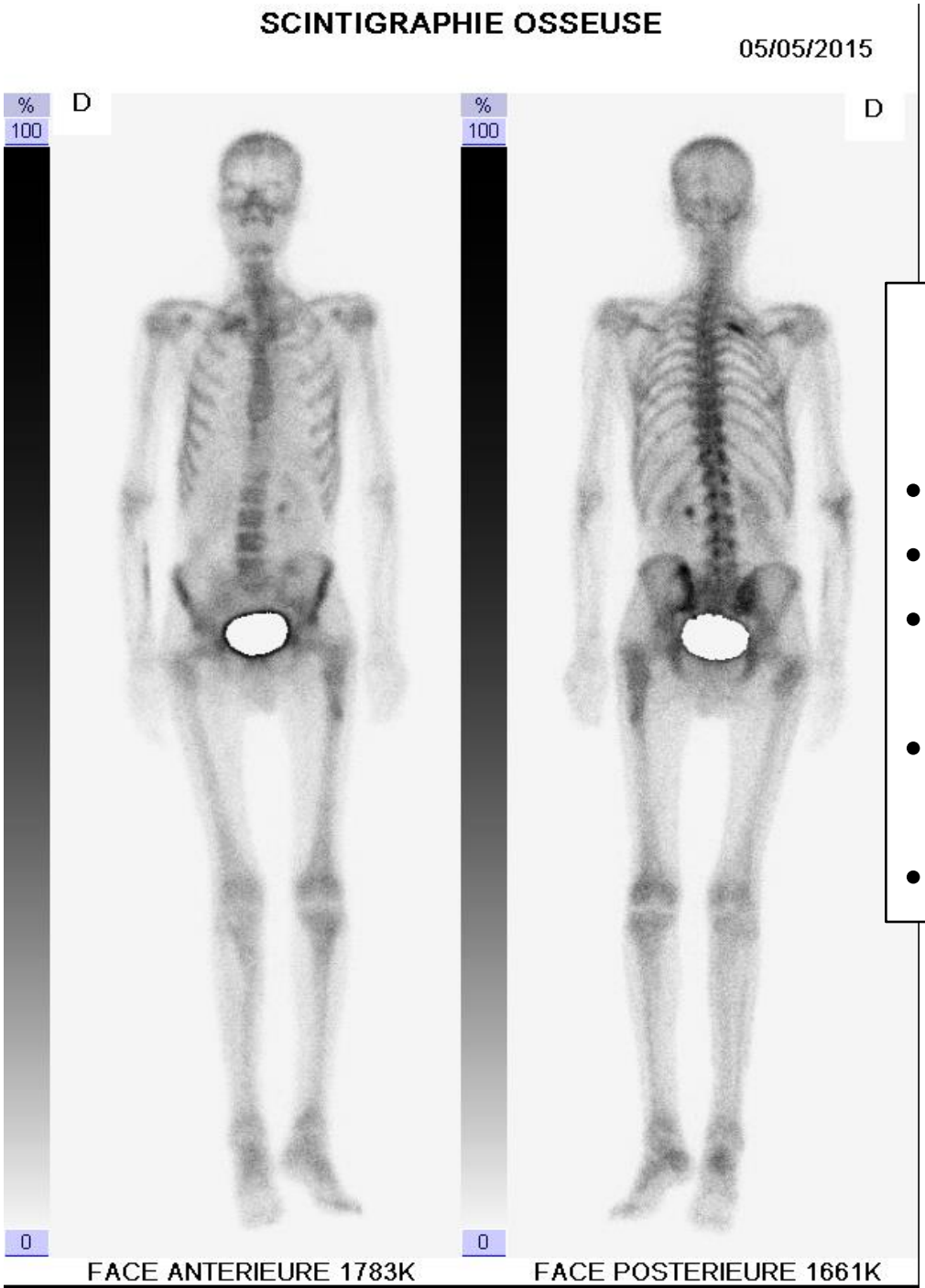

Clinical presentation

- M, 65 yo
- NSCLC L upper lobe T2aN3 M1b
- Lytic metastases 3rd L rib, prox. epi-meta-diaphyseal L femur
- Onset of L buttock pain 1 month ago
- Pelvis MDCT: Normal

SPECT+/CT- pattern?

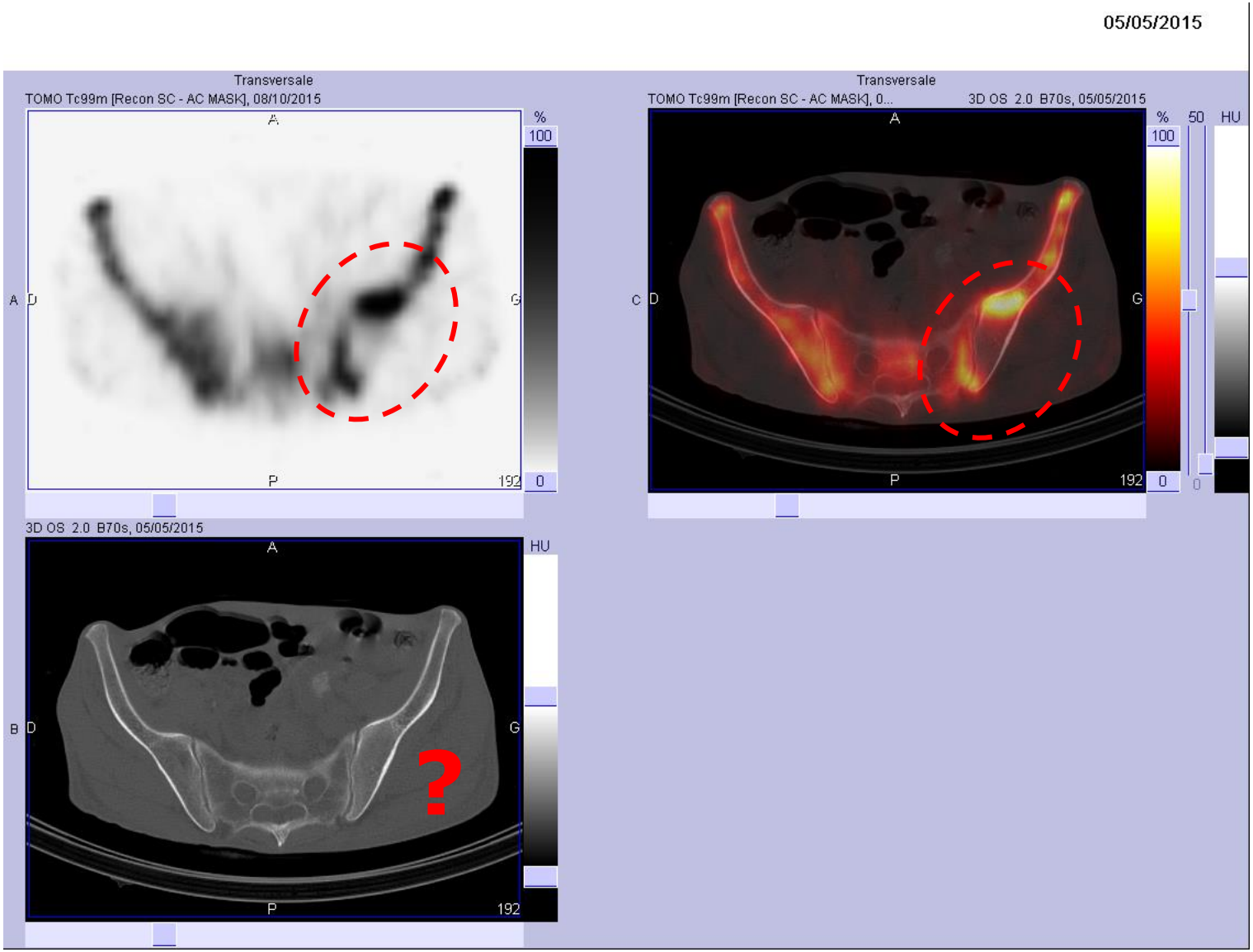

SPECT+/CT-/MRI+ pattern!

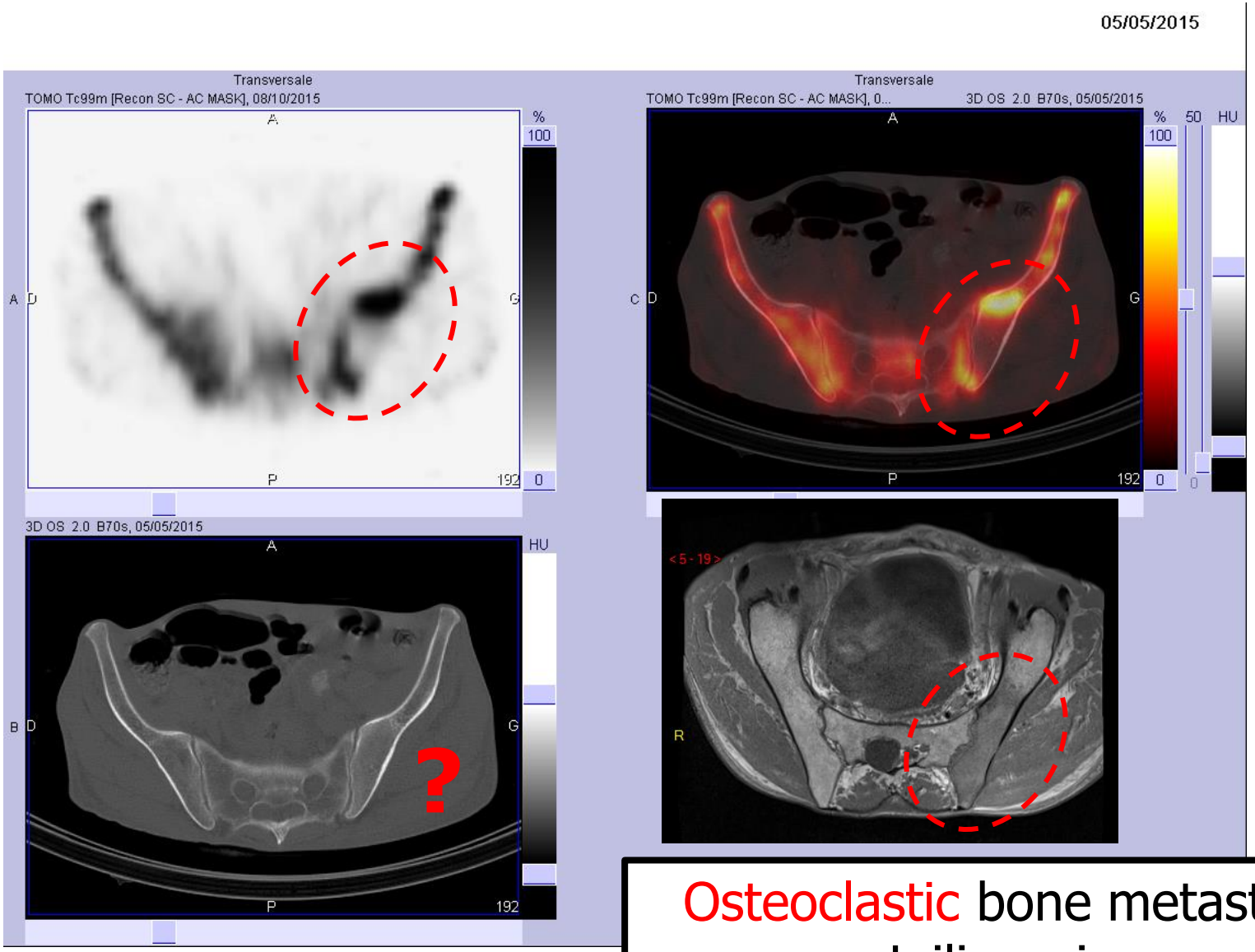

Osteoclastic bone metastasis
L iliac wing

Lytic bone lesions
RX/CT appearance

Differential Diagnosis of Solitary Lucent Bone Lesions

- **Fibrous Dysplasia (FD)**
- **Osteoblastoma**
- **Giant Cell Tumor**
- **Metastasis / Myeloma**
- **Aneurysmal Bone Cyst (ABC)**
- **Chondroblastoma / Chondromyxoid Fibroma**
- **Hyperparathyroidism (brown tumors) / Hemangioma / Hydatid cyst**
- **Infection**
- **Non-Ossifying Fibroma (NOF)**
- **Eosinophilic Granuloma (aka HCL) / Enchondroma**
- **Solitary Bone Cyst**

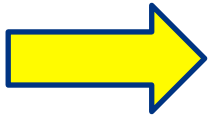

Mnemonic :
FOGMACHINES

Lytic bone lesions
Scintigraphic appearance

Differential Diagnosis of Solitary Lucent Bone Lesions

- **Fibrous Dysplasia**
- **Osteoblastoma**
- **Giant Cell Tumor**
- **Metastasis / Myeloma**
- **Aneurysmal Bone Cyst**
- **Chondroblastoma / Chondromyxoid Fibroma**
- **Hyperparathyroidism (brown tumors) / Hemangioma / Hydatid cyst**
- **Infection**
- **Non-ossifying Fibroma**
- **Eosinophilic Granuloma (aka LCH)/ Enchondroma**
- **Solitary Bone Cyst**

No uptake

Dorsalgie inflammatoire révélant une vertèbre évidée

Présentation clinique

- F, 48 ans
- Juillet 2017 : Survenue de douleurs vertébrales interscapulaires lors d'une course à pied, d'aggravation rapidement progressive, avec crises douloureuses durant 1 mois puis douleurs s'amendant partiellement
- Réveils nocturnes
- Dérouillage matinal: 1h30
- Douleurs partiellement calmées par les antalgiques de palier 2
- A l'examen: EVA 5-6/10
- Pas d'AEG (pas d'asthénie, pas de perte de poids, pas de fièvre, pas de sueurs nocturnes)
- ATCD: WPW traité par radiofréquence en 2012, capsulite de l'épaule bilatérale, D en 2011 puis G en 2016, traitée par kinésithérapie, fracture traumatique du carpe D ostéosynthésée en 2010
- Pas d'intoxication alcoolo-tabagique

Bilan biologique

- NFS: RAS
- CRP = 2 mg/L
- Electrophorèse des protéines sériques normale
- Calcémie et phosphorémie normales
- Fonction rénale et enzymes hépatiques: RAS

IMAGERIE

TDM du rachis cervico-dorso-lombaire

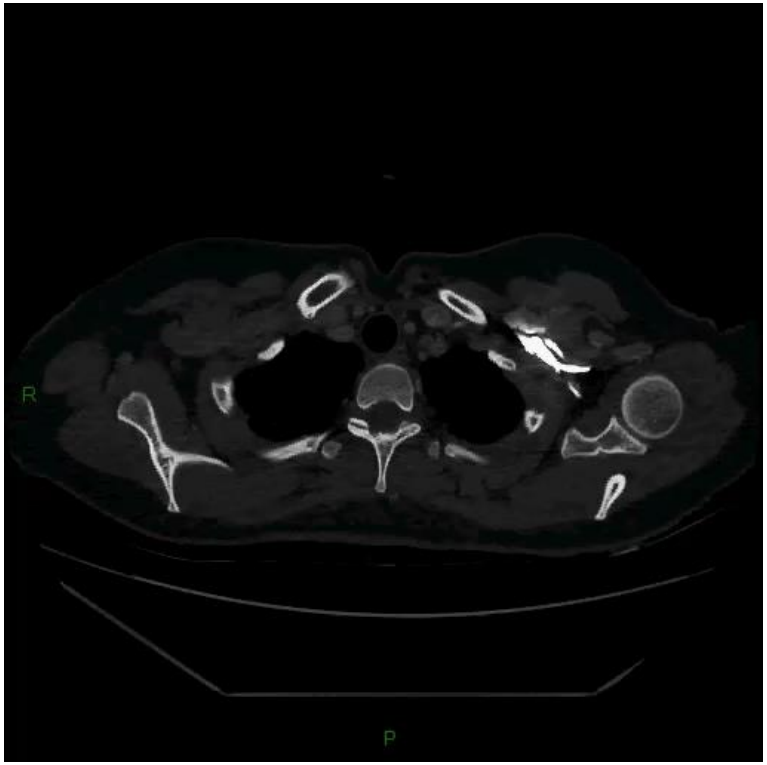

TEP/TDM au FDG
Rachis

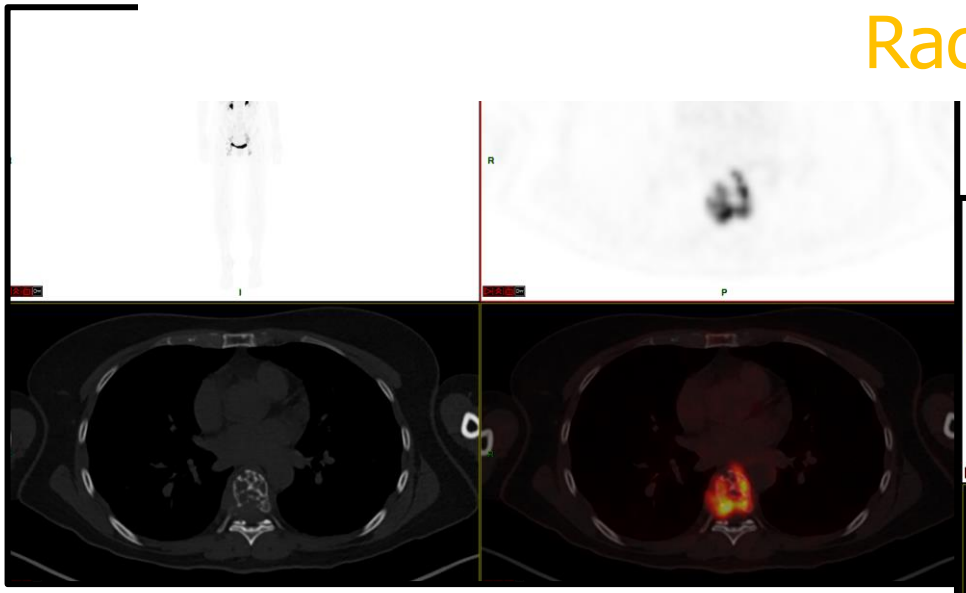

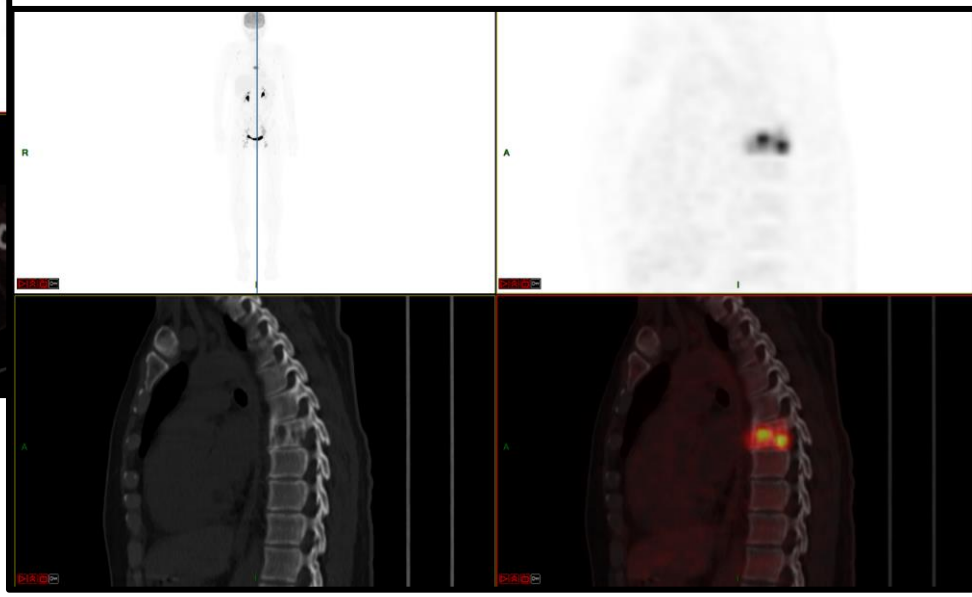

Lésion de T7 intensément hypermétabolique (SUVmax = 21)

Diagnostic ?

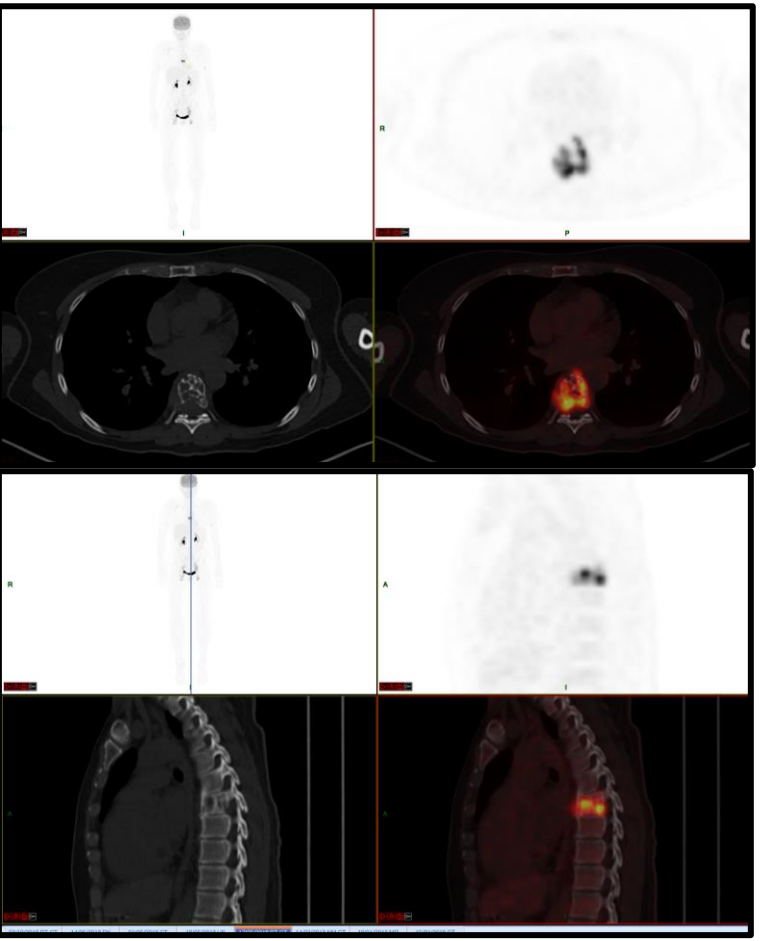

1. Métastase ostéolytique
2. Myélome/plasmocytome
3. Lymphome
4. Hémangiome vertébral
5. Histiocytose langerhansienne
6. Infarctus vertébral

TEP/TDM au FDG
Aires inguinales

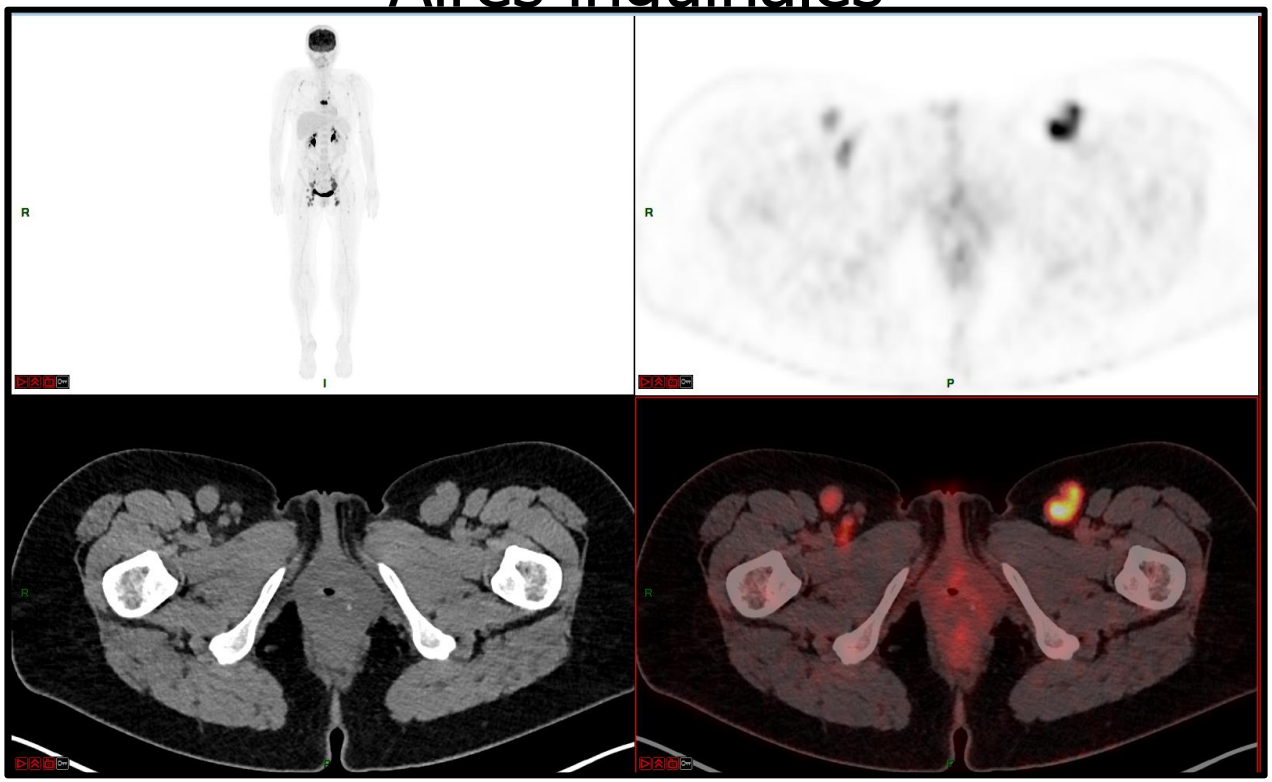

Polyadénomégalie (en règle supracentimétrique) hypermétabolique (en règle SUVmax ≥ 5) des chaînes
sus-claviculaires, axillaires, mammaires internes, pelviennes et inguinales bilatérales associées à la lésion de T7 intensément hypermétabolique (SUVmax = 21)

Diagnostic (bis) ?

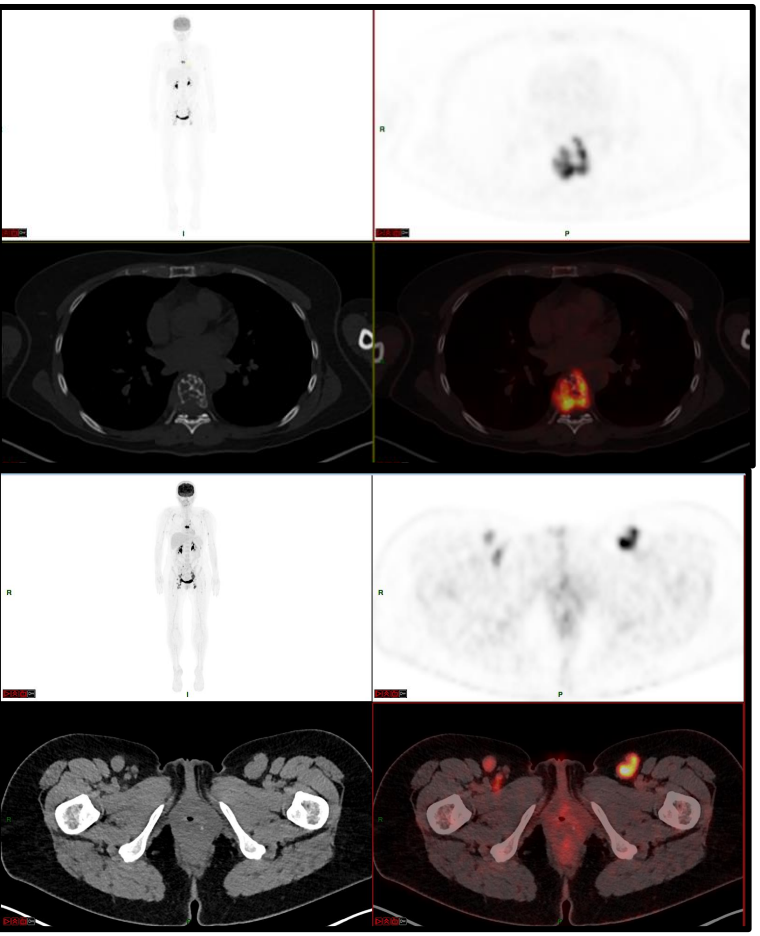

1. Métastase ostéolytique
2. Myélome/plasmocytome
3. Lymphome
4. Hémangiome vertébral
5. Histiocytose langerhansienne
6. Infarctus vertébral

Quelle est la procédure diagnostique à suivre ?

1. IRM corps entier
2. Myélogramme par ponction sternale
3. Biopsie ostéo-médullaire sternale
4. Biopsie ECT-guidée d'une adénopathie inguinale
5. Biopsie sous TDM de la lésion de T7

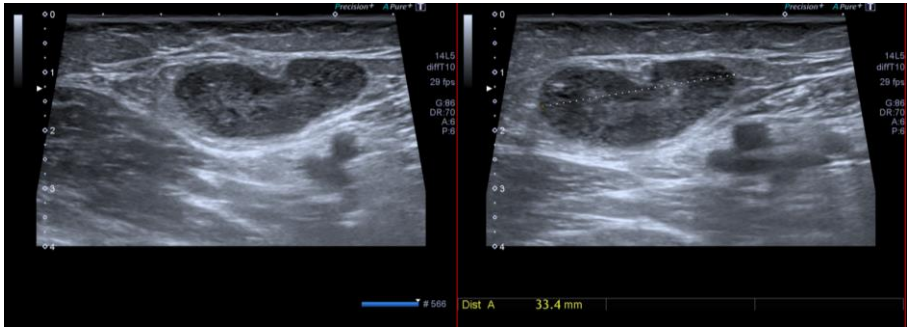

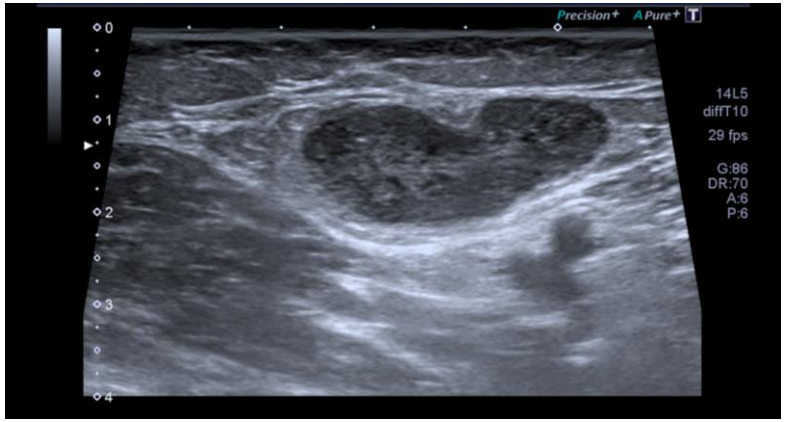

Diagnostic anatomo-pathologique sur biopsie adénopathie inguinale G

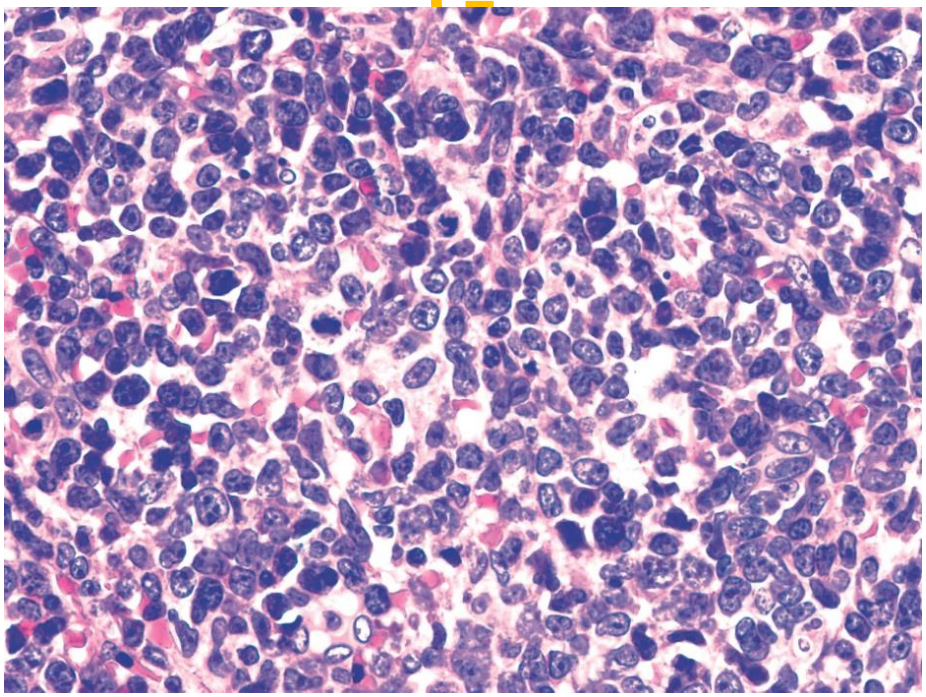

Morphologie et expression les cellules folliculaires de BCL2+ CD10+ BCL6+ sont en faveur d'un **lymphome folliculaire**

DISCUSSION

SPECT/CT osseuse: hypofixation vertébrale diffuse (vertèbre froide) Gamme diagnostique

- Métastase ostéolytique
- Myélome/plasmocytome
- Lymphome
- Hémangiome vertébral
- Histiocytose langerhansienne
- Infarctus vertébral

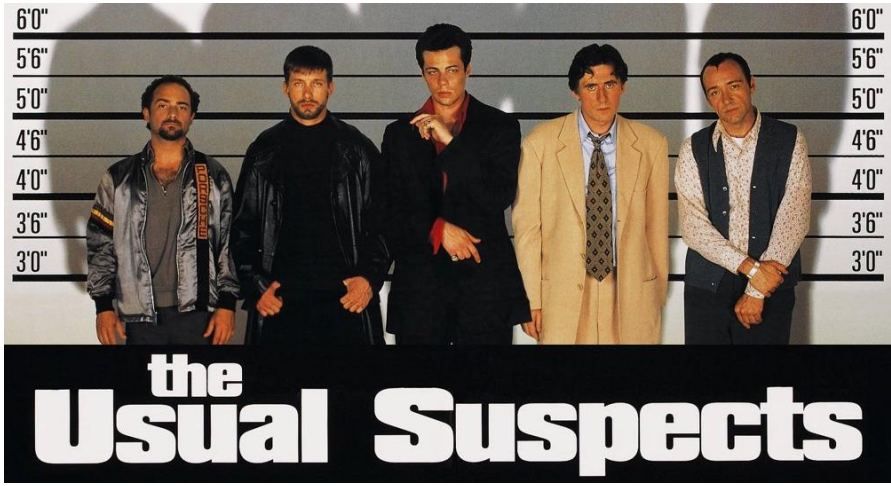

LW Bassett. AJR 1981; 136: 129-131

Tumeurs à cellules rondes : Des tumeurs « passe-muraille »

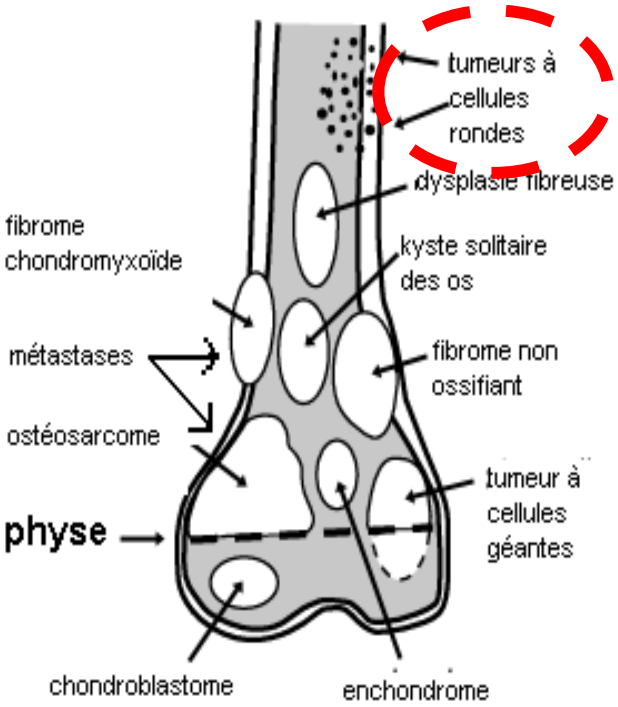

Madewell JE, et al. Radiol Clin North Am 1981

- Lymphomes
- Neuroblastome
- Sarcome d'Ewing/PNET
- Rhabdomyosarcome
  - Chondrosarcome mésenchymateux
  - Médulloblastome
  - Synovialosarcome dédifférencié
  - Ostéosarcome à petites cellules

Li S, et al. Adv Anat Pathol 2010

Physiopathologie, histoire naturelle, imagerie

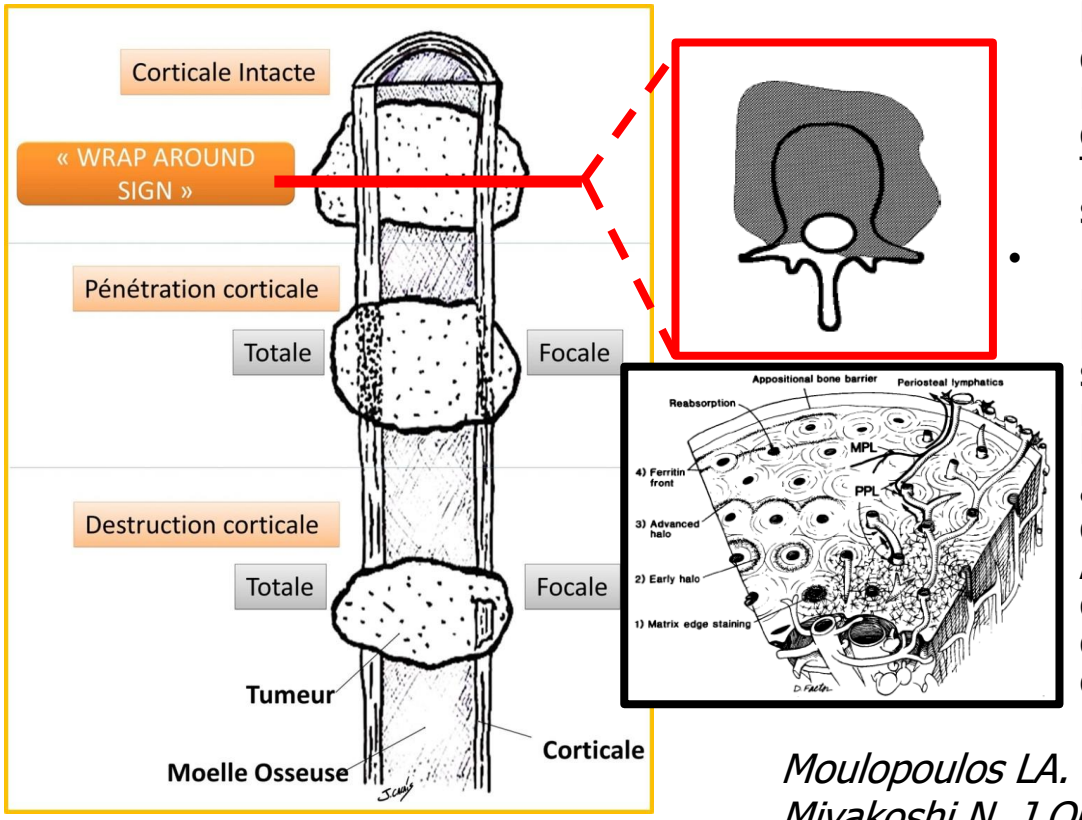

- La TDM est ici prise en défaut en raison d'un envahissement osseux par dissémination hématogène ou par contiguïté mais à destruction trabéculaire minime et sans rupture corticale, typique du lymphome, alors que l'imagerie métabolique SPECT osseuse et TEP revêt une sensibilité lésionnelle supérieure
- Les tableaux radiologiques tirent leurs phénotypes des 2 caractéristiques de l'envahissement osseux par le lymphome : soit par contiguïté, auquel cas il existe une rupture corticale, soit par dissémination hématogène, auquel cas la corticale est amincie et repoussée (« soufflée ») mais demeure intacte pour une longue période
A l'extrême, la tumeur peut perforer la corticale sans la détruire et se présenter comme une masse des partie molles enveloppant la pièce osseuse:

Wrap around pattern

Moulopoulos LA. Leukemia & lymphoma 1999;34(1-2):179-84
Miyakoshi N. J Orthop Sci 2003; 8:207–212
Jeong SY. Korean J Lab Med 2007;27:383-7

Plasmocytome/Myélome/Lymphome
Aspect TDM

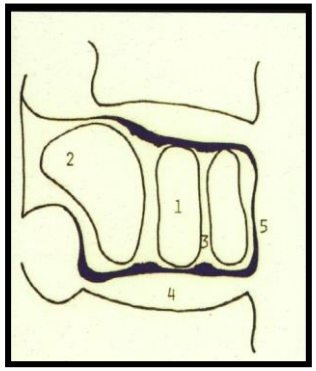

1. Amande ostéolytique a grand axe vertical
2. Pédicule évidé
3. Cloisons denses verticales compartimentant l'ostéolyse
4. Plateaux vertébraux condensés
5. Corticale antérieure soufflée ou détruite

Aspect radiologique typique: 50% (rachis mobile)

- Au cours de l'extension osseuse du lymphome et du myélome, l'infiltration tumorale prend naissance dans la moelle hématopoïétique
- En théorie, il en découle que l'envahissement du rachis est diffus, de manière homogène ou hétérogène, pour les hémopathies malignes, alors qu'il est focalisé pour les métastases des tumeurs solides

JD Laredo et coll. Vertebral tumors and pseudotumors. Radiol Clinics North Am 2001; 39: 137-163

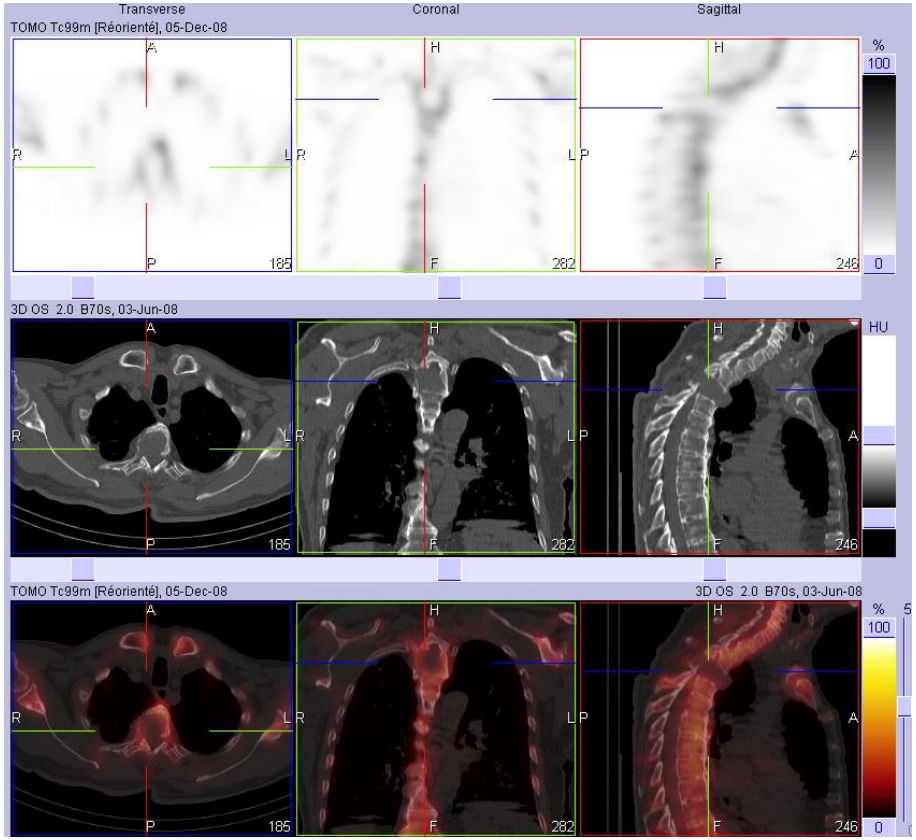

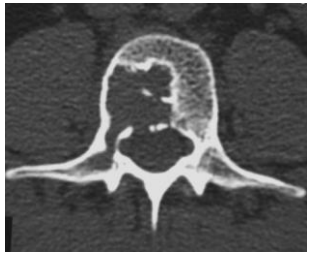

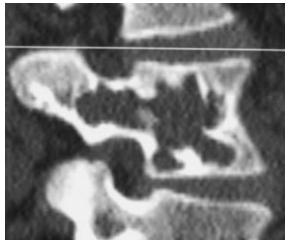

Plasmocytome

- Lésion ostéolytique expansive avec une corticale ou une coque périostée respectée voire épaisse
  Présence de qq cloisons intra tumorales persistantes épaisses

- Contraste entre l'évidement de la vertèbre et le respect relatif de la corticale et de qq travées intra lésionnelles verticales

- 90% des plasmocytomes solitaires évoluent en myélome à 10 ans

Plasmocytome solitaire/Myélome
Aspect IRM

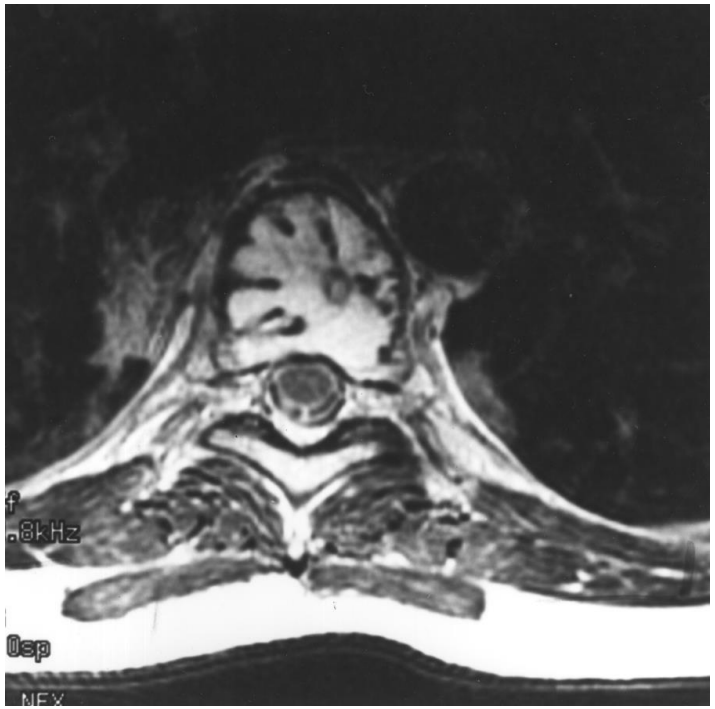

Rachis lombaire

Coupe axiale pondérée en T2

Configuration en "mini-brain" pathognomonique !?

NM Major, et al. AJR 2000;175: 261–263

Modalités d'imagerie planaire de 1ère ligne
Radiographies centrées & scintigraphie CE

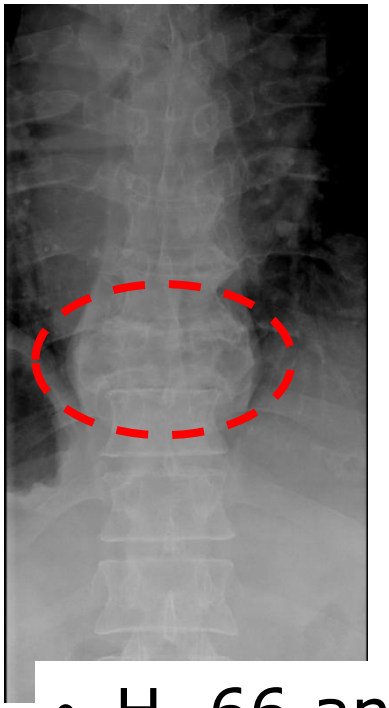

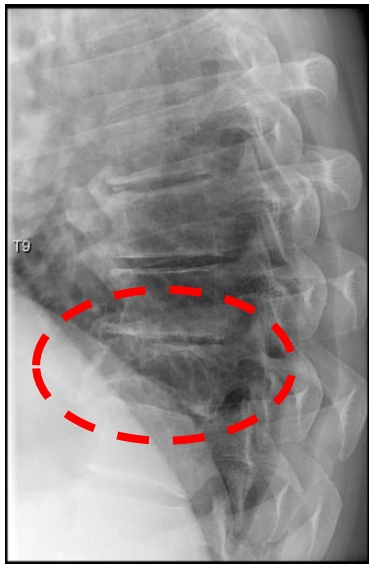

- H, 66 ans
- Asymptomatique
- Découverte TDM fortuite lésion T9
- Incertitude diagnostique:
  - Hémangiome ?
  - Dysplasie fibreuse ?

SPECT/CT rachis entier:
CT+SPECT/CT
Coupes axiales/coronales/sagittales

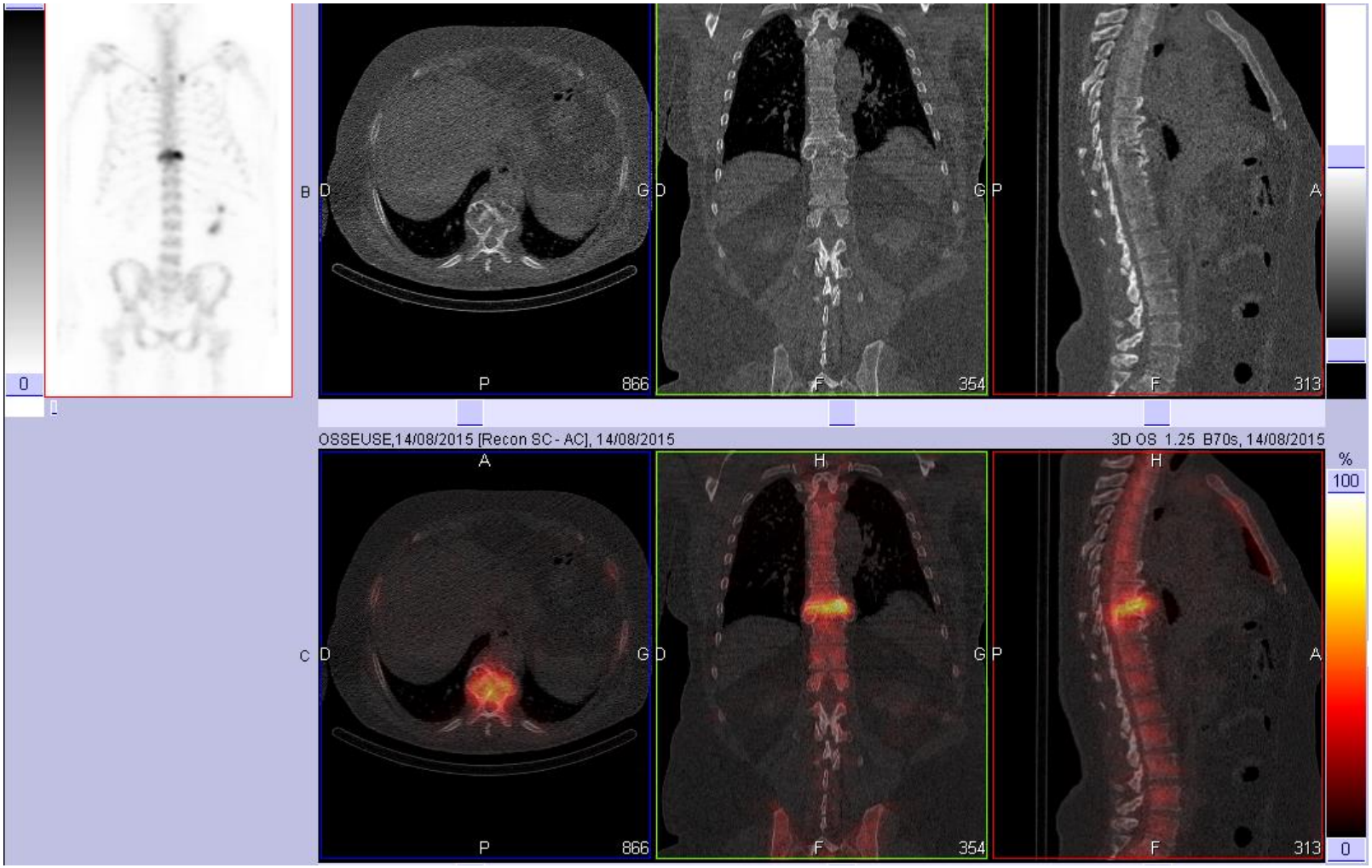

SPECT/CT rachis dorsal: SPECT+SPECT/CT+CT Coupes sagittales

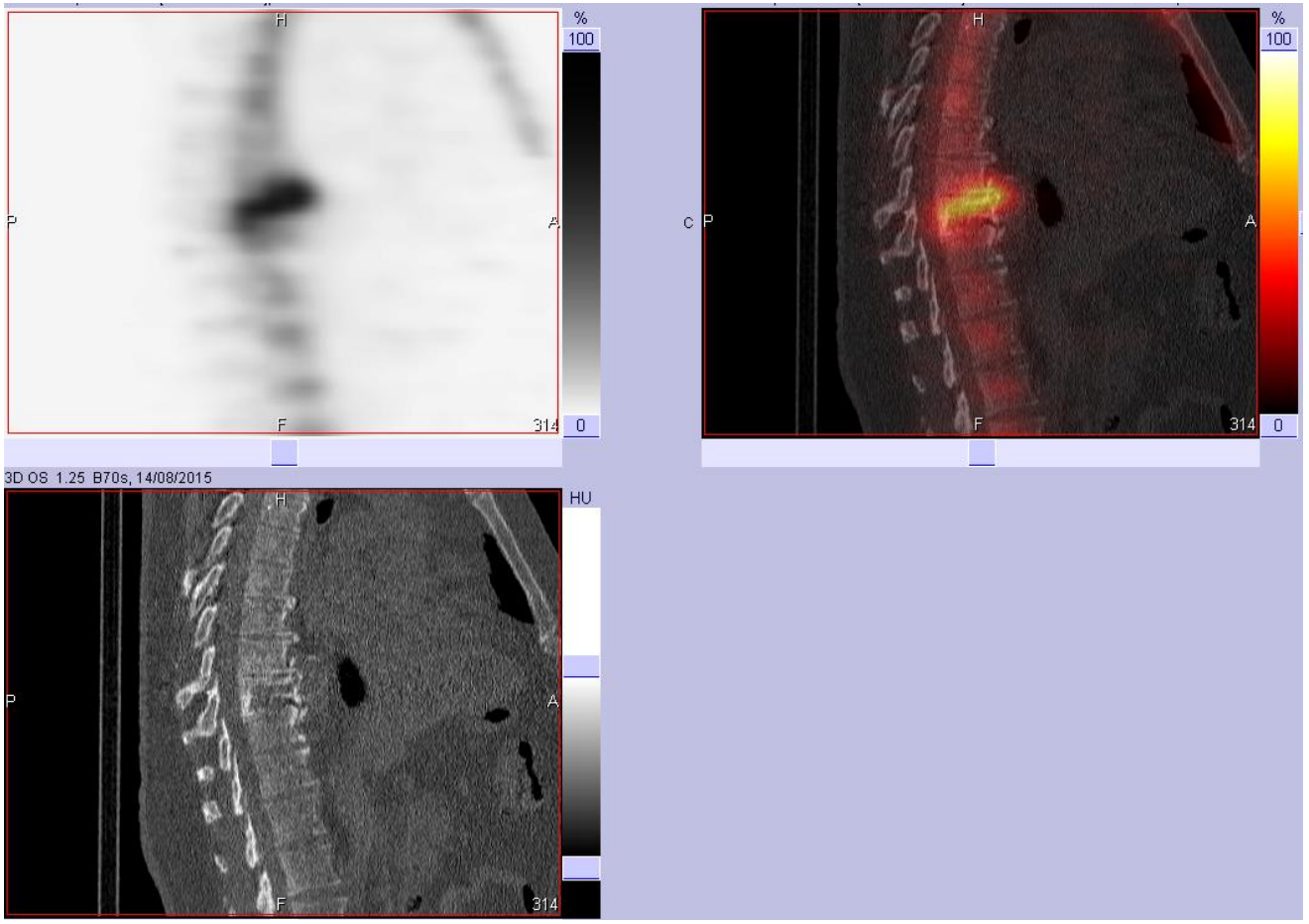

SPECT/CT rachis entier: Représentation fused VRT Pseudo-face postérieure

PET/CT rachis entier
Coupes sagittales

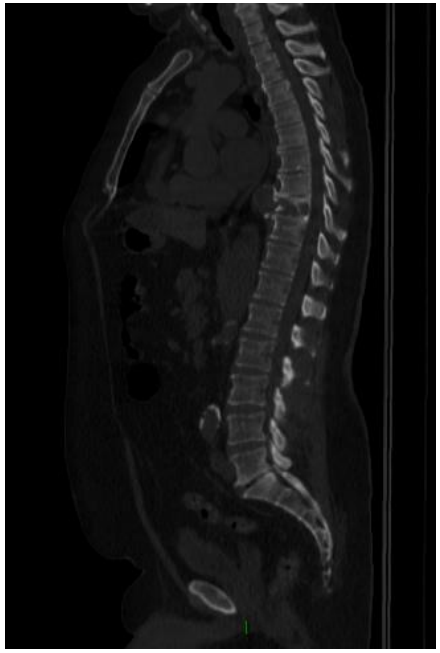

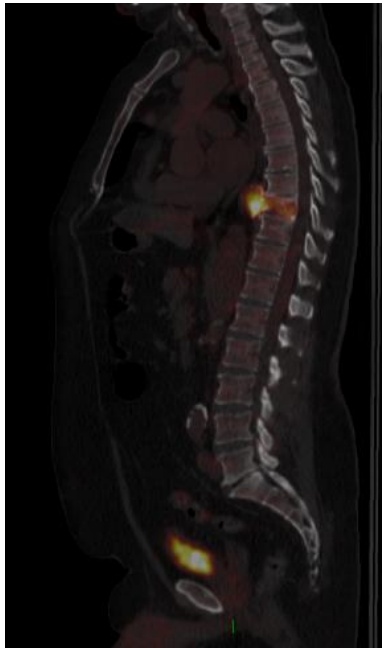

SPECT/CT OS
vs
PET/CT FDG

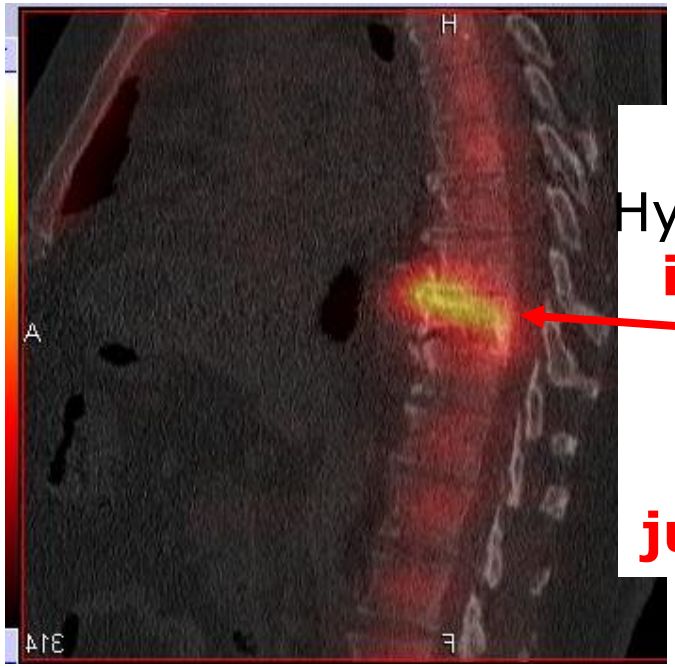

TEP:
Hypermétabolisme
intra-lésionnel

SPECT:
Hyperfixation
événements
juxta-lésionnels

Biopsie scano-guidée:
Dysplasie fibreuse

Enchondoma vs low grade chondrosarcoma

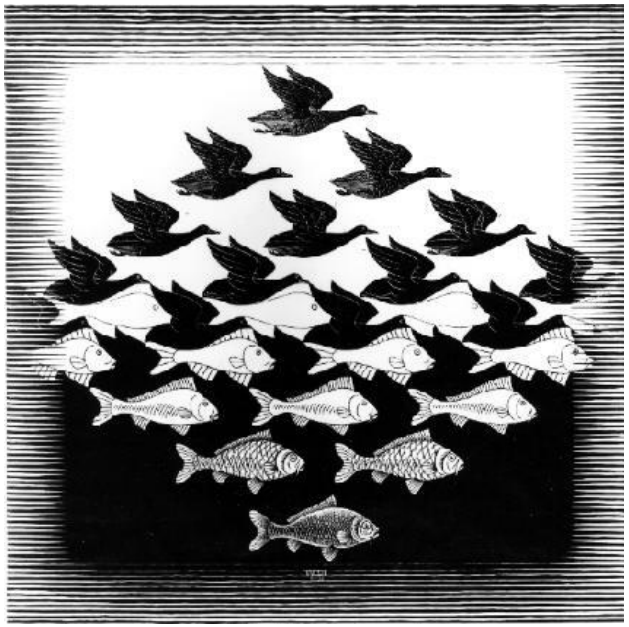

DIFFERENTIAL DIAGNOSIS: MISSION IMPOSSIBLE ?

Clinical context

- M, 75 years old
- Prostate cancer
  - T2N0Mx
  - Gleason 8 (4+4)
  - PSA = 5 ng/mL
- No bone pain
- Baseline bone scan

SCINTIGRAPHIE OSSEUSE SPECT-CT

25/11/2014

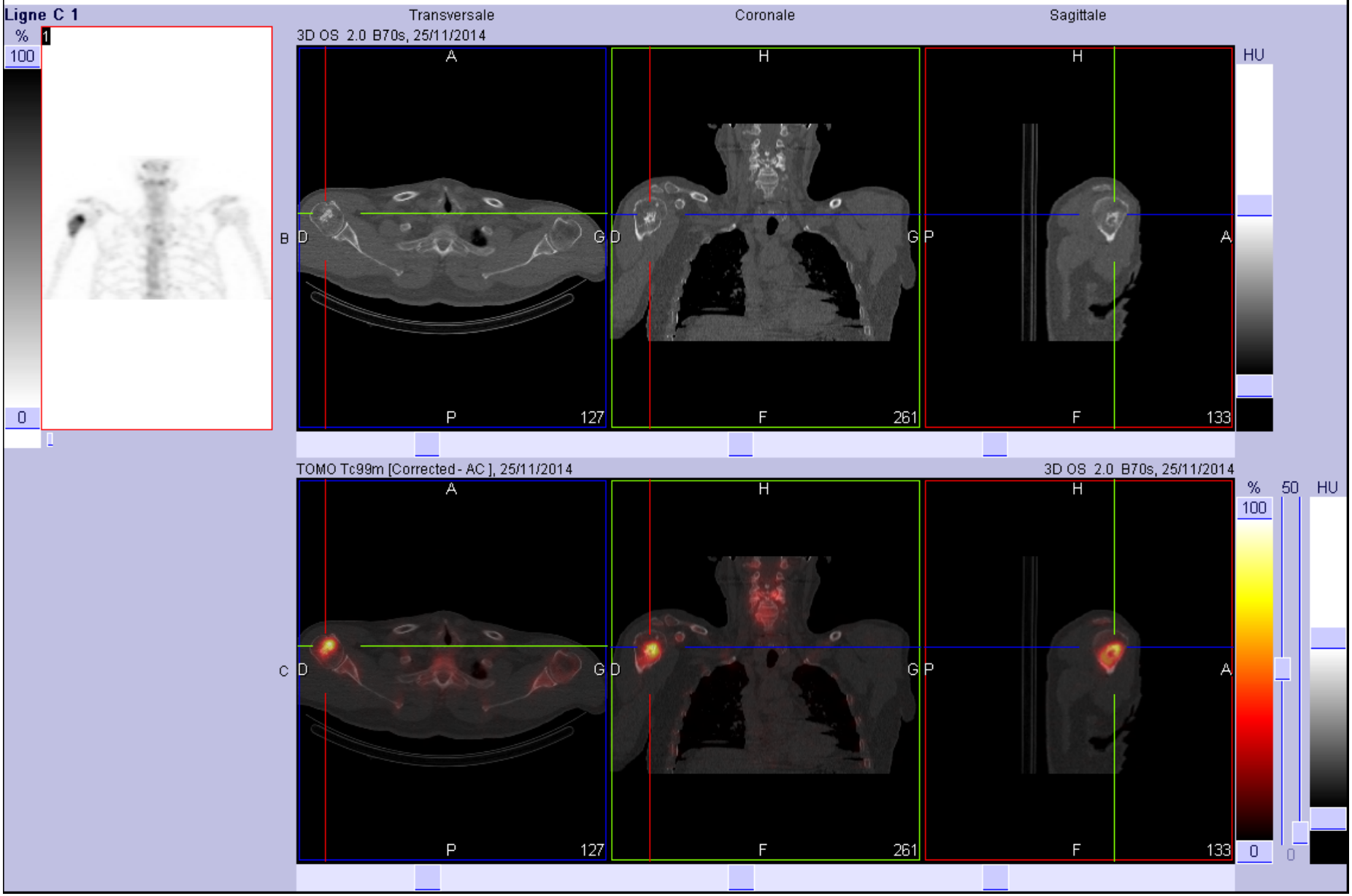

25/11/2014


Coronale
TOMO Tc99m [Réorienté], 27/08/2015
H
%
100
A D G
F
283
0
Coronale
TOMO Tc99m [Réorienté], 27/08/2015
3D OS 2.0 B70s, 25/11/2014
H
%
50
HU
100
C D G
F
283
0
0
3D OS 2.0 B70s, 25/11/2014
H
HU
B D G
F
283

R Humerus prox. epimetaphysis MRI
T1 FATSAT GADO – T2 SPAIR
Coronal views

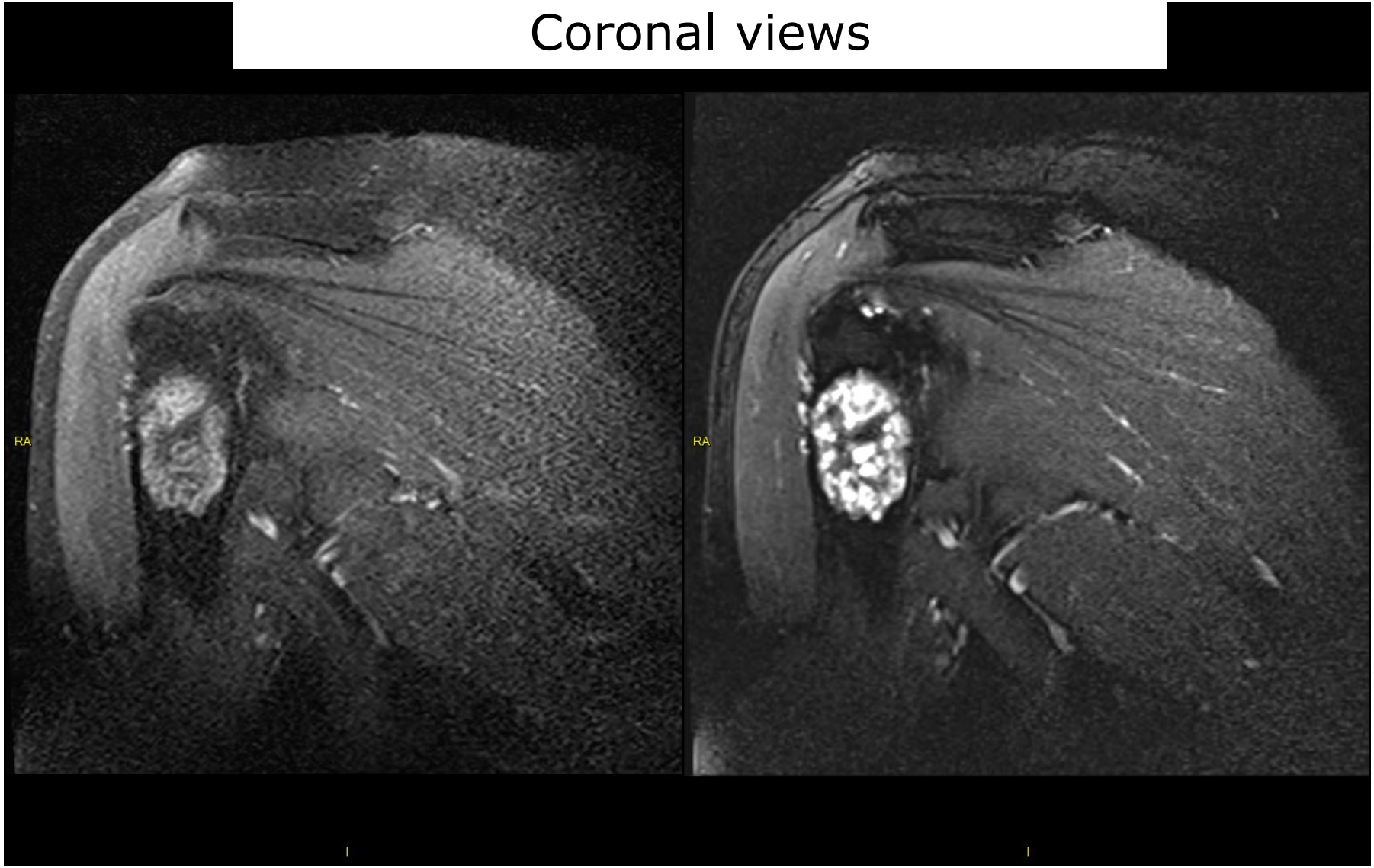

PET SCAN AS GATEWAY TO DISCOVERY OF CHONDROGENIC TUMOR

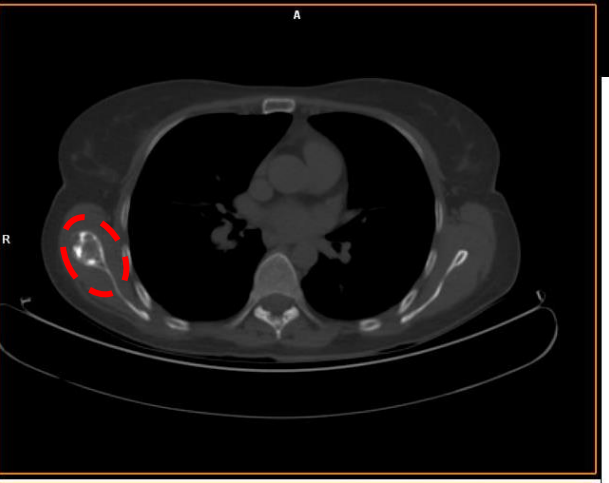

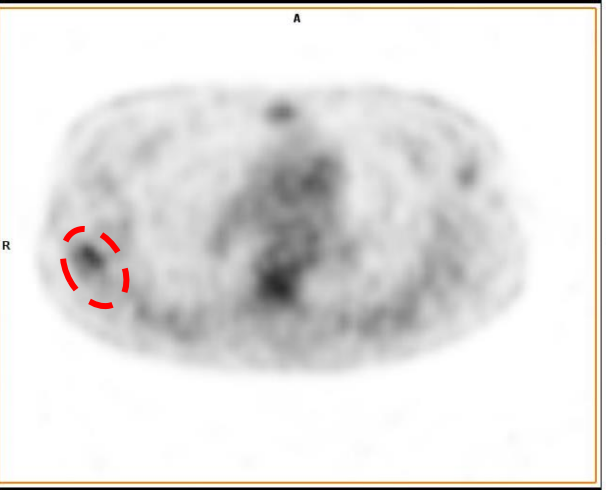

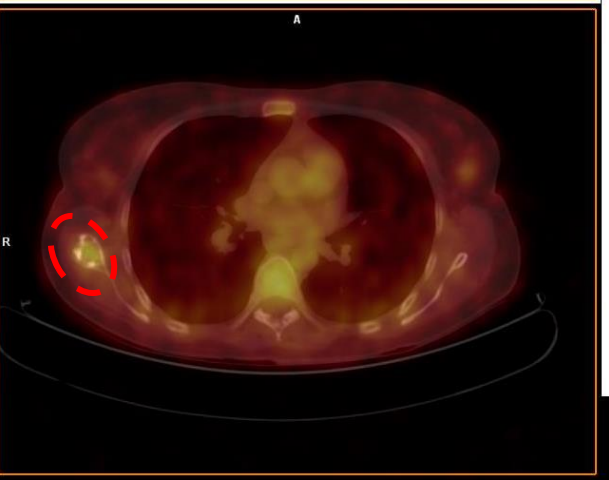

- F, 43 years old
- R breast bifocal cancer (tubular adenocarcinoma)
- No skeletal pain
- FDG PET: Baseline work-up

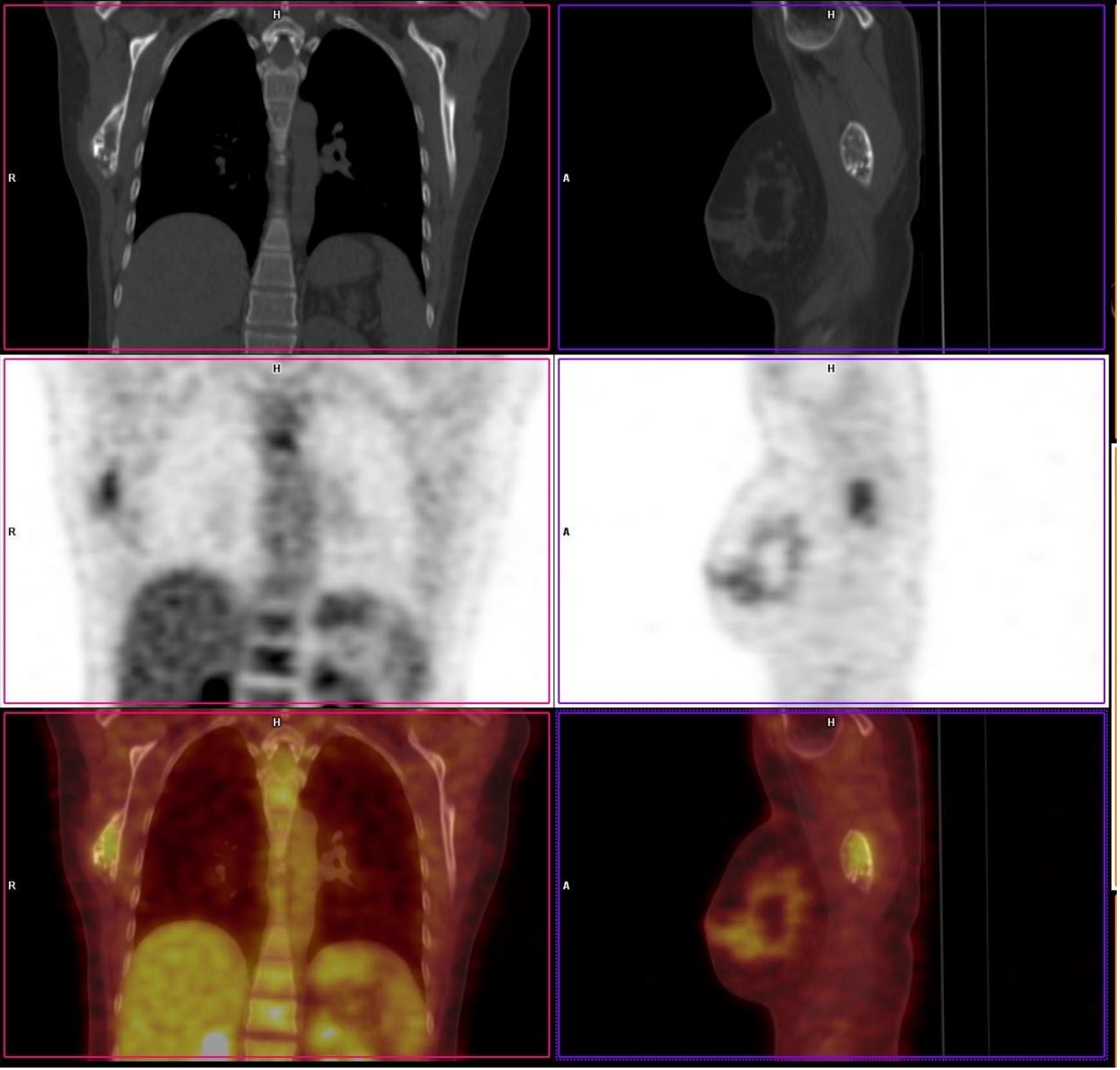

- SUVmax= 2.5 on baseline PET
- SUVmax stable on post-chemo PET 2 months later

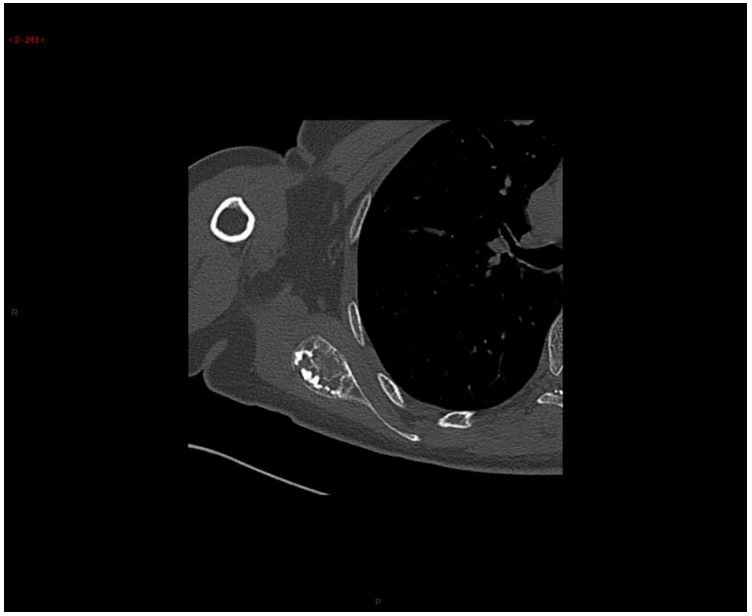

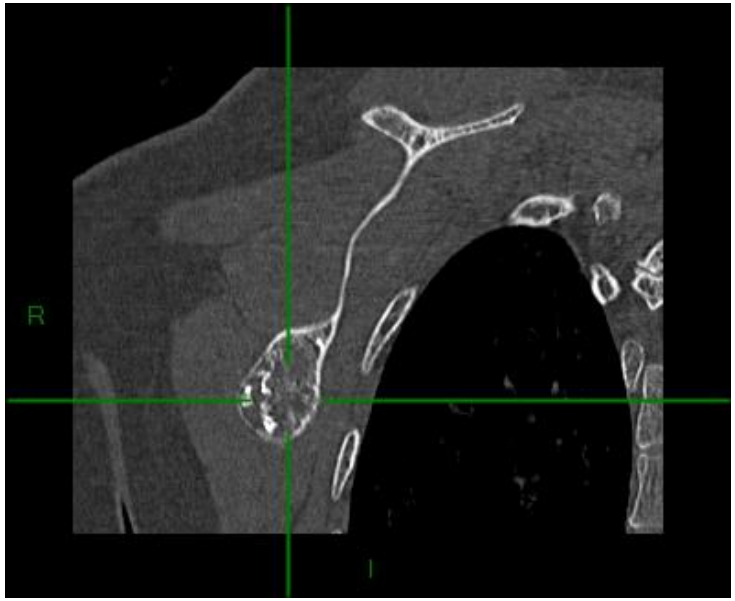

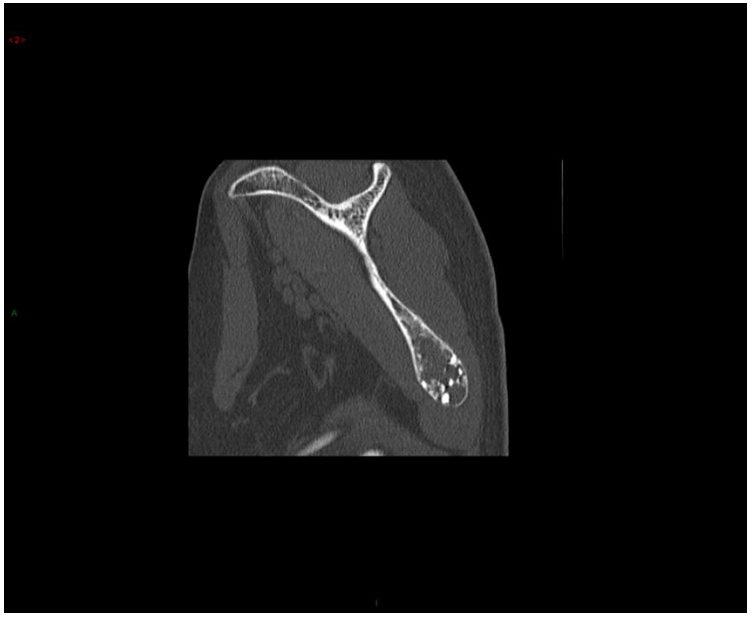

MDCT Right scapula
Transaxial + MPR Cor & Sag

- Tumor matrix: pop corn pattern
- Bone expansion++
- Endosteal scalloping+
- Cortical effraction++

FDG PET/CT - chondroblastoma

- FDG uptake
- ostelytic lesion
- epiphyseal localization

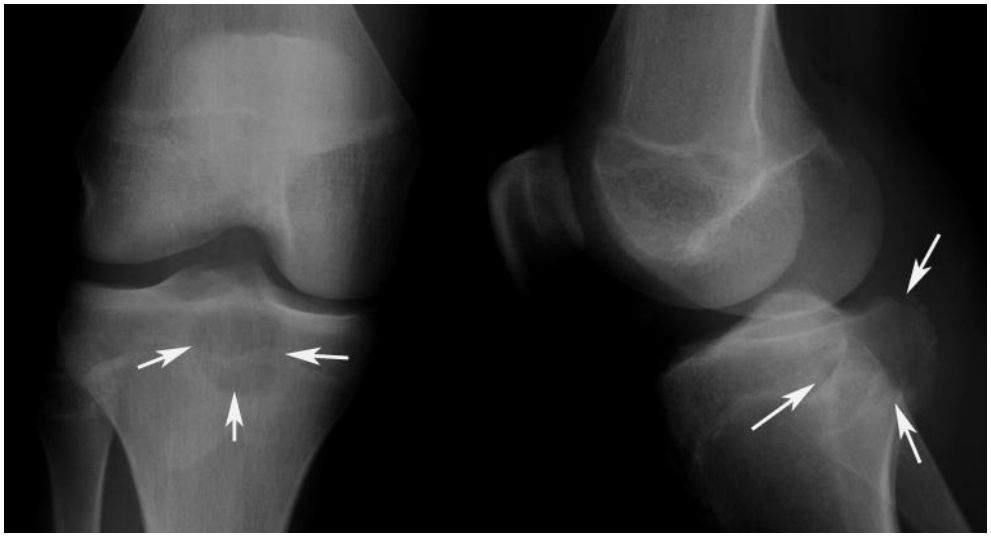

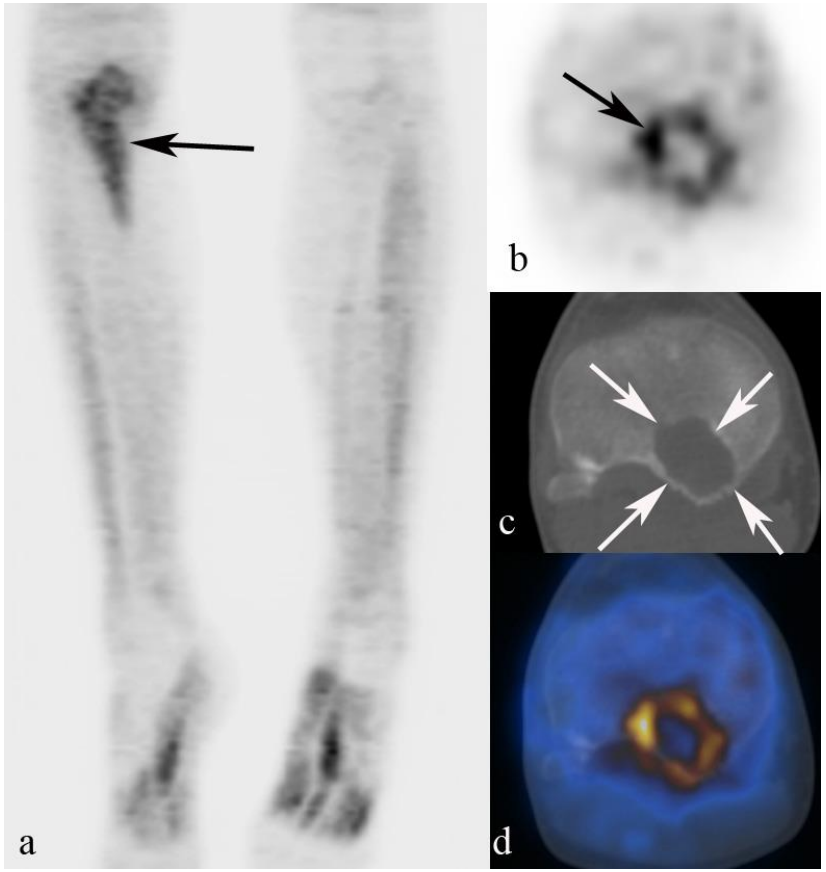

Enchondroma vs chondrosarcoma (any grade)
1) Clinical criteria

- Pain
  - Lesion-related:
    - 80% chondrosarcoma
    - 35% enchondroma
- Referred pain excluded

Parlier-Cuau C, Eur J Radiol 2011

Enchondroma vs low grade chondrosarcoma
2) Morphological imaging criteria

- X-Rays+CT
  - Size > 7.5 cm
  - Cortical thickening
  - Bone expansion
  - Endosteal scalloping
- MRI
  - Low-signal islands surrounded by hyper T1-weighted images
  - HyperT1 islands surrounded by low signal on T2-weighted FATSAT images at the periphery of the main tumour mass

Brien EW, Mirra JM. Benign and malignant cartilage tumors of bone and joint: their anatomic and theorical basis with an emphasis on radiology, pathology and clinical biology. I. Skeletal Radiol 1997; 26: 325-53.

Brien EW, Mirra JM. Benign and malignant cartilage tumors of bone and joint: their anatomic and theorical basis with an emphasis on radiology, pathology and clinical biology. II. Skeletal Radiol 1999; 28: 1-20.

Enchondroma vs. chondrosarcoma: A simple, easy-to-use, new magneticresonance sign. D Vanel, J Kreshak, F Larousserie, M Alberghinib, J Mirrab,M de Paolisc, P Picci. Eur J Radiol 82 (2013) 2154–2160

Enchondroma vs low grade chondrosarcoma
3) Metabolic imaging criteria
a) 99mTc-BP SPECT/CT or 18F-NaF PET/CT

- Increased uptake!?
- Heterogeneous uptake!?

➢ Planar whole body scan
➢ Qualitative

✓ Ill relevant!
✓ Poor inter reader agreement!

Murphey MD, Radiographics 1998;18 (5): 1213-37

Whole body planar bone scan: Uptake magnitude & heterogeneity level Enchondroma vs chondrosarcoma

Table 7
Degree and Pattern of Radionuclide Uptake in Bone Scintigraphy of Enchondromas and Chondrosarcomas

Radionuclide Uptake	Enchondroma (n = 67)	Chondrosarcoma (n = 51)
Degree (P < .0005)*		
Grade 1	26 (39)	3 (6)
Grade 2	27 (40)	6 (12)
Grade 3	14 (21)	42 (82)
Pattern (P = .001)		
Homogeneous	47 (70)	19 (37)
Heterogeneous	20 (30)	32 (63)

Note.—Numbers in parentheses are percentages.
*Grade 1 = uptake less than in the anterior iliac crest, grade 2 = uptake similar to that in the anterior iliac crest, grade 3 = uptake greater than in the anterior iliac crest.

Murphey MD, Radiographics 1998;18 (5): 1213-37

Why you may observe **increased** **uptake** by chondrogenic tumors on bone scintigraphy?

- Mineralization process by chondrogenic tumor
- Calcification zones ± tumor necrosis-associated
- Pathological fissures/fractures
- Peritumoral healthy bone reaction (incl. periosteal accretion)

Why you may observe **decreased** **uptake** by chondrogenic tumors on bone scintigraphy?

- Poor or un-differenciation of chondrogenic tumor
- Bone destruction by tumor-activated osteoclasts
- Tumor necrosis areas
- Intra-tumoral fibrosis

Grimaud E, Histol Histopathol (2002) 17: 1103-1111

PET quantification for differential EC/CS ?

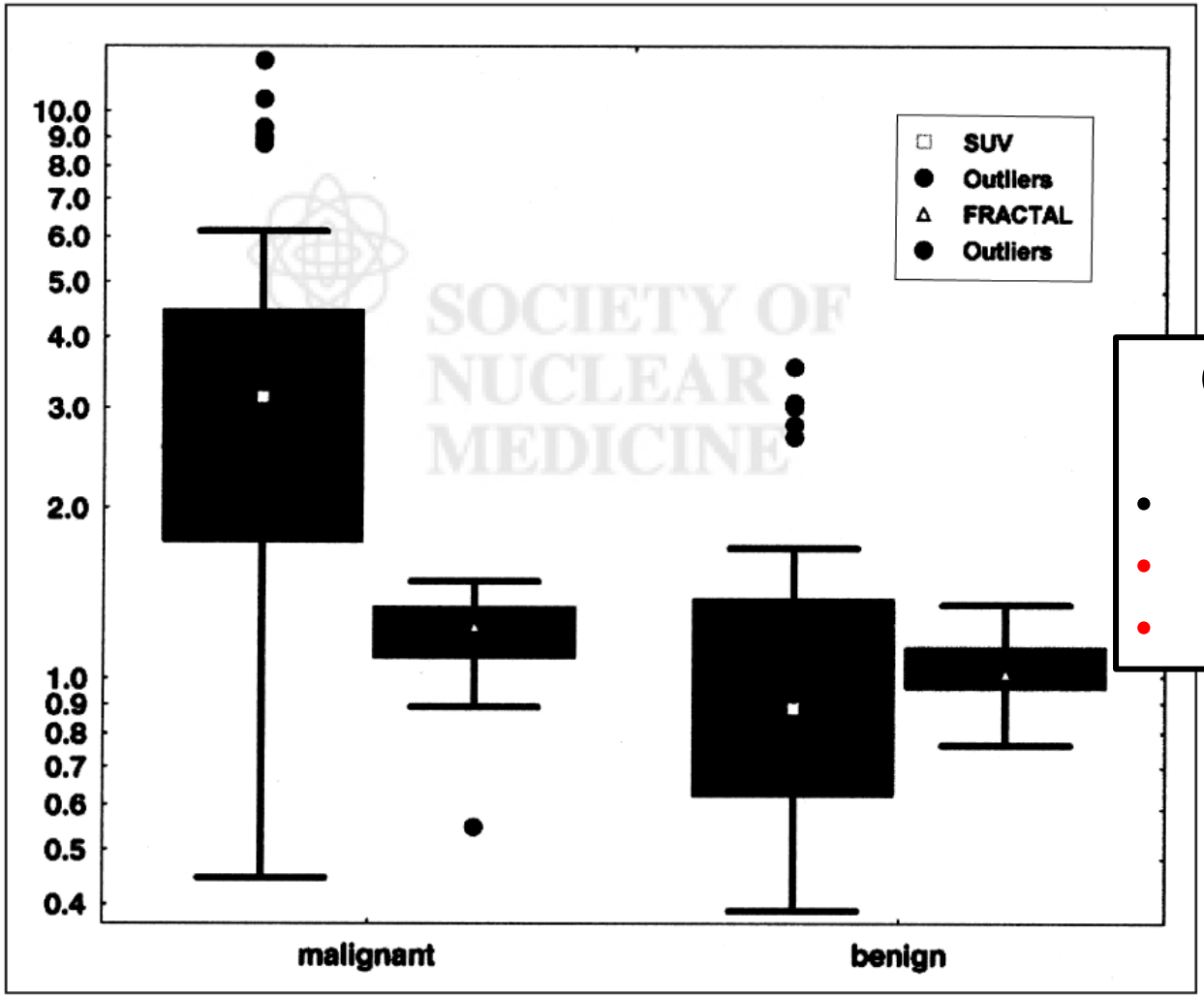

Quantitative indexes:

- Magnitude
- Heterogeneity
- Kinetics

Box–whiskers plots of average 18F-FDG uptake (SUV) at 60 min and average of fractal dimension for all malignant (n = 37) and all benign (n = 46) lesions

Dimitrakopoulou-Strauss A. J Nucl Med 2002; 43: 510–518

PET quantification for differential EC/CS ? (C't'd)

Parameter	SUV	FD	SUV, FD	SUV, FD, VB, K1–k4, Ki
Sensitivity (%)	54.05 (20/37)	71.88 (23/32)	64.52 (20/31)	75.86 (22/29)
Specificity (%)	91.30 (42/46)	81.58 (31/38)	88.89 (32/36)	97.22 (35/36)
Accuracy (%)	74.70 (62/83)	77.14 (54/70)	77.61 (52/67)	87.69 (57/65)

Magnitude+Heterogeneity+Kinetics

Fibrous dysplasia- Pitfall in lung cancer staging with FDG PET/CT

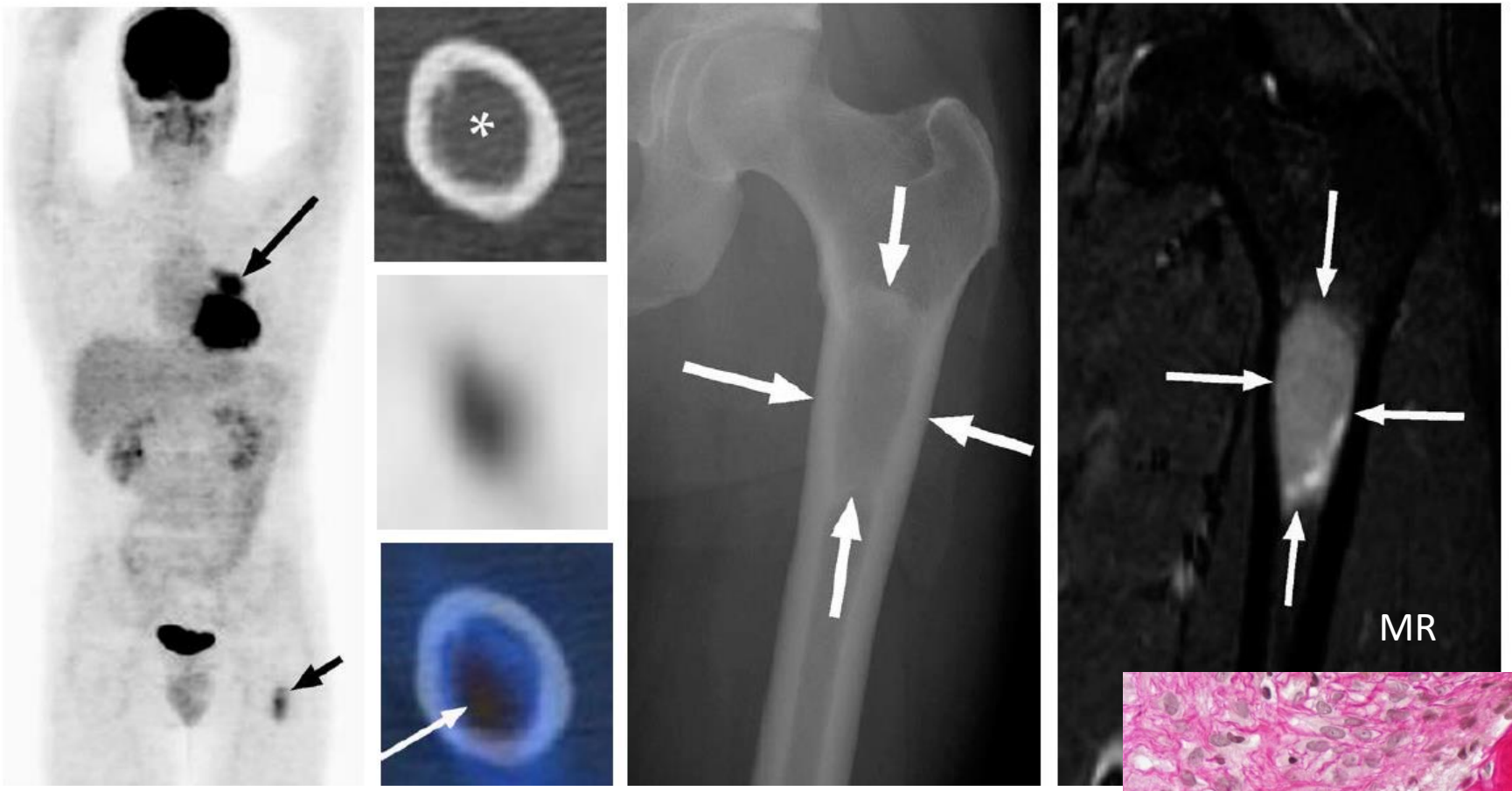

FDG PET/CT

x-ray

K Strobel et al. Skeletal Rad 2007

Histology

Fibrous dysplasia
Basic roentgenographic types

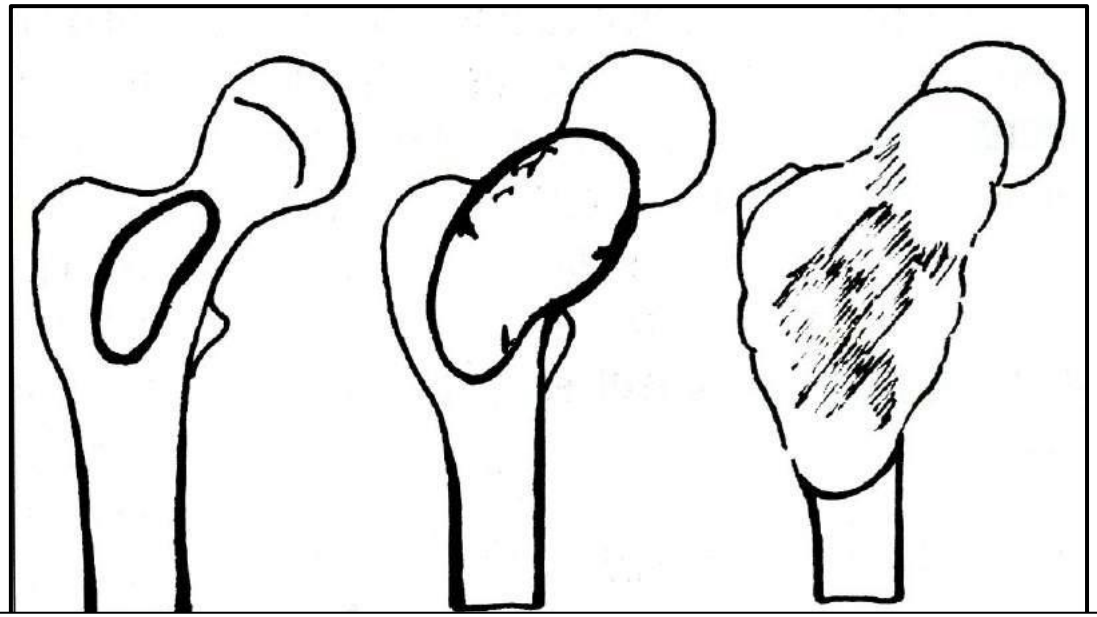

Type I Type II Type III

Type I: "ground-glass" or pagetoid appearance (60% of cases)
Type II: The cystic appearance
Type III: The mottled or "soap bubble" pattern

JD Laredo, Conduite à tenir devant une image osseuse unique d'allure tumorale. Sauramps Ed, 2004

Fibrous dysplasia (monostotic)
Epidemiology and lesions distribution

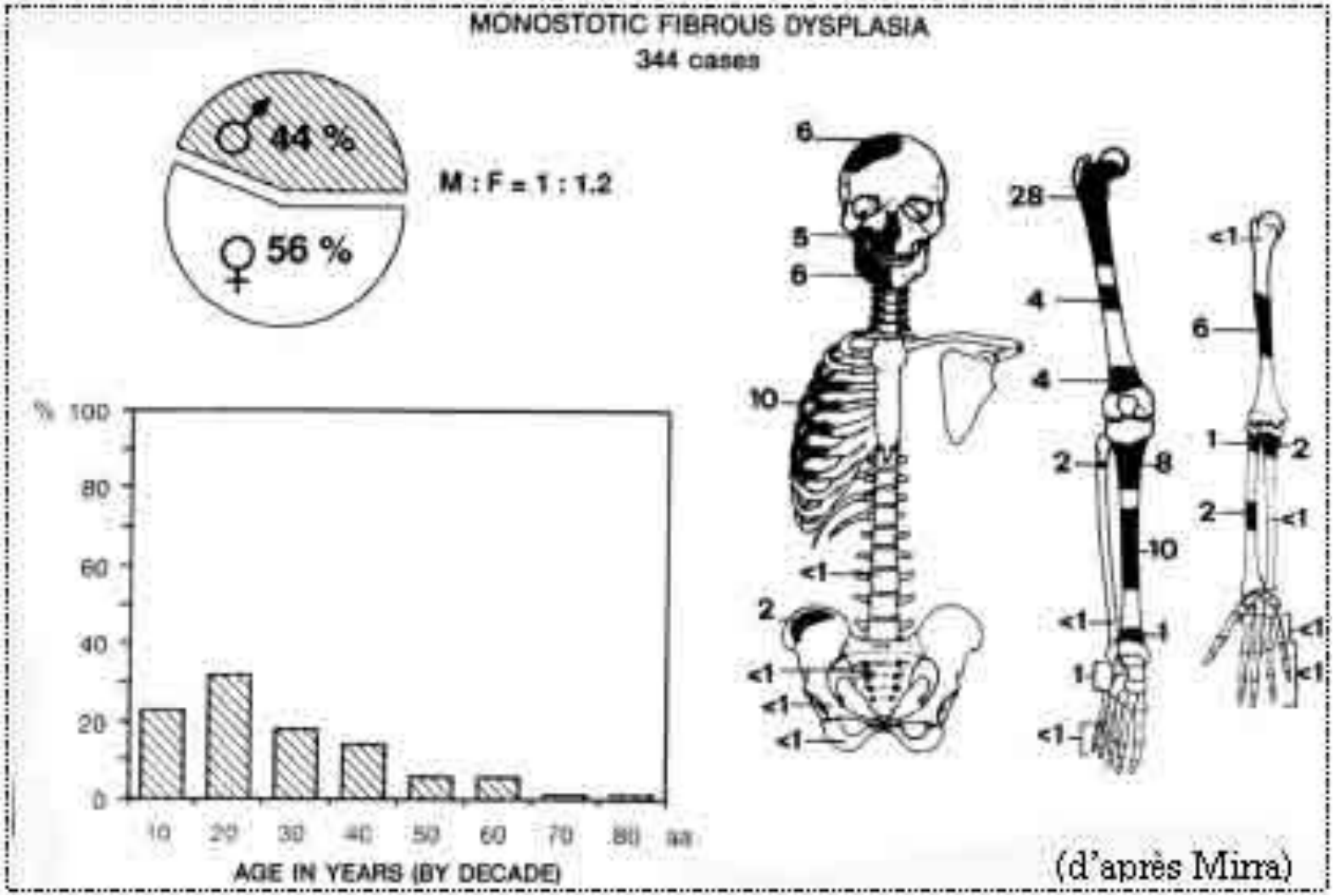

Osteoblastoma mimicking osteosarcoma in FDG PET/CT imaging

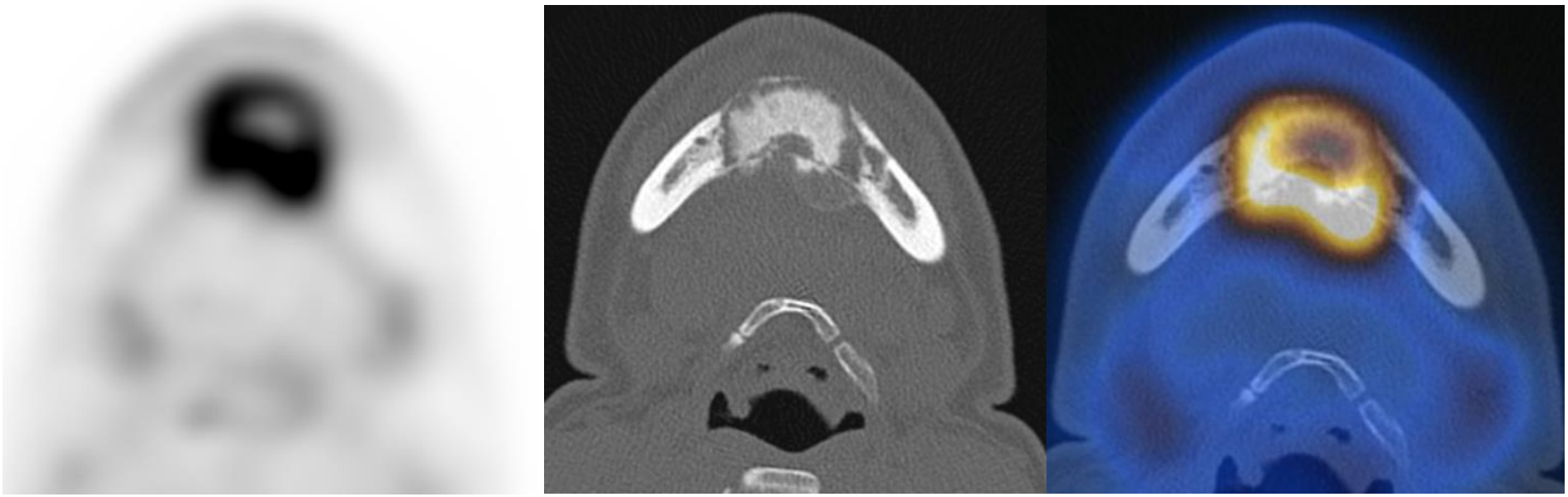

Strobel et al. CNM 2013

Osteosarcoma mimicking osteoblastoma in XR/CT/MRI

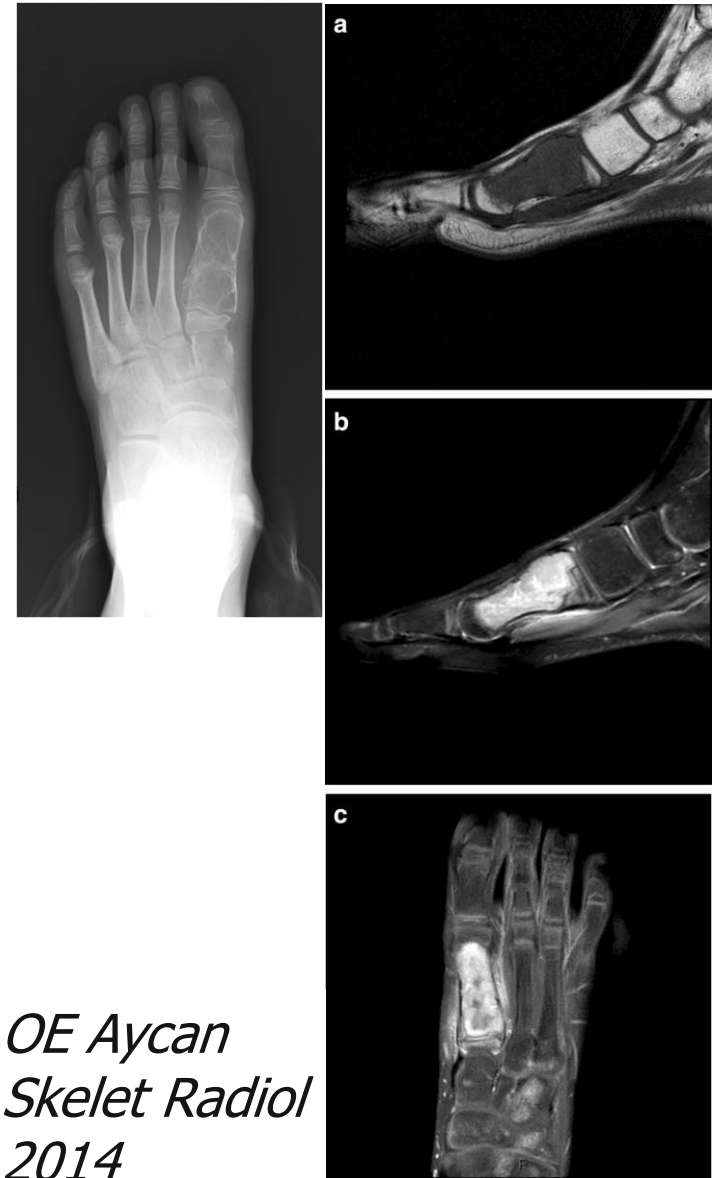

OE Aycan Skelet Radiol 2014

Classification of Osteosarcoma	
Classification	%
Primary high-grade, intramedullary	75
Mixed pattern (73%)	
Bone rich/sclerosing (9%)	
Cartilage rich (5%)	
Spindle cell rich	
Malignant histiocyte rich	
Telangiectatic	
Small cell rich (Ewing-like)	
Benign giant cell rich	
Epitheloid cell rich	
Primary low-grade, intramedullary	4–5
Fibrous dysplasia-like (50%)	
Nonossifying fibroma-like (25%)	
Osteoblastoma-like (15%)	
Chondromyxoid fibroma-like (10%)	
Secondary intramedullary	6
Multifocal	1–2
Intracortical	0.2
Juxtacortical	7–10
Parosteal (65%)	
Periosteal (25%)	
High-grade surface (10%)	
Osteosarcoma of jaw	6

Mirra JM, ed. *Bone Tumors.* Philadelphia, PA: Lea & Febiger; 1989:249–389

Osteoid osteoma

- SPECT/CT or fluoride PET/CT very helpful for diagnosis and therapy planning: high focal uptake on bone scan with nidus on CT
- often misinterpreted on MR because of extensive edema
- might have FDG uptake

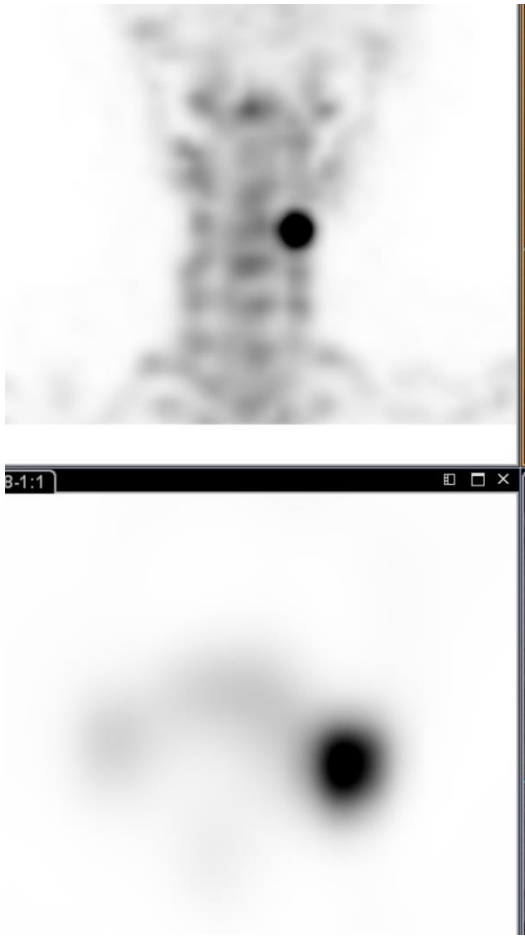

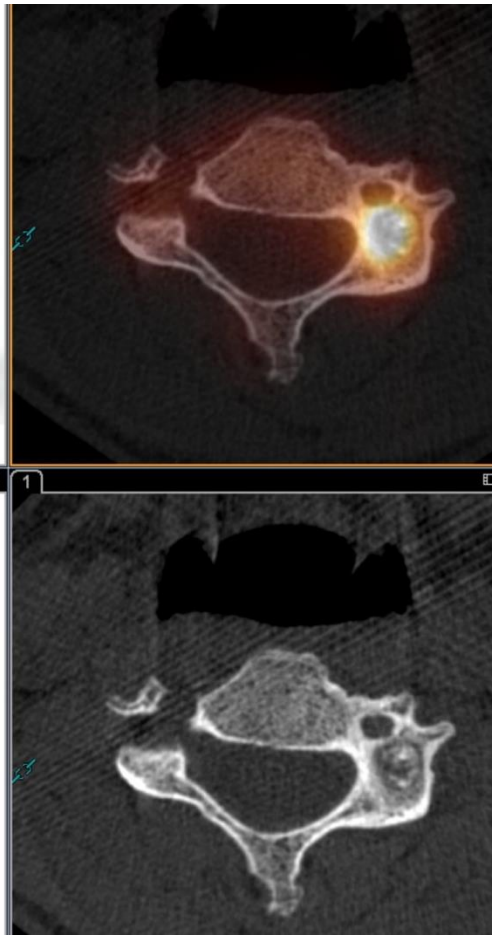

Osteoid osteoma sacrum – fluoride PET/CT

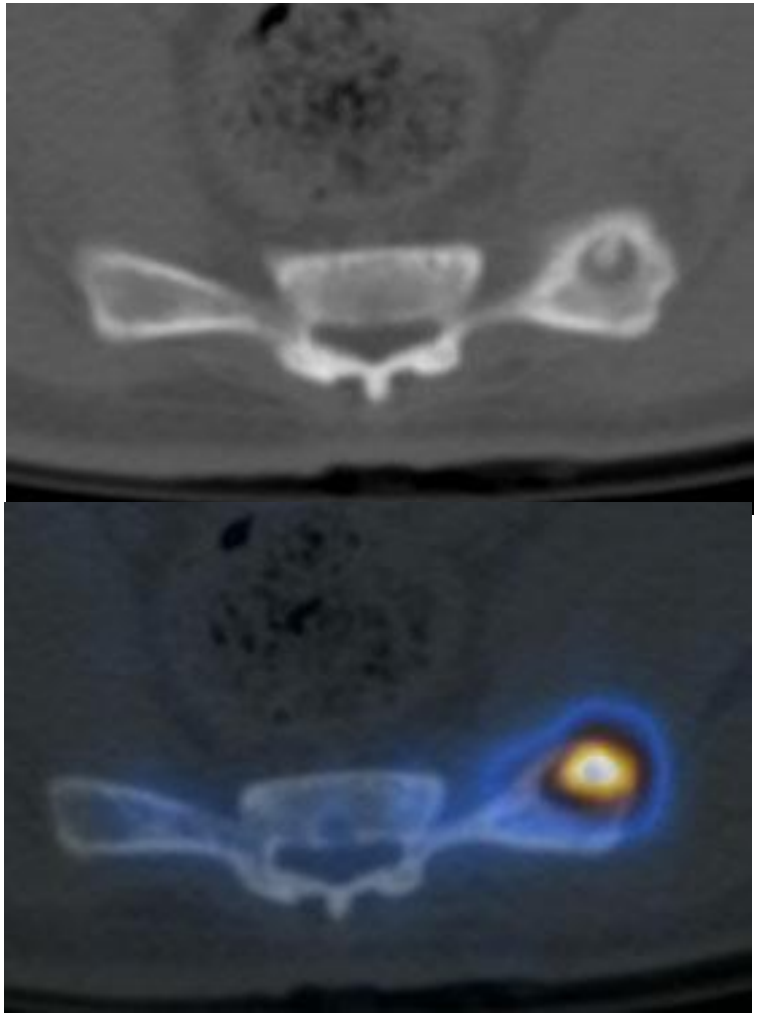

Aneurysmal Bone Cyst (ABC)

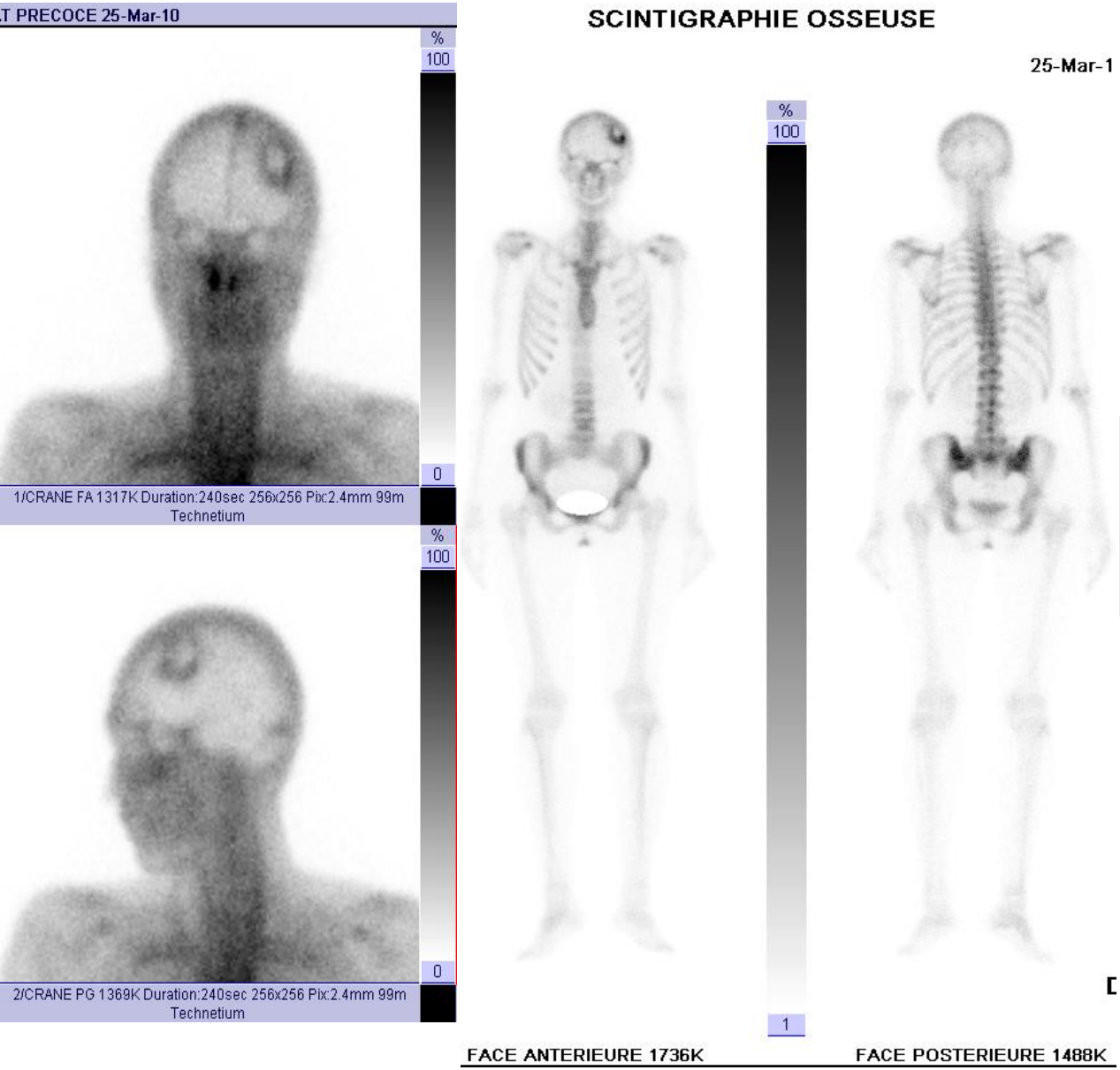

- 32 year old patient
- Headache of recent onset
- L fronto-parietal lump
- Neurological exam. OK

ABC: Skull SPECT/CT

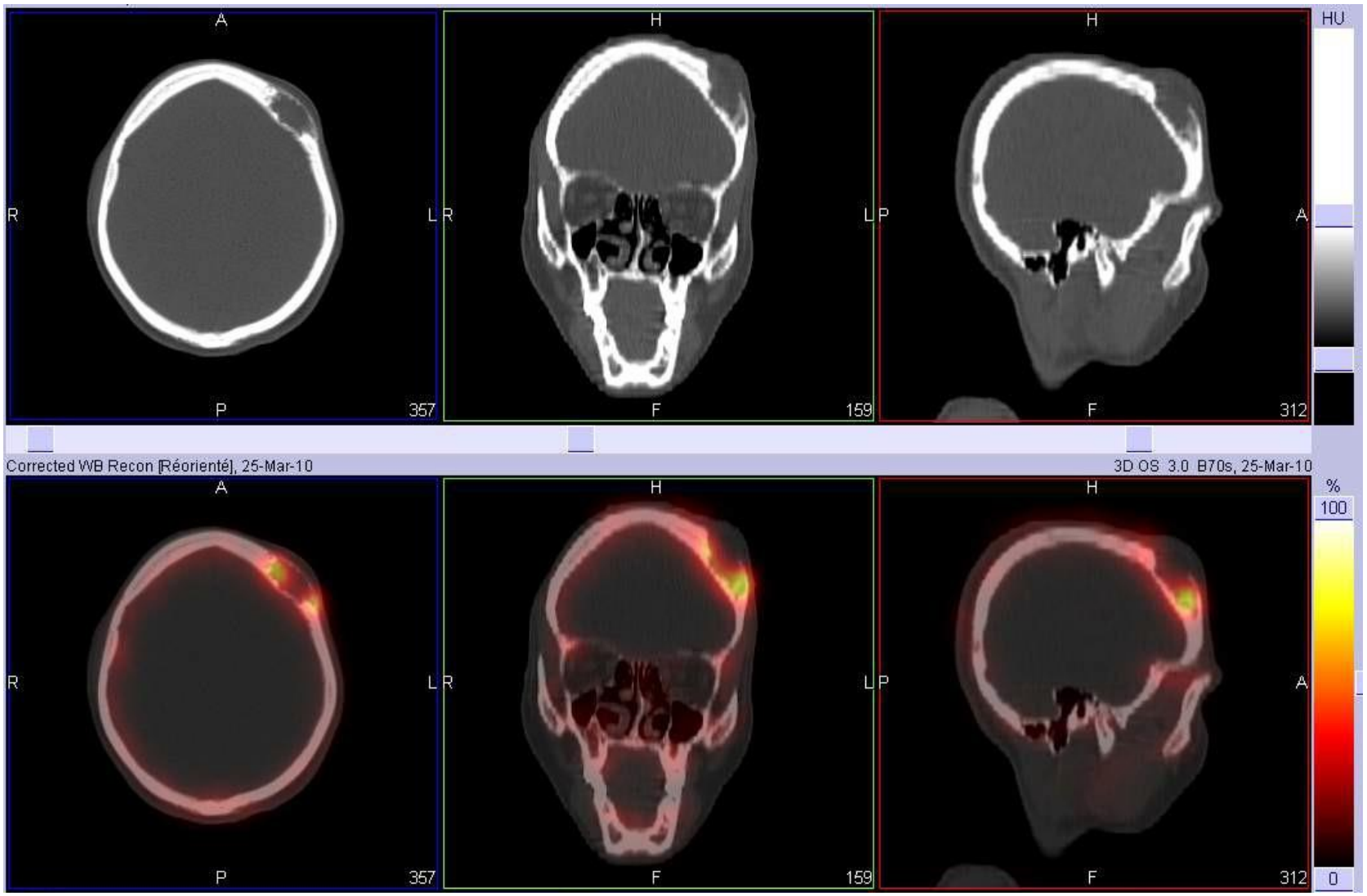

SPECT/CT
fused VRT display

Skull planar blood pool ant. view

Bone scintigraphy

MDCT VRT

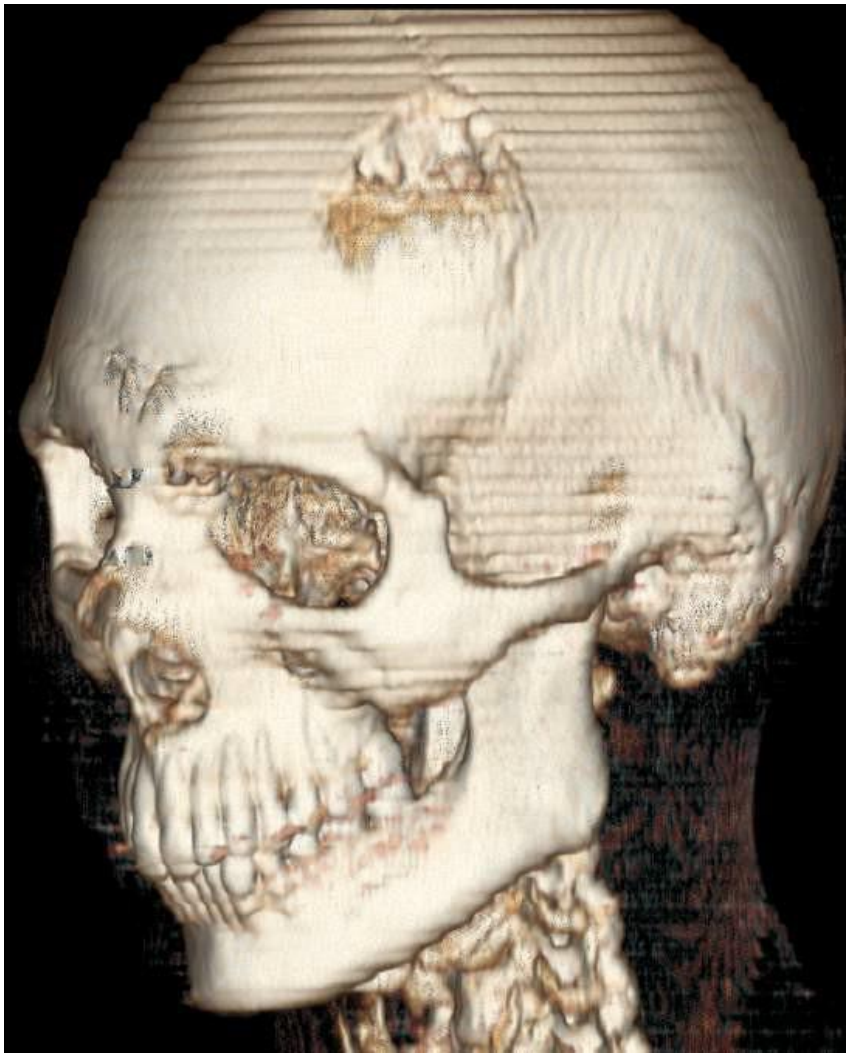

ABC: CT vs MRI

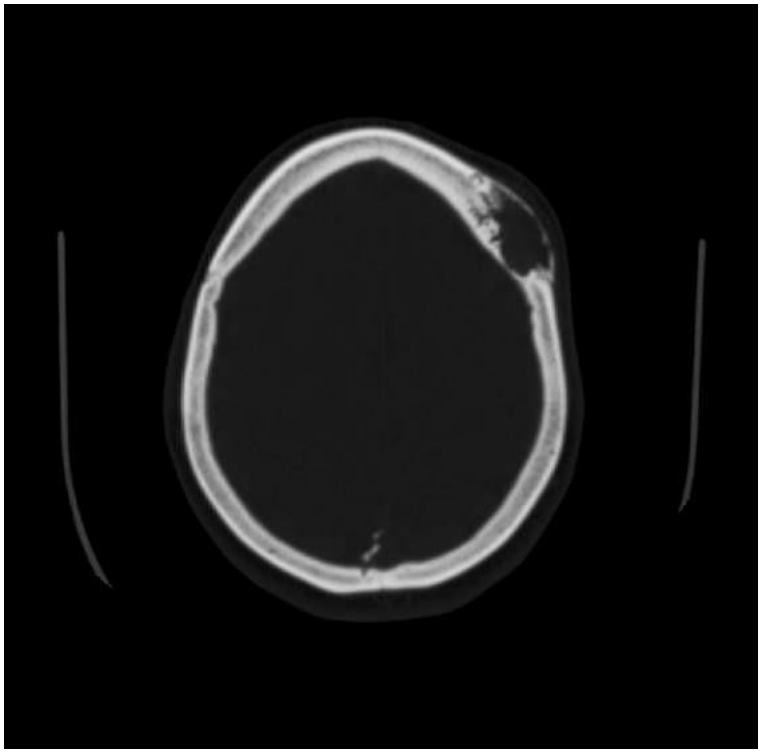

Lytic expansile lesion
Lesion matrix calcifications
Outer and inner tables involved

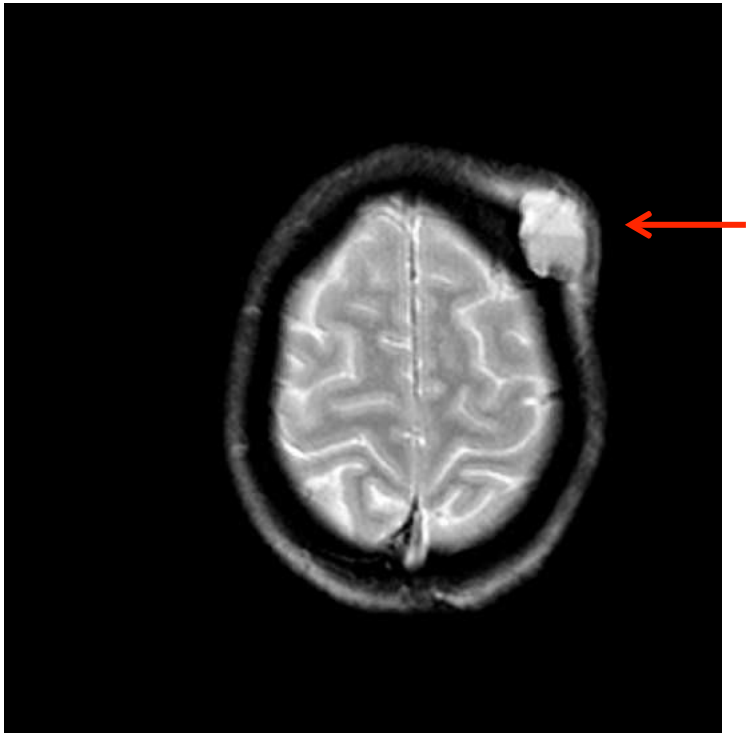

Fluid/fluid level appearance

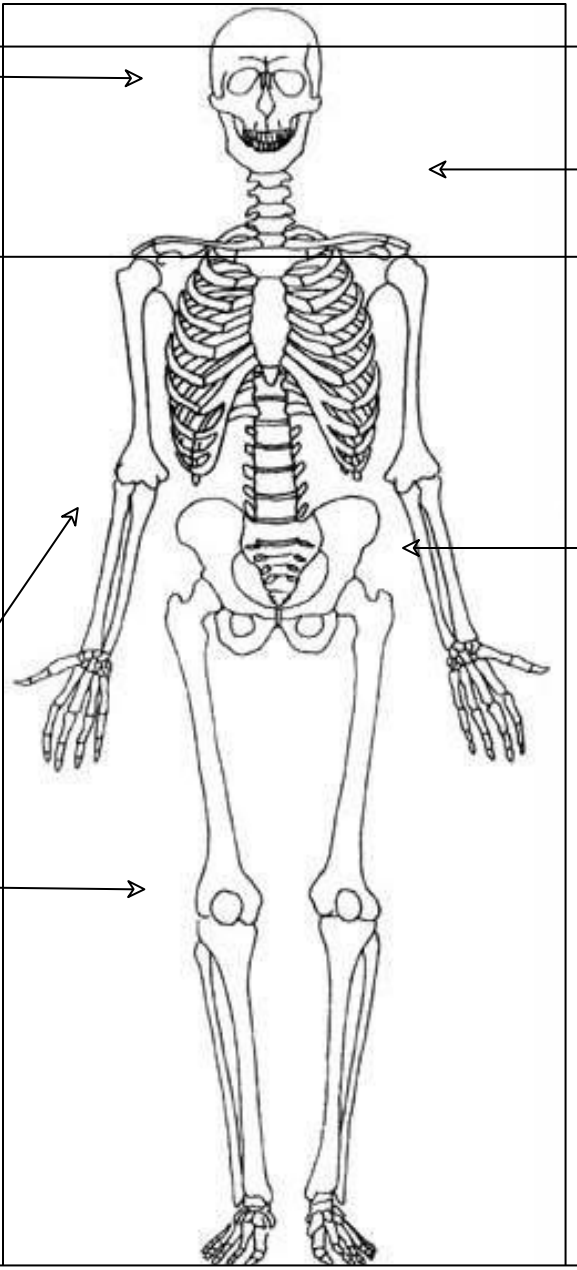

Incidence: 0.4 / 100.000

Skeletal distribution of ABC

fibrous cortical defect/non-ossifying fibroma

- localization: metaphysis long bones
- x-ray diagnostic (normally no need for SPECT/CT)
- no touch lesion
- might have increased FDG uptake

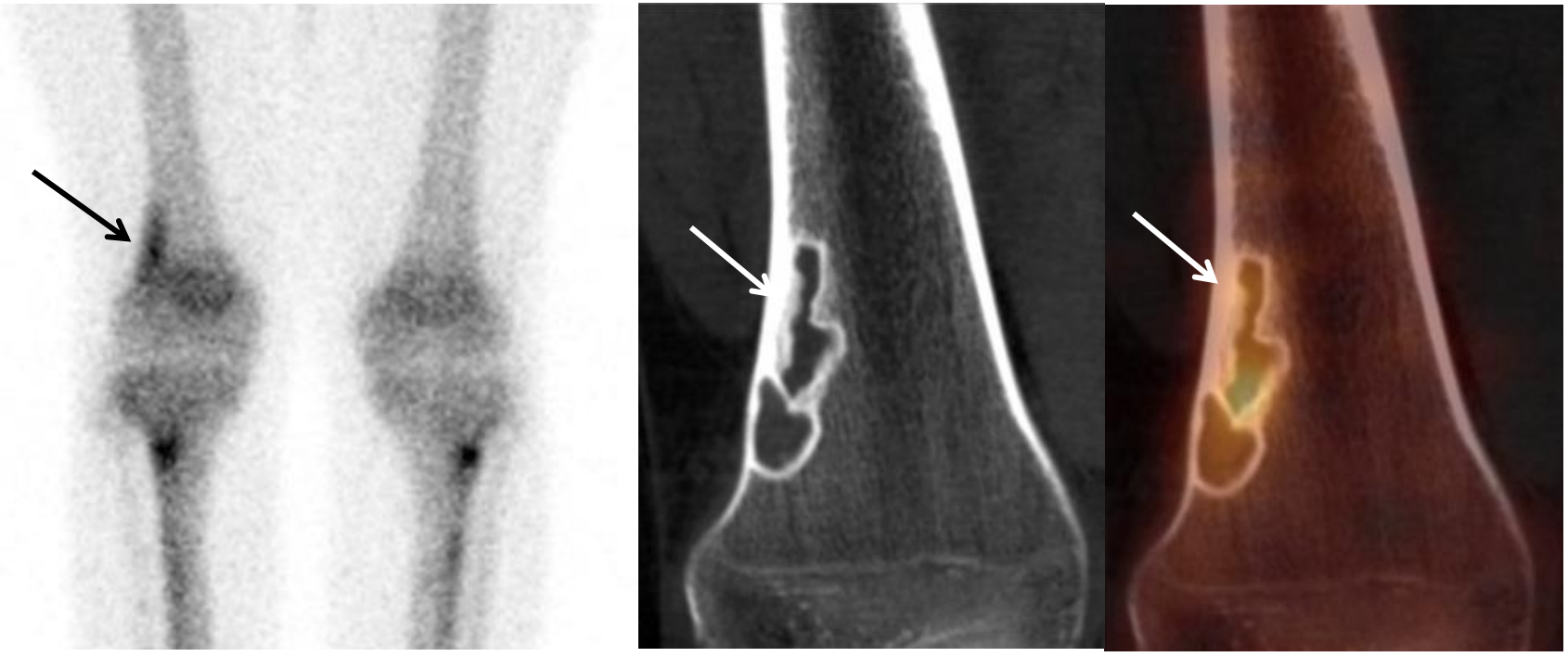

fibrous cortical defect/non-ossifying fibroma – pitfall in tumor staging with FDG PET/CT

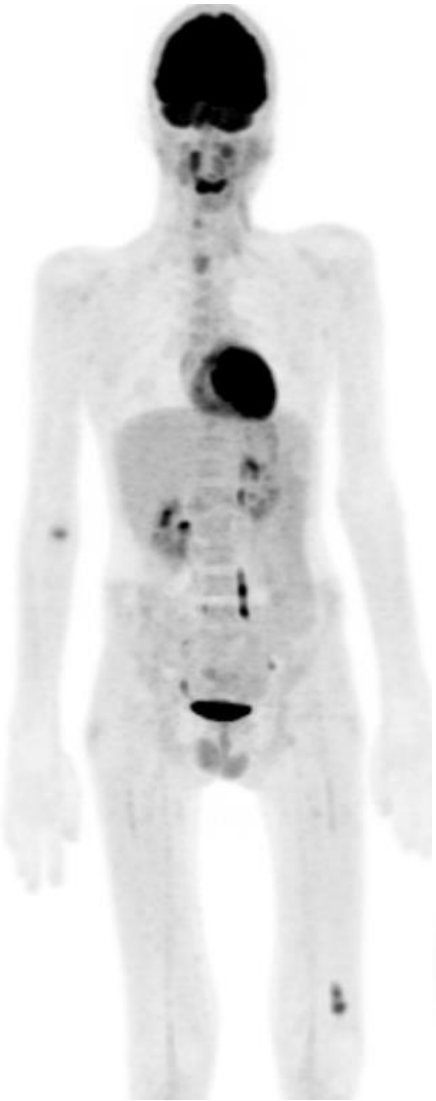

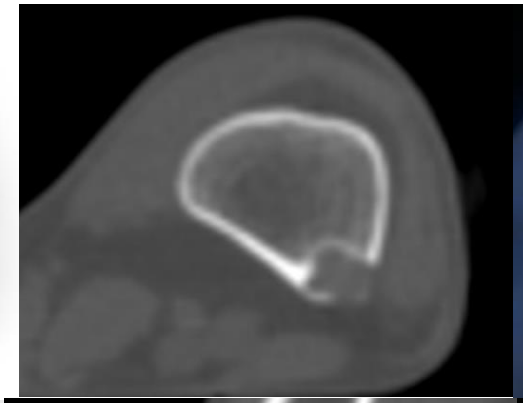

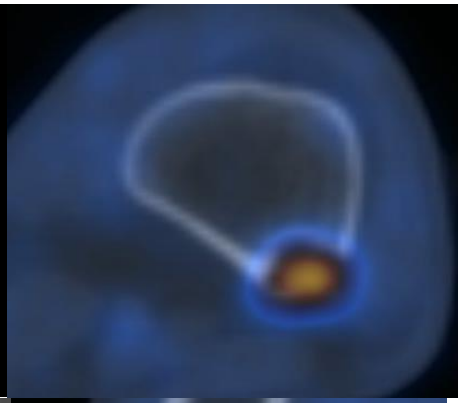

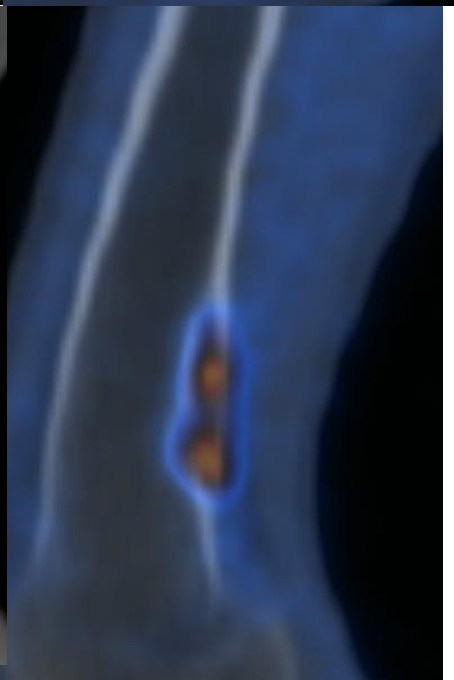

6. Cortical and periosteal reaction

Cortical and periosteal reaction

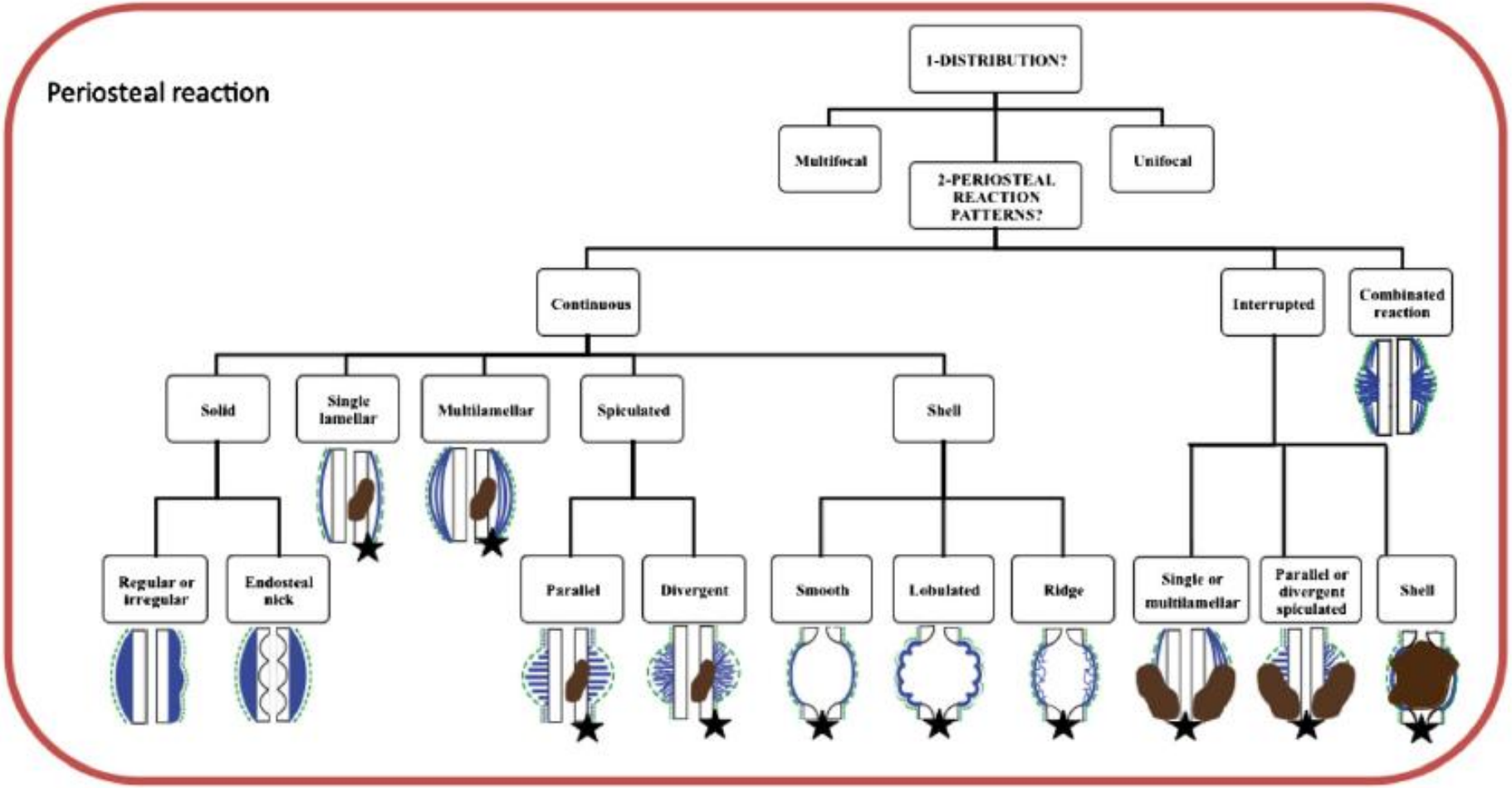

D Bisseret, Skeletal Radiol 2015

Bisphosphonates-(99mTc) biodistribution Osteolytic metastasis model

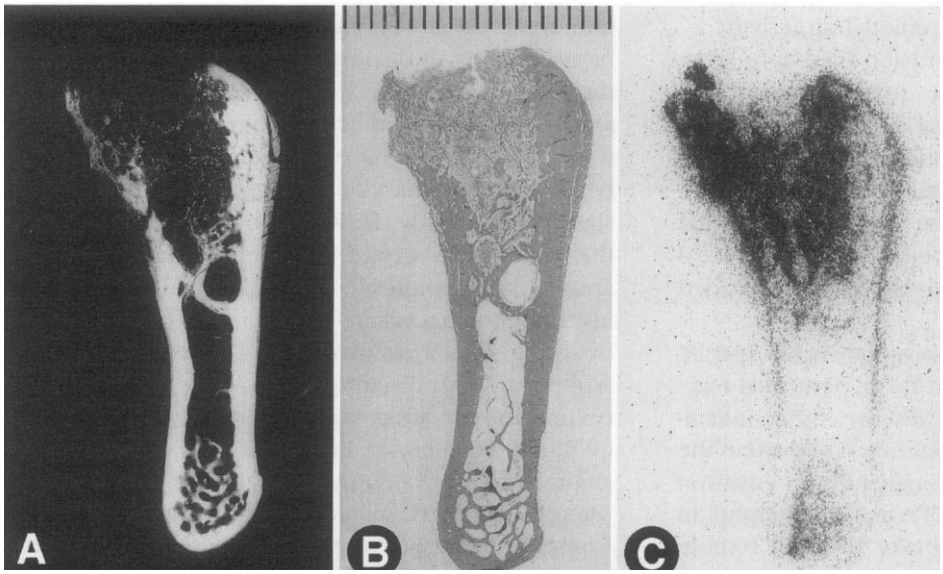

Methods

- Patients (n=7) bearing mandibular osteolytic metastases from head & neck carcinoma
- Injection of BP-(^{99m}Tc) then osseous surgical removal
- Autoradiography and contact macroradiography

• Results

- Peritumoral uptake (=immature bone) and periosteal of radioactivity from ^{99m}Tc-BP

M Tsuchimochi, J Oral Maxillofac Surg 1999

Mistaken identity:
Painful L tibia for 6 months in a 20 yo F…
…A diagnostic trap avoidable without biopsy!

Clinical presentation

- F, 25 yo
- Shop employee
- Pain in L leg
  - Unilateral
  - Chronic (> 6 mo)
  - Initially mechanical rhythm
  - Then triggering night awakening
- Past medical history: nil

Provisional clinico-roentgenographic diagnosis:
Tibial periostitis (*aka shin splints*) or overuse stress fracture

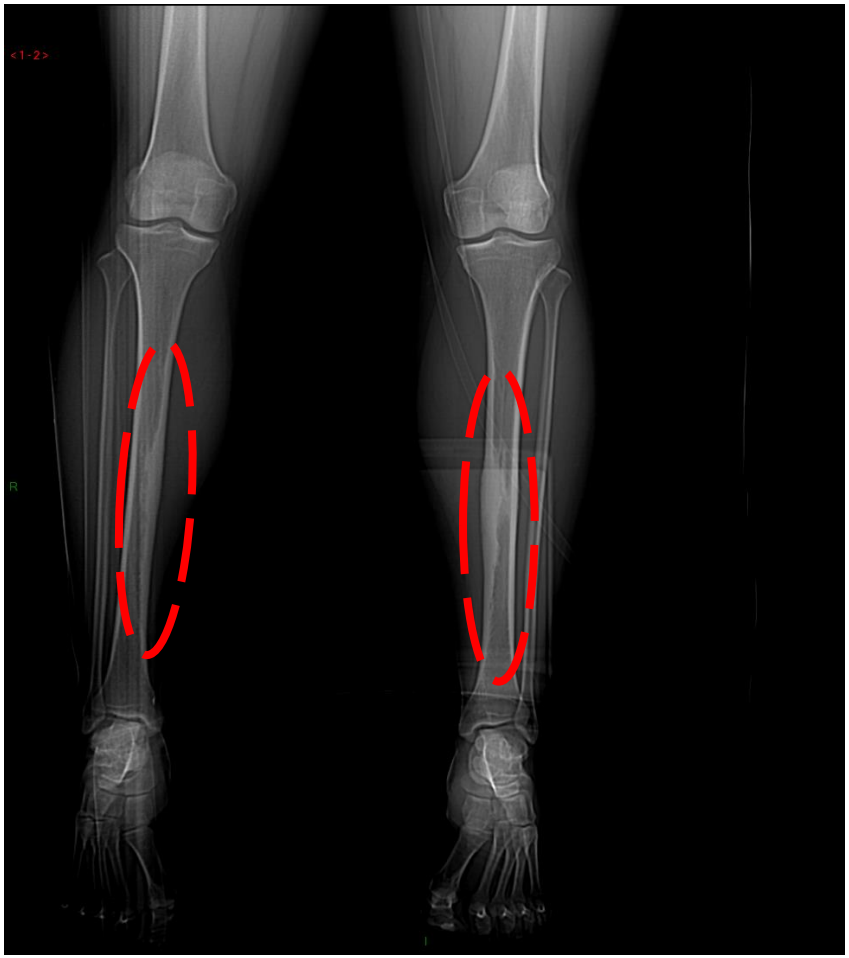

Scout view
Lower limbs skeleton

Reviewing CT scout images: Observations of an expert witness.
RH Daffner.
AJR 2015; 205:589–91

Bone scintigraphy
Planar blood pool LL AP spot views + WBS

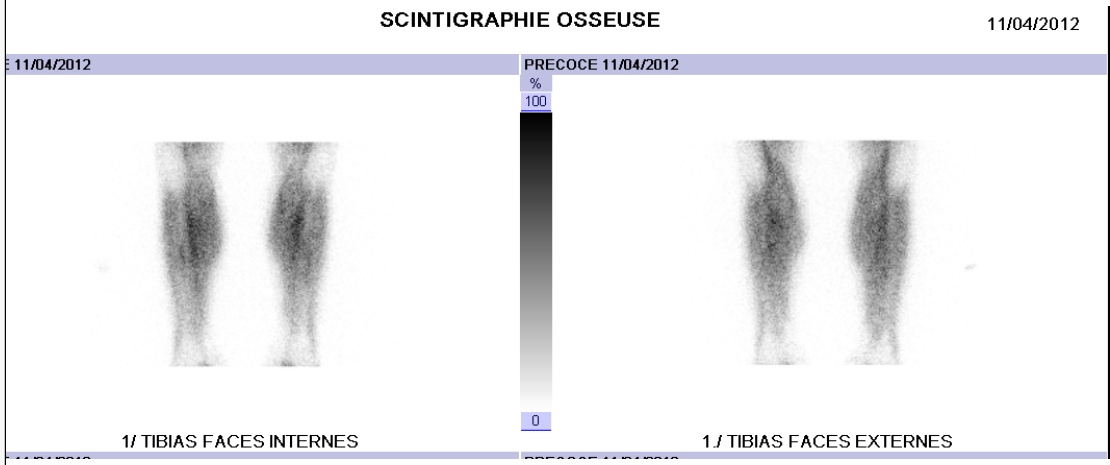

SPECT/CT tibias
Axial & coronal views

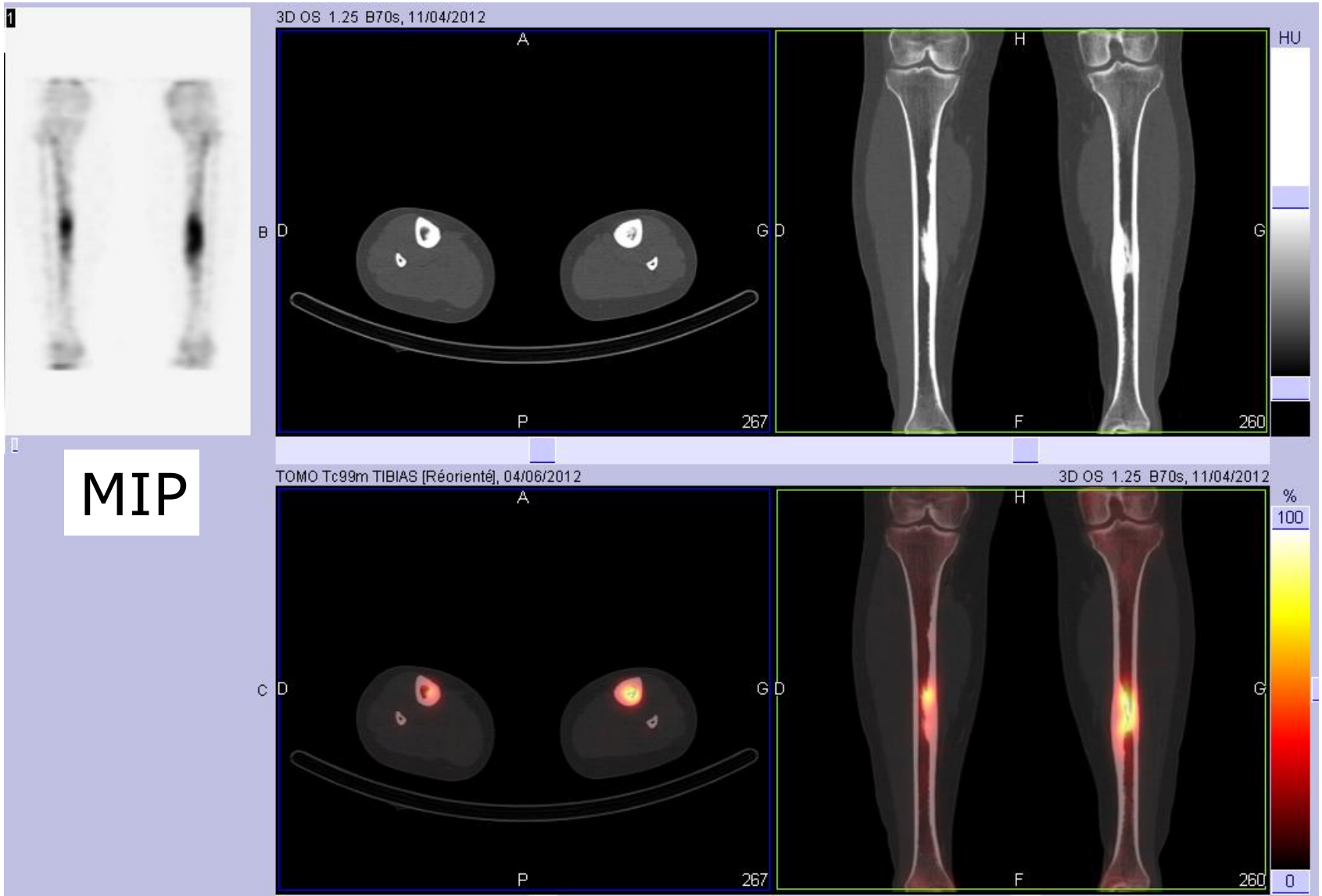

SPECT/CT tibias: Fused VRT

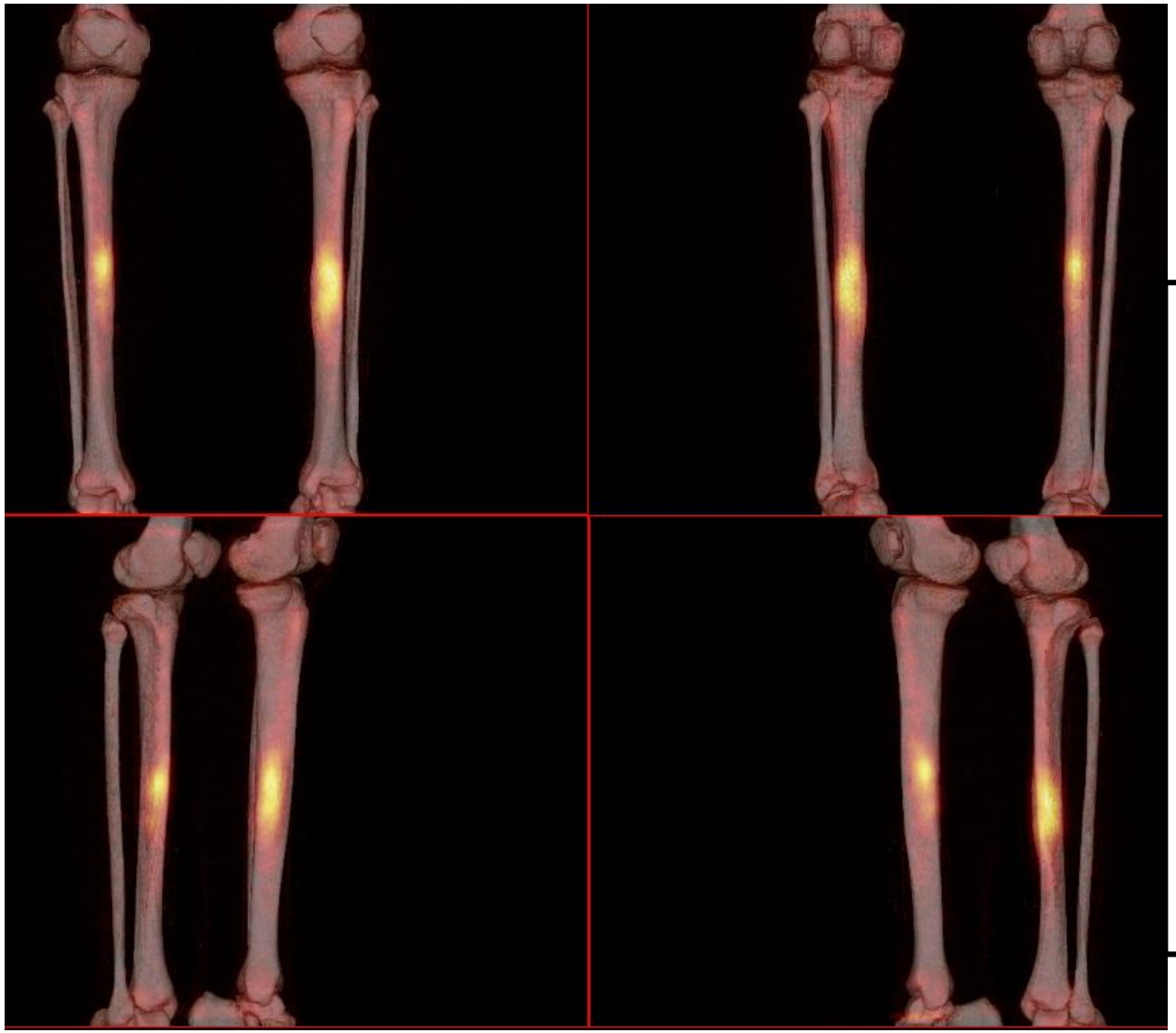

SPECT+/CT+
congruent pattern
Hyperostosis/hyperosteo blastosis cortical epicenter on both endosteal and periosteal aspects, bilateral and almost symmetrical of tibial diaphyses
Metaphyses and epiphyses spared

MRI tibias coronal view T1

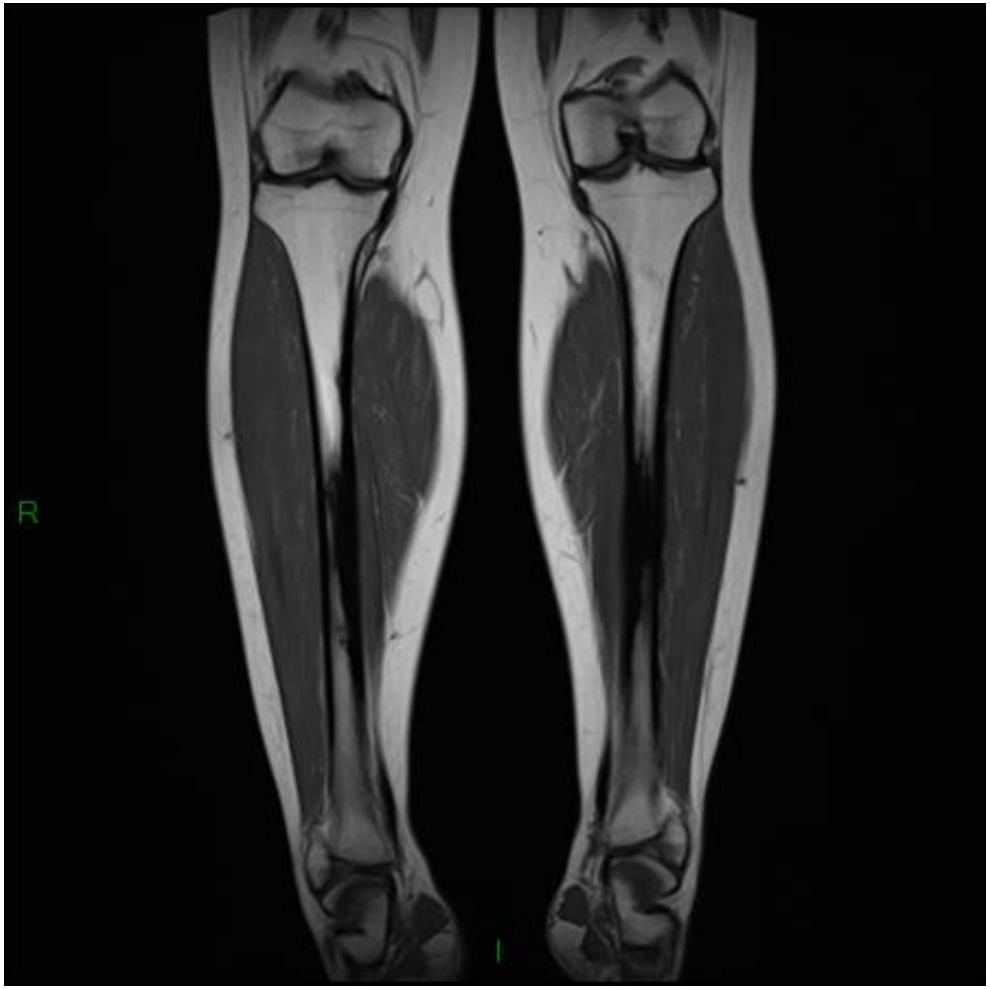

MRI tibias coronal view T1 Gd-enhanced

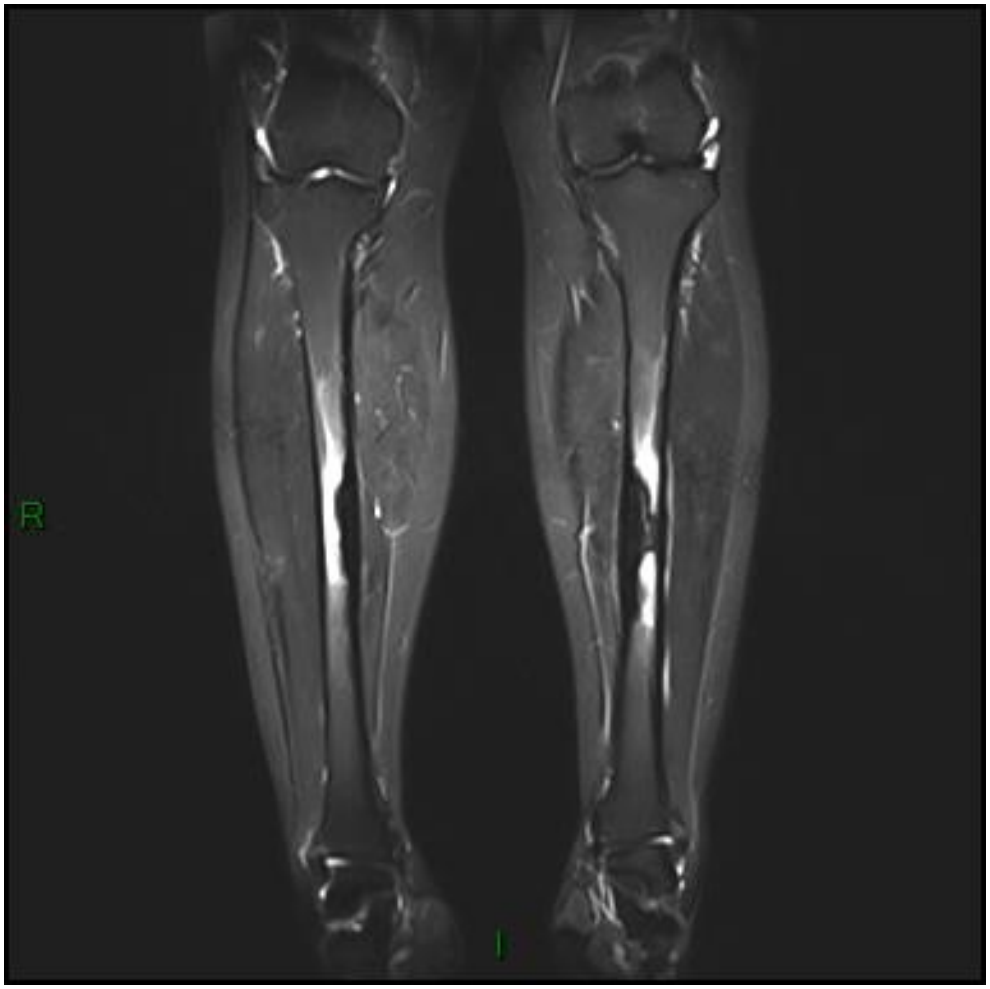

Tibias: coronal views
MRI-CT-SPECT correlation

MRI T1	CT *low dose*
MRI T1 Gd	Fused VRT

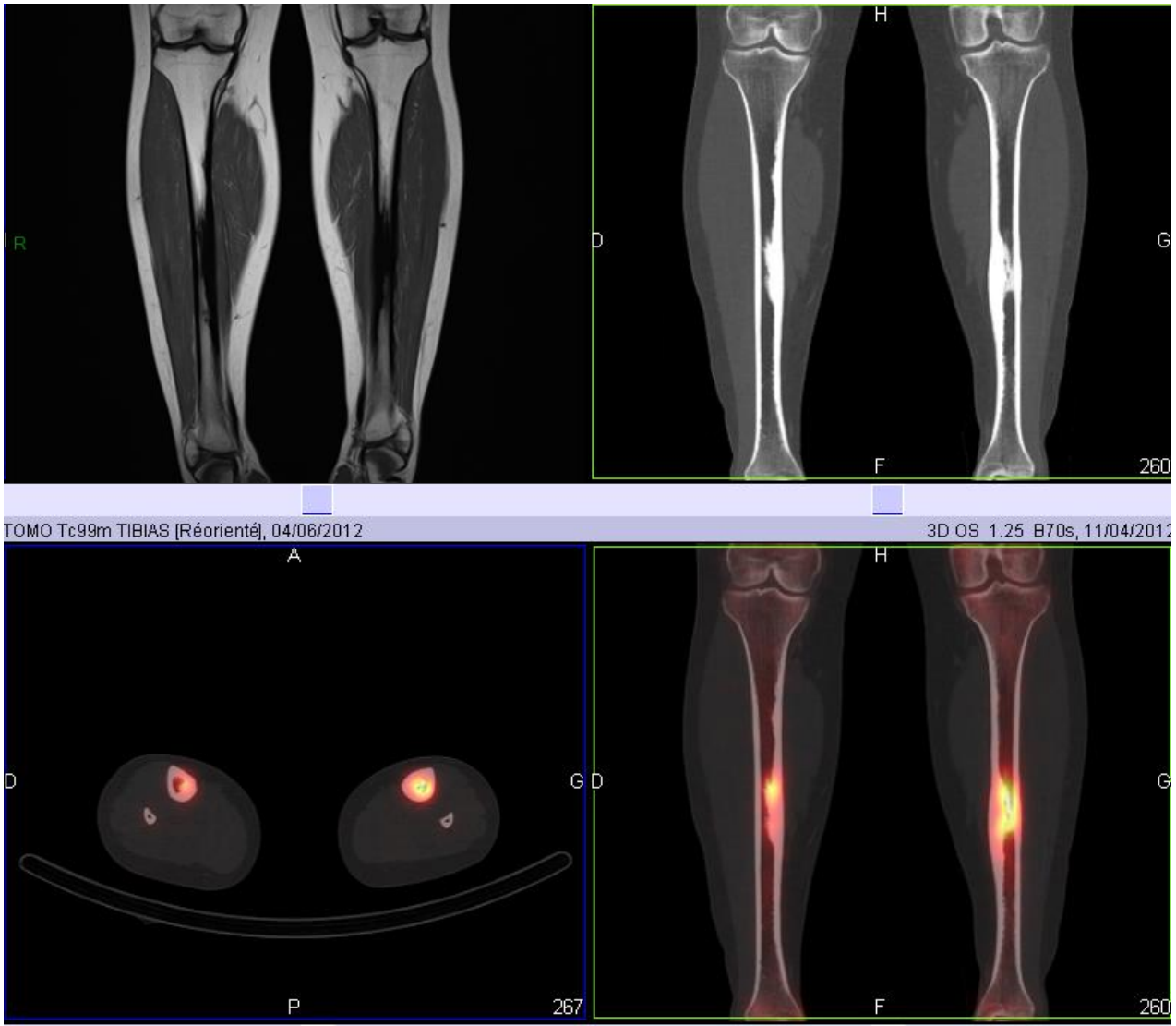

Diagnosis, please!?

1. Melorheostosis
2. Camurati-Engelmann disease
3. Shin splints
4. Erdheim-Chester disease
5. Schnitzler syndrome

Diagnosis, please!?
Correct answer

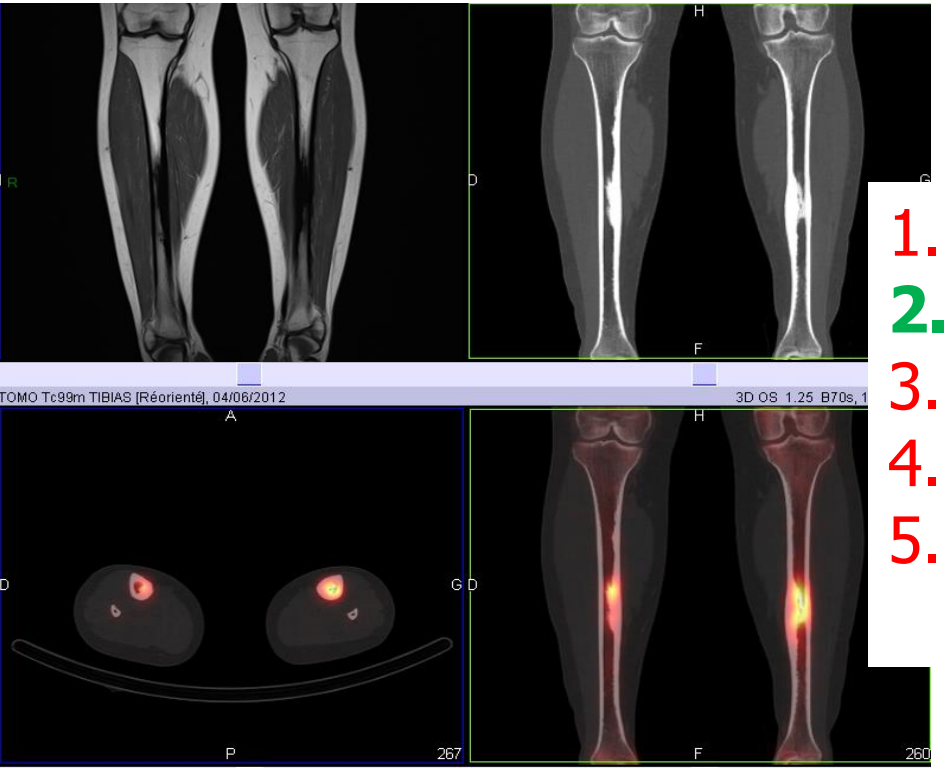

1. Melorheostosis
2. **Camurati-Engelmann disease**
3. Shin splints
4. Erdheim-Chester disease
5. Schnitzler syndrome

NON-INVASIVE IMAGING GROUNDED DIAGNOSIS

Progressive diaphyseal dysplasia [PDD]

(aka Camurati-Engelmann disease)

Confirmation with careful familial medical history taking with patient:

Likely PDD in mother and sister!

Camurati-Engelmann disease
Identity card

- Rare inherited disorder, featured by an extended bone dysplasia with increased diaphyseal thickness of tubular bones
- CED begins during childhood and mainly involves tibia, femur, humerus, cubitus, ulna, and skull basis
- Clinical syndrome encompasses osseous pain chiefly localized at legs, muscular weakness, with atrophy, waddling gait, fatigability, severe recurrent headaches, delayed puberty
- Plain X-rays: Cortical elongated thickening, periosteal and endosteal, of tubular bones diaphyses, in a symmetrical fashion, with stenosis/obliteration of medullary spaces (aftermath of intramembranous ossification disturbance!)
- Other abnormalities: Blood (anemia, leucopenia, increased ESR at contrast with CRP within normal limits), and vascular bed (Raynaud's phenomenon)

Nosology, genetics & therapy: An update

- Group of genetic osteosclerotic disorders
  - Neo-natal severe osteosclerotic dysplasias
  - Increased bone density dysplasias without bone shape alteration
  - Increased density dysplasias with metaphyseal and/or diaphyseal involvement

- Genetics: CED is expressing a dominant autosomal transmission but may appear de novo

- CED is triggered by TGFβ1 gene mutations.
  TGFβ1 is a key factor to recruit mesenchymal cells in osteoblastogenesis pathway.
  TGFβ1 is also disturbed in osteopoikilosis

- Therapy: Corticosteroids long-standing regimen

*W Van Hul. BoneKEy Reports **1**: 97 (2012)*

Camurati-Engelmann disease
Dysplasia of intramembraneous ossification

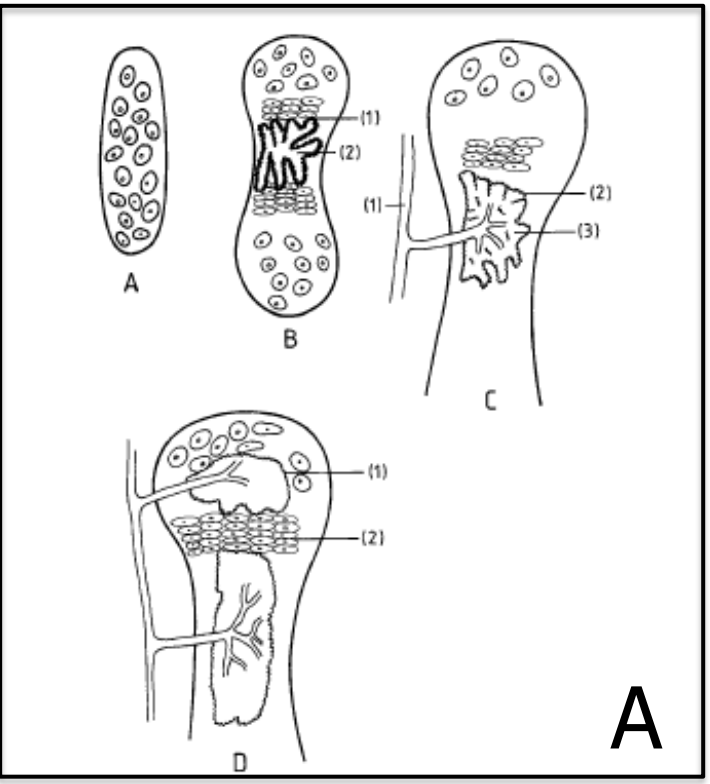

2 ossification pathways
for
human skeleton

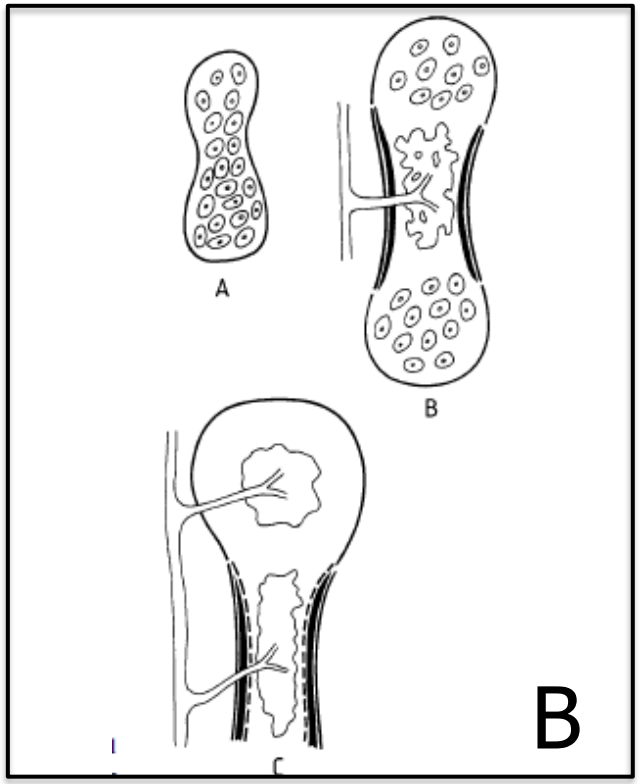

Endochondral bone formation (A) is a fundamental mechanism for longitudinal bone growth during vertebrate development. Cartilage, an avascular tissue, is replaced by bone in a process called endochondral ossification. During this process, the epiphyseal growth plate undergoes morphogenesis A region of resting chondrocytes differentiates into a zone of proliferating chondrocytes that then hypertrophies and finally undergoes apoptotic cell death, while being replaced by bone. The net result is lengthening of the bone, while the thickness of the growth plate remains relatively constant.
Intramembraneous bone (B), formed without cartilaginous models. With intramembranous bone formation, bone arises directly from mesenchyme. Target bones are tubular bones, and flat bones, and found in the cranial vault and facial region.

DIFFERENTIAL DIAGNOSIS

INSTANTIATION & PATTERN RECOGNITION

Differentials gamut: Tibial bilateral cortical increased uptake/osteosclerosis in adult

- ✓ Periostitis & tibial stress fractures by overuse (young or middle-aged)
- ✓ Chronic Recurrent Multifocal Osteomyelitis (CRMO)/SAPHO
- ✓ Metabolic osteopathies (Looser's zones/Milkman's fractures in osteomalacia)
- ✓ Erdheim-Chester disease (ECD)
- ✓ Myelofibrosis
- ✓ Tumors & pseudo-tumors:
  - ➢ Melorheostosis
  - ➢ Ribbing disease
  - ➢ Blood malignancies (lymphoma,…)
  - ➢ Peripheral osteo-medullary metastases
  - ➢ Pierre-Marie-Bamberger hypertrophic pulmonary osteoarthropathy

Ribbing disease
(Hereditary multiple diaphyseal sclerosis)

Seeger LL et al. Ribbing disease (multiple diap
sclerosis): Imaging and differential diagnosis.
AJR 1996; 167: 689-694

- Ribbing disease and CED sometimes decrypted as 2 phenotypes of same condition
- Autosomal recessive transmission
- Clinical manifestations occur in middle-aged individuals (on mature skeleton)
- Involvement of tubular bones
  - Exclusive
  - Unilateral or assymetrical and asynchrone
- Protracted course towards stabilization

Periostitis & stress fracture
Zwas classification

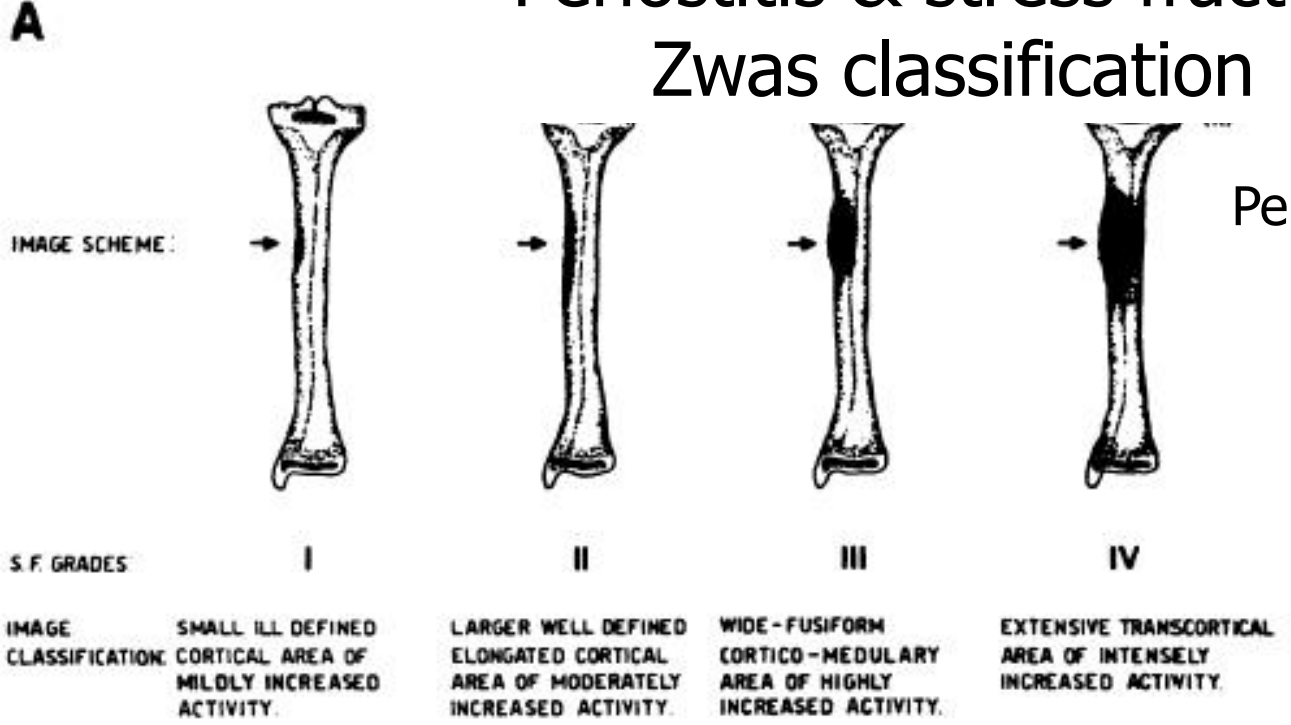

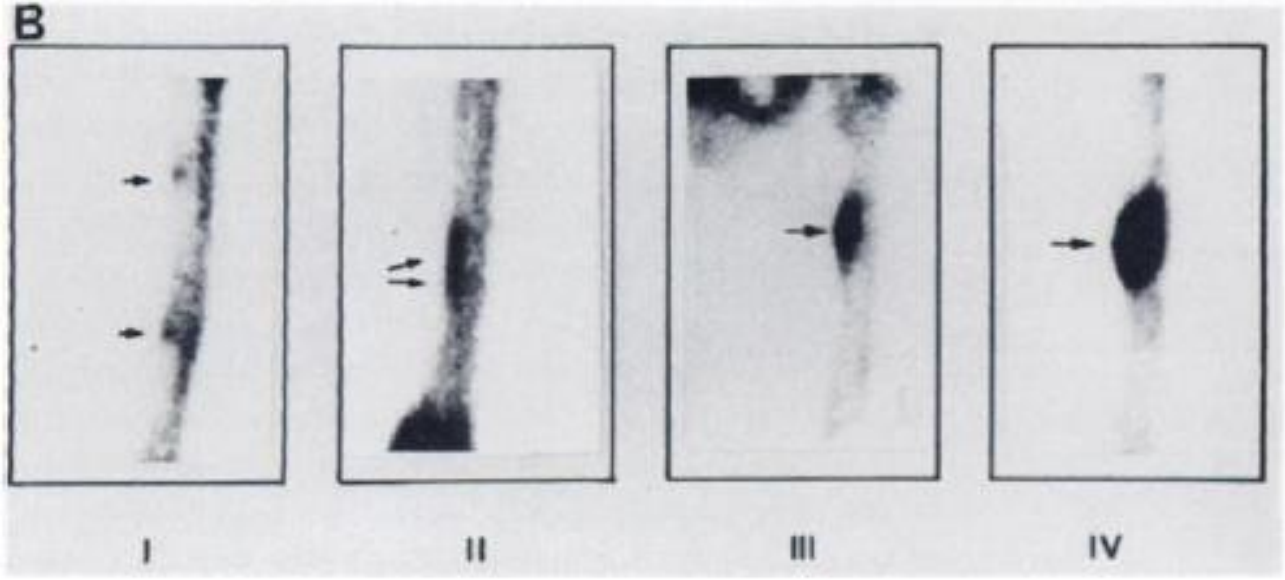

Periostitis & stress fracture
Planar bone scan
classifications

- Milgrom (1984)
- Zwas (1987)
- Matin (1987)

✓ Very similar
✓ Grounded on increased uptake thickness
✓Zwas = Best trade-off between diagnostic accuracy and in-the-field practice!

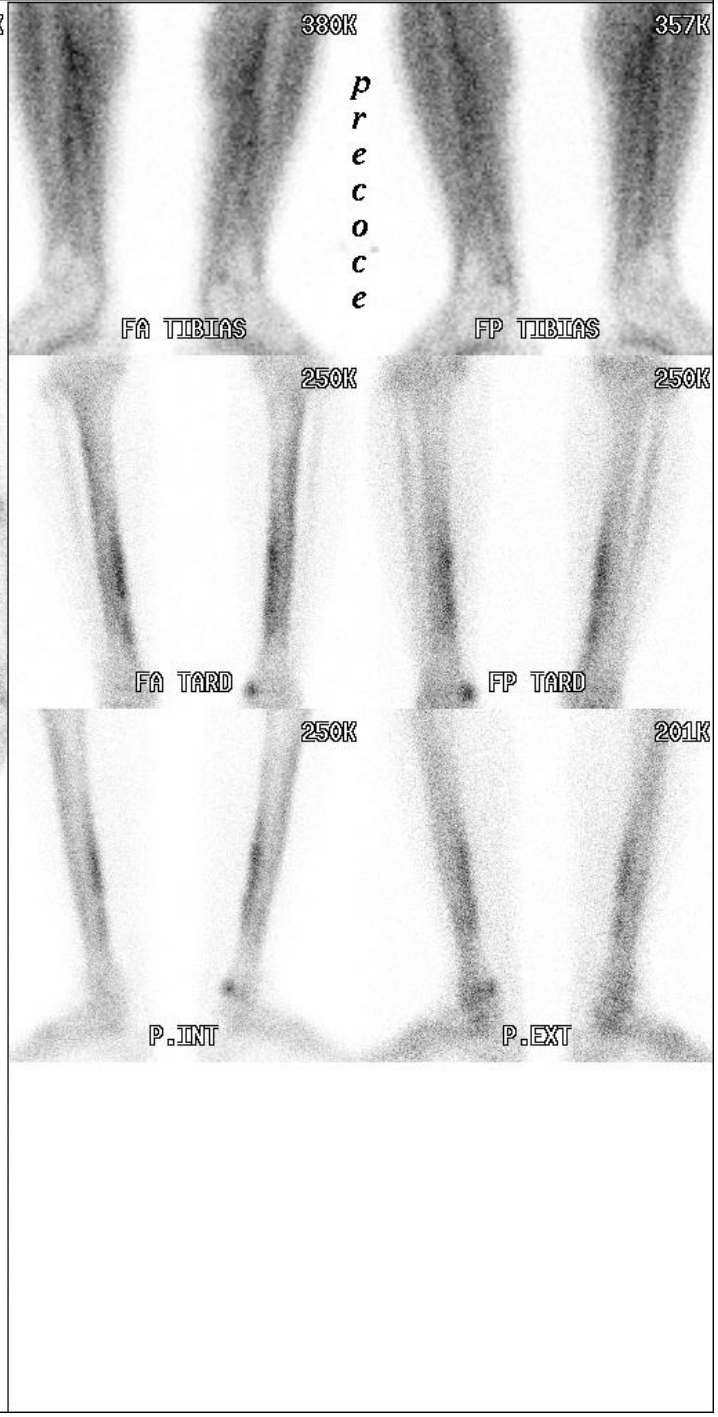

<u>Clinical presentation</u>:
M, 25 yo
Soccer player
Mechanical pain
R+L tibias (4 months)

<u>Plain X-rays</u>:
Unconspicuous

<u>Bone scan</u>:
R+L tibial periostitis
+
osseous tears L tibial malleolus

Hypertrophic osteo-arthropathy
Osteolytic metastasis R acetabulum
Causative primitive: NSCLC

Differential diagnosis lower limbs skeleton:

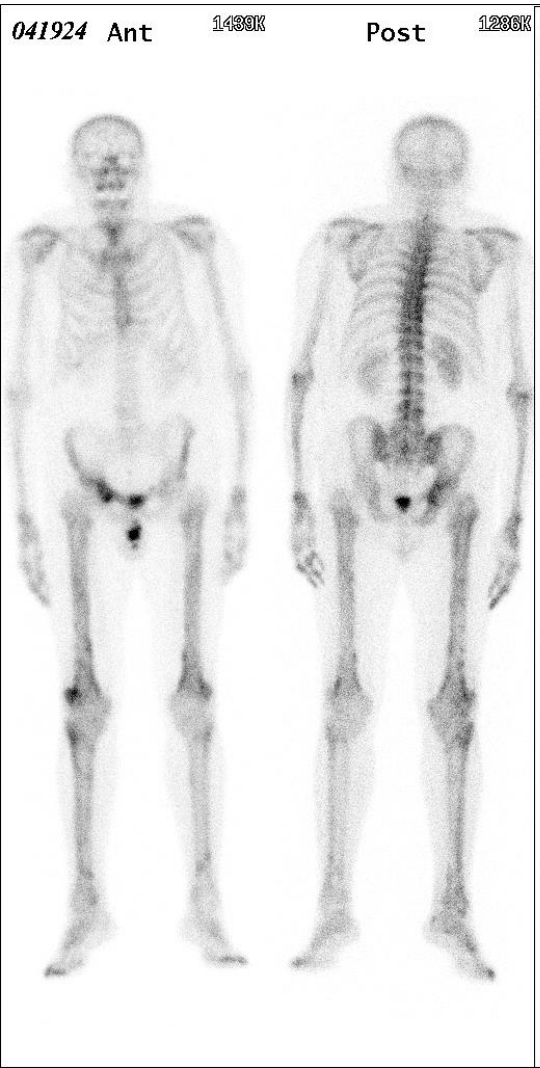

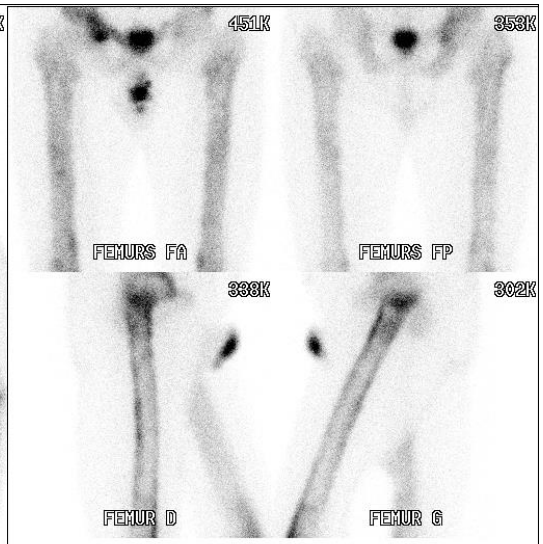

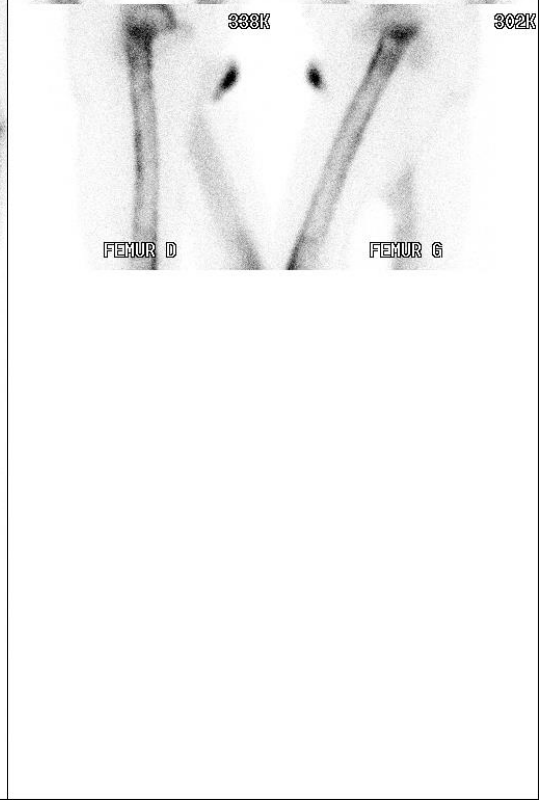

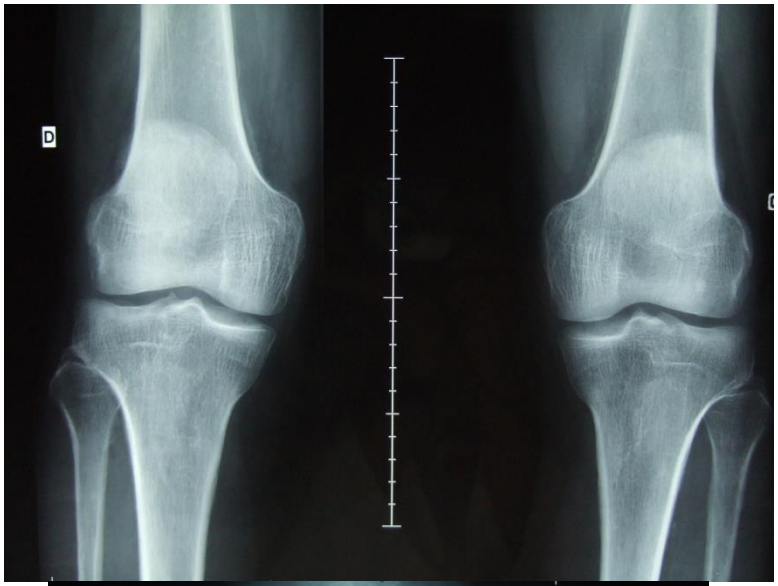

Scintigraphic patterns at **regional scale** (lower limbs skeleton) & **systemic scale** (total skeleton) (1/3)

Maladie de Erdheim-Chester

Syndrome de Schnitzler

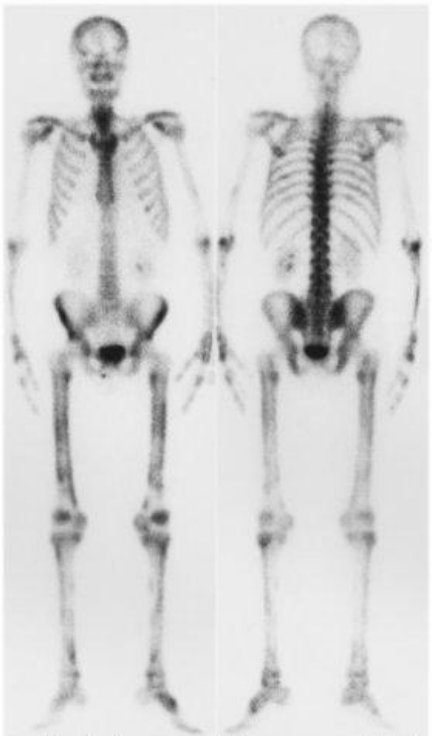

Ostéoarthropathie hypertrophiante pneumique

Envahissement métastatique osseux

(pseudo-) cold knees

hot knees (epimetaphyseal sclerosis)

Scintigraphic patterns at **regional scale** (lower limbs skeleton) & **systemic scale** (total skeleton) (2/3)

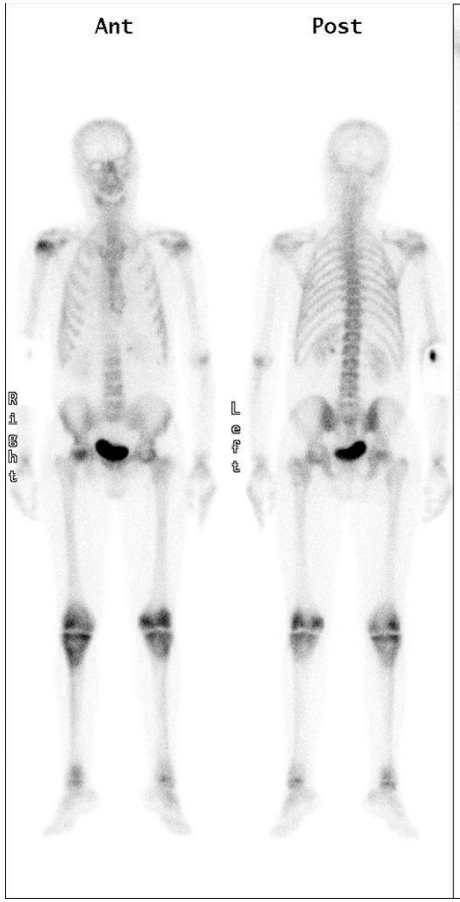

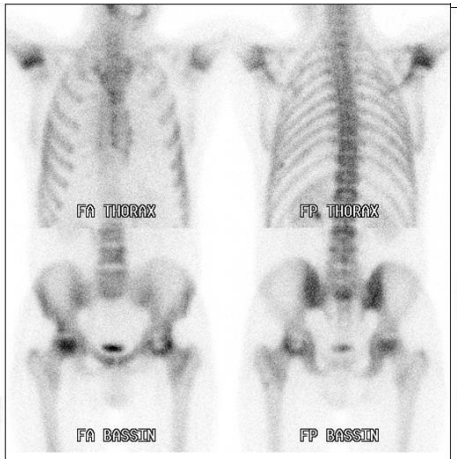

OSTEONECROSE MULTIFOCALE

– *Homme de 48 ans*

– *Cancer du larynx opere*

– *Corticotherapie prolongee recente*

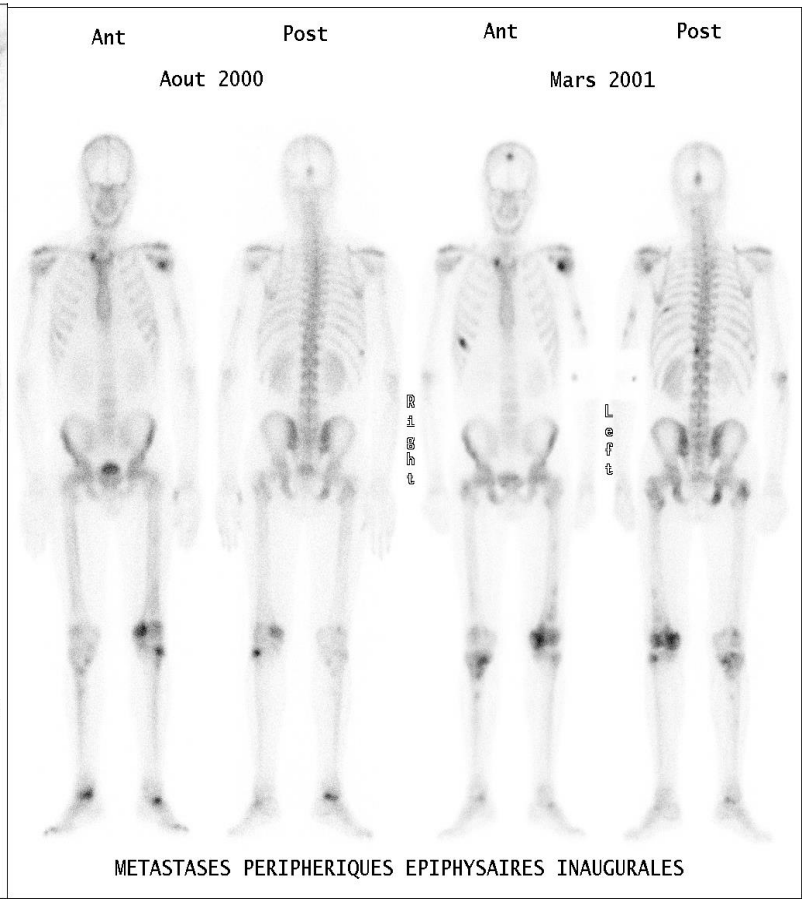

METASTASES PERIPHERIQUES EPIPHYSAIRES INAUGURALES

Scintigraphic patterns at **regional scale** (lower limbs skeleton) & **systemic scale** (total skeleton) (3/3)

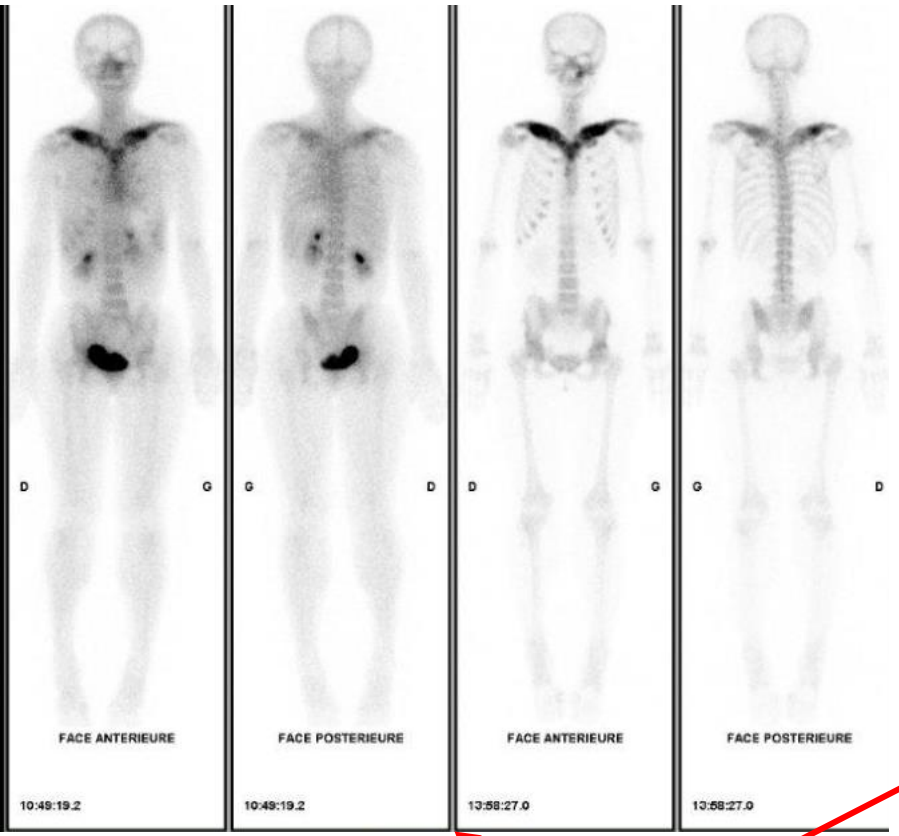

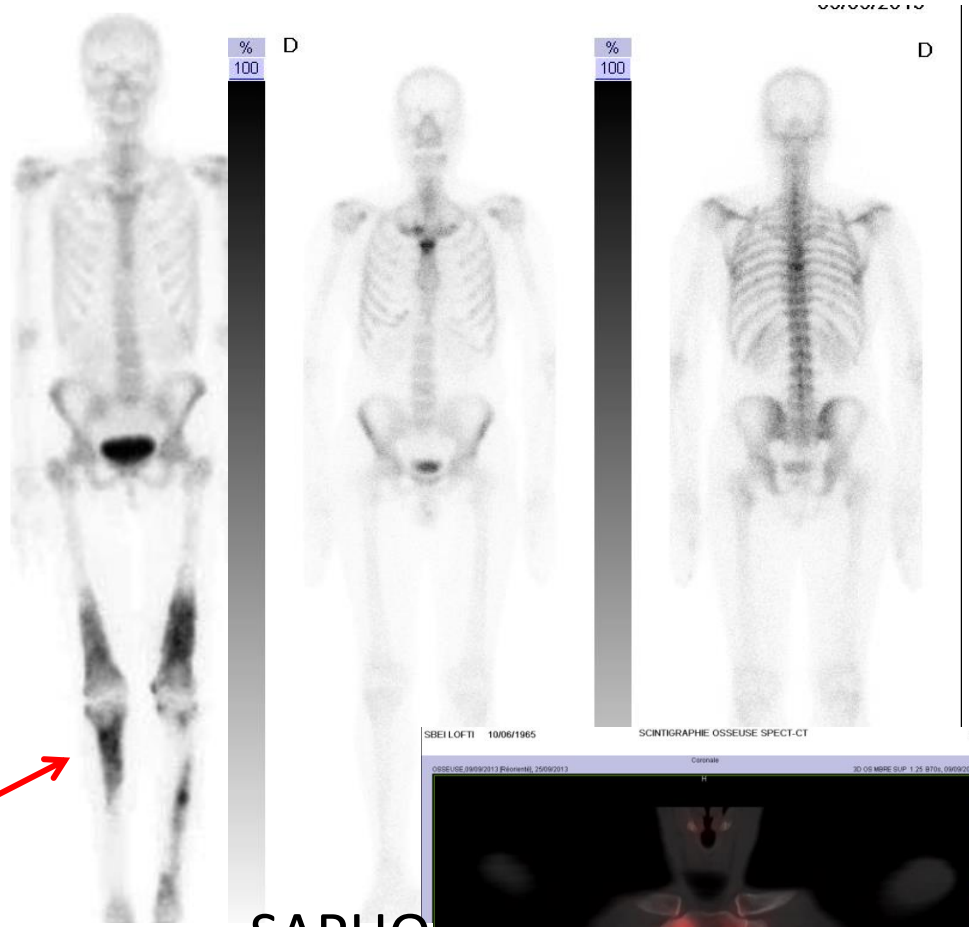

SAPHO

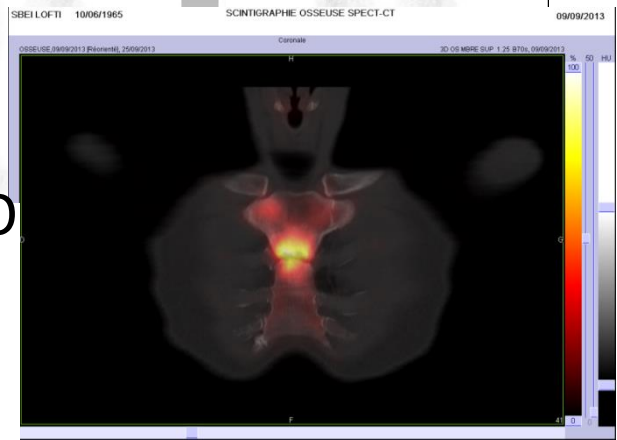

CRMO:

Bilateral diametaphyseal increased uptake sleeves

Regional pattern

Melorheostosis

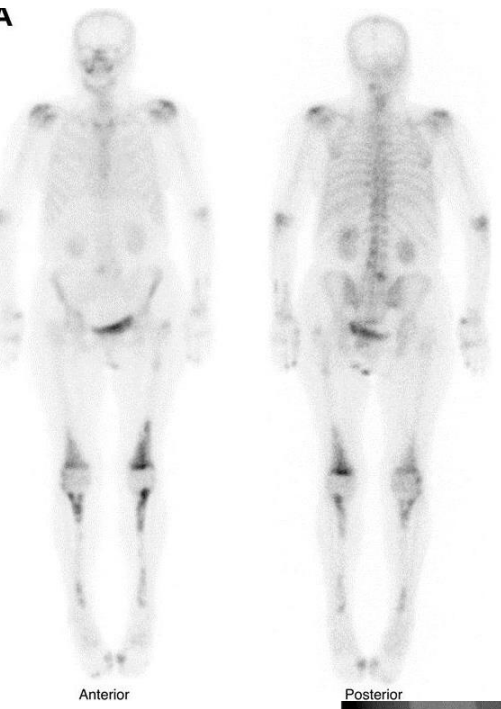

Li Sonoda
Clin Nucl Med
2011

- Periosteal hyperostosis
- Usually apparent in early childhood, 50% develop symptoms by age 20
- RX/CT: Asymmetric cortical hyperostosis in contiguous bones, often with an appearance of melting candle wax
- Bone scan appearance : moderate increase of tracer uptake in an asymmetric linear pattern
- Condition can be polyostotic, involving contiguous bones across the joints along the sclerotomal distribution

Key messages

- Unfrequent condition
- Misleading clinical presentation
- Radio-scintigraphic picture usually stereotyped
- Familial history taking
- Biopsy avoidable++

Bibliographic landmarks

- ✓ Greenspan A. Sclerosing bone dysplasias- a target-site approach. Skeletal Radiol 1991; 20: 561-583.
- ✓ de Vernejoul MC. Sclerosing bone disorders. Best Pract Res Clin Rheumatol 2008; 22 (1): 71-83.
- ✓ Vanhoenacker FM, de Beuckeleer LH, Van Hul W, Balemans W, Tan GJ, Hill SC, De Schepper AM. Sclerosing bone dysplasias: genetic and radioclinical features. Eur Radiol 2000; 10: 1423-33.
- ✓ Momose M. et al. Camurati–Engelmann disease on a 99mTc-HMDP bone scan. Eur J Nucl Med Mol Imaging 2008; 35:2143
- ✓ Robins PD, Blake MP, Robinson PS. SAPHO Syndrome mimicking metastases on bone scintigraphy. Clinical Nuclear Medicine 1998; 23: 696.
- ✓ Fukumitsu N, et al. Bone scintigraphy in polyostotic fibrous dysplasia. Clinical Nuclear Medicine 1999; 24: 446.
- ✓ Cift H, Unay K, Ozkan K, Akcal MA, Eceviz E. Four extremity fractures in a patient with renal osteodystrophy. J Ren Care 2010; 36: 21-4.
- ✓ D.C. Davis et al. Melorheostosis on three-phase bone scintigraphy - case report. Clinical Nuclear Medicine 1991; 17:561-564.

7. Activity

Activity
What do you mean!?

- Bone lesion turn-over = (99mTc)-BP bone scan
- Bone lesion metabolism+inflammatory reaction = FDG PET/CT, MRI

Bone island/enostosis

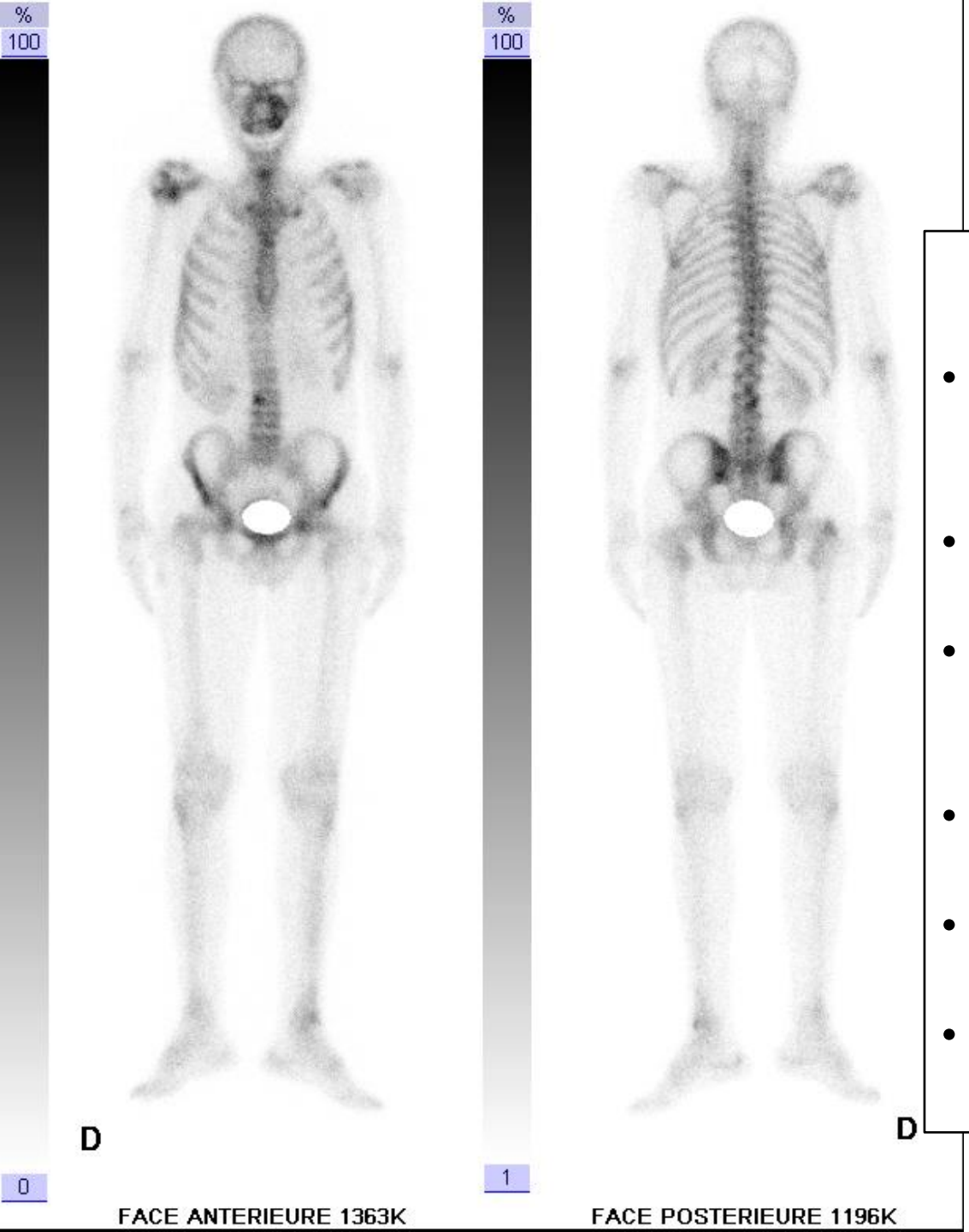

Clinical setting

- Pollakiuria revealing a prostate carcinoma
- PSA total initial = 23 ng/mL
- Prostatectomy in Feb 2009 followed by hormonotherapy
- PSA = 8 ng/mL
- No bone symptoms
- Medical history: Traumatic fractures

SPECT/CT lumbar spine

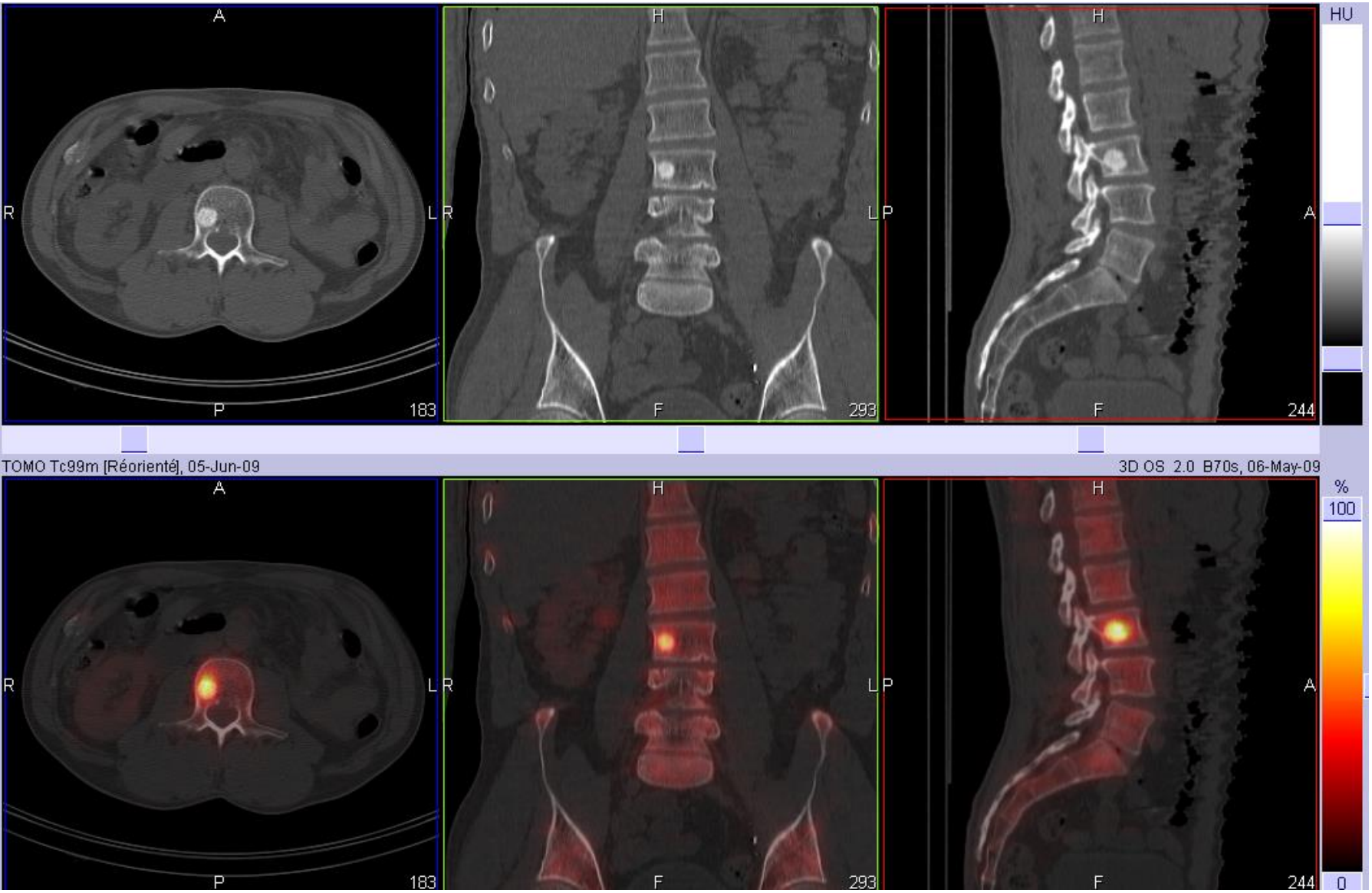

Lumbar spine
SPECT/CT Fused VRT

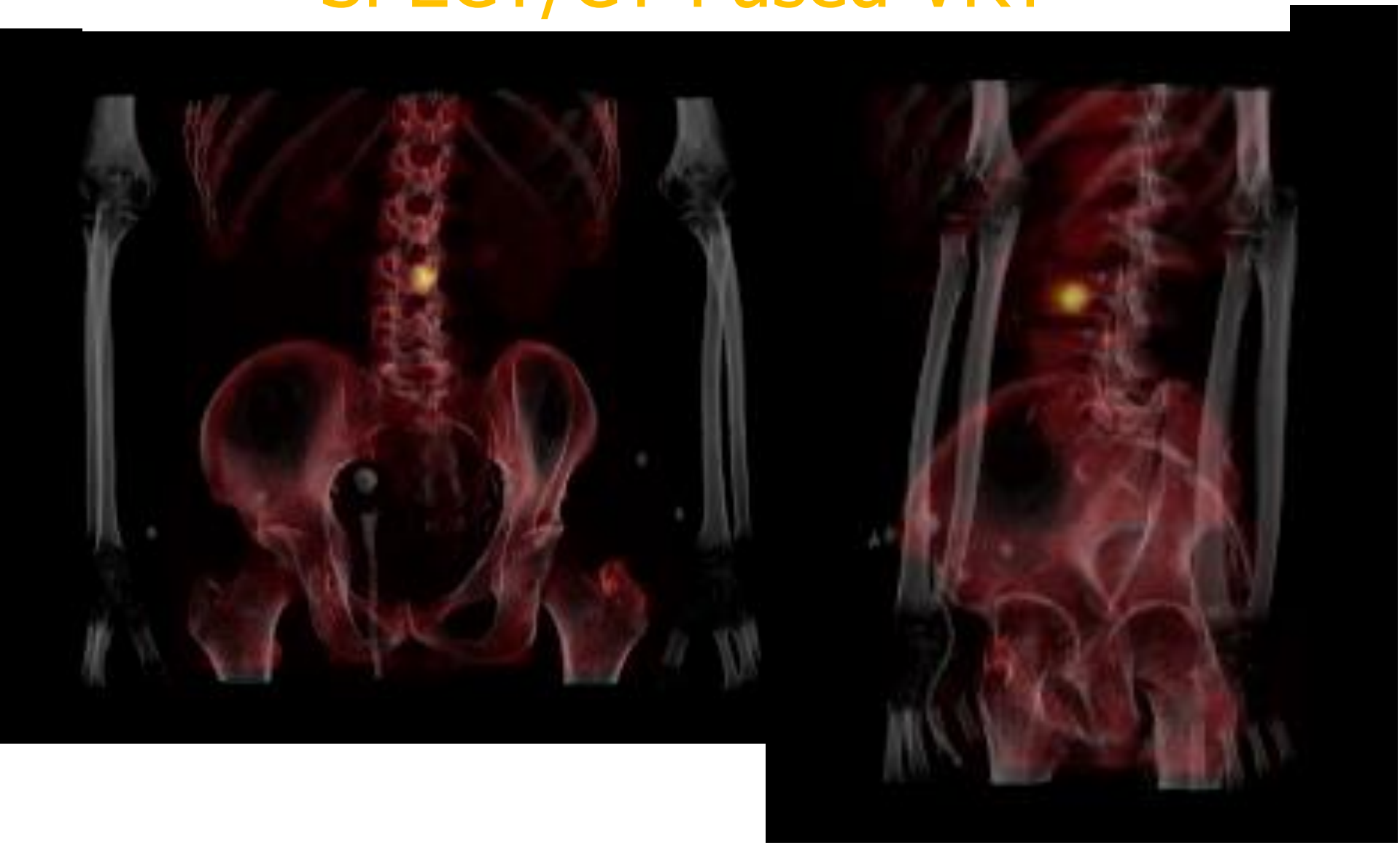

Solitary focal sclerotic lesion
A diagnostic dilemma in CT?

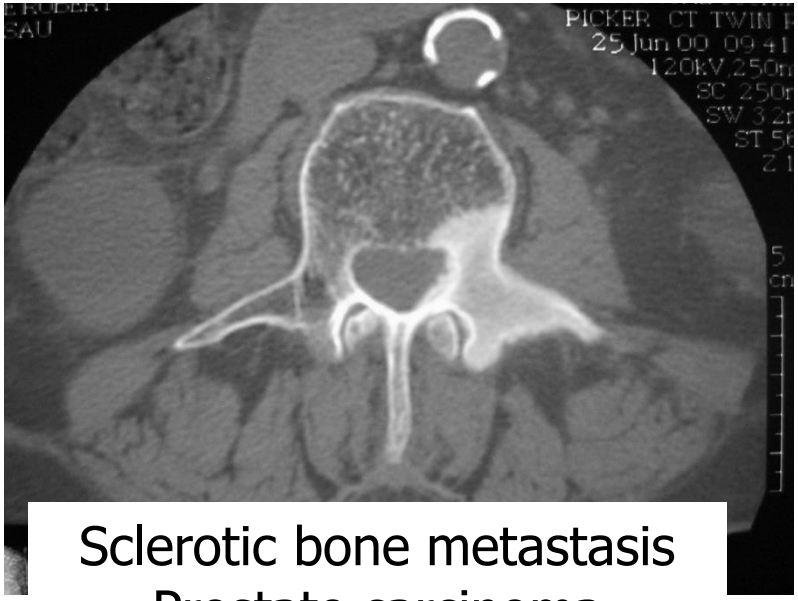

Sclerotic bone metastasis
Prostate carcinoma

- Low density area, rule-of-thumb < cortical density
- Matrix texture heterogeneous
- Fuzzy borders
- Frequent cortical disruption
- Pedicle often invaded

CT acquisition set up in diagnostic protocol mandatory for deciphering differential!

Bone island (enostosis)

- Sclerotic nodule, very high density
  rule-of-thumb > cortical density
  Matrix texture homogeneous
- Geometry rounded or elongated
- Developed in full spongiosa
  But neighbouring cortical shell
- Intact cortical
- Size varies between 1 mm and 2 cm
- Borders clear-cut and spiculated
  In continuity with cancellous trabeculae
- Pedicle rarely involved

Distinguishing untreated sclerotic/osteoblastic metastases from bone islands using CT attenuation measurements

- Mean and maximum CT attenuation values of enostoses were 1190 ± 239 HU and 1323 ± 234 HU, respectively
- Mean and maximum CT attenuation values of osteoblastic metastases were 654 ± 176 HU and 787 ± 194 HU, respectively
- Using a cutoff of 885 HU for mean CT attenuation, the AUC was 0.982, sensitivity was 95%, and specificity was 96%
- Using a cutoff of 1060 HU for maximum CT attenuation, the AUC was 0.976, sensitivity was 95%, and specificity was 96%

Ulano, A AJR 2016; 207: 362–368

Distinguishing untreated sclerotic/osteoblastic metastases from bone islands using CT attenuation measurements (C't'd)

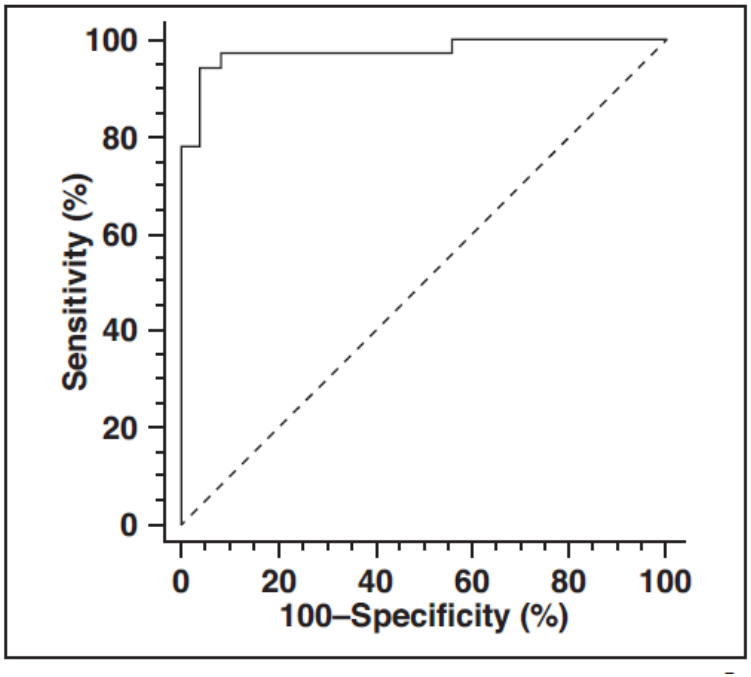

AUC of 0.982 for maximum attenuation

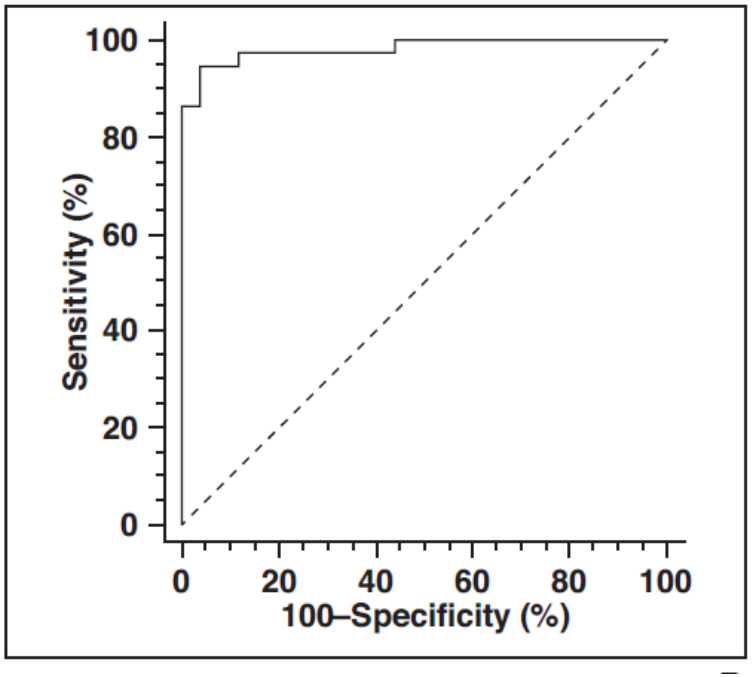

AUC of 0.976 for mean attenuation

Bone island:
Comparison of measurements
HU densities (CT) and turn-over rate (SPECT)

Uptake ratio
BI/spongiosa:
=
4,5

Densities:
BI = 600 HU
Spongiosa=100 HU

Sclerotic metastasis
Carcinoid tumor

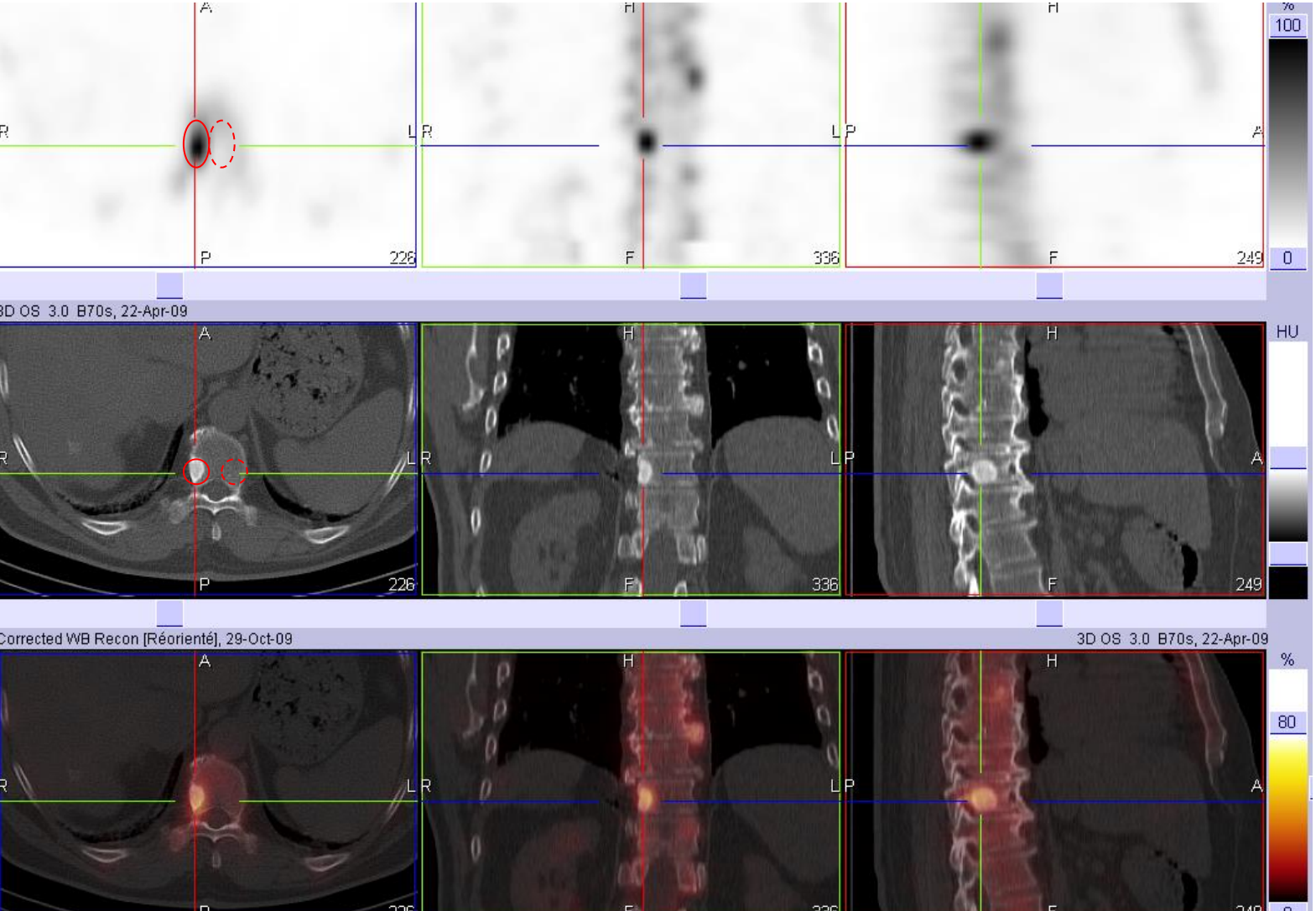

Uptake ratio
BM/spongiosa:
=
3,7

Densities:
BM = 500 HU
Spongiosa=100
HU

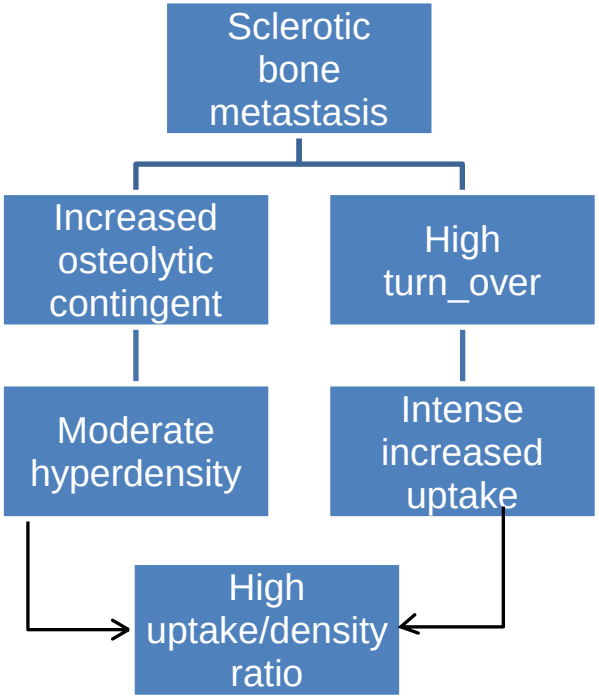

Sclerotic metastases vs sclerotic dysplasia?:

SPECT/CT « Ratios of ratios »

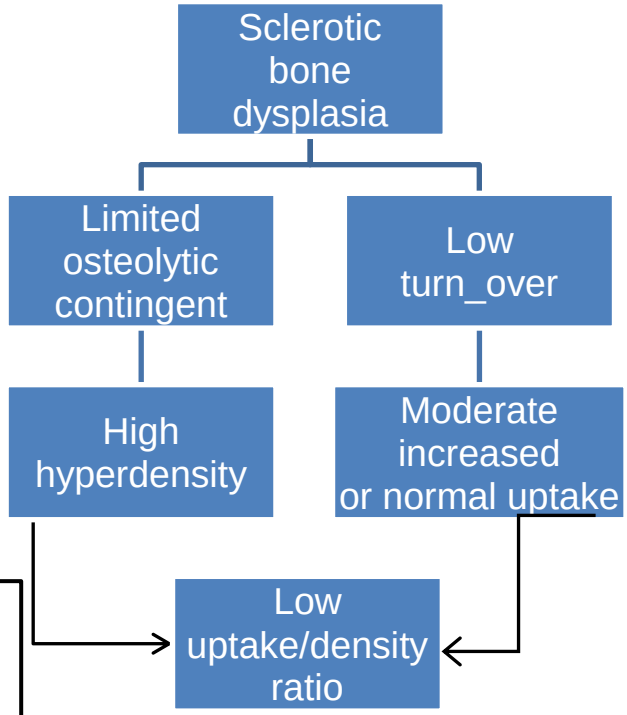

Achong DM. Increased uptake in a vertebral bone island seen only on SPECT. Clin Nucl Med 2007; 32(8): 620-3.

Uncoupled increased density and increased turn-over in bone mets?

Rationale

Sclerotic metastases …
always associated to bone resorption

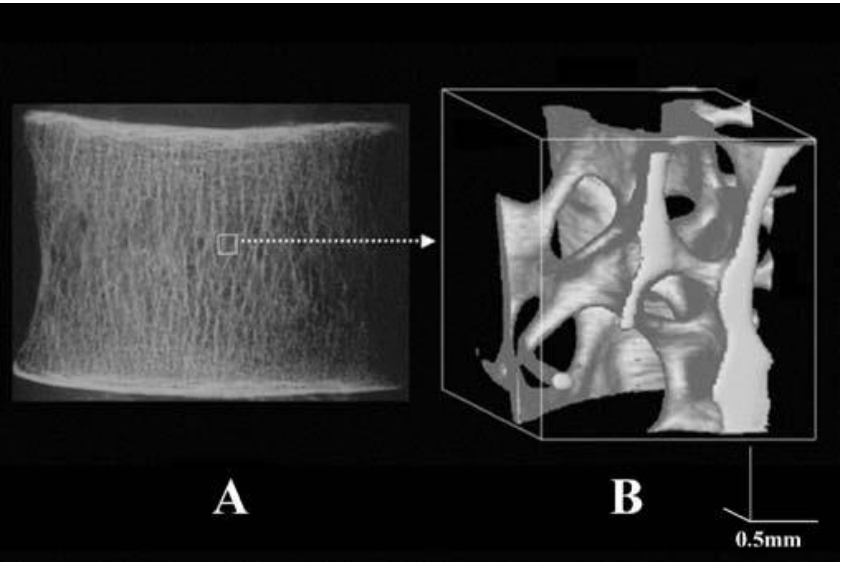

Normal vertebra

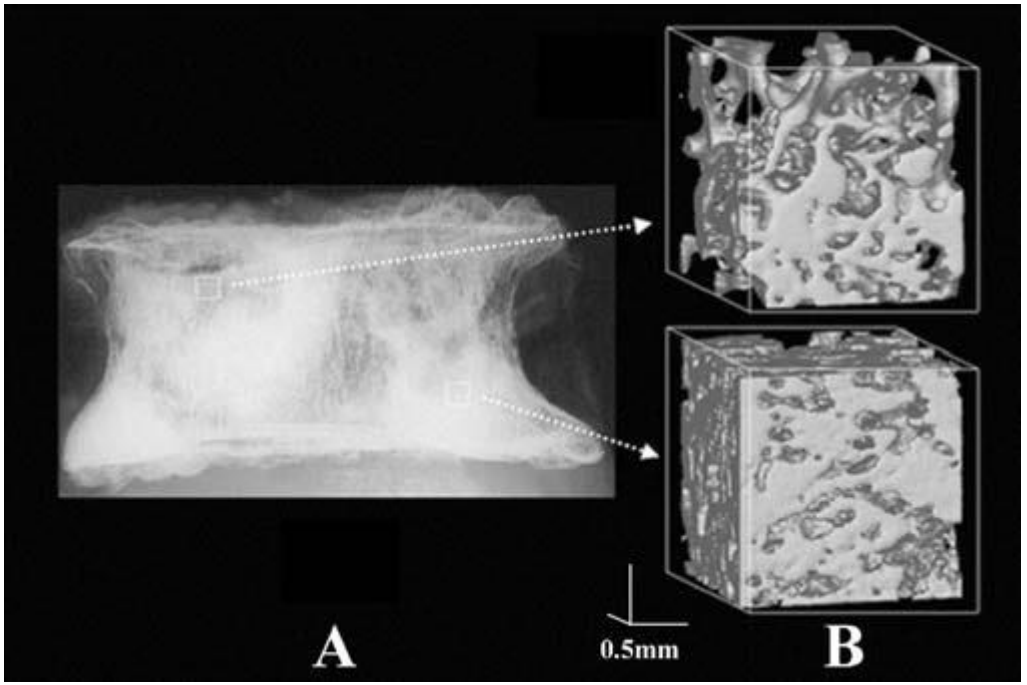

Sclerotic metastasis

Tamada, Skeletal Radiology 2005

« Fifty shades of grey »: Hounsfield CT scale

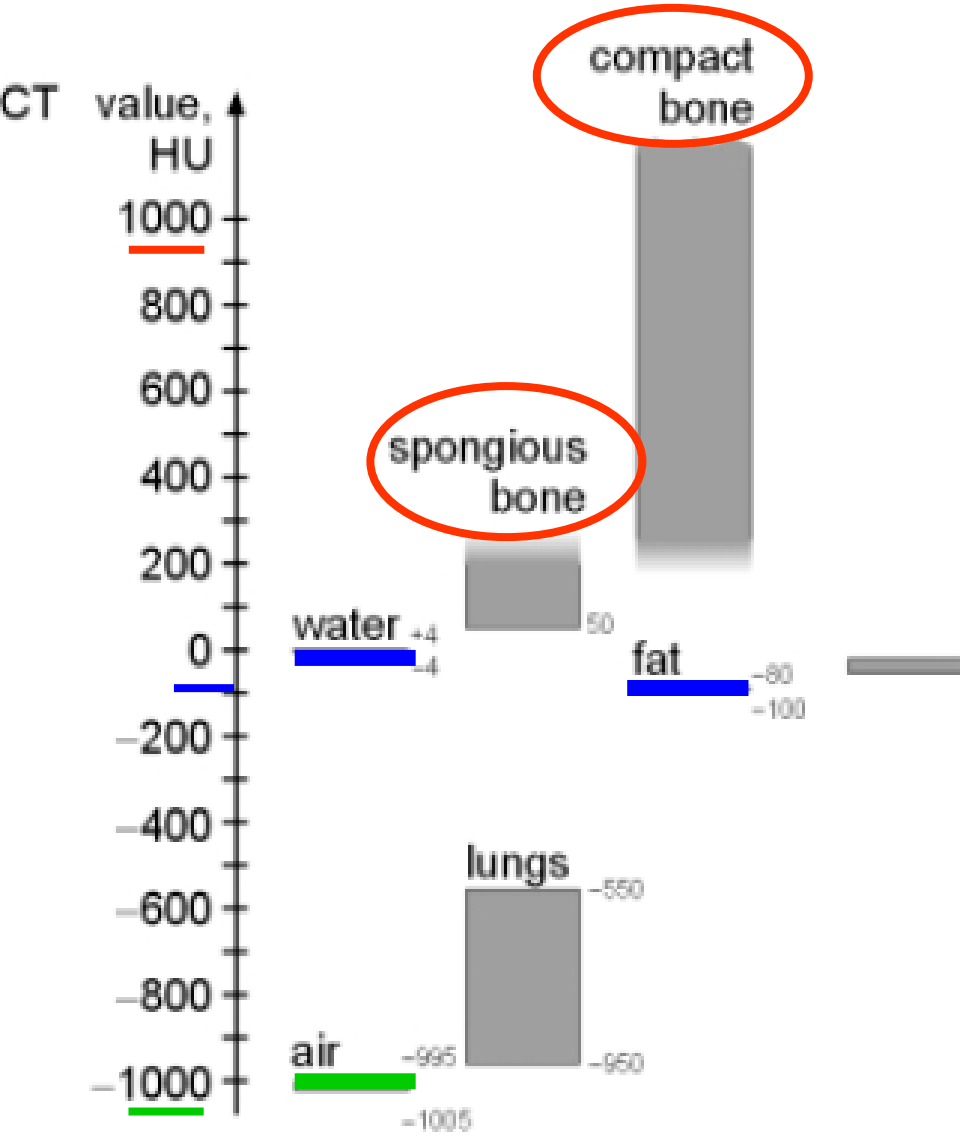

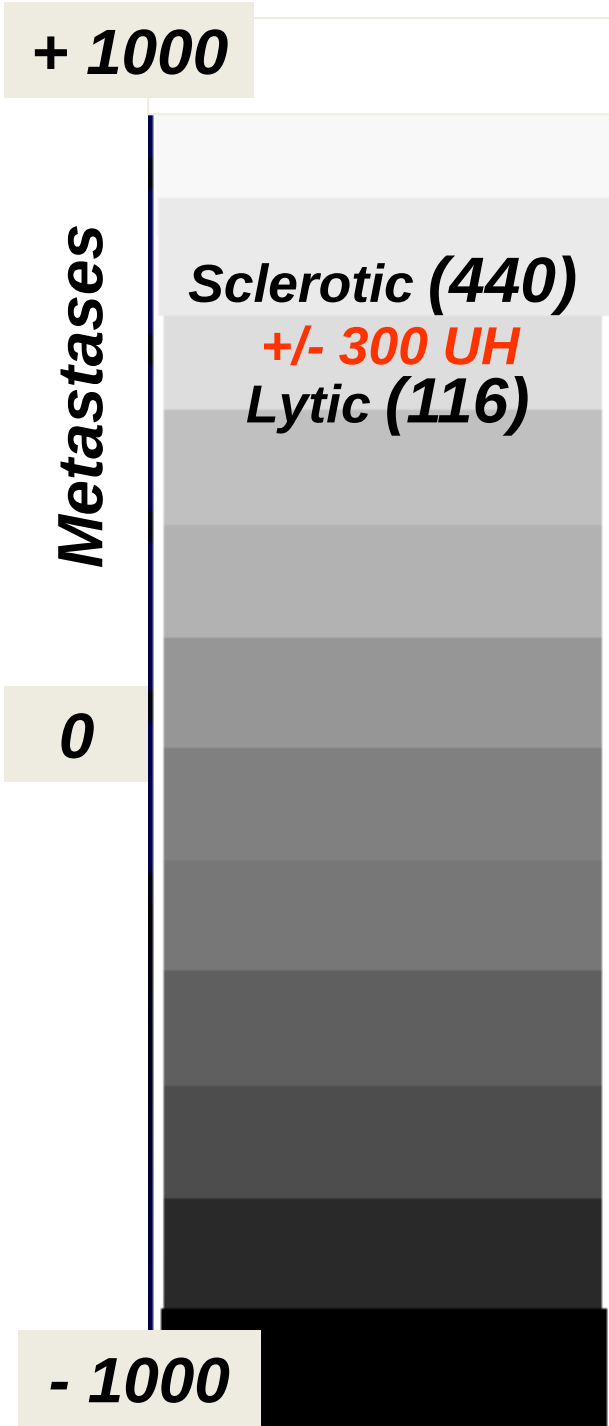

Kalender CT 2000 / Vassiliou CEM 2007 / Quattrocchi SR 2007

FDG PET/CT:
SUV in benign and malignant bone tumors

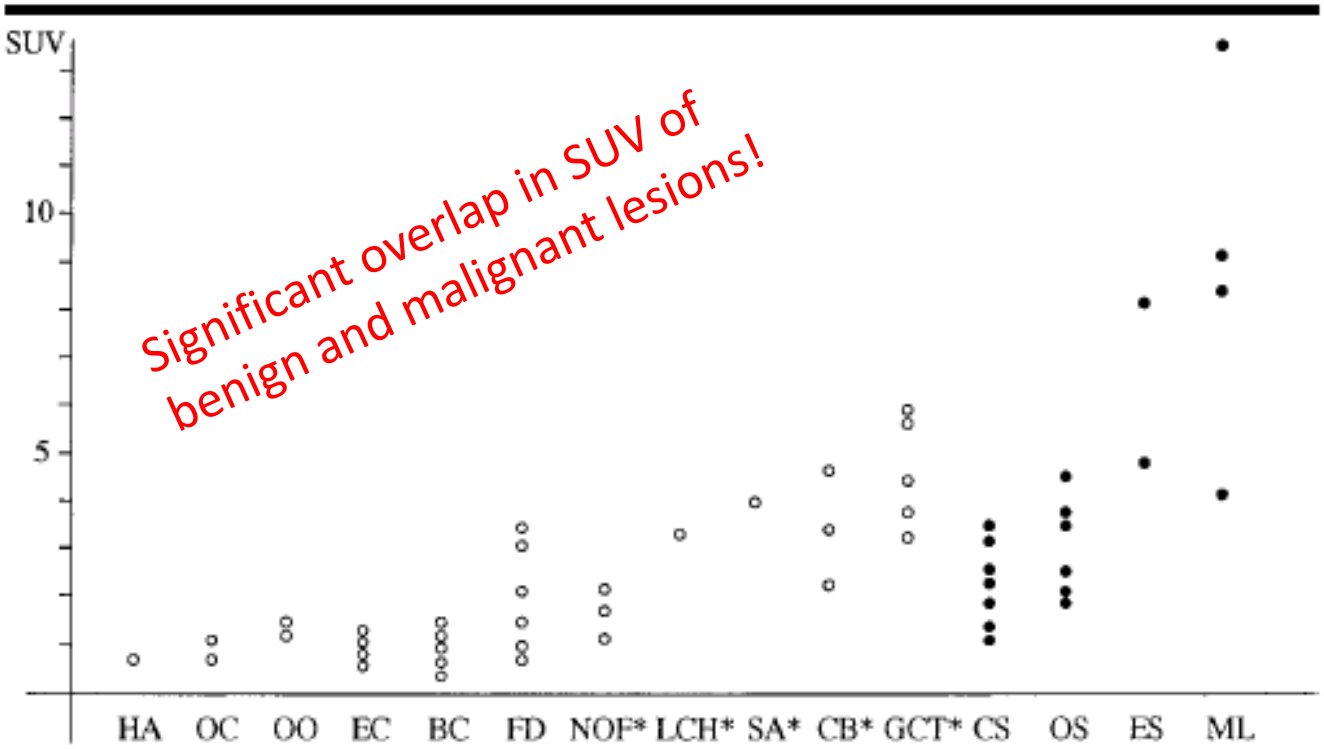

Figure 1. Graph shows SUVs of primary bone tumors and tumorlike lesions. ○ = benign lesions, ● = malignant tumors, and ⋆ = histiocytic or giant cell–containing lesions. SUVs were 3.52 ± 1.42 for histiocytic lesions, 1.31 ± 0.76 for nonhistiocytic benign lesions, and 4.34 ± 3.19 for malignant tumors. *BC* = bone cyst, *CB* = chondroblastoma, *CS* = chondrosarcoma, *EC* = enchondroma, *ES* = Ewing sarcoma, *FD* = fibrous dysplasia, *GCT* = giant cell tumor, *HA* = hemangioma, *LCH* = Langerhans cell histiocytosis, *ML* = malignant lymphoma, *NOF* = nonossifying fibroma, *OC* = osteochondroma, *OO* = osteoid osteoma, *OS* = osteosarcoma, *SA* = sarcoidosis.

Aoki et al., Radiology 2001

Painful lump in the thigh in a patient on follow-up for a prostate cancer

Clinical presentation

- M, 63 year-old
- Perception by patient of a painful lump at antero medial portion of right mid-thigh, 6 months ago
- Medical history: Prostate cancer diagnosed in 2013
  - Radical prostatectomy in January 2014
  - Patient cannot remember if he underwent a MDCT or a bone scan in baseline work up!
  - Last PSA dosage: 0.01 ng/mL

X-Rays right femur

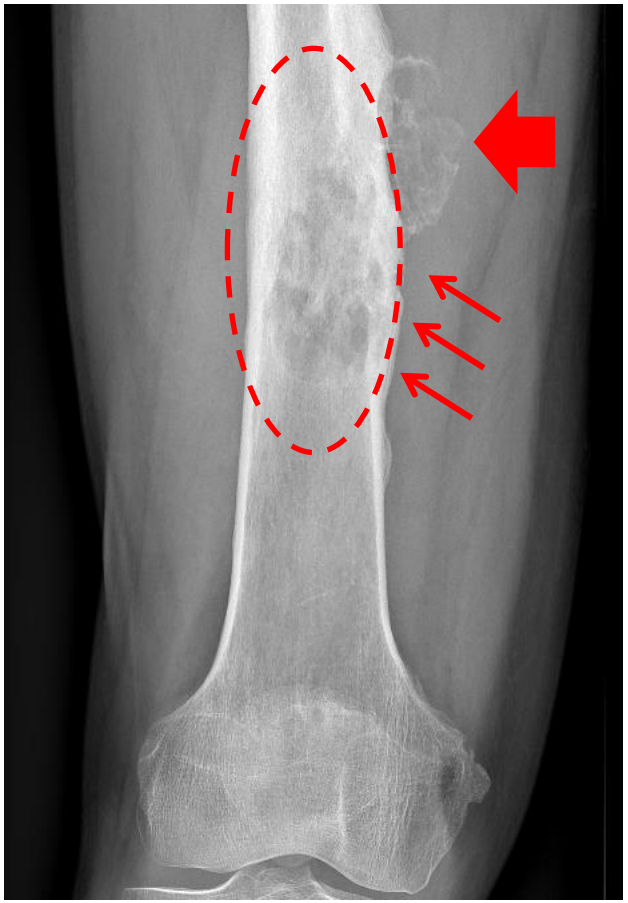

MDCT femurs

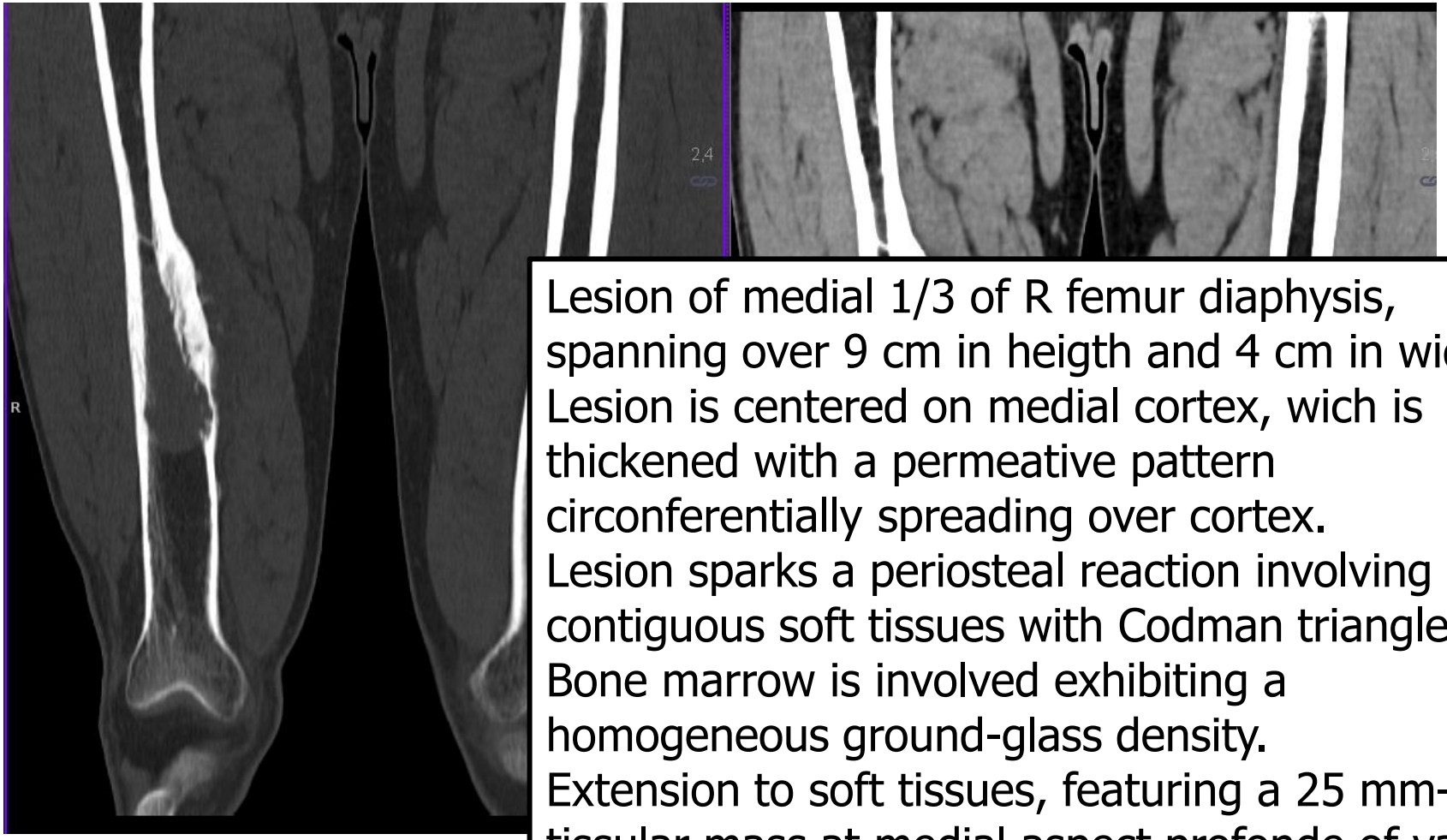

Lesion of medial 1/3 of R femur diaphysis, spanning over 9 cm in heigth and 4 cm in width.
Lesion is centered on medial cortex, wich is thickened with a permeative pattern circonferentially spreading over cortex.
Lesion sparks a periosteal reaction involving contiguous soft tissues with Codman triangle.
Bone marrow is involved exhibiting a homogeneous ground-glass density.
Extension to soft tissues, featuring a 25 mm-tissular mass at medial aspect profonde of vastus intermedius muscle.
No skip lesion.
Sparing of R hip and knee joints.

MRI Right femur
T1 & T1 IV FATSAT
Sagittal views

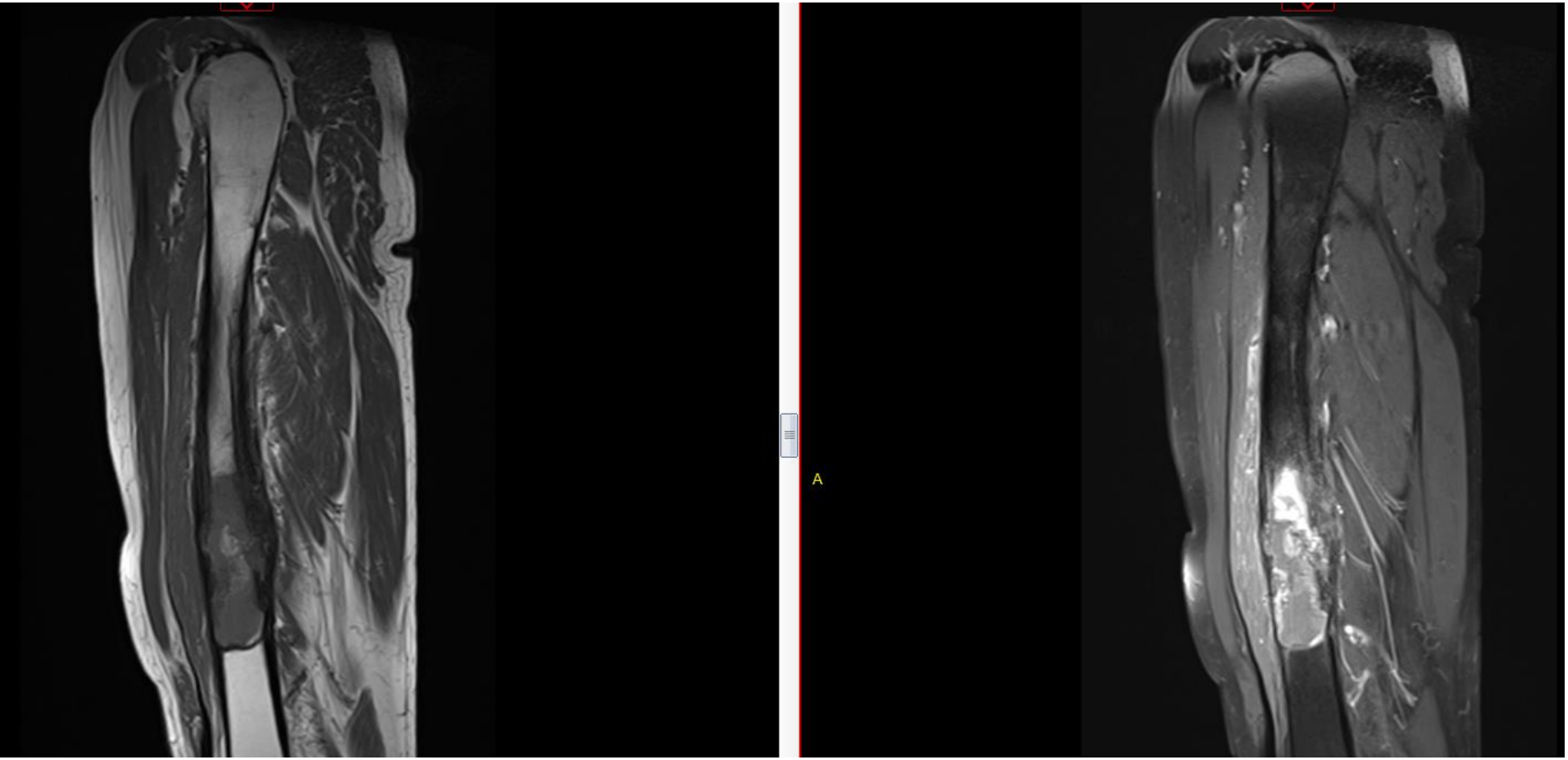

Bone scintigraphy

Whole body planar scan

Bone scintigraphy

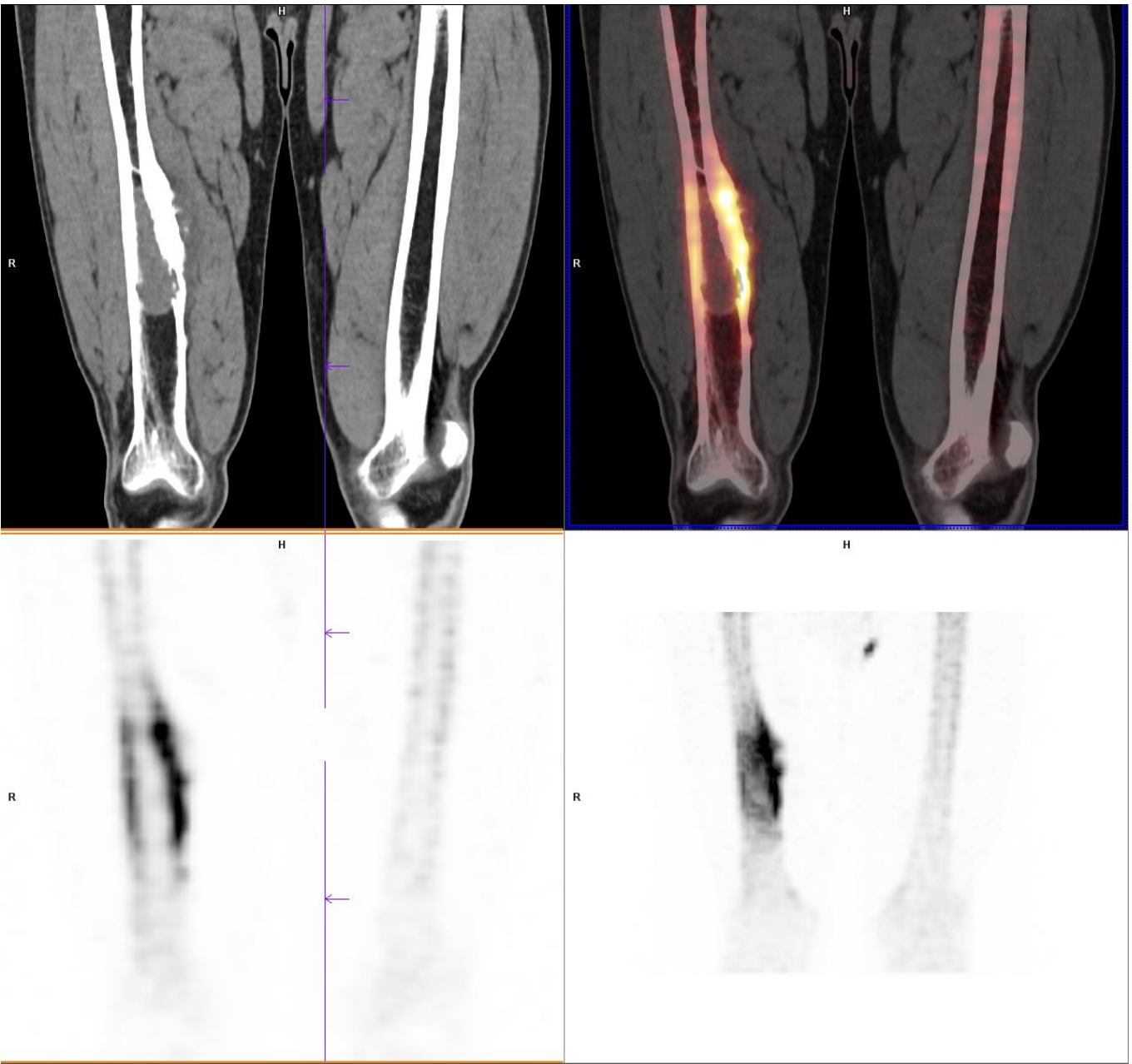

SPECT/CT
Femurs
Oblique coronal views
Soft tissue window

Bone SPECT/CT
Fefmurs
Transaxial views
Bone window

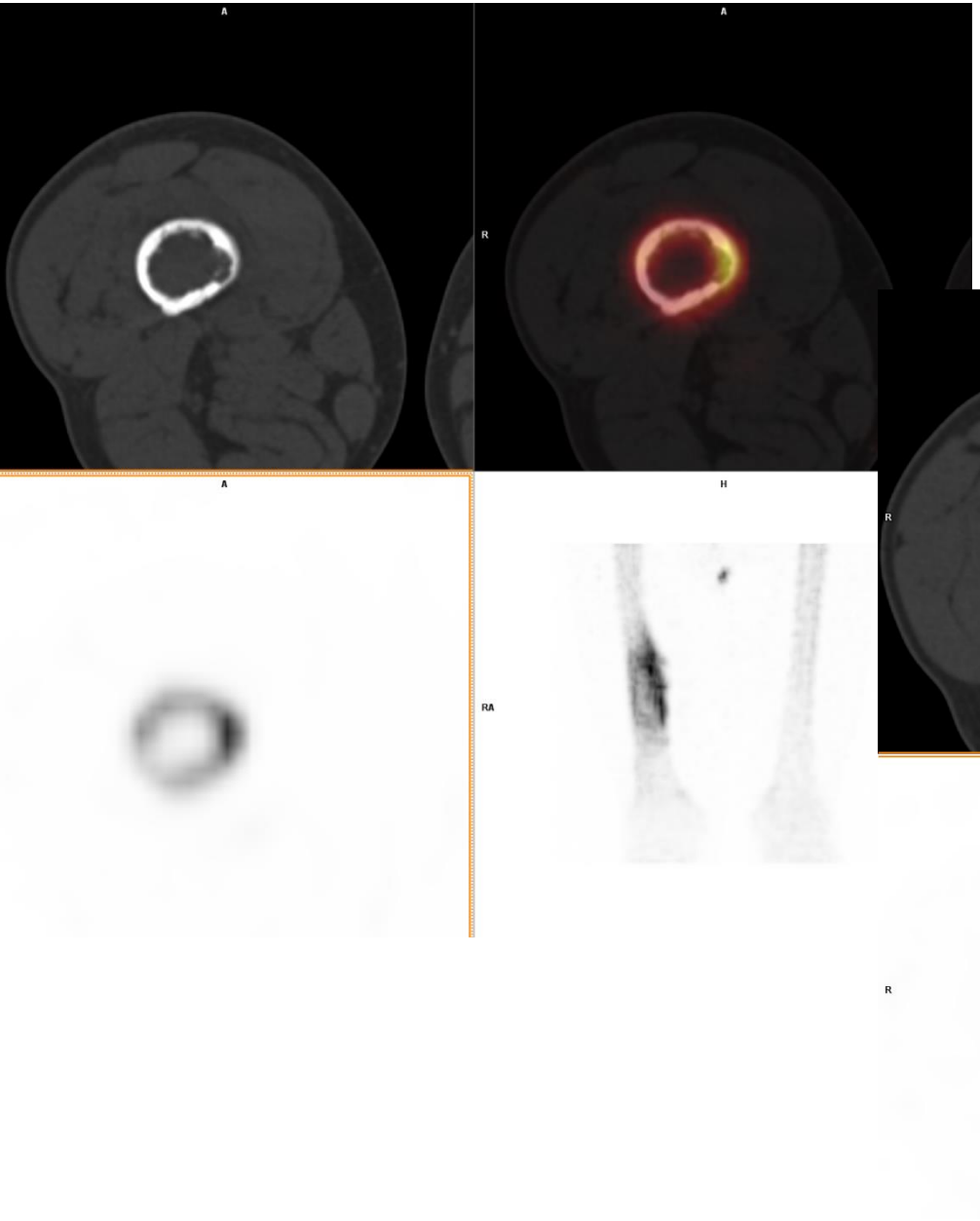

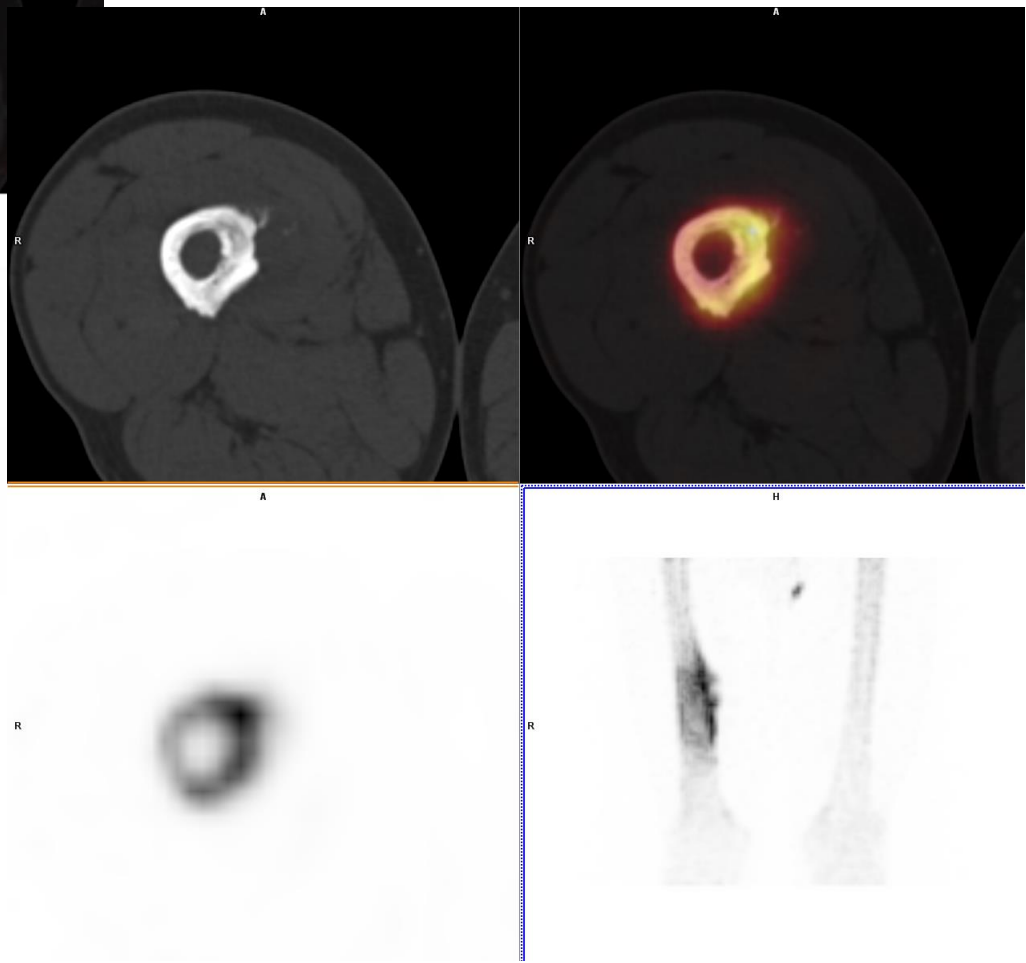

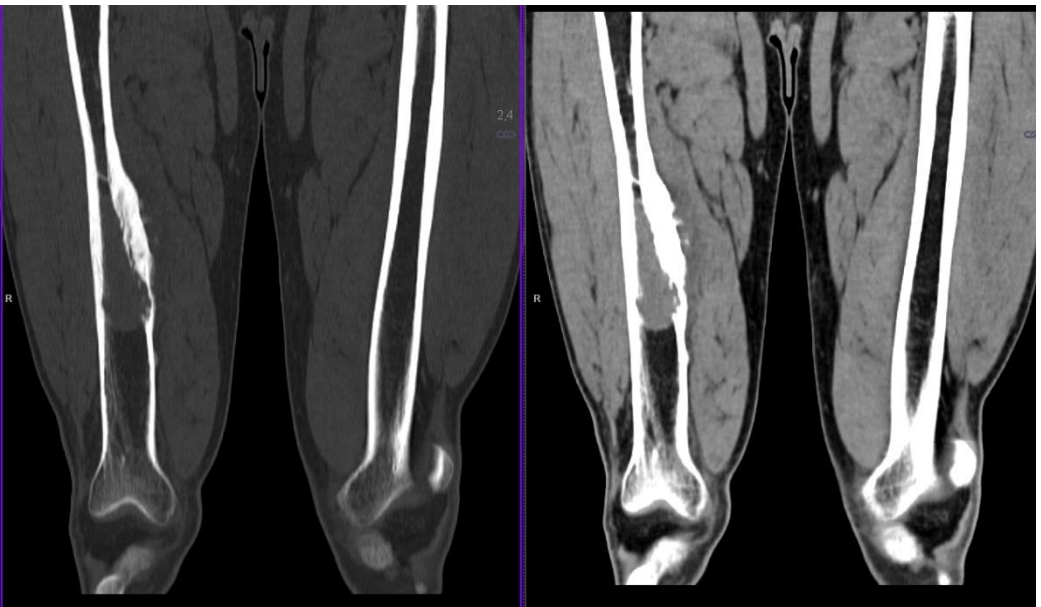

Most plausible diagnosis?

1. Bone metastasis
2. Subacute osteomyelitis
3. Lymphoma
4. Osteosarcoma
5. Paget disease

Most plausible diagnosis?

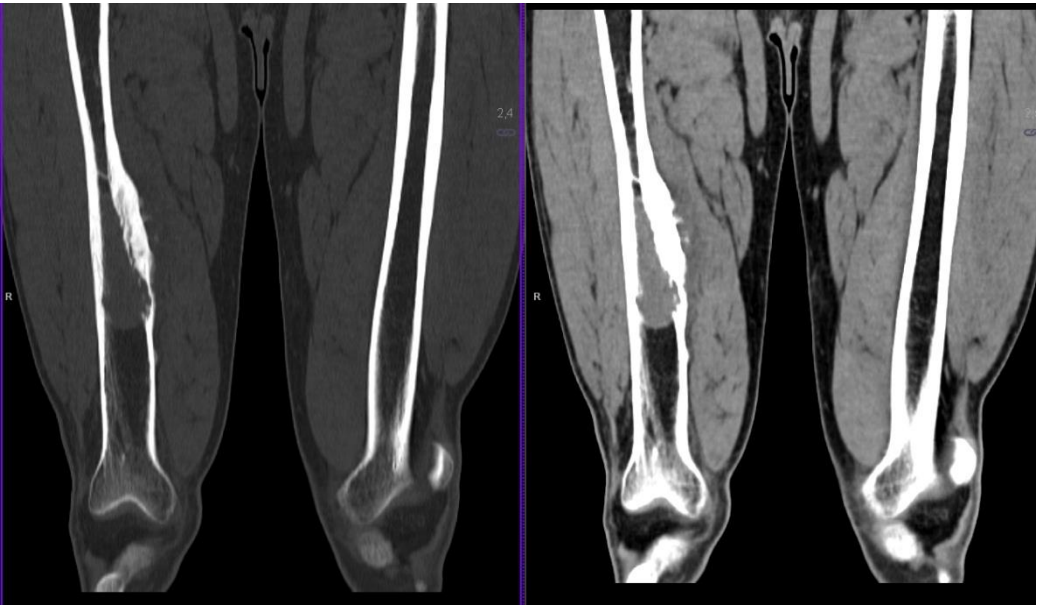

1. Bone metastasis
2. Subacute osteomyelitis
3. Lymphoma
4. Osteosarcoma
5. Paget's disease

Comparison
Plain X-rays vs scout view

Daffner RH. Reviewing CT scout Images: Observations of an expert witness. AJR 2015; 205: 589-91

Johnson PT, et al. The CT scout view: does it need to be routinely reviewed as part of the CT interpretation? AJR 2014; 202:1256-63

Diagnostic procedure & work-up

- CT-guided femur biopsy
  - Pathology: Undifferentiated tumor – focal osteoformation (Discussion GSF-GETO)
  - Ultimated diagnosis: Osteosarcoma conventional type de high malignancy grade 1/3 medial diaphysis R femurdroit
- Baseline work-up: Negative
  - MDCT thorax: normal/PET: FDG-avid area corresponding to primitive bone tumor
- Assessment after 1 cycle of neo-adjuvant chemotheray Doxorubicine-Cisplatin: local expansion
- Decision of surgery ASAP

FDG PET/CT
Femurs reoriented coronal views
Bone window

FDG PET/CT
Femurs reoriented coronal views
Soft tissues window

Tumor R femur, at 1/3 medial-1/3 caudal segment, FDG-avid, involving bone marrow (SUVmax = 21.9) and invading muscular tissues (SUVmax = 18.9) from medial cortical.

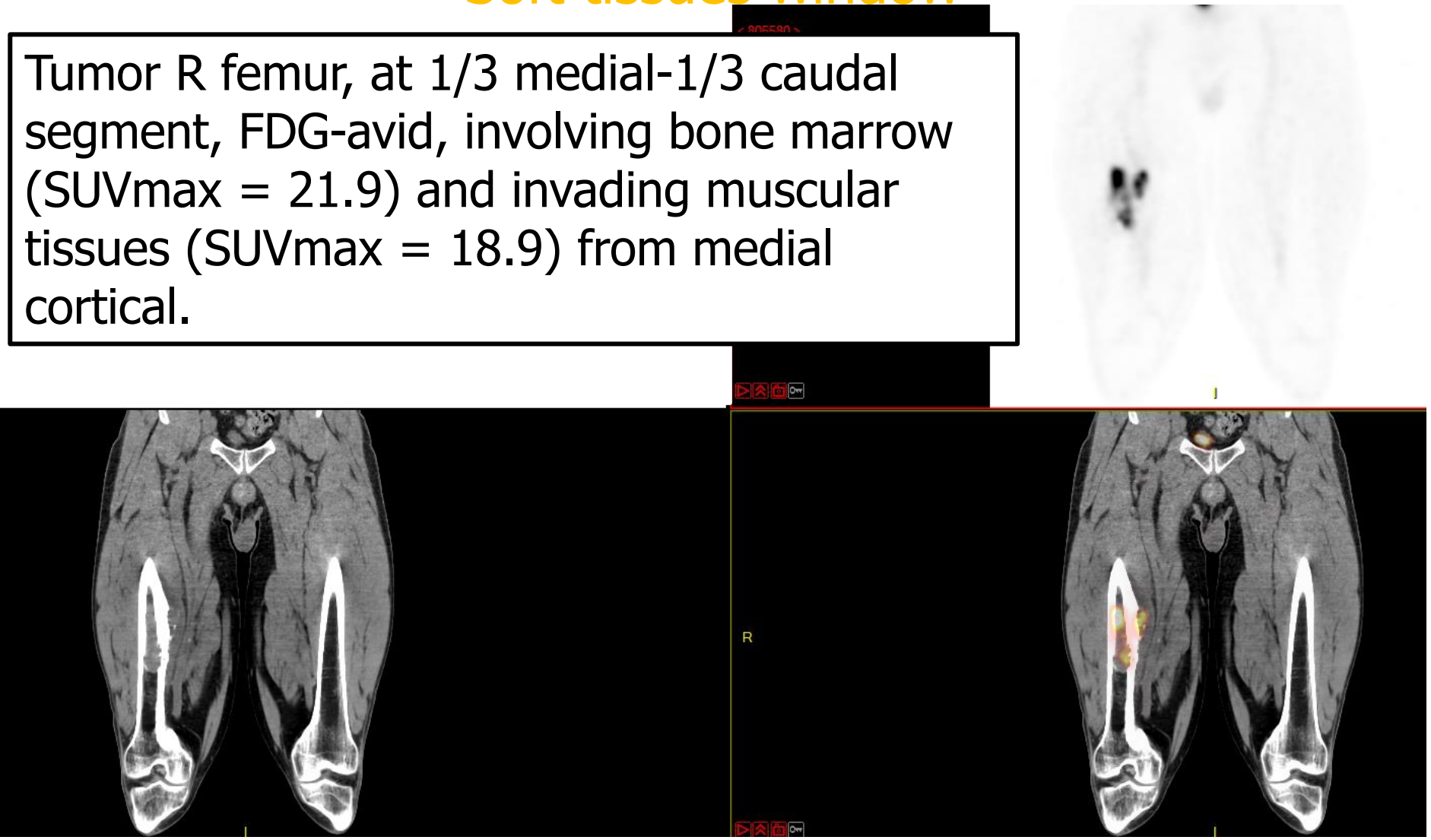

FDG PET/CT
Femurs axial views
Bone window

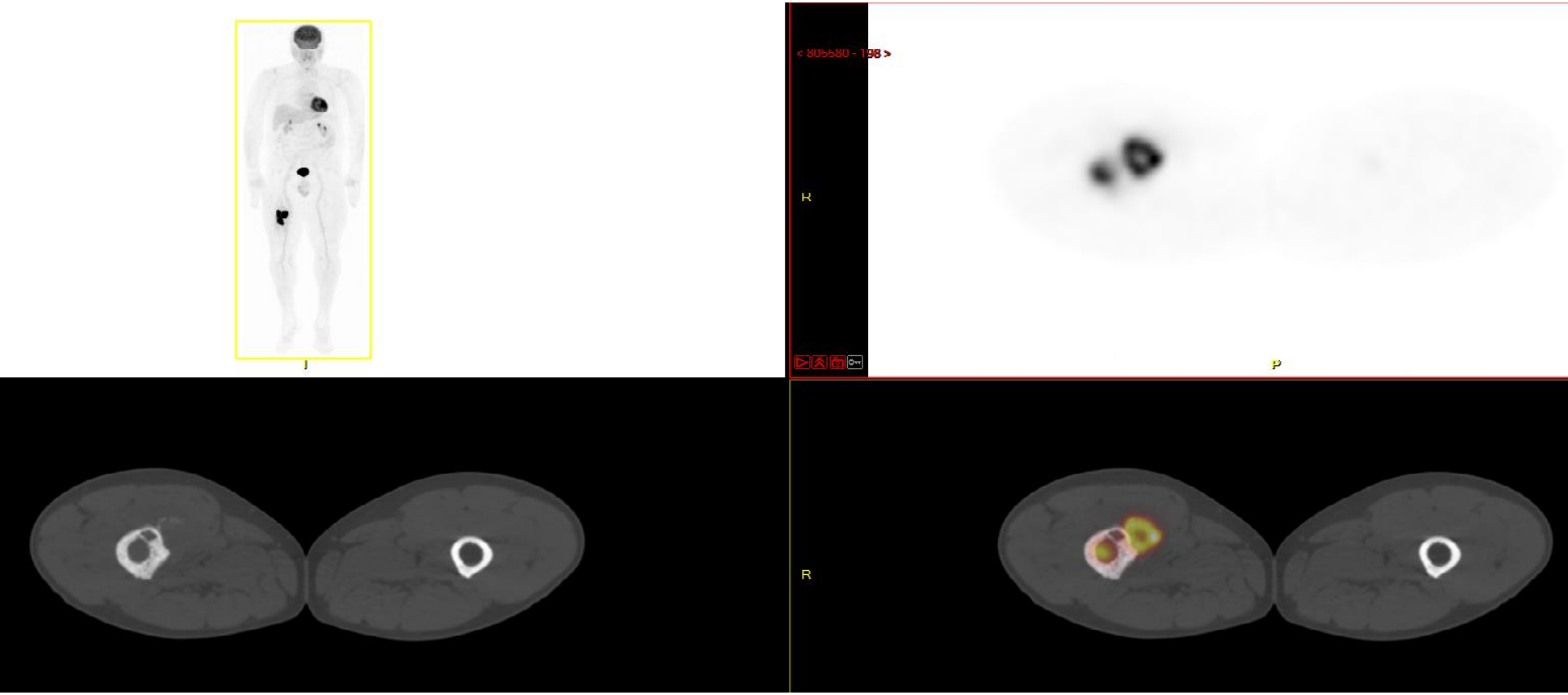

FDG PET/CT
Femurs axial views
Soft tissue window

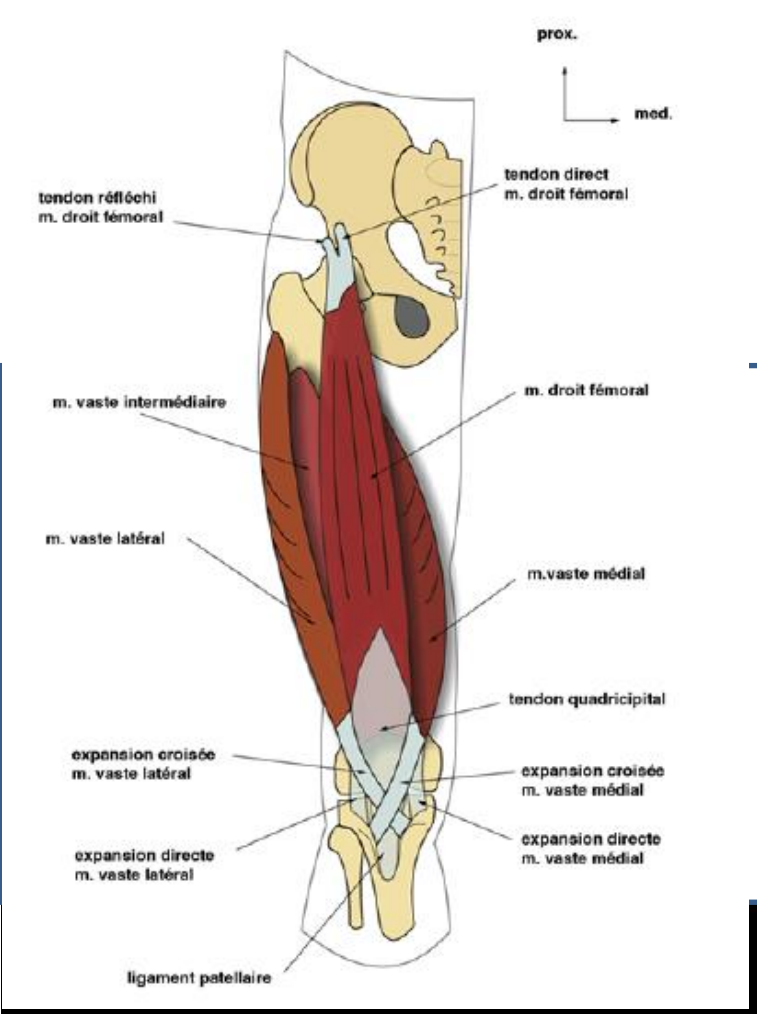

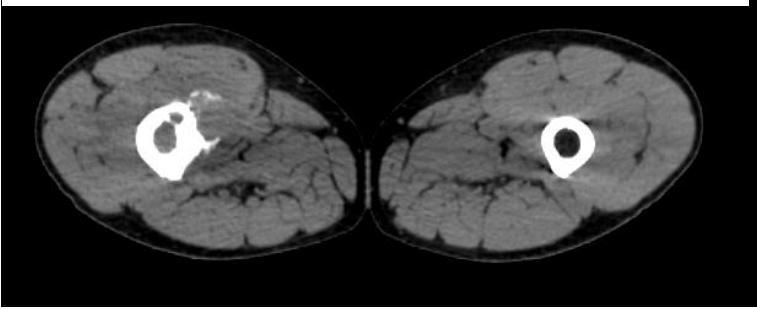

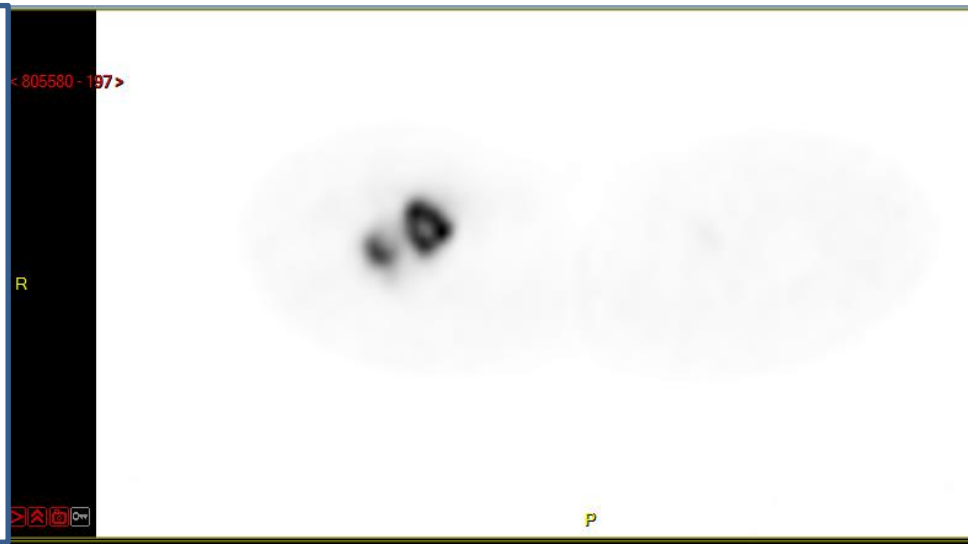

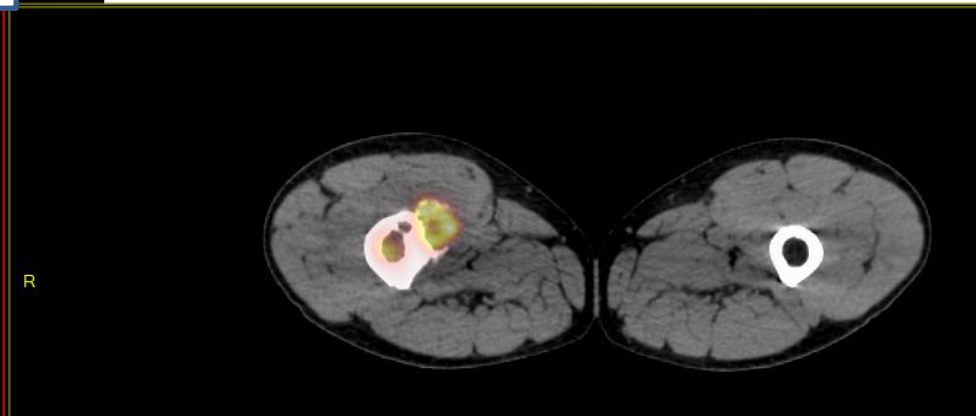

Surgical procedure

- En bloc resection of tumor over 17 cm of femoral diaphysis
- Reconstruction by massive diaphyseal graft
- Osteosynthesis by one-piece nail-plate LCP

DISCUSSION

- Diagnostic pathway
- Differential diagnosis gamut

Osteosarcoma

- Most common primary bone tumor after myeloma
- Ages 10-25 years or ages 40+ with other diseases
- Metaphysis of long bones, rarely diaphysis
- RX/CT: large, destructive, lytic or blastic mass with permeative margins; may break through cortex and elevate periosteum; sunburst pattern due to new bone formation in soft tissue
- Bone scintigraphy:
high heterogeneous uptake
with clear-cut margins,
extended pattern of uptake

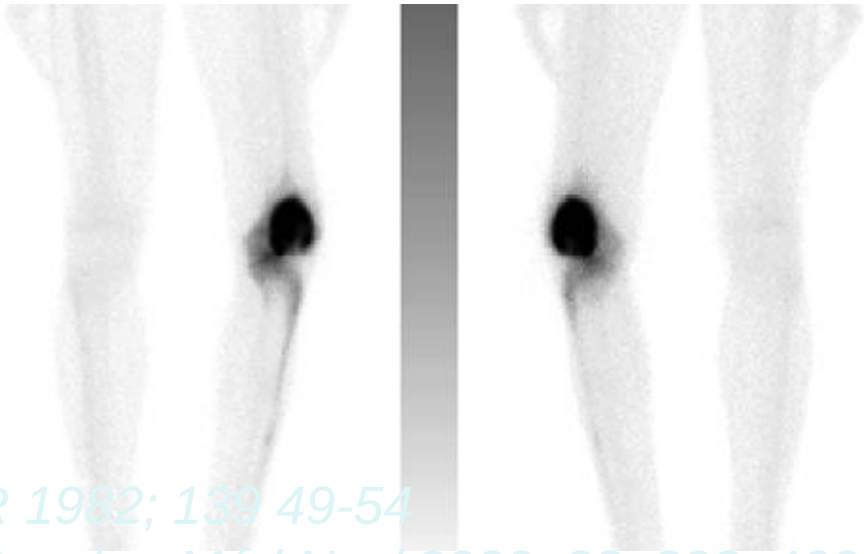

F Chew, AJR 1982; 139 49-54

A Girma, F Paycha, Méd Nucl 2009; 33: 398–409

Clinical interest of bone-seeking radionuclides in osteosarcoma

Uptake and localization of 99mTc-Methylene Diphosphonate in mouse osteosarcoma. Hiroshi Nakashima, Hironobu Ochi, Natsuo Yasui, Hideki Hamada, and Keiro Ono. Eur J Nucl Med (1982) 7: 531-535

« On the microautoradiography, the activity of 99mTc-BP was localized in the mineralized matrix of tumor bone and was almost nil in the nonmineralized matrix (osteoid) and the tumor cells »

PET diagnosis of pulmonary metastases in osteogenic sarcoma. N Tse et al. Am J Clin Oncol 1994; 17 (1): 22-25

« We report the case of a patient with (…) metastatic osteogenic sarcoma (…) who presented with pulmonary nodules, in whom [18F] fluoride ion/PET imaging was useful in confirming the nature of the pulmonary nodules »

Caution!

Localization OS

Younger patients: metaphysis

Older patients: diaphysis+++

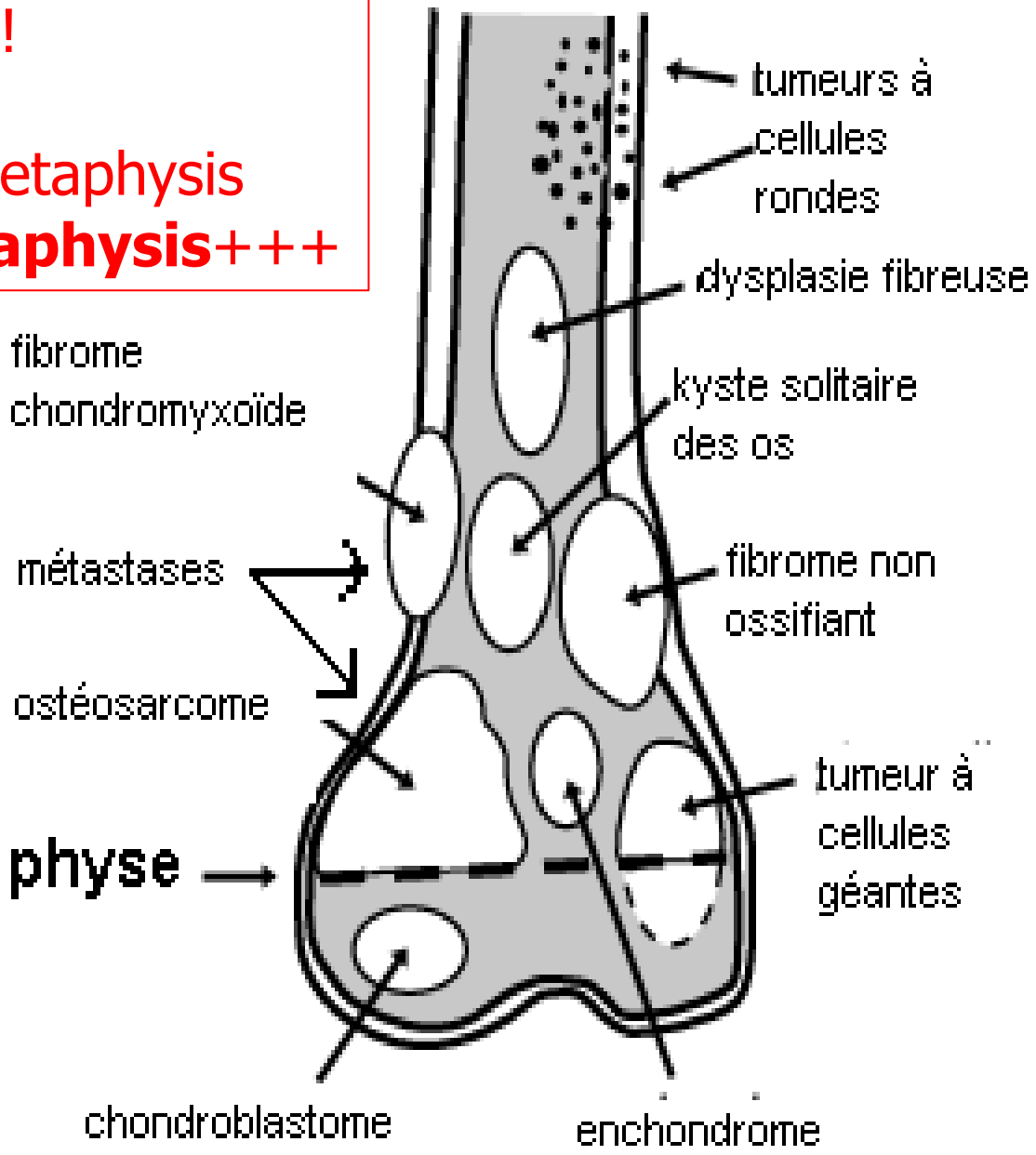

Adapted from:

Madewell JE, et al. Radiol Clin North Am 1981

DIFFERENTIALS

Ostéosarcome vs sarcome d'Ewing

Caractéristiques	Ostéosarcome	Sarcome d'Ewing
Epidémiologie	10-20 ans	5-30 ans
Tissu élaboré par la tumeur	Matrice ostéoïde	Origine mésenchymateuse
Aspect radiologique	Lodwick de type II & III	Lodwick de type II & III
Localisation physaire	Os longs > os plats Métaphyse (diaphyse)	Os plats, os courts, Os longs: diaphyse (métaphyse)
Configuration scintigr. osseuse	Hétérogène/Marges nettes Métastases pulmonaires hyperfixantes	Homogène/Marges imprécises Métastases pulmonaires non fixantes
Anomalies de signal IRM	HypoT1/HyperT2 hétérogène	HypoT1/HyperT2 hétérogène
Avidité tumorale pour le FDG	Suv max : 2-4 SO ≥ TEP	Suv max : 4-7 SO < TEP

A Girma, F Paycha, Méd Nucl 2009;

Métastases pseudo-sarcomateuses du cancer de la prostate

Métastases pseudo-sarcomateuses

[Sunburst Periosteal Reaction in a Bony Metastasis]

BREIT, ROBERT; VAN DER WALL, HANS; EMMETT, LOUISE; STOREY, GEOFFREY; ALLMAN, KEVIN

Clinical Nuclear Medicine. 25(5):392-393, May 2000.

A whole-body bone scan shows multiple sites of increased uptake in the vertebral column, right sacroiliac joint, and the right femur, suggesting the presence of metastatic disease. The abundant uptake in the femoral cortex corresponds to the site of the sunburst reaction (arrow). Below this is another site of focal uptake (arrowhead) corresponding to the lesion present on the plain radiograph (*).

[Sunburst Periosteal Reaction in a Bony Metastasis]

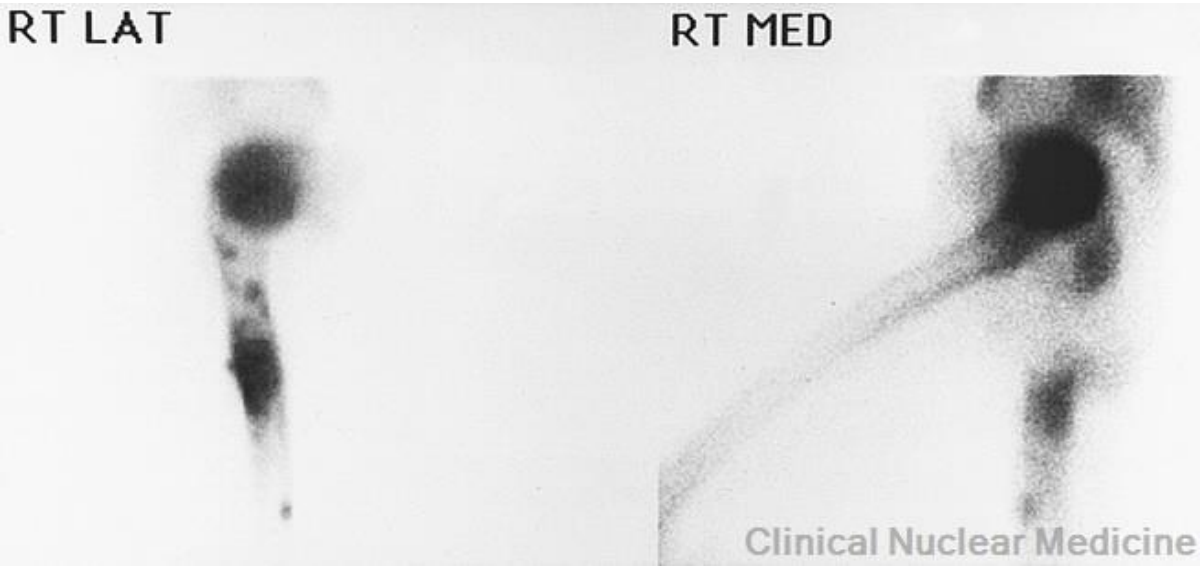

- Regional scintigraphic views of the right femur. The lateral and medial views show extensive posterolateral cortical uptake and multiple focal areas elsewhere in the cortex.

Sunburst Periosteal Reaction in a Bony Metastasis

BREIT, ROBERT; VAN DER WALL, HANS; EMMETT, LOUISE; STOREY, GEOFFREY; ALLMAN, KEVIN

Clinical Nuclear Medicine. 25(5):392-393, May 2000.

doi:

Fig. 1. A 92-year-old man had increasingly severe pain in the right hip. He reported a history of resection of the right kidney because of transitional cell carcinoma 6 years previously. A plain radiograph of the right proximal femur shows a permeating destructive lesion of the cortex with radiating spicules associated with periosteal elevation, giving a sunburst appearance. Below this is another site of permeating destruction within the trabecular bone of the medulla (*). The sunburst periosteal reaction is most commonly reported with primary bone tumors such as osteosarcoma (1). Transitional cell carcinoma, a rare metastatic cause of the sunburst reaction, has been reported in 3 of 70 cases since 1936 (2). Other reported causes were prostatic carcinoma (29%); gastrointestinal, breast, and bronchogenic carcinoma; and neuroblastoma.

Métastases pseudo-sarcomateuses

Cas Viggo-Petersen

Douleurs de cuisse gauche.
ATCD: Cancer de la prostate.
Radiographies avec 2 contrastes différents

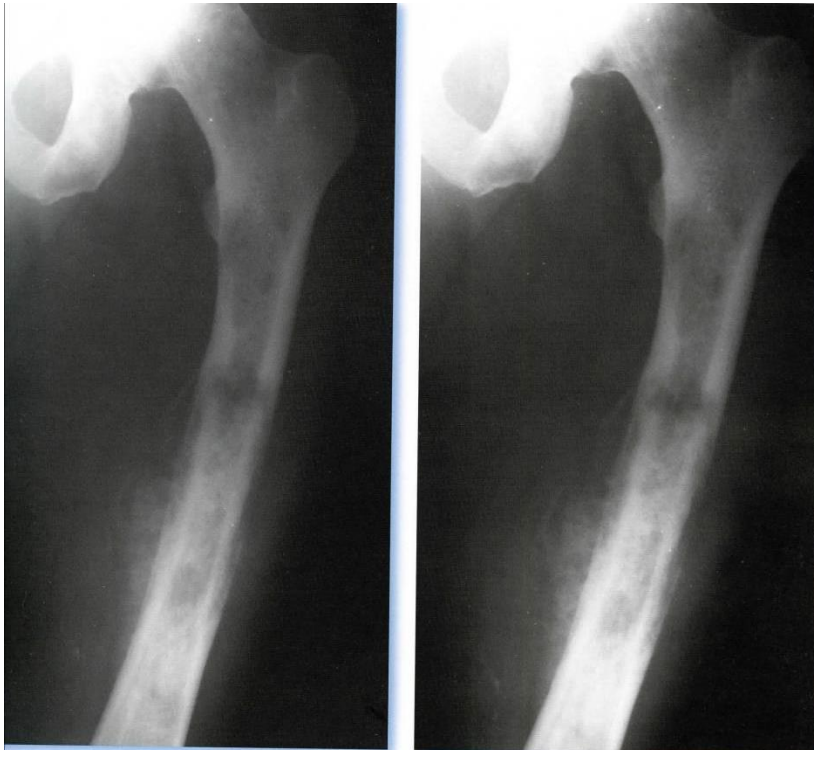

Cas Viggo-Petersen

Diagnostic

Métastase peudo-sarcomateuse d'un cancer de la prostate.

Clés

- l'association d'une ostéolyse de type mité et d'une réaction périostée irrégulière avec ossification floride en feu d'herbe est très évocatrice d'un sarcome
- cet aspect pseudo-sarcomateux est cependant connu dans les métastases des cancers de la prostate, diagnostic à évoquer compte-tenu de l'antécédent, et de la rareté des ostéosarcomes sur os sain à cet âge
- les métastases pseudo-sarcomateuses sont très rares en dehors du cancer de la prostate

- Métastase pseudo-sarcomateuse étendue solitaire excep

Référence


Anthologie des concours de radiologie rhumatologique des journées Viggo-Petersen
Jean-Denis Laredo et Ghazi Ayoub
Tome 1
Pfizer

Ostéomyélite chronique
Histoire naturelle

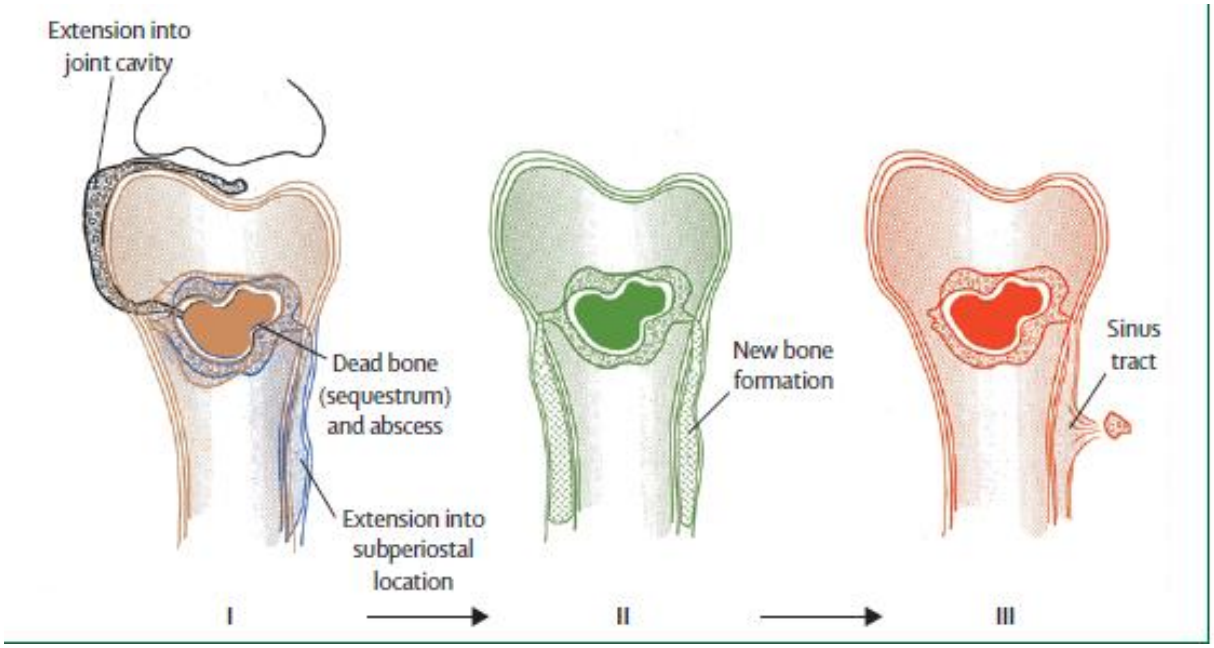

Modèle OM chronique hématogène de l'os long continu

Ostéomyélite chronique
Radiographies/TDM/Scintigraphie osseuse

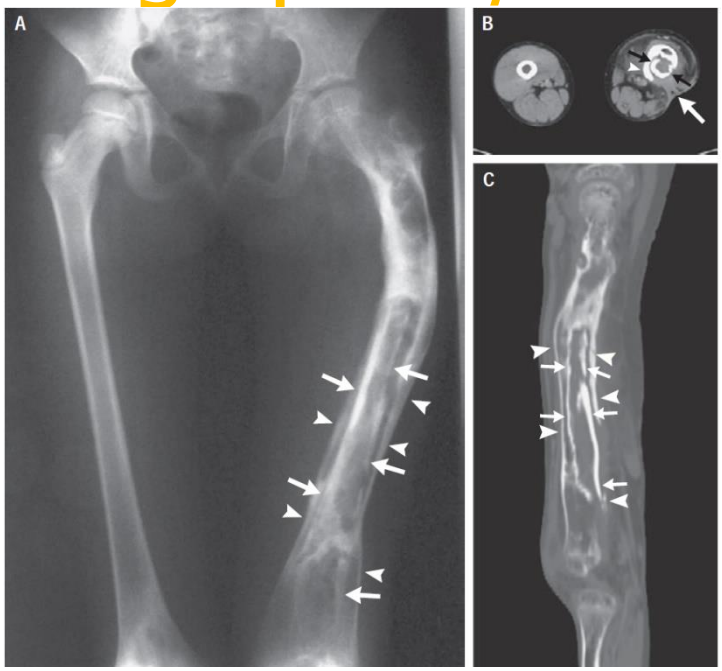

- Radiographies/TDM:
  - Os longs: fémur, tibia
  - Ostéolyse méta(-dia)physaire centro-osseuse à géométrie longitudinale cerclée d'un liseré de condensation: aspect d'os dans l'os
  - Réaction périostée
  - Infiltration des tissus mous adjacents
  - Extension articulaire fréquente

Scintigraphie osseuse

- Hyperfixation intense hétérogène
- Congruente à l'ostéolyse
- Hyperfixations satellites des articulations voisines classiques

Ostéomyélite chronique
Configuration IRM "en cible"

1. Coeur de cible: cavité renfermant l'abcès hypo-T1/hyper-T2
2. Couche périphérique à l'abcès: tissu de granulation richement vascularisé hyper-T1 (séquences sans et avec contraste) /hyperT2

   (signe de la pénombre:

   Se: 30%/Sp>95%)
3. Cerne de condensation osseuse réactionnelle hypo-T1/hypo-T2
4. Zone péri-abcès d'œdème médullaire, hypo-T1/hyper-T2

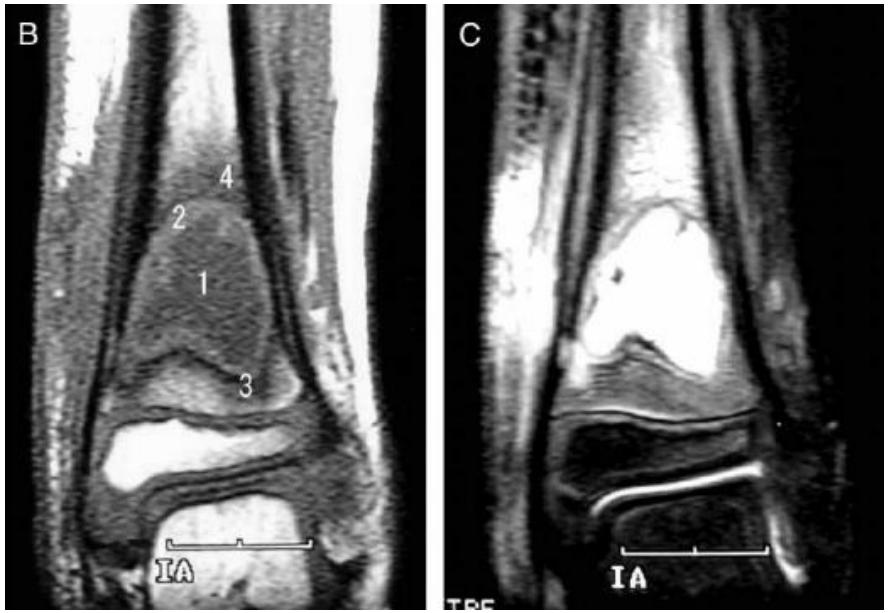

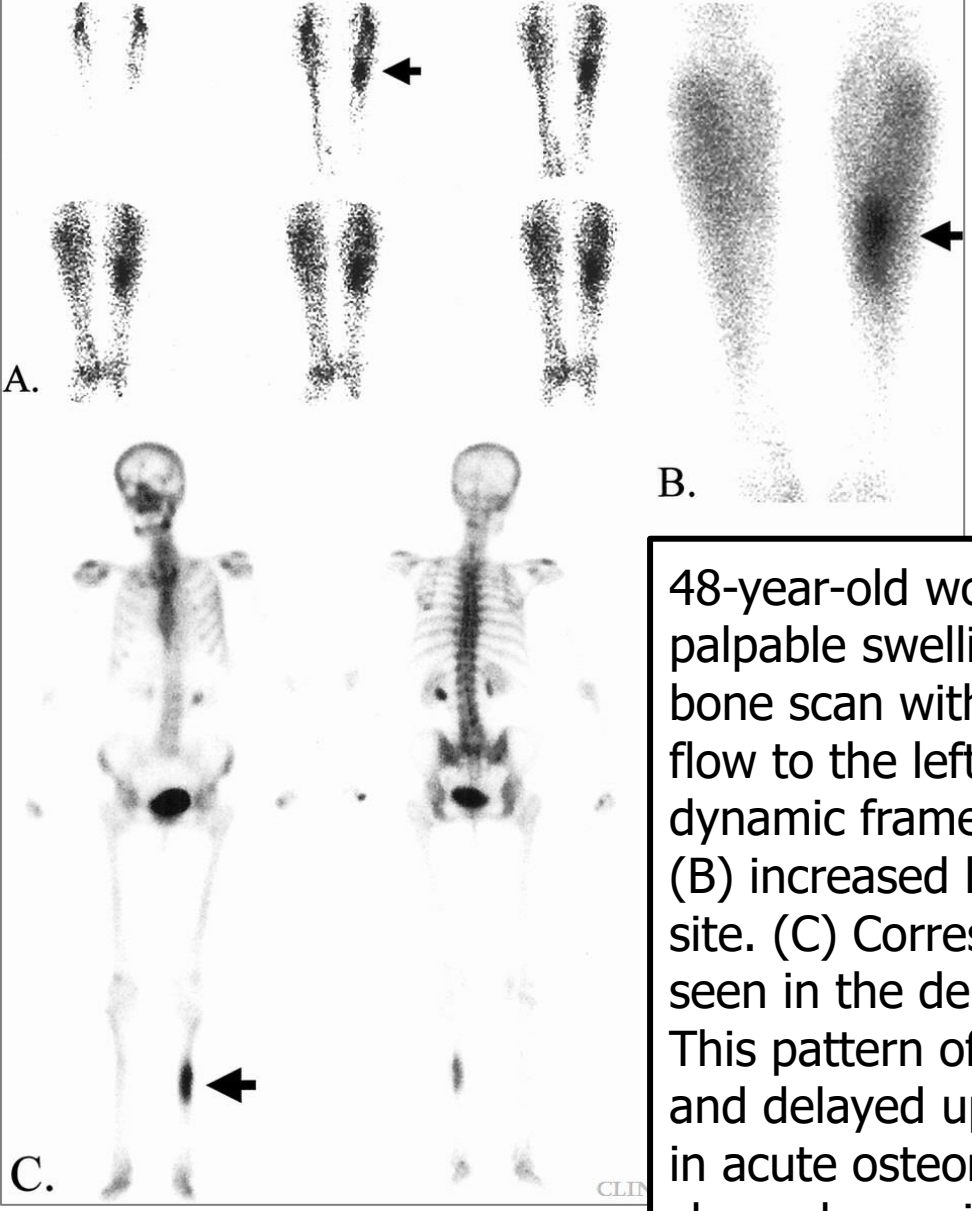

Unusual Presentation of Solitary Bone Metastasis From Breast Carcinoma Mimicking Acute Osteomyelitis of the Left Midtibial Shaft

Salem S, et al. Clin Nuclr Med 2000; 25: 480-481

48-year-old woman with breast carcinoma had a tender palpable swelling in the left midtibial shaft. A 3-phase bone scan with Tc-99m MDP revealed (A) increased blood flow to the left midtibial shaft (arrow) in the early dynamic frames acquired every 6 seconds. In addition, (B) increased blood pool activity is evident at the same site. (C) Corresponding intense increased focal uptake is seen in the delayed static images acquired 2 hours later. This pattern of remarkable increased flow, pooled blood, and delayed uptake is similar to the findings usually seen in acute osteomyelitis. Whole-body delayed images showed no evidence of any other bony metastases. A needle biopsy of the left midtibial lesion confirmed bony metastasis from breast carcinoma. The incidence of a solitary bone metastasis below the knee is rare.

Atteintes osseuses des lymphomes

Lymphome non hodgkinien :
Ostéolyse mitée (Lodwick type II)
de la diaphyse fémorale D

- <u>Lymphome osseux primitif</u>

Lésion solitaire: 80%-90% des cas
Squelette appendiculaire majoritairement atteint:
Fémur (20%), tibia (13%), humérus (10%)
Métaphyse et/ou diaphyse
Ostéolyse mitée, réaction périostée

- <u>LH & LNH</u>

Atteinte squelette axial: 75%-80%
LNH: Phénotype lytique: 80%
Ostéolyse perméative ou mitée
LH: Phénotype condensant: 45%
Localisation solitaire peu fréquente (30%)

KA Ruzek, The multiple faces of lymphoma of the musculoskeletal system, Skeletal Radiol 2004

Sequestra in PBL

Sequestra in Primary Lymphoma of Bone: Prevalence and Radiologic Features

Michael E. Mulligan [1,2]
Mark J. Kransdorf [2,3]

OBJECTIVE. Our objective was to determine the prevalence and spectrum of radiologic features of sequestra (detached pieces of bone separated from the involved segment) in cases of primary lymphoma of bone. This is a feature of primary lymphoma of bone that, to our knowledge, has not been reported previously. Recognizing sequestra is important, because a limited differential diagnosis of entities exists when this finding is seen.

MATERIALS AND METHODS. We retrospectively reviewed all the clinical and pathologic information and radiologic studies in our archives on 434 cases of skeletal lymphoma. Of these, 246 met our criteria for consideration as cases of primary lymphoma of bone. All cases were pathologically proved. Plain radiographs were available for review in all cases, and CT scans were available in 46. Data on the presence or absence of sequestra, their size and appearance, the bone involved, and the site of involvement were recorded in each case.

RESULTS. Sequestra were noted in 28 (11%) of the 246 cases. The size varied from 2 to 45 mm (average, 12 mm), and multiple sequestra were seen in 17 cases. They were seen in the long bones (15 cases), axial skeleton (10 cases), and three other sites (scapula, calcaneus, and third metatarsal).

CONCLUSION. Sequestra have been reported in a variety of conditions, including osteomyelitis, eosinophilic granuloma, fibrosarcoma, malignant fibrous histiocytoma, and desmoplastic fibroma. Because sequestra were seen in 11% of the cases of primary lymphoma of bone reviewed in this study, we believe that lymphoma should also be included in the differential diagnosis when a sequestrum is noted on imaging studies.

AJR 1993;160:1245–1248

Paget’s disease

Différentiel: Rx+TDM

- La maladie de Paget monostotique est minoritaire: 20 % des tableaux cliniques
- Topographie:
  - rachis 78 %
  - pelvis 70 %
  - **fémur 65 %**
  - tibia 44 %
  - crâne 39 %

Distribution épi-méta-diaphysaire

- Critères radiologiques cardinaux:
  - » Raréfaction initiale
  - » Epaississement cortical et spongieux
  - » Densification variable de l'os spongieux
  - » Elargissement/déformation de la pièce osseuse
- Epaississement des corticales et densification de l'os spongieux ➡ dédifférenciation cortico-spongieuse

Différentiel
Apport de l'IRM

- Le stade 3 (condensant) de l'atteinte pagétique se caractérise par un hyposignal T1 et T2 résultant de l'augmentation de l'épaisseur trabéculaire, la sclérose et la fibrose médullaire
- L'évolution à terme du stade 3 de la maladie de Paget est la transformation graisseuse de la moelle osseuse, accompagnée de phénomènes d'œdème, donnant alors un hypersignal T1 et T2

Suggested Readings

- Fogelman I Gnanasegaran G, van der Wall H Radionuclide and Hybrid Bone Imaging: Springer; 2012.
- Aoki J, Watanabe H, Shinozaki T, Takagishi K, Ishijima H, Oya N, et al. FDG PET of primary benign and malignant bone tumors: standardized uptake value in 52 lesions. Radiology. 2001;219(3):774-7.
- Dehdashti F, Siegel BA, Griffeth LK, Fusselman MJ, Trask DD, McGuire AH, et al. Benign versus malignant intraosseous lesions: discrimination by means of PET with 2-[F-18]fluoro-2-deoxy-D-glucose. Radiology. 1996;200(1):243-7.
- Horger M, Eschmann SM, Pfannenberg C, Vonthein R, Besenfelder H, Claussen CD, et al. Evaluation of combined transmission and emission tomography for classification of skeletal lesions. AJR Am J Roentgenol. 2004;183(3):655-61.
- Strobel K, Exner UE, Stumpe KD, Hany TF, Bode B, Mende K, et al. The additional value of CT images interpretation in the differential diagnosis of benign vs. malignant primary bone lesions with 18F-FDG-PET/CT. Eur J Nucl Med Mol Imaging. 2008;35(11):2000-8.
- Sharma P, Mukherjee A, Karunanithi S, Nadarajah J, Gamanagatti S, Khan SA, et al. 99mTc-Methylene diphosphonate SPECT/CT as the one-stop imaging modality for the diagnosis of osteoid osteoma. Nucl Med Commun. 2014;35(8):876-83.
- von Schulthess GK. Molecular Anatomic Imaging: PET/CT, PET/MR and SPECT/CT. 3 Rev ed. ed: Wolters Kluwer; 2015.

8. Crossing or not the joint?

Cartilaginous vertebral end-plates and disc: Metastasis vs malignant bone tumour behaviour

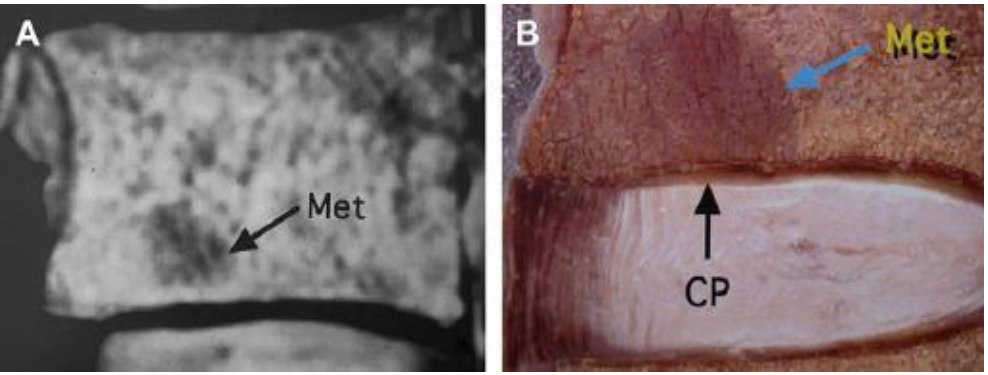

A. MRI T1-sequence: Metastatic nodule displaying hyposignal contiguous to intersomatic space
B. Anatomical slice evidencing metastatic lesion sparing cartilaginous vertebral plates

- ✓ Cartilaginous vertebral plates (CP) and intervertebral disc block the way of cancer cells crossing from one vertebra to the neighbouring one
- ✓ Deteriorated disc and/or CP loose this property+++
- ✓ 3 malignant tumours are notorious to cross the disc:
  - ✓ Lymphoma
  - ✓ Chordoma
  - ✓ Chondrosarcoma

Kakitsubata Y. Joint Bone Spine 2009; 76: 50-56
Takuya F. Spine 1997; 22: 1905-1912

Lymphoma

- Hodgkin lymphoma: 45% sclerotic form
- Non Hodgkin lymphoma: 5% sclerotic form

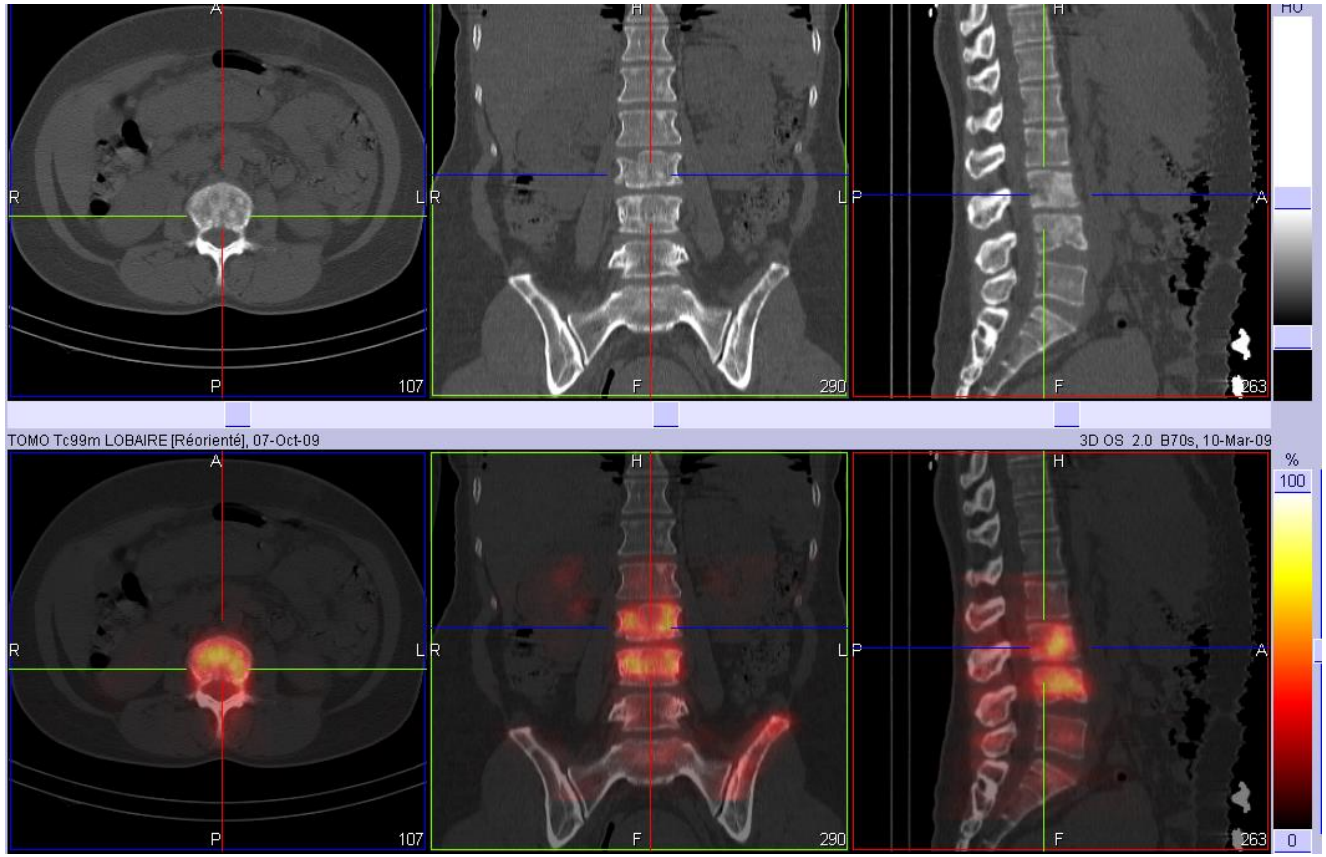

Localisations sclerotic form of L3-L4: Large cell B lymphoma

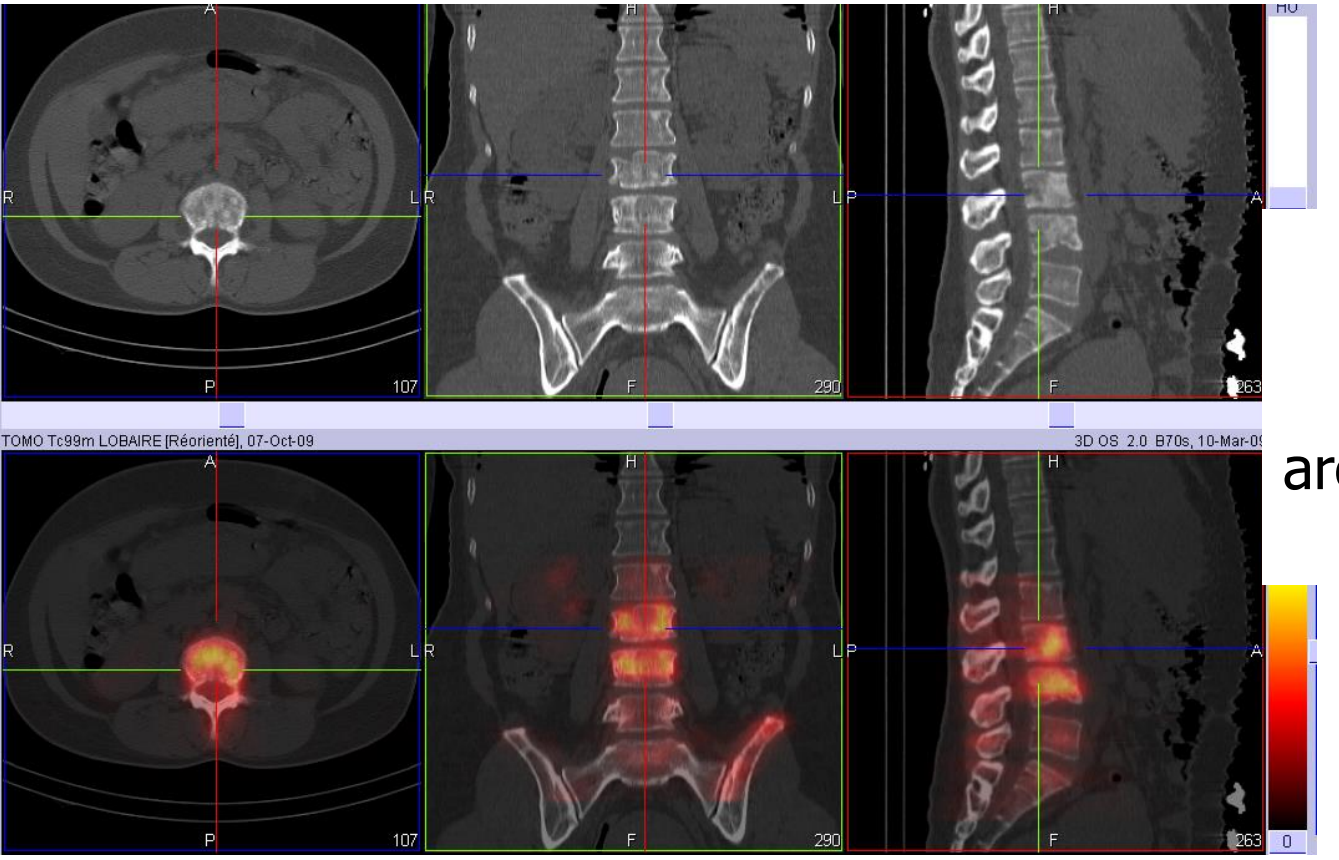

SPECT/CT pattern
Intense hot spots matching sclerotic areas in L3 et L4 bodies and L iliac wing

Lymphoma tumoral infiltration starts in hematopoietic marrow.
In theory, one surmises invasion of spine occurs in a diffuse way, homogeneous or heterogeneous, in hematological malignancies, in contradistinction of a focal way for bone metastases.
Differential: Skeletal tuberculosis

Kim HJ, et al. Spinal involvement of hematopoietic malignancies and metastasis: differentiation using MRI. Clin Imaging 1999; 23: 125-33

Myeloma:
NaF-(18F) PET/CT
Extensive lytic lesion crossing SIJ

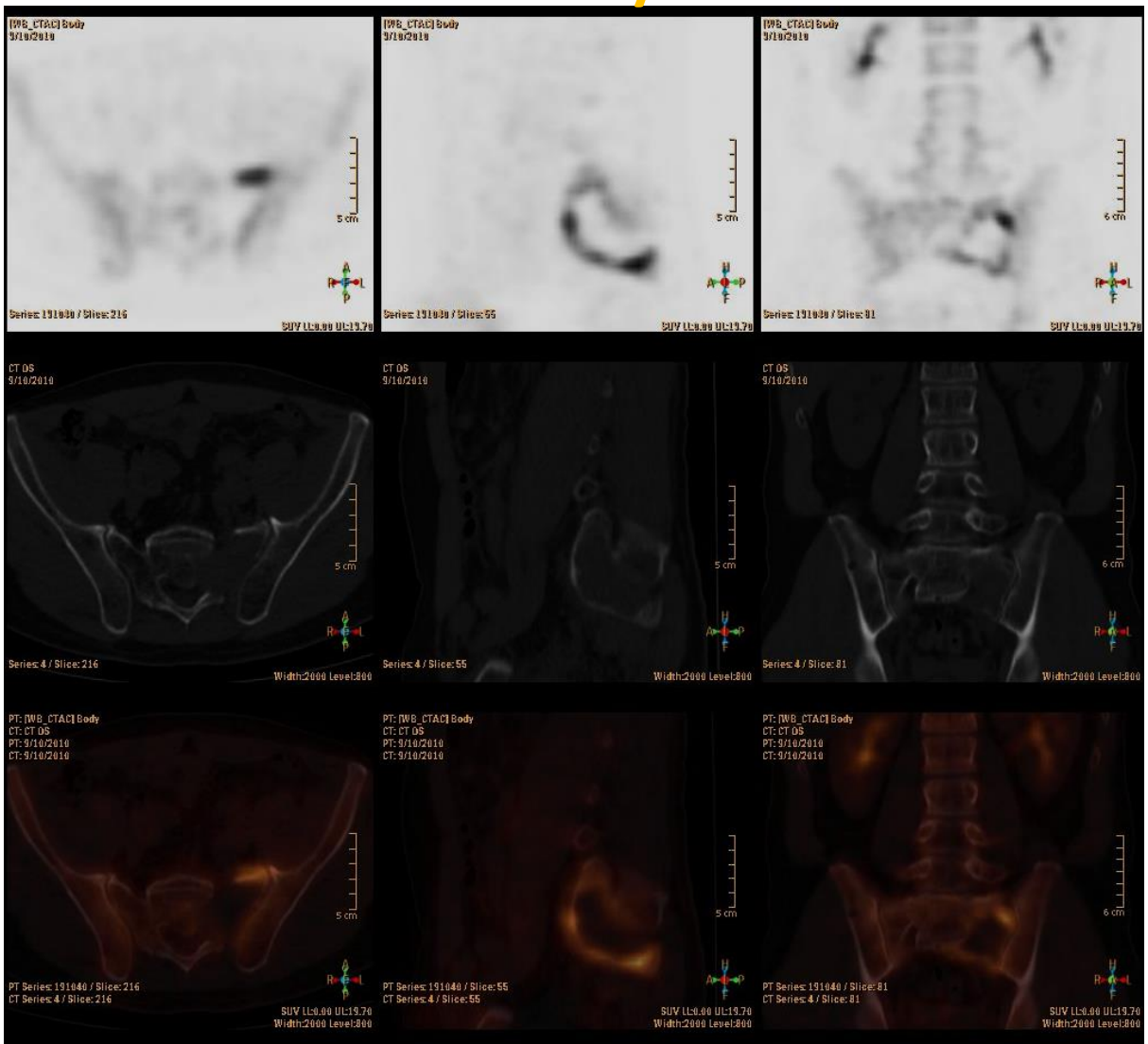

Clinical context

- Male, 55 year old
- Myeloma on treatment
- Painful sacral recurrence

9. Soft tissue component

Soft tissue component

- A soft tissue component extending outside bone typically indicates an aggressive lesion
- Soft tissue should be assessed for
  1. Density (eg fat, fluid, or air)
  2. Presence of calcification or ossification (should be distinguished whenever possible++)
  3. Gas bullae should be searched for to unearth abscess
  4. Secondary changes in the bone adjacent to a soft tissue abnormality
- Benign lesions may be associated with soft tissue mass
  - Osteomyelitis
  - GCT
  - ABC
- Determine whether a bone lesion is invading soft tissues or soft tissue mass is invading bone

Rule of the origin

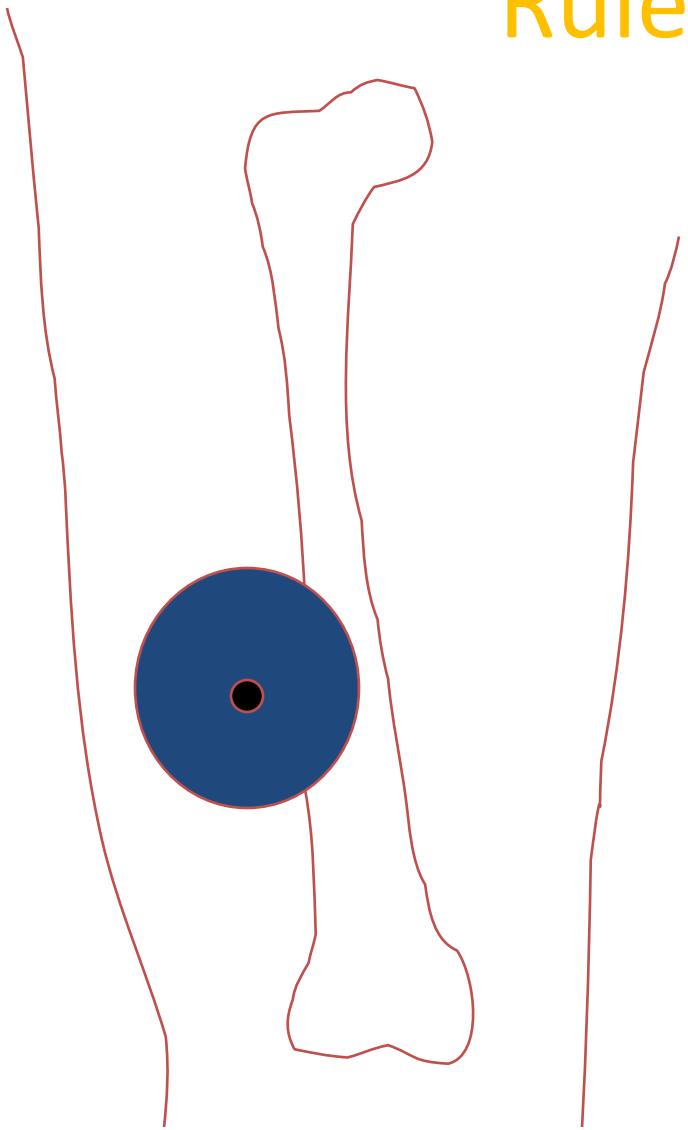

EXTRA-OSSEOUS

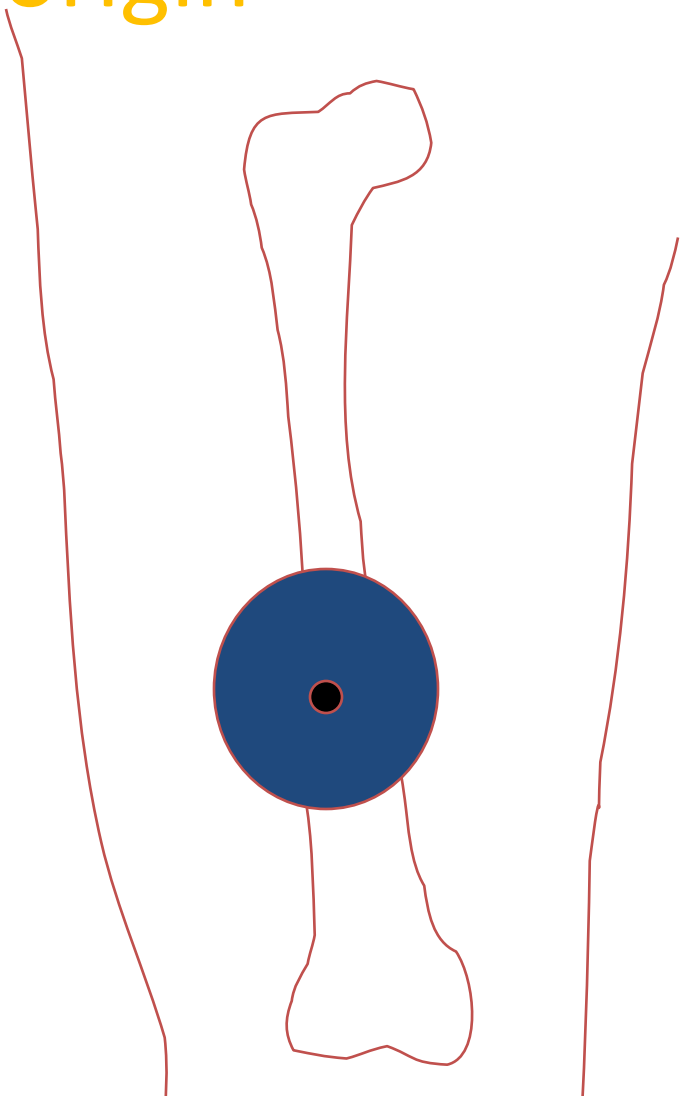

INTRA-OSSEOUS

Chordoma
Cross-sectional anatomical imaging

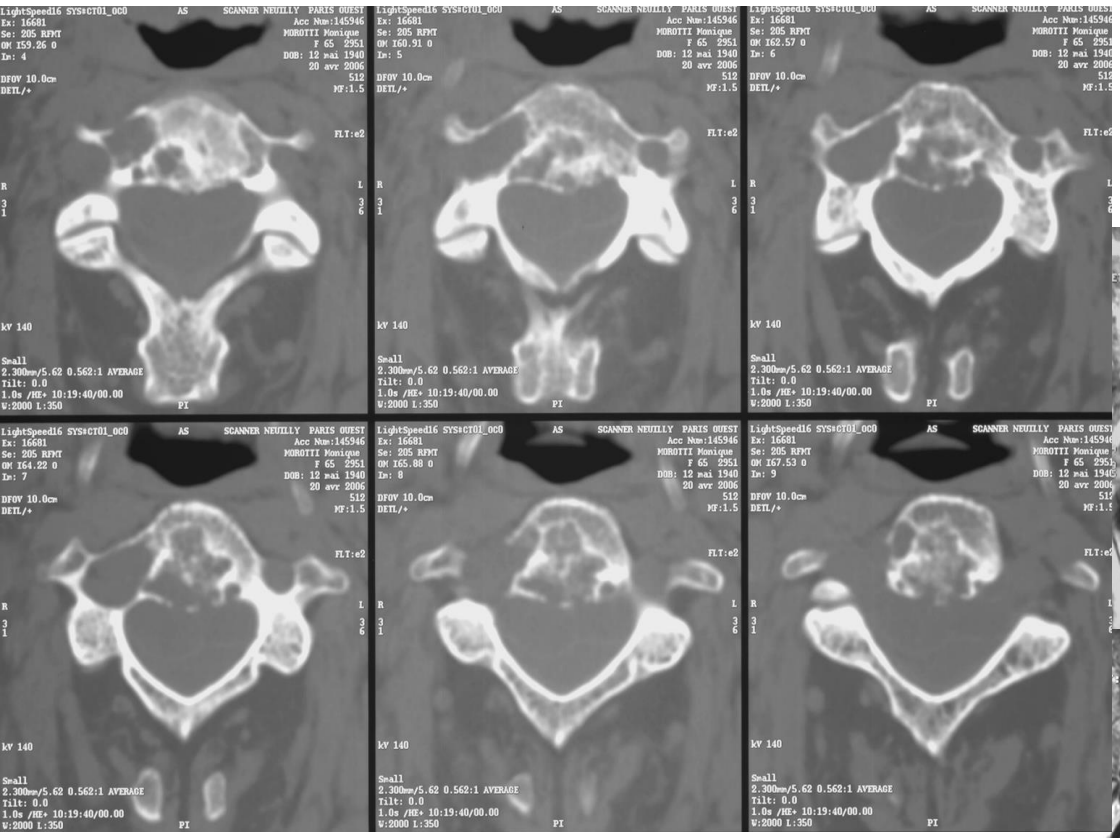

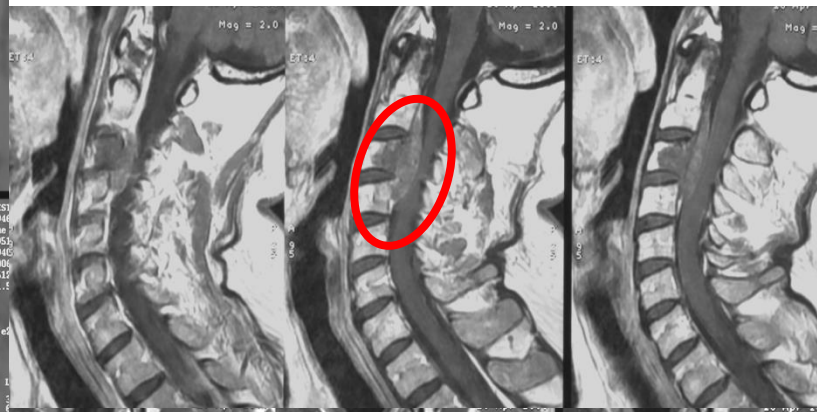

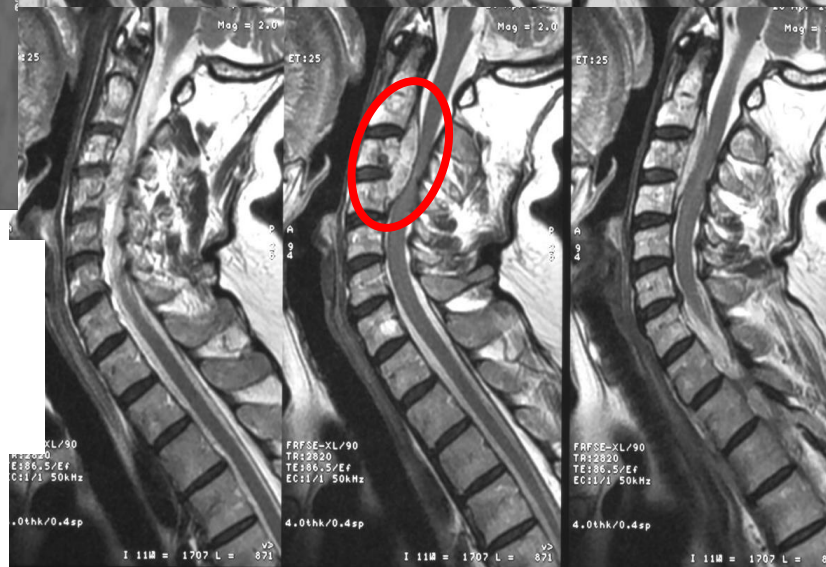

CT: Osteolysis vertebral body+ epidural spread

MUSHROOM PATTERN

Sag MRI hypoT1/hyperT2

Bone scintigraphy

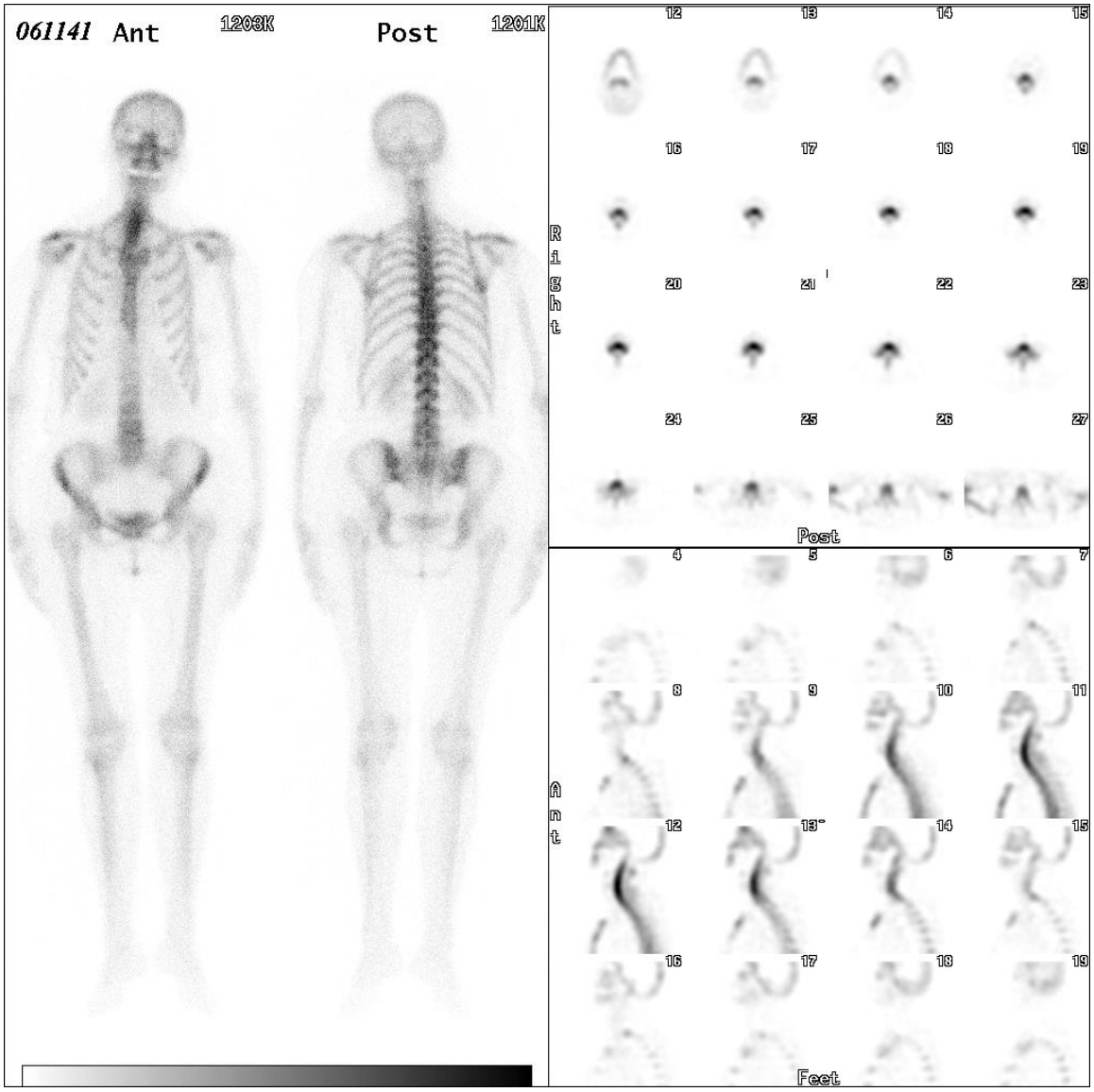

Subormal!

Chordoma
The key facts

- Rare tumors arising from vestigial embryonal notochord remnants
- Axial distribution : sacro-coccygeal (60 %) > spheno-occipital (25 %) > spine (15 %) [1/3 cervical segment]
- Vertebral body location most frequent
- Intervertebral disk invasion
- Epidural extension
- Local aggressiveness entailing high recurrence risk
- Therapy = resection ± proton beam therapy (Bragg peak++)
- Key prognostic factor : *en bloc* excision ++

Double discrepancy: Pivotal findings pointing to chordoma

1) Extra-osseous extension

>>

Intra-osseous spread

2) Anatomical cross-sectional imaging

(MDCT, MRI) dramatically positive in contrast to negative cross-sectional metabolic imaging (bone SPECT/CT, FDG PET/CT)

Un piège diagnostique potentiellement létal :
chordome révélé par une vaste lésion lytique de C3 normofixante à la scintigraphie osseuse aux bisphosphonates-(^{99m}Tc).

Médecine Nucléaire - Imagerie fonctionnelle et métabolique - Vol. 30 - n° 07 - 2006

10. Number

Number

Multifocal osteolytic

- Lytic metastases
- Myeloma/Mult. plasmocytomas
- Lymphoma (non-Hodgkin)
- Secondary avascular necrosis
- Osteomyelitis
- Fibrous dysplasia
- Langerhans cell histiocytosis
- Hyperparathyroidism
- Sarcoidosis

Multifocal osteosclerotic

- Blastic metastases
- Treated metastases
- Lymphoma (Hodgkin)
- Insufficiency fractures
- Paget's disease
- Osteopoikilosis
- Gardner syndrome
- Melorheostosis
- Congenital stippled epiphyses
- Mastocytosis
- Tuberous sclerosis

Number
Osteolytic/Osteoclastic lesions

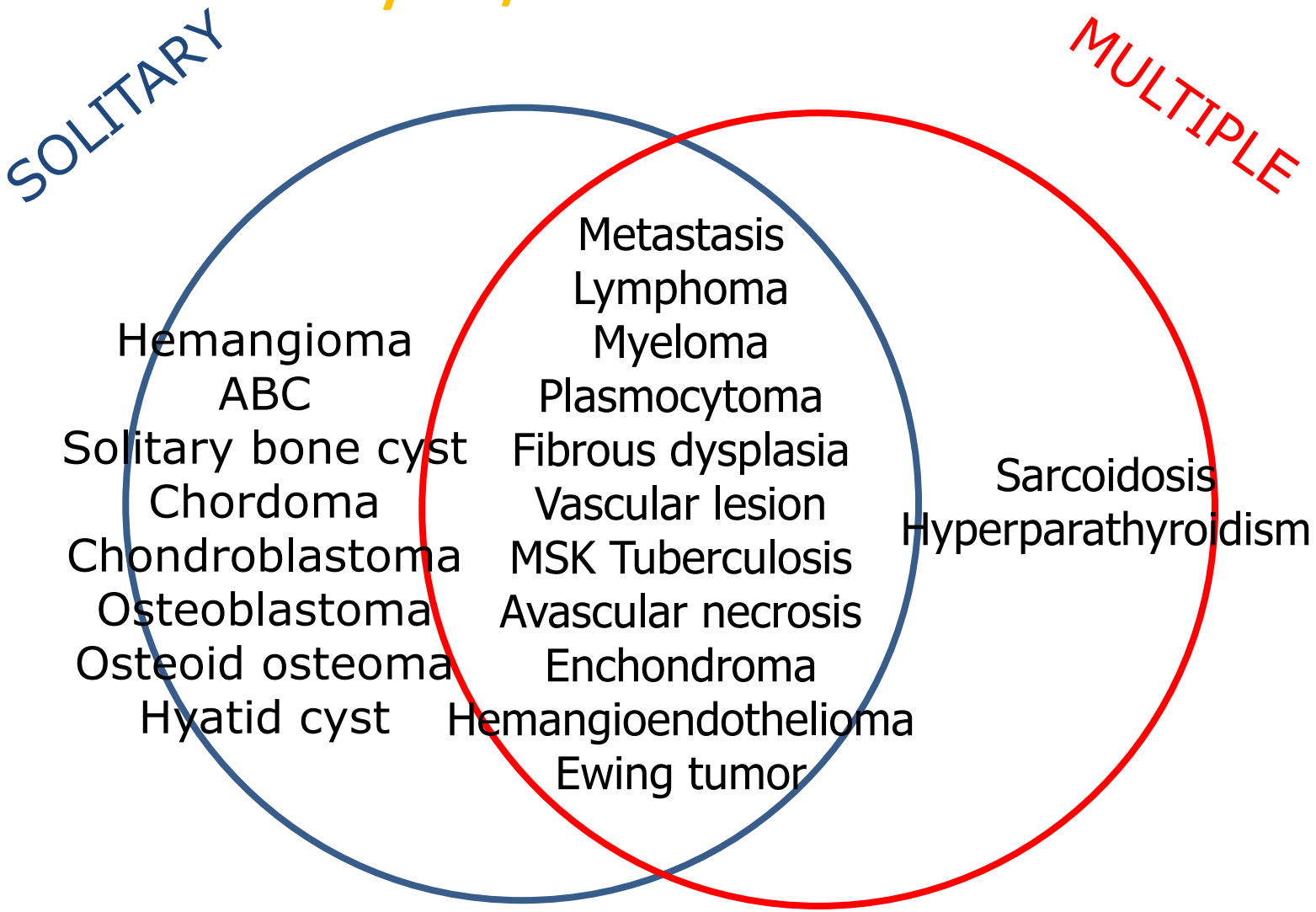

SCINTIGRAPHIE OSSEUSE

02/07/2012

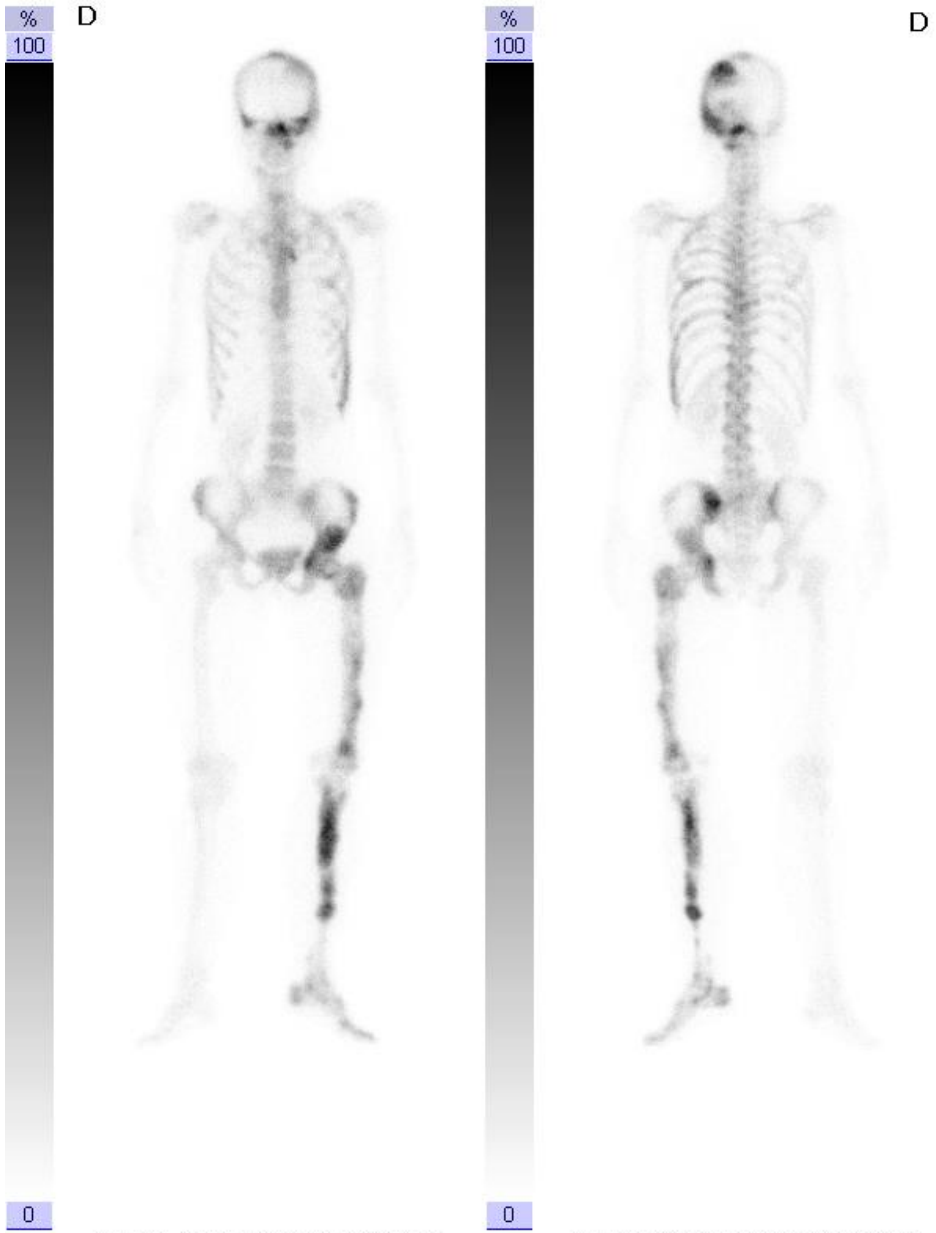

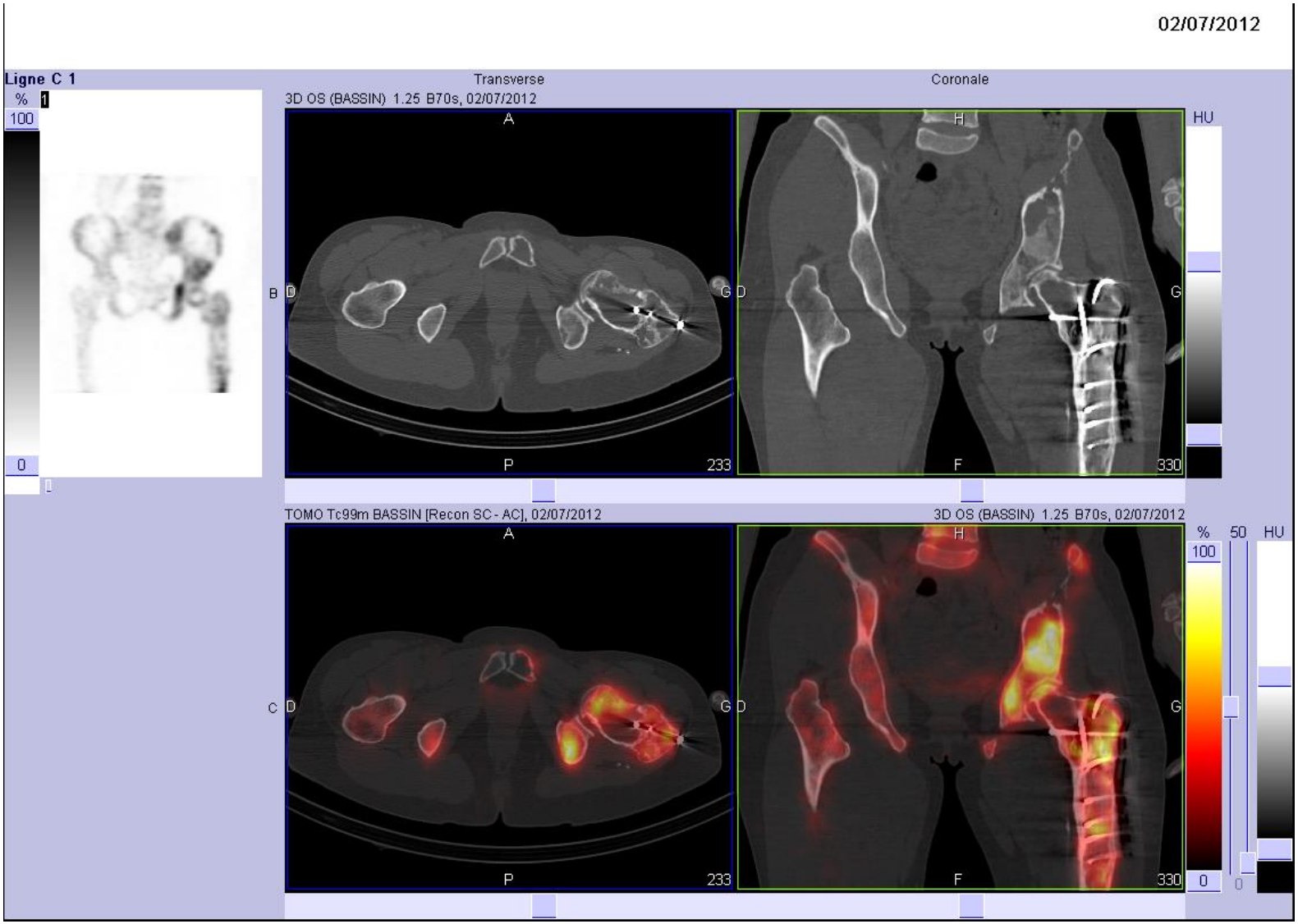
02/07/2012
Ligne C 1
Transverse
Coronale
%
1
100
0
3D OS (BASSIN) 1.25 B70s, 02/07/2012
A
B
D
G
P
233
H
F
330
HU
TOMO Tc99m BASSIN [Recon SC - AC], 02/07/2012
3D OS (BASSIN) 1.25 B70s, 02/07/2012
C
%
50
HU

SCINTIGRAPHIE OSSEUSE

02/07/2012

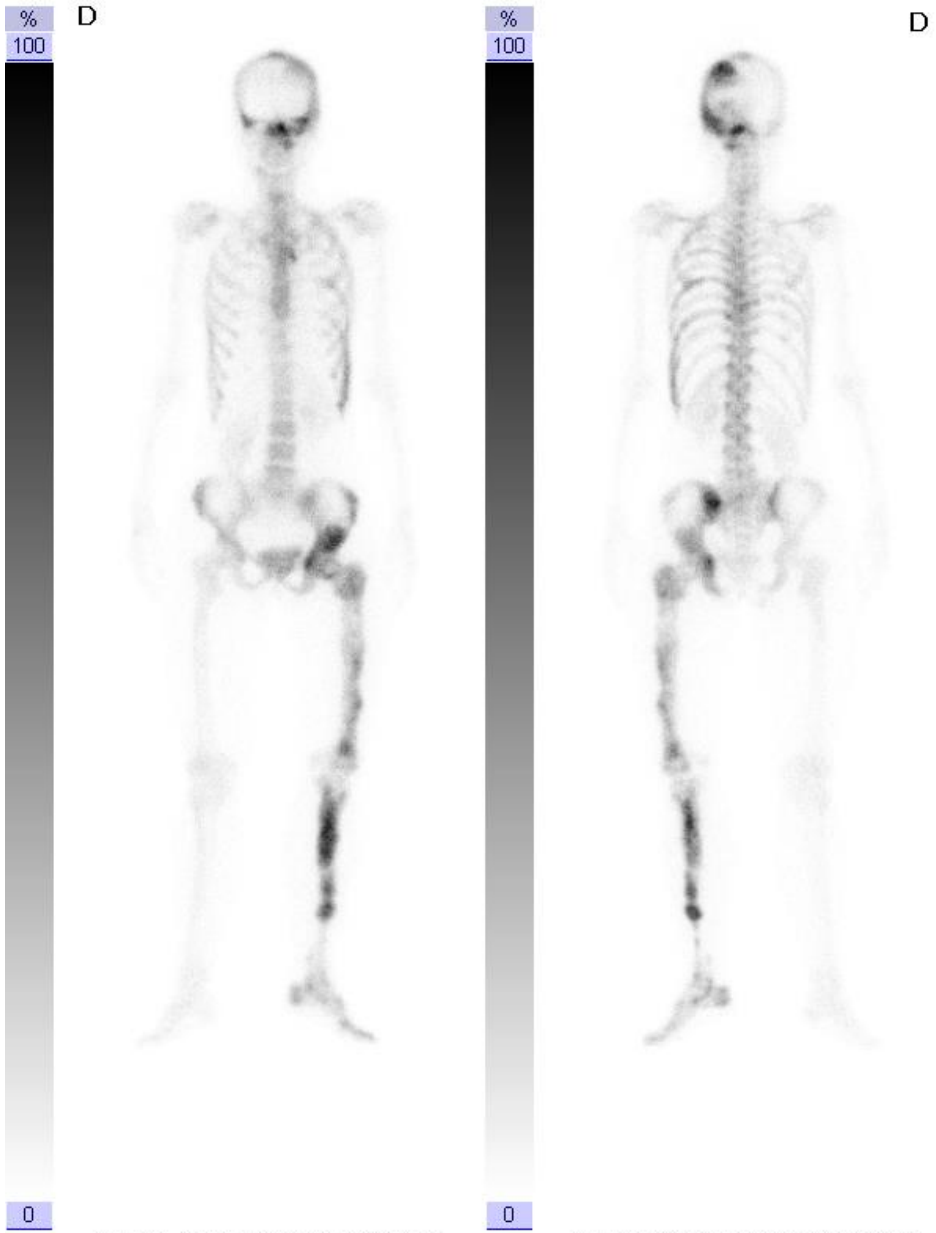

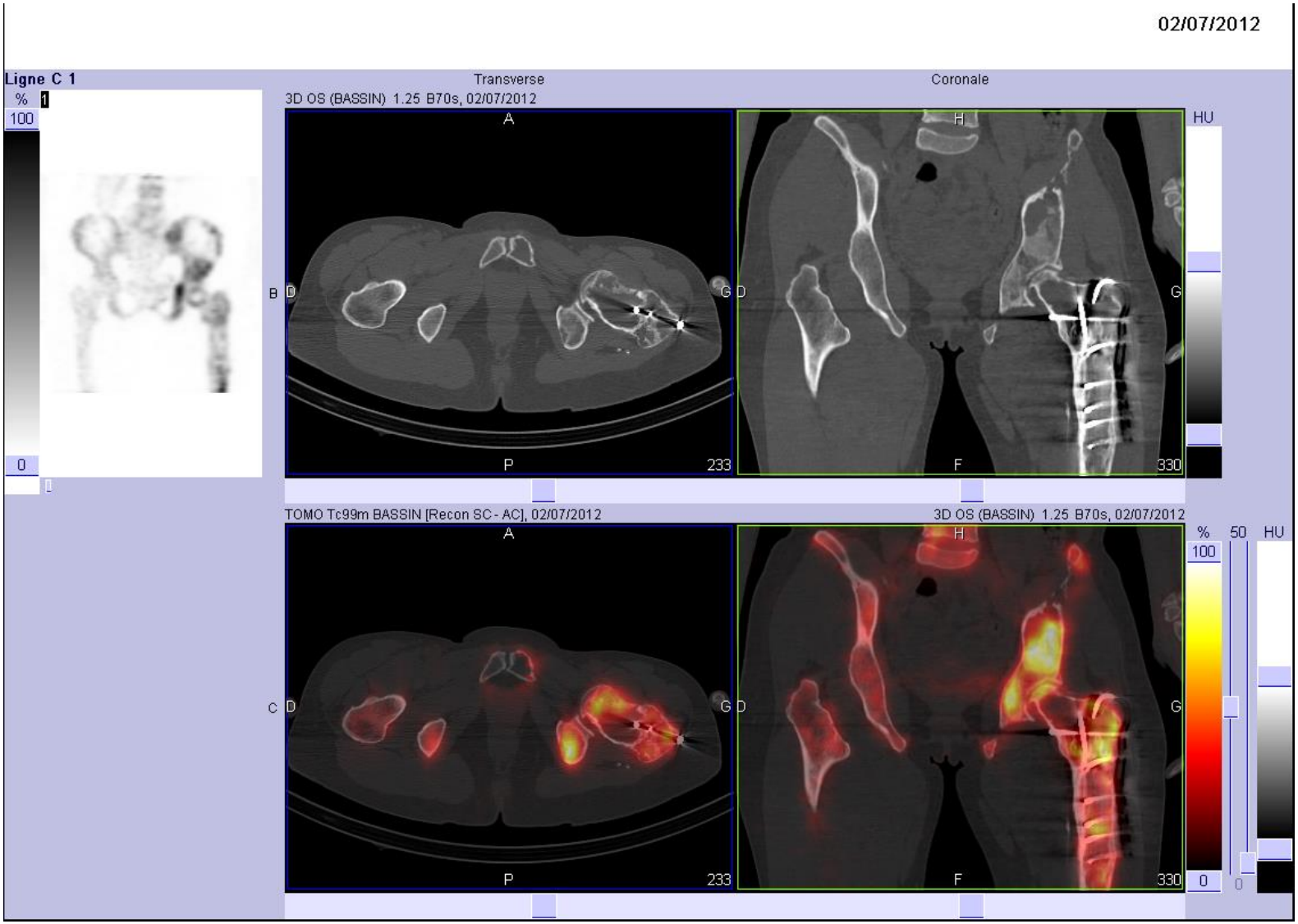
02/07/2012
Ligne C 1
Transverse
Coronale
%
1
100
0
3D OS (BASSIN) 1.25 B70s, 02/07/2012
A
B
D
G
P
233
H
F
330
HU
TOMO Tc99m BASSIN [Recon SC - AC], 02/07/2012
3D OS (BASSIN) 1.25 B70s, 02/07/2012
C
%
50
HU

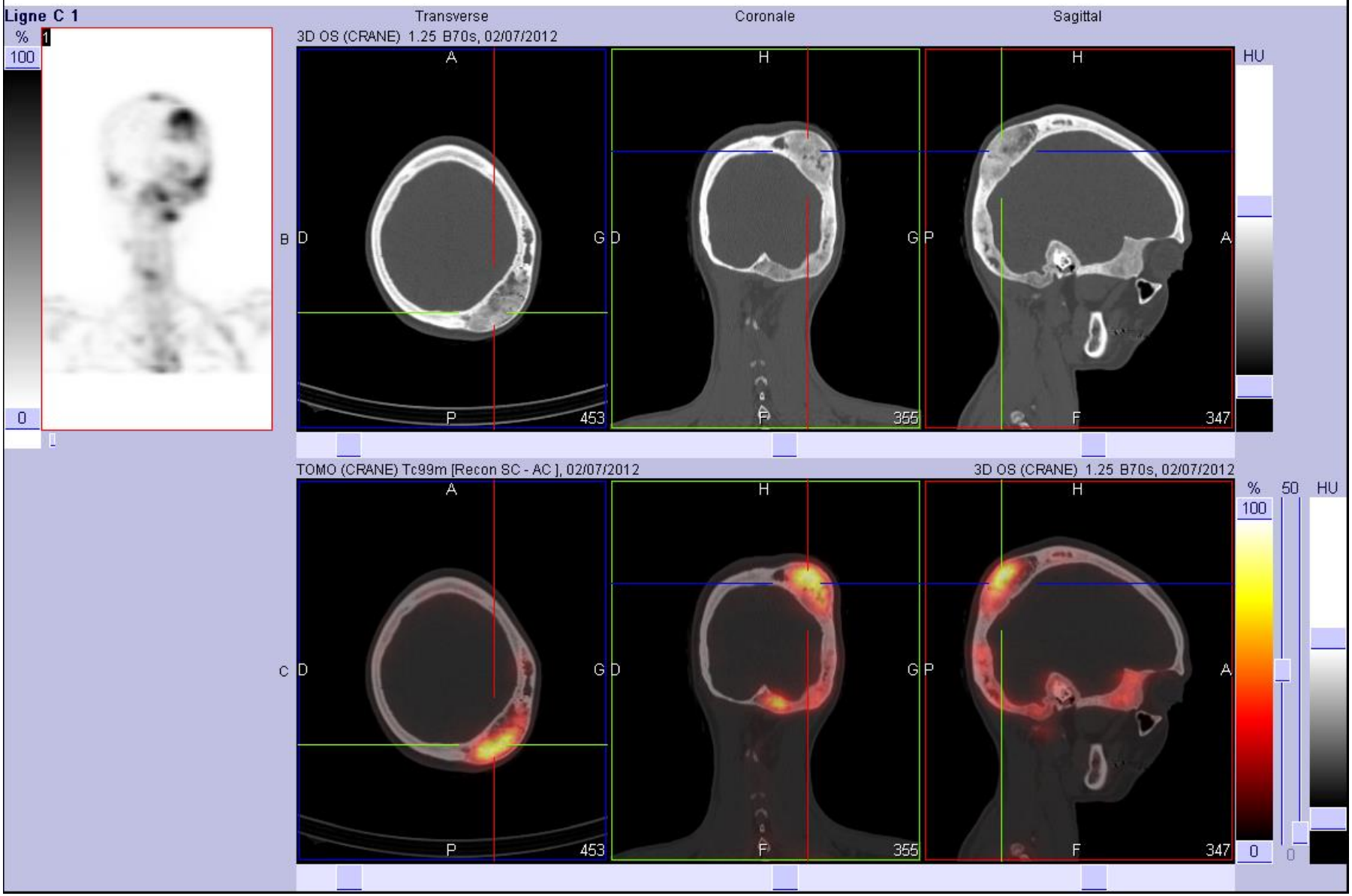
Ligne C 1
Transverse
Coronale
Sagittal
3D OS (CRANE) 1.25 B70s, 02/07/2012
%
100
0
HU
A
H
H
B
D
G
D
G
P
A
P
453
F
355
F
347
TOMO (CRANE) Tc99m [Recon SC - AC], 02/07/2012
3D OS (CRANE) 1.25 B70s, 02/07/2012
%
50
HU
100
0
C
P
453
F
355
F
347

02/07/2012

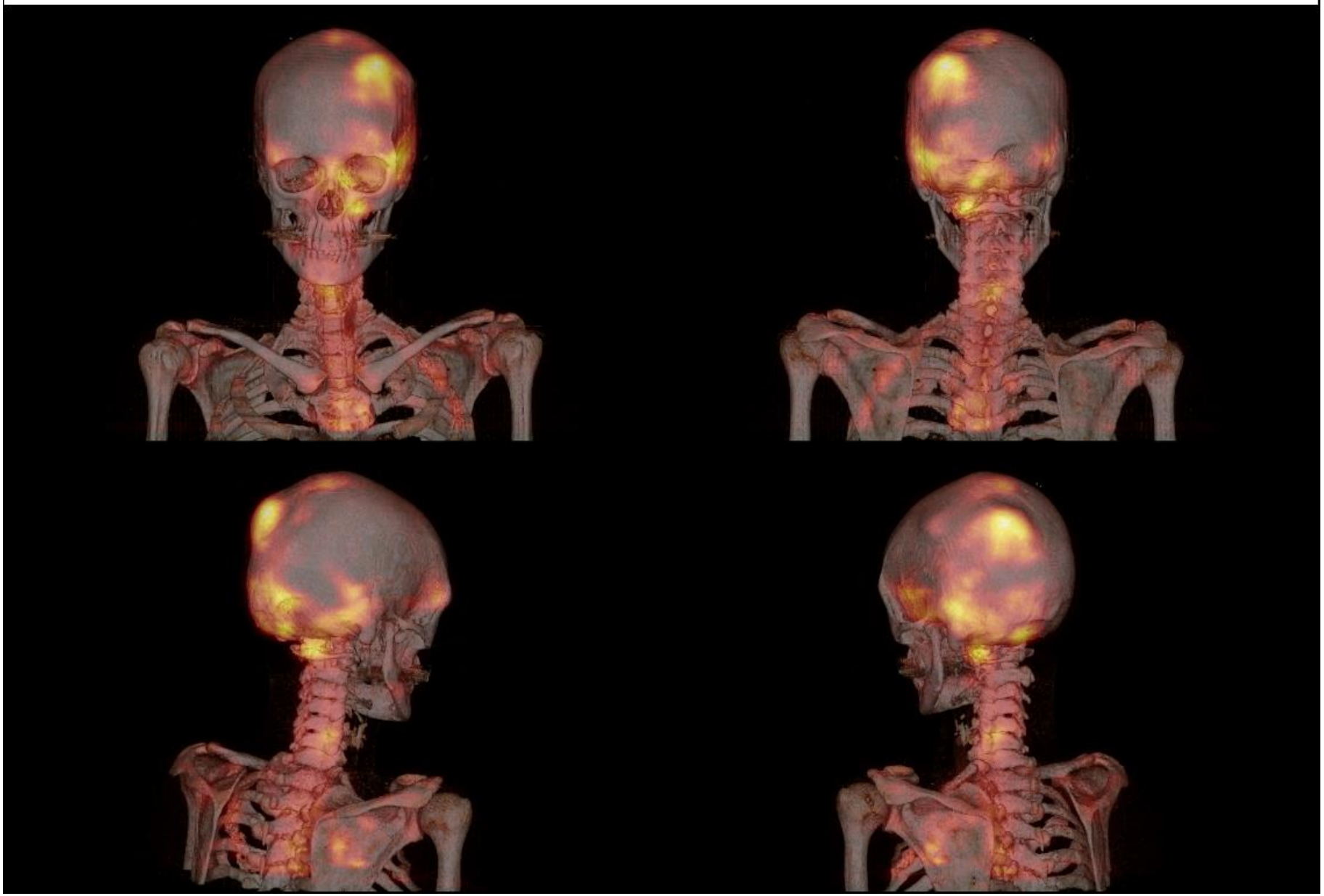

Polyostotic fibrous dysplasia

Particular case of incidentaloma noticeable by:

- ✓ Agreement between X-rays, CT, MRI and bone scan disturbancies
- ✓ Extensive feature of scintigraphic disturbancies
- ✓ Hemimelic (hemi-skeletal) distribution
- ✓ Deformation of tubular bones and flat bones

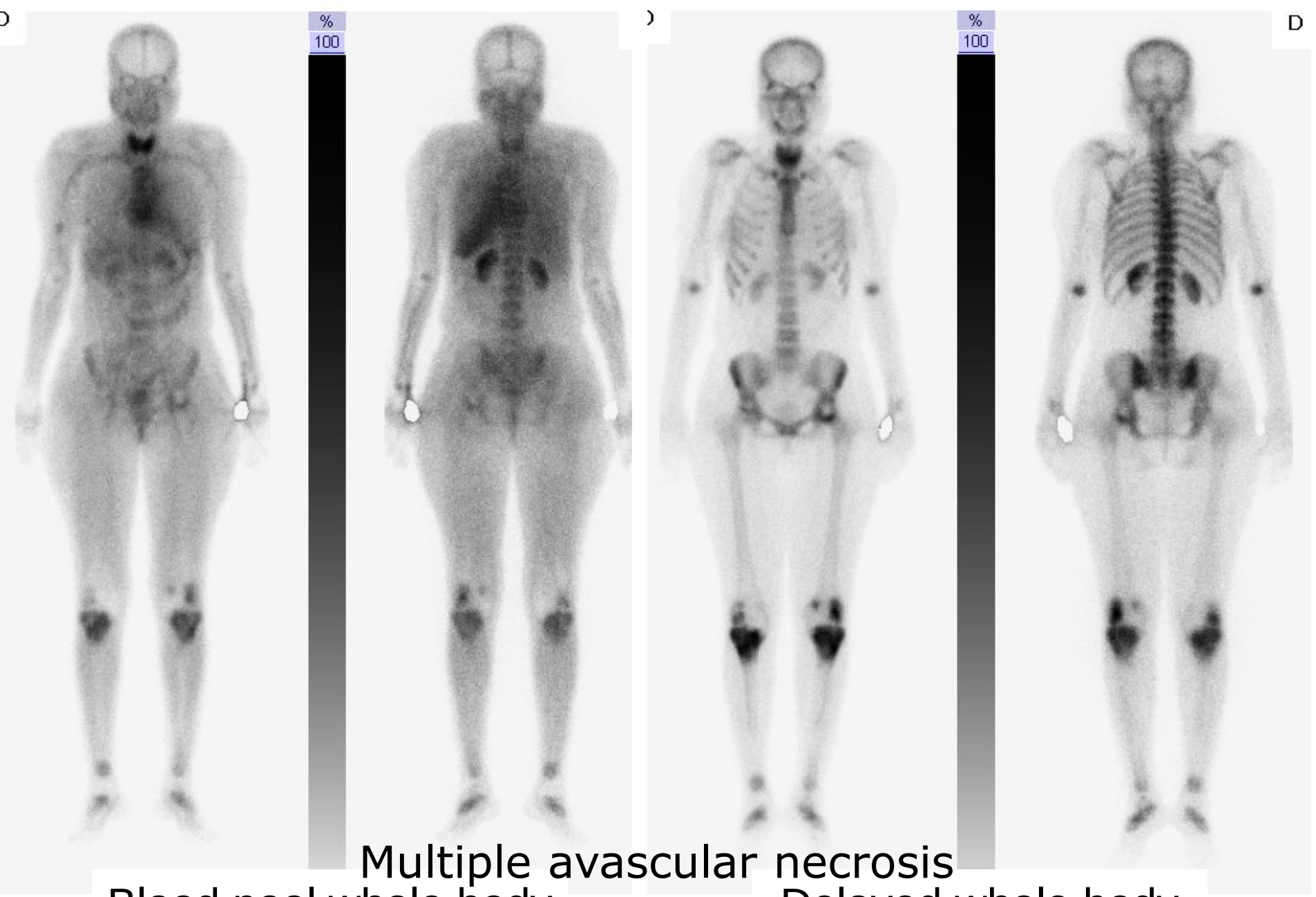

Multiple avascular necrosis

Blood pool whole body

Delayed whole body

Number
Osteosclerotic/Osteoblastic lesions

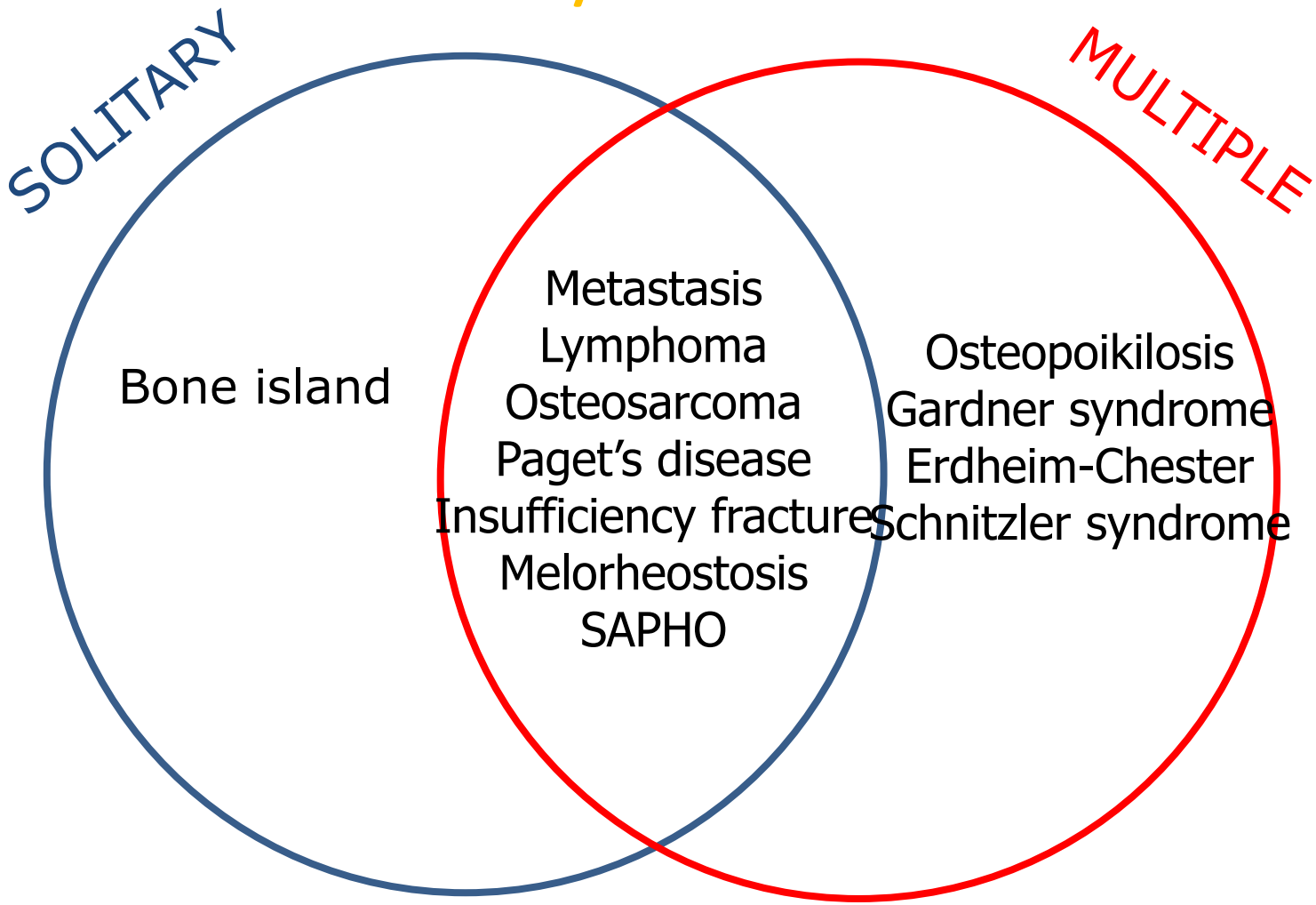

Multiple osteosclerotic/osteoblastic lesions
Still an URO
(unknown radiological object)!?

1. More prevalent thoraco-abdomino-pelvic MDCT incidentalomas reported because of high density contrast
2. More baffling systemic conditions than for multiple osteolytic/osteoclastic lesions
3. FDG PET frequently negative
4. CT-guided biopsy technically arduous to perform and pathological material difficult to analyze

Cancer lobulaire invasif du sein: l'insaisissable ?

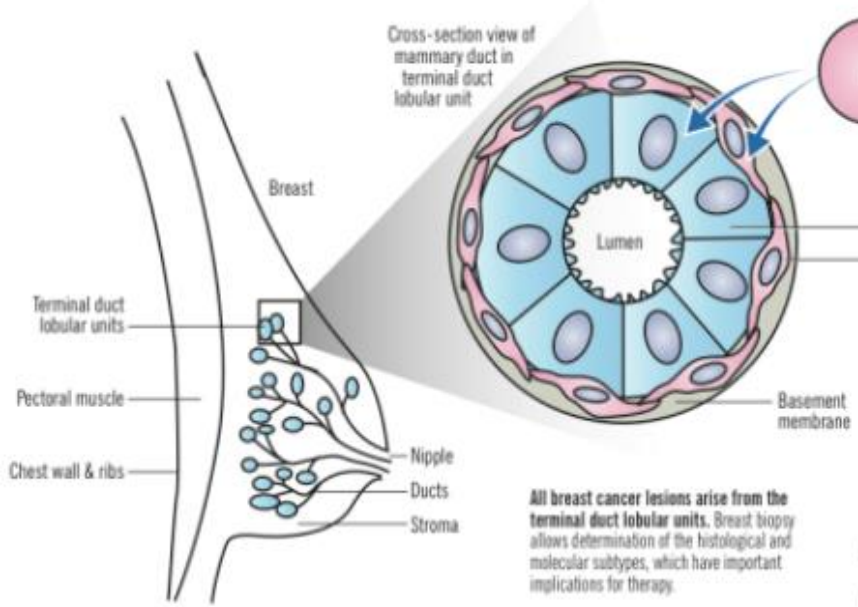

All breast cancer lesions arise from the terminal duct lobular units. Breast biopsy allows determination of the histological and molecular subtypes, which have important implications for therapy.

Normal breast stem cells or progenitor cells transform into breast cancer cells. The cancer cel are similar in phenotype to the normal basal and luminal cells of the ductal structure.

Basal or myoepithelial cells
- Contractile cells for milk ejection
- *Estrogen receptor* –
- Progesterone receptor –

Luminal or epithelial cells
- Respond to hormonal stimulatio for milk production
- *Estrogen receptor* +
- Progesterone receptor +/–

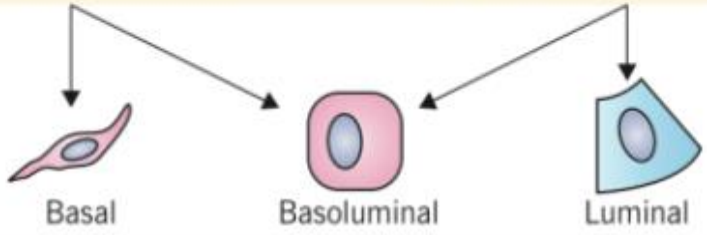

Histological subtypes	Ductal	Lobular
Preinvasive cancer 25% Cells limited to basement membrane	**Ductal carcinoma in situ (DCIS)** 80% May spread through ducts and distort duct architecture 1% progress to invasive cancer per year Usually unilateral	**Lobular carcinoma in situ (LCIS)** 20% Does not distort duct architecture Same genetic abnormality as ILC – E-cahderin loss 1% progress per year Can be bilateral
Invasive cancer 75% Extension beyond the basement membrane	**Invasive ductal carcinoma (IDC)** 79% Usually from DCIS precursor Cause fibrous response, producing a palpable mass on examination Metastasis through lymphatics and blood	**Invasive lobular carcinoma (ILC)** 10% Usually from LCIS precursor Minimal fibrous response, presents less often with palpable mass Metastasis through abdominal viscera to GI, ovaries, uterus Almost always ER+

Molecular subtypes	Triple negative ER–, PR–, HER2–	HER2+	Luminal B	Luminal A
% of breast cancers	15-20%	10-15%	20%	40%
Receptor expression		HER2		ER+/PR+
Histologic grade Level of cell differentiation	High (grade III)			Low (grade I)
Prognosis Correlates to histologic grade	Poor			Good
Response to medical therapy	Chemotherapy	Trastuzumab		Endocrine

TEP TDM FDG

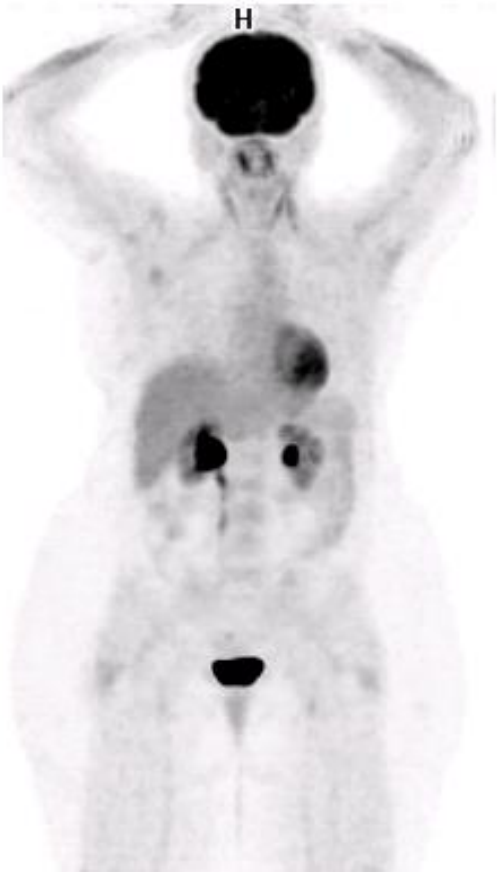

Décembre 2014

Octobre 2015

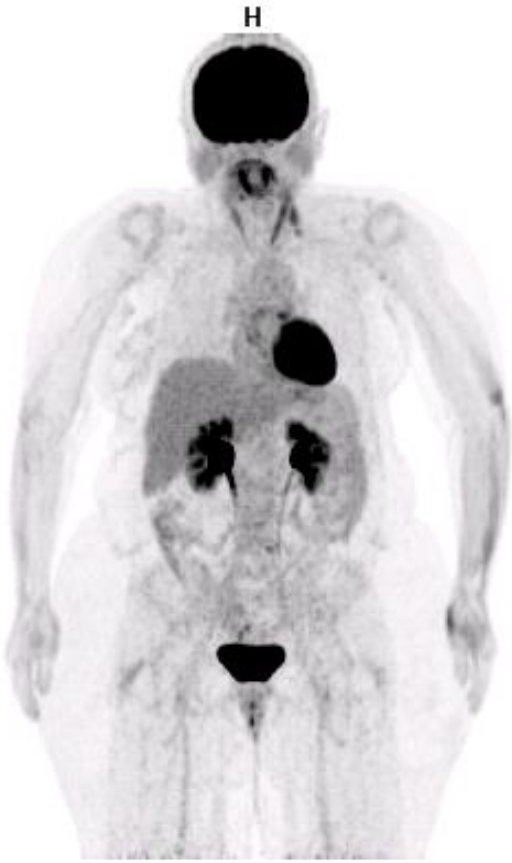

Mars 2016

Mars 2016

Octobre 2015

Décembre 2014

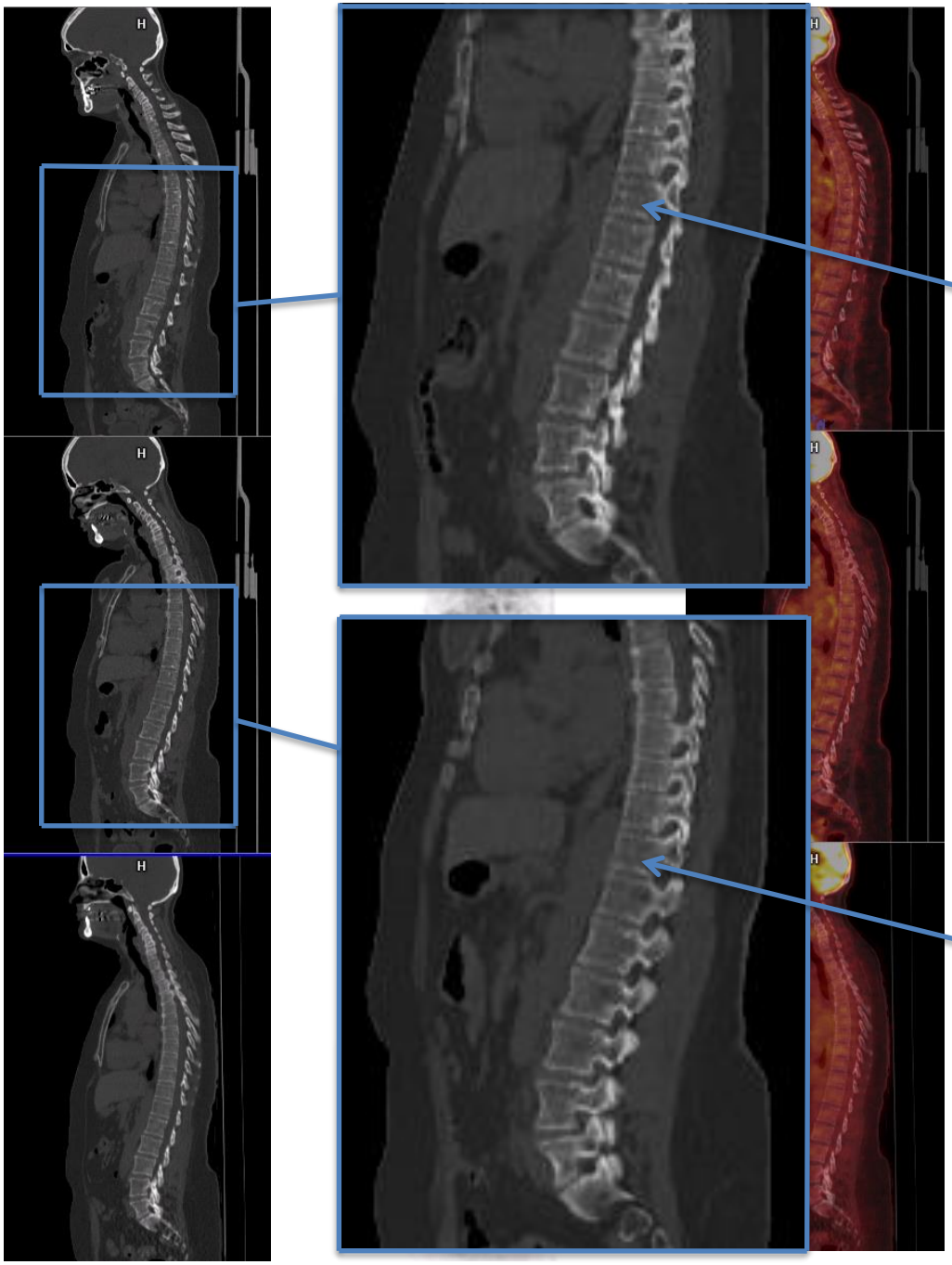

JNM The Journal of NUCLEAR MEDICINE

Comparison of ^{18}F-FDG PET/CT for Systemic Staging of Newly Diagnosed Invasive Lobular Carcinoma Versus Invasive Ductal Carcinoma

Molly P. Hogan, Debra A. Goldman, Brittany Dashevsky, Christopher C. Riedl, Mithat Gönen, Joseph R. Osborne, Maxine Jochelson, Clifford Hudis, Monica Morrow and Gary A. Ulaner

J Nucl Med 2015; 56:1674–1680

Conclusion

Comparaison de l'intérêt de la TEP TDM FDG vs scintigraphie osseuse + TDM dans le bilan d'extension :

- IDC: TEP TDM FDG > scintigraphie osseuse + TDM

  Les métastases osseuses des IDC sont plus souvent ostéolytiques donc inconstamment fixantes sur la scintigraphie osseuse aux (99mTc)-BP qui fixe les lésions ostéoblastiques et non ostéoclastiques (Se : 60%-100%). Ces lésions expriment une plus forte affinité pour le FDG

- ILC: TDM > TEP TDM FDG + scintigraphie osseuse

  Les métastases osseuses de ILC présentent une plus faible affinité pour le glucose donc peu fixantes sur la TEP FDG. Les lésions sont majoritairement ostéocondensantes mais à turn over lent, donc faiblement fixantes en scintigraphie osseuse, mais visibles sur le scanner en fenêtre osseuse.

Aggressive or quiescent?

Decision!

Quiescent (Q) status
=
All Q criteria fulfilled!

- Non-symptomatic
- Medical history = 0
- Biology: Normal
- X-Rays and MDCT
  - Osteolysis: Lodwick-Madewell IA or IB
  - Osteosclerosis: Homogeneous, density > cortical
  - Cortex: Normal appearance
  - Periosteal reaction: Absent or compact
- Bone scintigraphy: No significant increased uptake
- FDG PET: No increased SUV
- Comparison to previous imaging tests: stable aspect

Quiescent (Q) status
=
Noli Me Tangere
(Don't touch lesions)

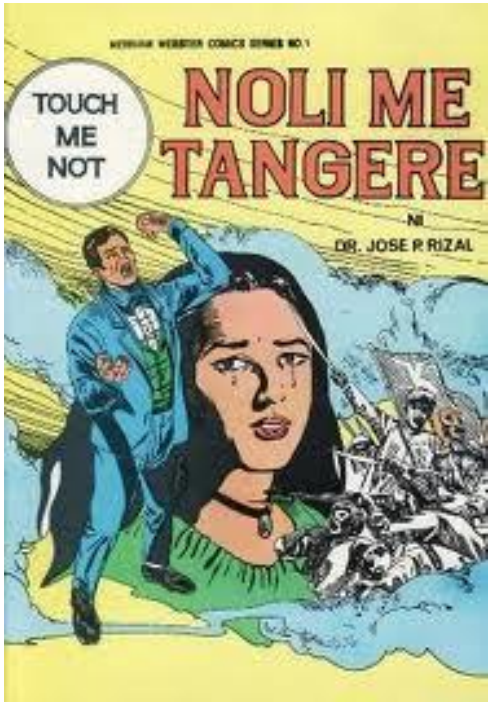

Aggressive (A) status if ≥1 A criteria fulfilled ⇒ **Biopsy**!

Tumoral image displaying any aggressive criteria

- Tumoral
  - Met or primitive
- Blood malignancy
- MSK infection
- Histiocytoses (LCH & non-LCH)

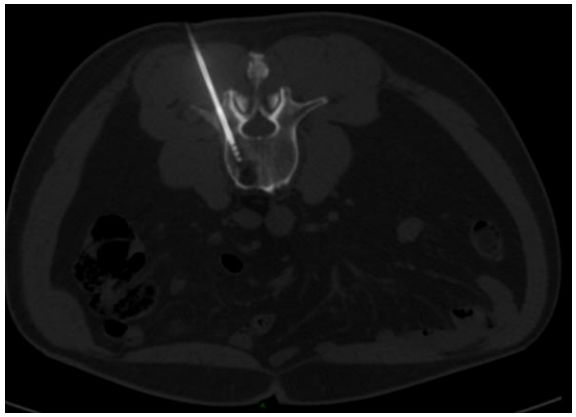

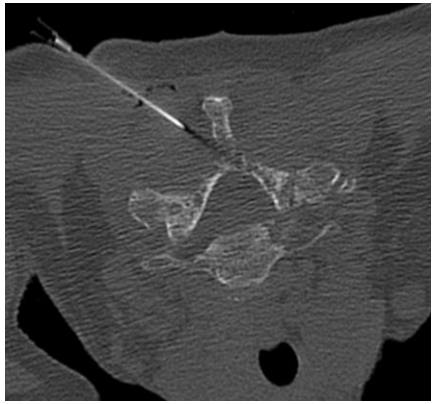

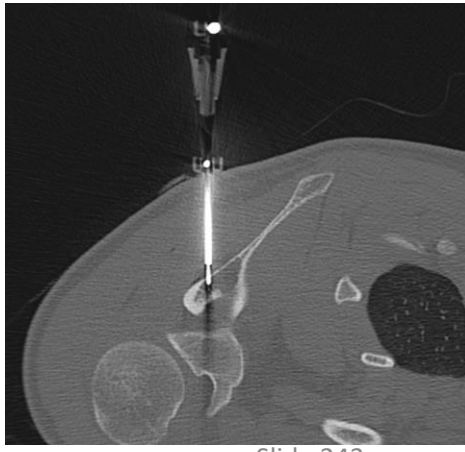

Conclusion

Tumor
Aggressiveness ⇆ Quiescence
A survival 10 criteria checklist for the imaging specialist

1. Localization
2. Age
3. Pain
4. Phenotype lytic/sclerotic
5. Margins
6. Activity/timeline
7. Cortical/Periosteum
8. Crossing or not the joint
9. Soft tissue expansion
10. Number (⇒ distribution)

Internet free dedicated links

- http://pathologyoutlines.com/bone.html
- http://njms2.umdnj.edu/tutorweb/introductory.htm
- http://www.rad.washington.edu/mskbook/
- https://link.springer.com/content/pdf/bfm%3A978-3-319-54018-4%2F1.pdf
- http://www.wheelessonline.com/ortho/2136

Websites last visited on May, 17, 2019